POLYURETHANES BASED ON FATTY ACIDS WITH IMPROVED BIOCOMPATIBILITY

Rodolfo Jesús González Paz

Dipòsit Legal: T. 1470-2012

Rodolfo Jesús González Paz

Polyurethanes based on fatty acids with improved biocompatibility

PhD THESIS

Supervised by

Dr. Virginia Cádiz and Dr. Gerard Lligadas

Departament de Química Analítica i Química Orgànica

UNIVERSITAT ROVIRA I VIRGILI

Tarragona

2012

UNIVERSITAT ROVIRA I VIRGILI

Departament de Química Analítica
i Química Orgànica
c/Marcel.li Domingo, s/n
Campus Sescelades
4007, Tarragona

Virginia Cádiz, Catedrática, y Gerard Lligadas, Profesor Lector, del Departamento de Química Analítica y Química Orgánica de la Universidad Rovira i Virgili,

CERTIFICAMOS:

Que el presente trabajo, titulado "Polyurethanes based on fatty acids with improved biocompatibility", que presenta Rodolfo Jesús González Paz para la obtención del título de Doctor, ha sido realizado bajo nuestra dirección en el Departamento de Química Analítica y Química Orgánica de esta Universidad y que cumple los requisitos para poder optar a la Mención Europea.

Tarragona, 24 de julio de 2012

Dra. Virginia Cádiz

Dr. Gerard Lligadas

Si un hombre quiere estar seguro de que camino ha de transitar,
que cierre los ojos y camine en la oscuridad...

San Juan de la Cruz

Agradecimientos

Inicialmente me gustaría agradecerle a mi directora Virginia Cádiz por haberme dado la oportunidad de crecer profesionalmente en su grupo de trabajo durante cuatro años, gracias por tus sabios consejos durante esta etapa de mi vida, he cambiado de forma positiva muchos aspectos personales. En segundo lugar, me gustaría agradecer enormemente a mi codirector Gerard Lligadas por su paciencia y constancia en corregir mis faltas durante este tiempo, hoy en día soy más profesional y humano. Quisiera agradecerle a Joan Carles Ronda por ser un gran ejemplo a seguir dentro del laboratorio, siempre dispuesto a trasmitir su amplio conocimiento y ayudar a quien lo necesita, muchas gracias por tus consejos dentro del campo científico, me ayudaron mucho a resolver problemas en los momentos más difíciles. De igual forma quiero agradecerle a Marina Galiá por sus sonrisas en momentos que lo necesitaba. Así como a los profesores que a pesar de no ser de nuestro grupo de trabajo siempre me mostraron una alta calidad humana y profesional, gracias por sus enriquecedoras clases y palabras, Angels Serra, Ana Mantecón, Toni Reina, Jordi Puiggali y Sebastián Muñoz-Guerra.

Compañeros de laboratorios, este camino sin su presencia no hubiese tenido sabor: Veteranos, Lucas, Kike, David, Mireia, gracias por su experiencia compartida, Cristina gracias por escucharme desde el comienzo, a pesar de que hablaba mucho y no me entendías nada, jejeje, sé que hemos formado una bonita y fuerte amistad, creo que ya entiendes un poco más mi forma de hablar, gracias por estar ahí en cada momento brindando tu ayuda y atención. Maryluz, siempre iluminando el camino con tu pureza, no olvidaré nuestras buenas conversaciones sobre la vida, para mi llegaste como una niñita y te irás como una mujer. Camilo, siempre de apariencia tranquila, pero internamente un gran pensador, gracias por hacerme reír y apoyarme. Alev y Zeynep, guerreras turcas, son mujeres de un corazón muy grande y muy capaces, sigan cultivando su crecimiento humano y profesional, las necesitamos. Marc a tí también te necesitamos, mantente constante y consciente como siempre. Adrián, Surya y Fiseha, compañeros fieles, hemos pasado muchos momentos juntos en este tiempo, días lluviosos y días muy alegres, gracias por escucharme y abrirse a contarme sus problemas y felicidades, no importa de que continente vengamos, Europa, Asia, África o América, somos humanos y ponerse en los zapatos del

otro, es el mejor doctorado que he hecho, gracias por enseñarme la vía. Asta, Marjorie, Silvia, Cristinas y compañeros del Azúcar, jeje, gracias por los buenos momentos en el café y en las comidas.

Me gustaría agradecerles a otras personas que de una u otra forma hicieron esto realidad, Ramón (RMN), Carlos (cafetería), vigilante del campus, señoras de la limpieza, Tere, Juan Luis, Olga, Tais, Avelina, Dunia y Jaume. Así como amigos que durante este ciclo de mi vida siempre estuvieron ahí, atentos, recordándome el presente con su aliento, José Luis, Pedro, Kiara, Miguel, Edgar, Virginia, Pablo, Silvana, Doza y la sangha del dojo zen Tarragona. Eliot muchas gracias por el diseño de la carátula, ya entiendo porque formas parte del equipo diseñador de *Reebok* en Barcelona, toda una obra de arte sin haberte dicho nada.

Vorrei ringraziare il Dr. Gianluca Ciardelli, per avermi dato l'opportunità di lavorare con il suo gruppo di ricerca e anche per essere sempre pronto ad aiutarmi in tutte le difficoltà. Ringrazio tutte le persone che ho incontrato nel gruppo e in Italia, che erano sempre pronte ad aiutare gentilmente, Marina, Clara, Monica, Susana, Antonella, Ruo, Piergiorgio, Valeria, Irene, Cristina, Fabiana, Simone, Pempa, Luiga, Lorenzo, Gabriela, Mariela, Laura, Paula, Maura, Rosana, Paolo, Gabriel, Andrea, Renata, Serena.

Quisiera dedicar esta tesis principalmente al Eterno Presente, por simplemente, estar ahí, a mi madre y familia por ser las bases a las que les debo todo y se merecen más. Pero sobre todo quiero dedicar esta tesis a la persona que incondicionalmente siempre ha estado presente apoyándome en todo momento y bajo cualquier circunstancia, Lindsay, le doy gracias a la vida por haberte encontrado al comienzo de esta etapa, te amo.

Table of contents

General introduction **1**

Sustainable development and renewable feedstocks 3

Scope and Objectives **13**

First part: Synthesis of polyurethanes via click chemistry **17**

Click chemistry in polymer science 19

Vegetables oils and fatty acids-derived polyurethanes 22

Chapter I. A Green Approach toward Oleic and Undecylenic Acids-derived Polyurethanes. 31

Chapter II. Thiol-yne Reaction on Alkyne-derivatized Fatty Acids: Biobased Polyols and Cytocompatibility of derived Polyurethanes. 57

Chapter III. Thiol-yne Reaction of Alkyne-derivatized Fatty Acids: Thiol- Reactive Linear Polyurethanes 81

Second Part: Biocompatibility of polyurethanes and functionalization strategies **101**

Biocompatibility of polyurethanes 103

Surface properties and modifications 109

Chapter IV. Study on the Interaction between Gelatin and Polyurethanes derived from Fatty Acids 121

Chapter V. Cytocompatible Polyurethanes from Fatty Acids through Covalent Immobilization of Collagen 147

Chapter VI. Enhancement of Fatty Acid-based Polyurethanes Cytocompatibility by Non-covalent Anchoring of Chondroitin Sulfate 175

General conclusions **197**

Appendices **201**

Appendix A. List of abbreviations 203

Appendix B. List of publications 206

Appendix C. Stages and meeting contributions 207

GENERAL INTRODUCTION

SUSTAINABLE DEVELOPMENT AND RENEWABLE FEEDSTOCKS

In 1987 the concept of sustainable development emerged after the Brundtland commission,[1] as the main goal to be achieved in response to the accelerated deterioration of the environment and consumption of feedstocks (Figure 1).[2] It was defined as the social and economic advance to assure human beings a healthy and productive life, without compromising the ability of future generations to meet their own needs.[3]

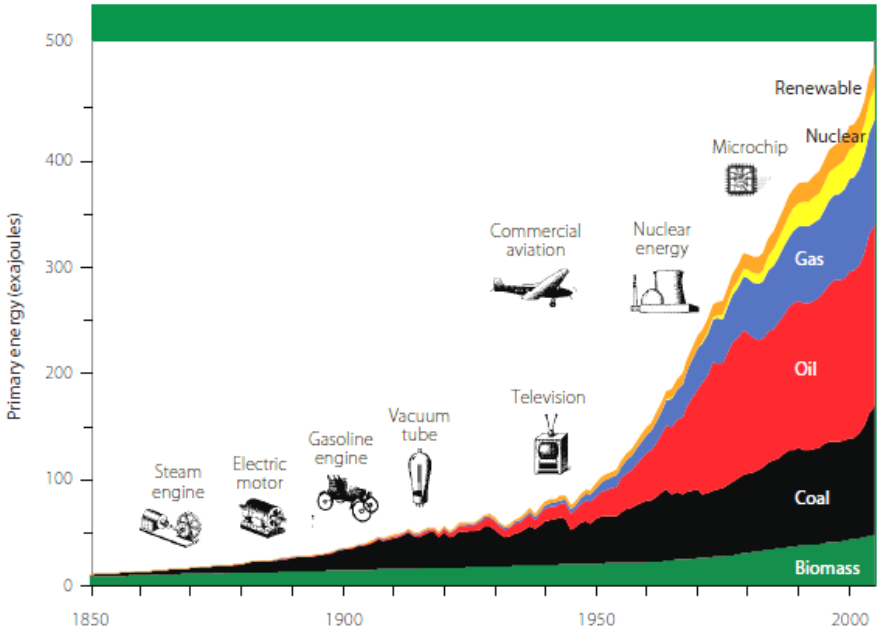

Figure 1. Rise in energy consumption (feedstocks) since the first industrial revolution.

In this regard, international environmental law has developed rapidly since 1992 United Nations Conference on Environmental and Development (UNCED)[4] and the treaty Convention on Biological Diversity (CBD),[5] that have had considerable impact as well on economic development and trade relations for the sustainable development. Also influential have been two documents issuing from UNCED: the Declaration of the Conferences (Rio Declaration) and the Agenda 21, a program of action setting out

[1] The Brundtland Commission, formally the World Commission on Environment and Development (WCED). Convened by the United Nations in 1983.
[2] United Nations , Department of Economic and Social Affairs, World Economic and Social Survey, The Great Green Technological Transformation, E/2011/50/Rev. 1ST/ESA/333, New York, p. vii, 2011.
[3] G. Brundtland, Our Common Future, Oxford University Press, Oxford, 1987.
[4] Report of the United Nations Conference on Environmental and Development, Rio de Janeiro, 1992. DOC. A/CONF.151/26/Rev.l (Vol. l- III), New York, 1993.
[5] Convention on Biological Diversity (CBD), Rio de Janeiro, 5 June 1992, in force 29 December 1993, UNTS vol. 1760, No. 30619, p. 79. See also the CBD website at www.biodiv.org.

measures required to protect and preserve the environment in the 21st century.[6] These documents were strongly reafirmed at the World Summit on Sustainable Development (WSSD)[7] in 2002 as a new environmental forum, called for the promotion of a sustainable use of biomass. It was recently shown that biomass can be produce in a volume sufficient for industrial utilization without compromising the food suply for the increasing global polution.[8] Chemists have much to contribute to meet this challenge. The consumption and production of chemicals in developing countries is growing much faster than in developed countries and could account for a third of global consumption by 2020. At the 2002 World Summit on Sustainable Development governments set the goal "that by the year 2020, chemicals will be produced and used in ways that minimize significant adverse impacts on the environment and human health".[9]

In this context, during the early 1990s the US Enviromental Protection Agency (EPA) coined the phrase Green Chemistry "To promote innovative chemical technologies that reduce or eliminate the use of generation of hazardous substances in the design, manufacture and use of chemical products". Over the last 12 years, Green Chemistry has gradually become recognized as both a culture and methodology for achieving sustainability. The main challenges of Green Chemistry and Engineering can be summarized as:

- Utilizing renewable instead of non-renewable feedstocks.
- Avoid toxic or dangerous chemicals to obtain safer products.
- Minimizing energy use.
- Minimizing waste and resource use, re-using products, recovering and recycling materials. So making processes globally more efficient.

Although there are some examples of green processes used in the industry, the total application of the main challenges of Green Chemistry and Engineering in the development of new chemical processes in the industry is not viable in most cases;

[6] The Rio Declaration 4 (1992) 31 ILM 874. For information about UNCED and for the texts of documents adopted at the Conference, see the website of the UN Department of Economic and Social Development, Sustainable Development section, at www.un.org/esa/sustdev.
[7] United Nations Report of the World Summit on Sustainable Development (WSSD) Johannesburg, South Africa, 2002. See Johannesburg Plan of Implementation, DOC. A/CONF.199/20, New York, 2002.
[8] J.O. Metzger, A. Huttermann, Naturwissenschaften: 96, 279-288, 2009.
[9] United Nations Report, Trends in Sustainable Development, Chemicals, Mining, Transport and Waste Management, Department of Economic and Social Affairs, Division for Sustainable Development, United, New York, p.2, 2010.

however, if part of these principles can be accomplished, the objective of sustainable development will be closer.

For the last 100 years fossil oil has been the cheapest raw material for energy and chemical production. Much of the materials and infrastructure of modern society has been built on the availability of this cheap source. This situation is now drastically and rapidly changing due to dwindling oil reserves in combination with increasing demand, with oil prices rising to up to 10 times those of 15 years ago. The previous low price of fossil oil provided little incentive to implement technologies that could improve energy efficiency, or replace fossil oils in industrial chemicals and materials production, even though substantial reductions in fossil oil consumption can be made easily and economically by applying existing technologies in these areas. However, recent decades have seen a rapid increase in industrialisation in the previous third world countries that are now approaching western countries in their life expectancy, living standards and energy consumption. Furthermore, global population growth, although predicted to level off in the latter half of this century, will still increase by 34% over the next 40 years. Therefore, even if substantial energy efficiency measures can be implemented, alternative sources for energy and material will still need to be found to satisfy future demand levels that could reach twice that of current consumption of fossil oil, if the global development and standard of living expectations are to continue being met.[10]

Nowadays, renewable raw materials make up an approximate 10-12% of the feedstocks used by the chemical industry and it is expected to increase under the B1 stabilization scenario[11] (Figure 2) for relative shares of the most important sources for the chemical industry. B1 is one of the stabilization scenarios considered by the Intergovernmental Panel on Climate Change (IPCC). It is one of the ideal scenarios among the possible ones and stipulates fast economic growth, rapid changes towards a service and information economy, population rising to 9 billion by 2050 and then declining, a reduction in material intensity and the introduction of clean and resource-efficient technologies, and a more integrated world. Oils and fats constitute the most

[10] A.S. Carlsson, J. L. Yilmaz, A.G. Green, S. Stymne, P. Hofvander, Eur. J. Lipid Sci. Technol: 113, 812-831, 2011.
[11] United Nations , Department of Economic and Social Affairs, World Economic and Social Survey, The Great Green Technological Transformation, E/2011/50/Rev. 1ST/ESA/333, New York, p. 14, 2011.

important renewable raw materials for the chemical industry (51 %), followed by carbohydrates (43 %) and other renewables such as proteins (6 %).[12,13]

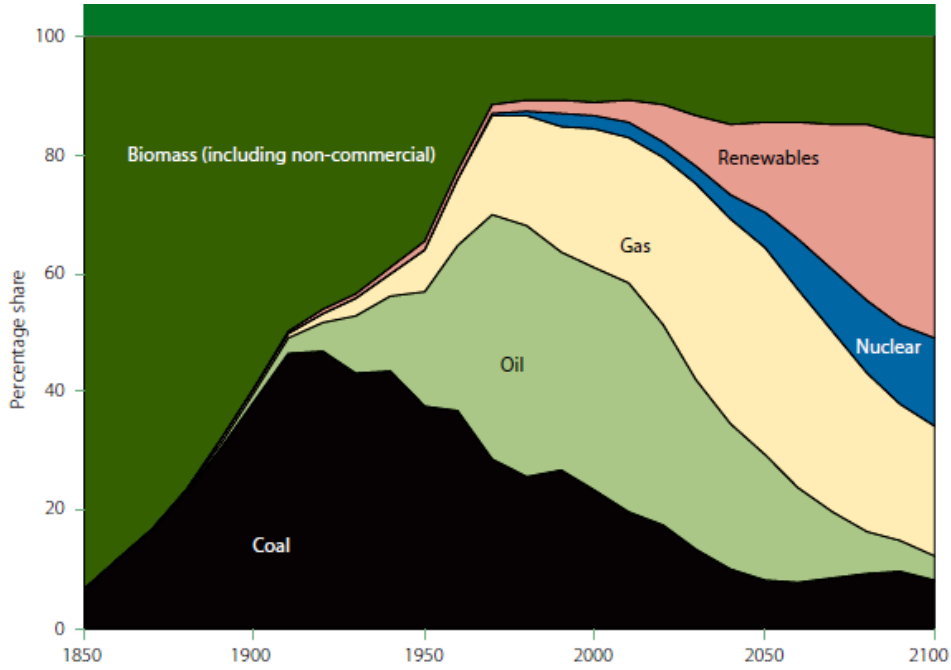

Figure 2. History and possible future of the global sources of feedstocks for the chemical industry.

Plant oils as renewable resources in polymer chemistry

The cost of plant oils 15 years ago was over five times higher than crude fossil oil; however, today they are approaching price parity. Thus, applications in which plant oils could not previously compete with fossil oil are now becoming economically viable. The annual global production of the major vegetable oils (from palm, soy, rapeseed, cotton, peanut, sunflower, palm kernel, olive, and coconut) amounted to 84.6 million tons (Mt) in 1999/2000 and increased to 137.3 Mt in 2009/2010 (an increase of 62%).[14] In addition, about 3.8 Mt of minor plant oils (from sesame, linseed, castor, corn) and about 22.1 Mt of animal fats (tallow, lard, butter, fish) were produced and consumed in 1999, growing moderately to 4.4 Mt and 24.5 Mt, respectively, in 2008.[15,16] Castor and linseed oil are almost exclusively used for industrial applications.

[12] Eissen, M.; Metzger, J.O.; Schmidt, E.; Schneidewind, U. Angew Chem Int Ed: 41, 414-436, 2002.
[13] J.O. Metzger, Eur. J. Lipid Sci. Technol: 111, 865-876, 2009.
[14] United States Department of Agriculture, Oilseeds: World Markets and Trade Monthly Circular http://www.fas.usda.gov/oilseeds/circular/Current.asp.
[15] F.D. Gunstone: Market report, Lipid Technol: 20, 264, 2008.

Interestingly, the production of castor oil increased by 38% from 0,43 Mt per year in 1999 to 0,60 Mt per year in 2008, whereas the production of linseed oil decreased by 12% from 0,73 Mt per year in 1999 to 0,64 Mt per year in 2008.[16]

The use of vegetable oils as raw materials in the chemical industry has become more important year by year. The annual global production of the oils and fats that are also used as oleochemical feedstock is shown in Figure 3 for 1999/2000 and 2009/10.[15, 16]

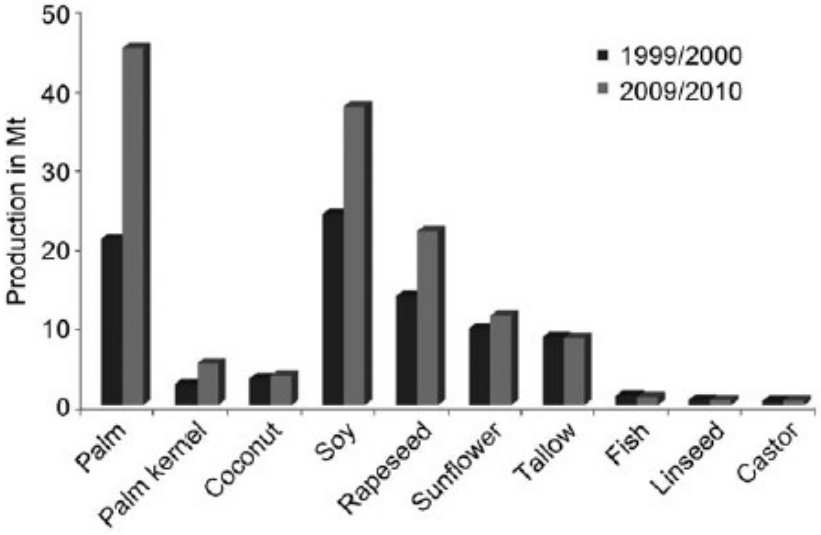

Figure 3. Production of oils and fats that are important as feedstock for the oleochemical industry in 1999/2000 and 2009/2010.

The use of vegetables oils as starting materials offers numerous advantages: for example, low toxicity, inherent biodegradability, and high purity,[17,18] thus they are considered to be one of the most important class of renewable resources for the production of biobased polymers. [19,20]

The main constituents of plant oils are triglycerides (Figure. 4), which are the product of esterification of glycerol with three fatty acids. Fatty acids account for 95%

[16] Oil World Annual, WORLD OILS & FATS, 2009: http://econ.mpob.gov.my/economy/annual/stat2009/ei_world09.htm.
[17] H. Bauman, M. Buhler, H. Fochem, F. Hisrsinger, H. Zoeblein, J. Falbe, Angew. Chem. Int. Ed. Engl: 27, 41-62, 1988.
[18] U. Biermann, W. Friedt, S. Lang, W. Luhs, G. Machmuller, J.O. Metzger, M.R. Klaas, H.J. Schafer, M.P. Schneider, Angew. Chem. Int. Ed: 39, 2206-2224, 2000.
[19] Y. Xia and R.C. Larock, Green Chem: 12, 1893-1909, 2010.
[20] L. Montero de Espinosa, M.A.R. Meier, Eur. Polym. J: 47, 837-852, 2011.

of the total weight of triglycerides and their content is characteristic for each plant oil (Table 1).

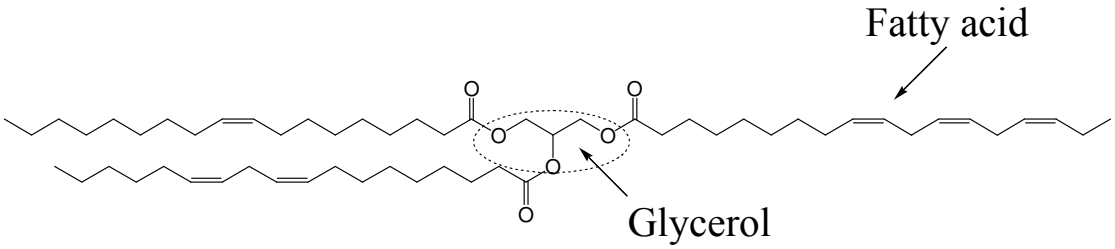

Figure 4. Triglyceride molecule, the main component of vegetable oils

Table 1. Fatty acid percentage distribution in various plant oils

Fatty acid	C:DB [a]	Canola	Corn	Castor	Linseed	Olive	Palm	Soybean	Sunflower	High oleic
Myristic	14:0	0,1	0,1	0	0	0	0,1	0,1	0	0
Myristoleic	14:1	0	0	0	0	0	0	0	0	0
Palmitic	16:0	4,1	10,9	1	5,5	13,7	44,4	11	6,1	6,4
Palmitoleic	16:1	0,3	0,2	0	0	1,2	0,2	0,1	0	0,1
Margaric	17:0	0,1	0,1	0	0	0	0,1	0	0	0
Margaroleic	17:1	0	0	0	0	0	0	0	0	0
Stearic	18:0	1,8	2	1	3,5	2,5	4,1	4	3,9	3,1
Oleic	18:1	60,9	25,4	3	19,1	71,1	39,3	23,4	42,6	82,6
Linoleic	18:2	21	59,6	4,2	15,3	10	10	53,2	46,4	2,3
Linolenic	18:3	8,8	1,2	0,3	56,6	0,6	0,4	7,8	1	3,7
Arachidic	20:0	0,7	0,4	0	0	0,9	0,3	0,3	0	0,2
Gadoleic	20:1	1	0	0	0	0	0	0	0	0,4
Eicosadienoico	20:2	0	0	0,3	0	0	0	0	0	0
Behenic	22:0	0,3	0,1	0	0	0	0,1	0,1	0	0,3
Erucic	22:1	0,7	0	0	0	0	0	0	0	0,1
Lignoceric	24:0	0,2	0	0	0	0	0	0	0	0
Ricinoleic	18:1	0	0	89,5	0	0	0	0	0	0
Dihydroxystearic	18:0	0	0	0,7	0	0	0	0	0	0
DB/Triglyceride		3,9	4,5	3,1	6,6	2,8	1,8	4,6	4,5	3

[a] C, number of carbon atoms; BD, number of C=C doble bonds.

Common fatty acids can be completely saturated but they can also present several double bonds. Besides, there is a number of naturally occurring fatty acids containing other functional groups such as hydroxyls or epoxides. The structures of some frequently studied fatty acids in polymer chemistry [20] are depicted in Figure 5.

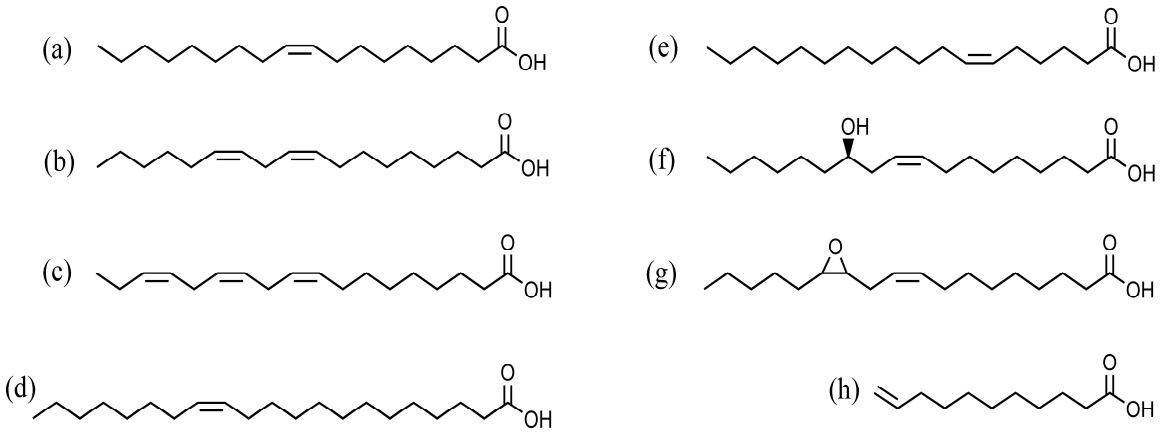

Figure 5. Fatty acids commonly used in polymer chemistry: (a) oleic acid, (b) linoleic acid, (c) linolenic acid, (d) erucic acid, (e) petroselinic acid, (f) ricinoleic acid, (g) vernolic acid, (h) 10-undecenoic acid.

Is possible to found up to 90 % of the same fatty acid fraction in some varieties of oils, as oleic and ricinoleic acids in high oleic sunflower and castor oils respectively. Undecenoic acid (Figure 5 h) can be obtained by heating ricinoleic acid under vacuum pyrolysis. Several mechanisms, including a MacLafferty-type rearrangement[21] (Scheme 1) and free-radical mechanism,[22] have been proposed for the transformation of ricinoleic acid into undecenoic acid and heptaldehyde. Undecenoic acid, is a C11 fatty acid with terminal carbon-carbon double bond that, owing to its bifunctional nature, has many possibilities to develop sustainable applications.

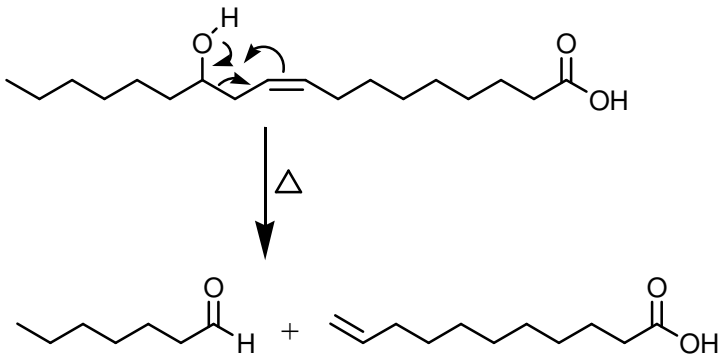

Scheme 1. MacLafferty-type rearrangement of ricinoleic acid to undecenoic acid and heptaldehyde.

[21] M. Van der Steen, C.V. Stevens, Chem. Sus. Chem: 2, 692-713, 2009.
[22] G. Das, R.K. Trivedi, A.K. Vasishtha, J. Am. Oil Chem. Soc: 66, 938- 941, 1989.

Triglycerides are highly functionalized molecules, and, therefore, have been used in the synthesis of cross-linked polymers via two main approaches. The first one takes advantage of the naturally occurring functional groups present in triglycerides, such as internal double bonds, alcohols, or epoxides, which can be polymerized using different methods. The second strategy depends on chemical modifications prior to polymerization. This approach solves the drawback of the low reactivity of natural triglycerides (which usually only contain double bonds) by introducing easily polymerizable functional groups, and thus widens the synthetic possibilities.[20, 23] The hydrolysis of triglycerides provides glycerol and a mixture of fatty acids. Glycerol is a widely used building block in polymer science finding application in the synthesis of polyurethanes, polyesters, or telomers. [24] On the other hand, fatty acids have been used for a long time by polymer scientists for the development of polymeric structures, [25] both directly (e.g. Scheme 2) and as building blocks for the synthesis of interesting monomers for polymer chemistry (e.g. Scheme 3).[26-28]

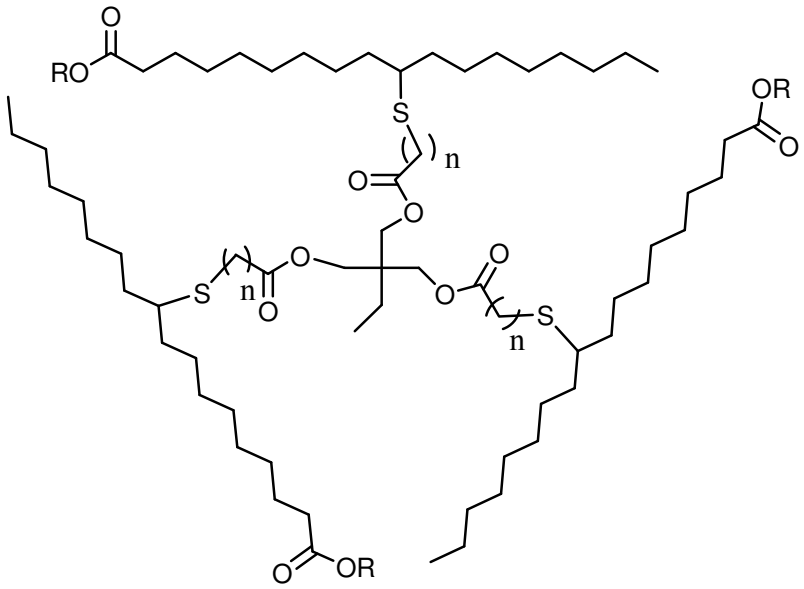

Scheme 2. Fatty ester trimerization by thiol-ene coupling.

[23] F.S. Guner, Y. Yagci, A.T. Erciyes, Prog. Polym. Sci: 31, 633-670, 2006.
[24] F. Jerome,Y. Pouilloux, J. Barrault, ChemSusChem: 1, 586-613, 2008.
[25] M.A.R. Meier, J.O. Metzger ,U.S. Schubert. Chem Soc Rev: 36, 1788-802, 2007.
[26] G. Lligadas, J.C. Ronda, M. Galia, V. Cádiz, Polymers: 2, 440-453, 2010.
[27] M. Desroches, M. Escouvois, R. Auvergne, S. Caillol, B. Boutevin, Polym. Rev : 52, 38-79, 2012.
[28] C. Lluch , J.C. Ronda, M. Galia, G. Lligadas, V. Cadiz. Biomacromolecules: 11, 1646-53, 2010.

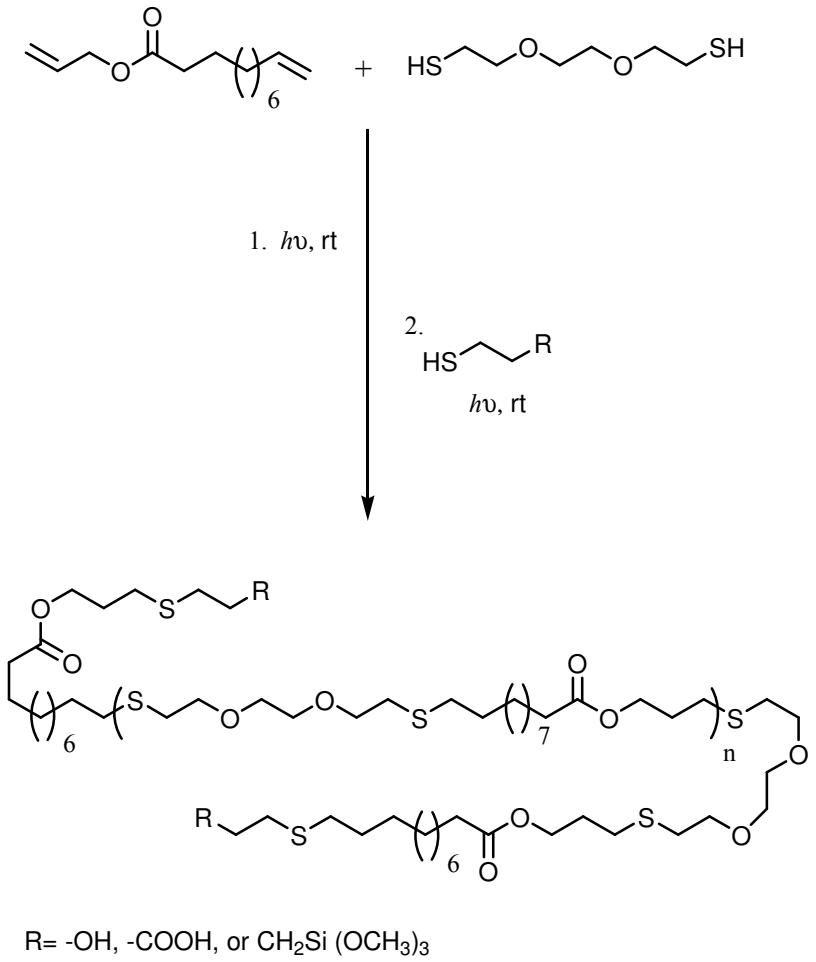

Scheme 3. Synthesis of telechelic monomers through a one-pot two thiol–ene click reactions from a fatty acid based monomer.

Several functionalization reactions of fatty acids or esters, some of them being advantageously solvent-free, are also reported in the reviewing papers of Schneider, [18, 29] or Metzger et al.,[30] and they are summarized on Scheme 4.

[29] M.P. Schneider, J. Sci. Food Agric: 86, 1769-1780, 2006.
[30] J.O. Metzger, Chemosphere: 43, 83-87, 2001.

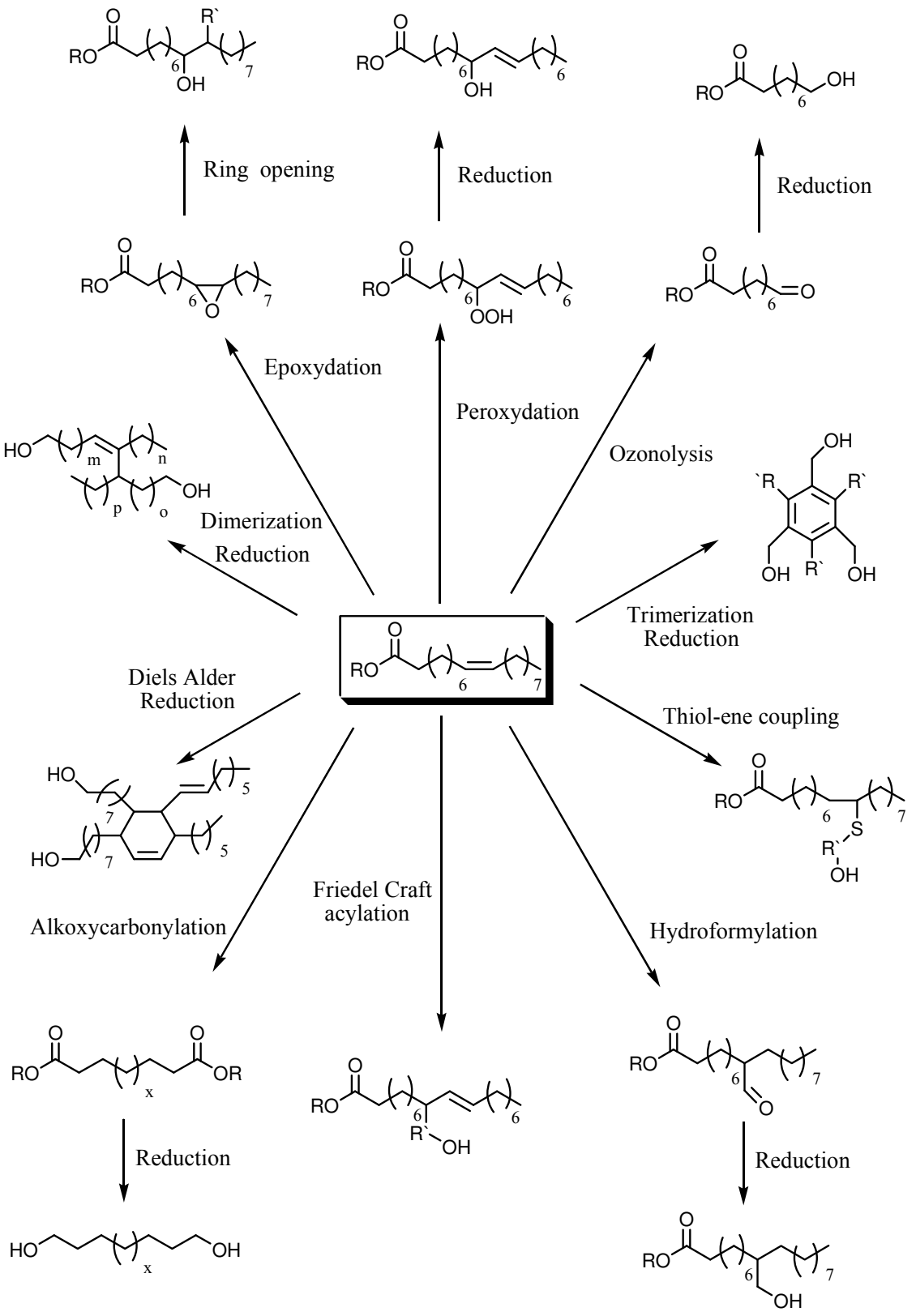

Scheme 4 . Modifications for the synthesis of monomers from fatty acids or esters.

SCOPE AND OBJECTIVES

Scope and Objectives

The emergence of the click chemistry concept greatly facilitates the synthesis of polymers following sustainability criteria. The thiol-ene coupling (TEC) and thiol-yne coupling (TYC) click chemistry of fatty acids obtained from plant oils is a promising addition to ease the preparation of fatty acid-derived monomers for polyurethanes synthesis. The main objective of this thesis was to develop new biobased polyurethanes from fatty acids derivatives as renewable resources using click chemistry. Moreover, as fatty acid-based polymers offer the advantage of being similar to biological macromolecules, for which the biological environment is prepared to recognize and deal with metabolically, we have also studied different strategies to enhance the biocompatibility of the synthesized polyurethanes in order to obtain new materials that could eventually be suitable for biomedical applications.

The work is presented in two parts. The first part collects the introduction, results and discussion which describe the preparation, characterization and properties of thermoplastic and thermosetting polyurethanes from fatty acid-based polyols, obtained by TEC and TYC click chemistry (chapters one to three). Oleic and 10-undecenoic acids derived from sunflower oil and castor oil, respectively, are used as starting reagents.

The second part (chapters four to six) of this thesis is focused on the enhancement of polyurethanes biocompatibility through bioactive molecules functionalization strategies, for tissue engineering purposes. Three approaches have been investigated:

(1) Blends of polyurethanes and gelatin
(2) Covalent surface modification of polyurethanes with collagen by plasma treatment.
(3) Ionic surface modification of polyurethanes with chondroitin sulfate by aminolysis treatment.

FIRST PART

Synthesis of polyurethanes via click chemistry

CLICK CHEMISTRY IN POLYMER SCIENCE

Thiol addition to double bonds (see Scheme 1) defined as thiol-ene click coupling, has emerged rencently as a powerful tool for synthetic purposes.[1,2] Click chemistry concept, introduced by Sharpless and colleagues in 2001, describes chemistry tailored to generates substances quickly and reliably by joining small units together.[3] Such a coupling reaction should meet several criteria: it should be modular, high-yielding, generate only harmless side products, it should be carried out under mild reaction conditions and it can be performance at ambient conditions with readily available starting materials.[4] Several thiol-based reactions (Scheme 1) have many of the aspects of click chemistry, namely they are rapid, proceed to high conversions under mild reaction conditions, react either neat or in benign solvents, and generally lead to one product that requires either little or no purification. This behavior allows for taking a series of thiols and creating/functionalizing/modifying an exceptional range of molecules and materials with physical, mechanical and chemical properties that can be altered to meet an extensive scope of requirements. [2]

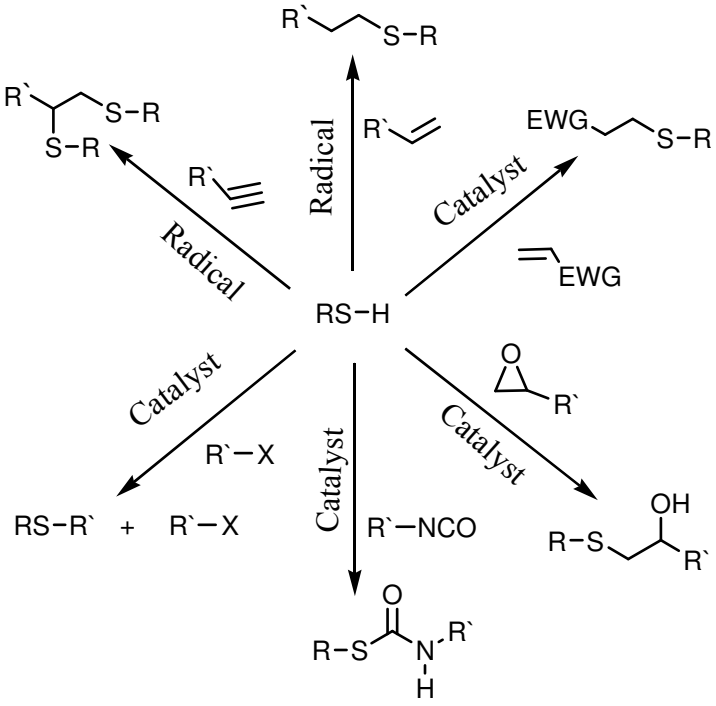

Scheme 1. Toolbox of thiol-click reactions. EWG = electron withdrawing group. X = Br, I.

[1] C.E. Hoyle, C.N. Bowman, Angew. Chem.Int. Ed: 49, 1540-1573, 2010.
[2] C.E. Hoyle,A.B. Lowe, C.N. Bowman, Chem. Soc. Rev: 39, 1355-1387, 2010.
[3] H.C. Kolb, M.G. Finn, K.B. Sharpless, Angew. Chem. Int. Ed: 40, 2004-2021, 2001.
[4] M.V. Dijk, D.T.S. Rijkers, R.M.J. Liskamp, C.F. van Nostrum, W.E. Hennink, Bioconjugate Chem: 20, 2001-2016, 2009.

Thiol-ene coupling (TEC) reactions have been used to synthesize polymers such as dendrimers and stars,[5,6] as well as to add functionality to a macromolecule.[7] The photochemicallly/ thermally-induced version of this reaction is known to proceded by a radical mechanism to give an anti-Markovnikov-type thioether (Scheme 2). [8] The click status of this reaction is supported by it being highly efficient, tolerance to many different reaction conditions/solvents, clearly defined reaction pathways/products, facile synthetic strategies from a range of easily obtained starting materials, as well as for being compatible with water and oxygen.[9]

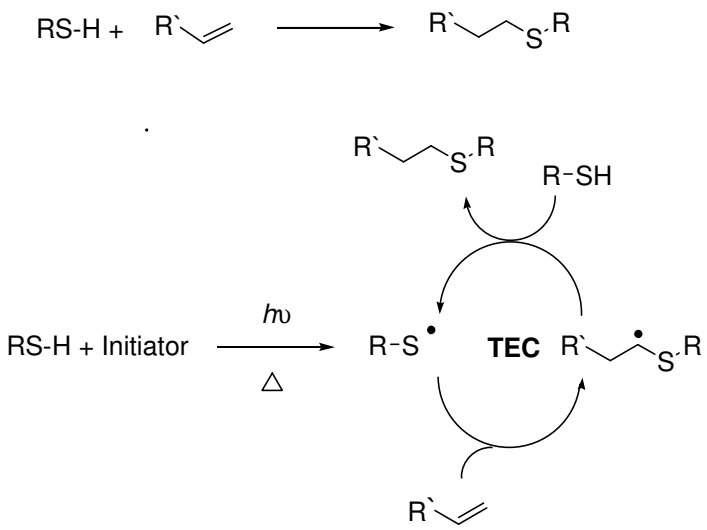

Scheme 2. The thiol-ene coupling (TEC) reaction.

In contrast, the thiol-yne radical coupling (TYC) has received much less interest.[10] The radical-mediated addition of a thiol to an yne has been known since the first half of the last century.[11] As with the TEC, the thiol-yne addition, in general proceeds rapidly under a variety of experimental conditions selectively yielding the (I) mono- or (II) bis-addition products (Scheme 3).

[5] K.L. Killops, L.M. Campos, C.J. Hawker, J. Am. Chem. Soc: 130, 5062-5064, 2008.
[6] J.W. Chan, B. Yu, C.E. Hoyle, A.B. Lowe, Chem. Commun: 4959-4961, 2008.
[7] M.A. Gauthier, M.I. Gibson, H.A. Klok, Angew. Chem., Int. Ed: 48, 48-58, 2009.
[8] a) F.R. Mayo, C. Walling, Chem. Rev: 27, 351-412, 1940, b) K. Griesbaum, Angew. Chem: 82, 276-290, 1970, c) S.Z. Zard, Radical Reactions in Organic Synthesis, Oxford University Press, Oxford, 2003.
[9] a) A. Dondoni, Angew. Chem. Int. Ed: 47, 8995-8997, 2008, b) Z. Jin, B. Xu, G.B. Hammond, Eur. J. Org. Chem: 1, 168-173, 2010.
[10] B.D. Fairbanks, T.F. Scott, C. J. Kloxin, K.S. Anseth, C.N. Bowman,Macromolecules: 42, 211-217, 2009.
[11] a) H. Bader, L.C. Cross, I. Heilbron, E.R.H. Jones, Chem. Soc. J: 1, 619-623, 1949, b) J.C. Sauer, J. Am. Chem. Soc: 79, 5314-5315, 1957.

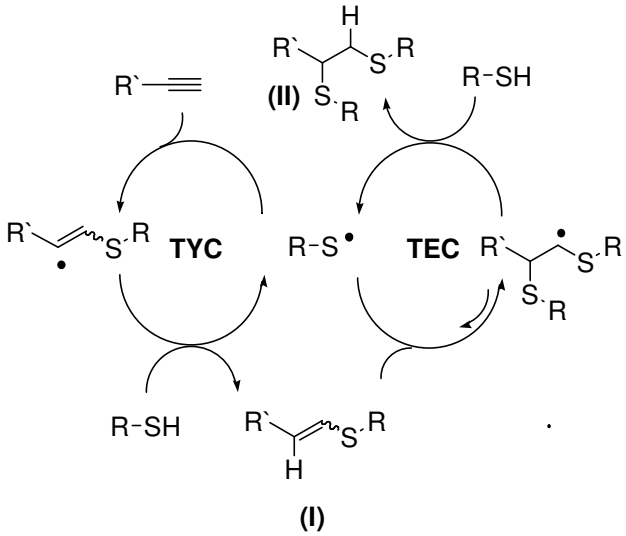

Scheme 3. Sequential addition and hydrogen abstraction steps of primary alkyne and the subsequent vinyl sulfide during a thiol−yne coupling.

In the last two years, TYC reactions have also become very popular and useful synthetic method in polymer science for the synthesis of dendrimers, hyperbranched polymers, and gels as well as postfuntionalization of readily synthesized polymers with proper funtional groups. Moreover, this efficient functionalization reaction was also applied for microprinting, the synthesis of lipid mimetics, and reactions on solid surfaces.[12]

Recently, click chemistry has also been applied for synthesis of polymers with biomedical applications.[4] Polymers can be applied in drug delivery system, as scaffolds for tissue engineering and repair, and as novel biomaterials. These applications have led to an increasing demand of well-defined polymers with tailorable properties. The emergence of the click chemistry concept greatly facilitated the synthesis of these polymers. The TEC and TYC click chemistry of fatty acids obtained from plant oils is a promising addition to ease the preparation of fatty acid-derived monomers for polyurethanes with potential biomedical purposes.

[12] a) D. Konkolewicz, C.K. Poon, A. Gray-Wealeb, S. Perrier, Chem. Commun: 47, 239-241, 2011, b) B.D. Fairbanks, E.A. Sims, S.K. Anseth, C.N. Bowman, Macromolecules: 43, 4113-4119, 2010, c) J.W. Chan, J. Shin, C.E. Hoyle, C.N. Bowman, A.B. Lowe, Macromolecules: 43, 4937-4119, 2010, d) A.B. Lowe, C.E. Hoyle, C.N. Bowman, J. Mater. Chem: 20, 4745-4750, 2010, e) M. Minozzi, A. Monesi, D. Nanni, P. Spagnolo, N. Marchetti, A. Massi, J. Org. Chem: 76, 450-459, 2011.

VEGETABLES OILS AND FATTY ACIDS-DERIVED POLYURETHANES

Basic chemistry of polyurethanes

Polyurethane (PU) is the general name of a family of synthetic polymers that contain the urethane moiety in their chemical repeat structure (Figure 1). PUs, having a relatively short history, of slightly more than 70 years, became one of the most dynamic groups of polymers, exhibiting versatile properties suitable for use in practically all the fields of polymer applications: foams, elastomers, thermoplastics, thermorigids, adhesives, coatings, sealants, fibers and so on. With a global production of 14Mt in 2006, PUs are the 6th most widely used polymer. Additionally, they are used in some specialty applications such as biomedical devices.

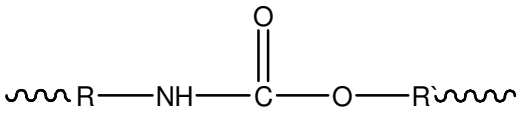

Figure 1. Urethane linkage

PUs are obtained by the reaction of an polyol and a polyisocyanate. Depending on the funtionality of the reactants, one can obtain linear or crosslinked polymers. Because this is a nucleophilic addition reaction, it is catalyzed by basic compounds such as tertiary amines and by metal compounds such as organotin. Urethane formation (Scheme 4 a) is actually an equilibrium reaction; the presence of catalyst therefore also increases the rate of the back reaction at high temperatures. Isocyanate not only reacts with primary amine (Scheme 4 b), but can also react with secondary amine such as the N-H in urethane or urea groups, even though the rate of reaction is much lower compared with that of the primary amine. The nucleophilic addition nature of the reaction with the secondary amine remains the same and so the chemical structure of the products (allophanate and biuret, with respect to the reaction with urethane and urea can be easily predicted (Scheme 4 c and d),. Allophanate or biuret formation leads to branching and crosslinking and is favored when excessive isocyanate is present.

In addition to the above two basic reactions, the reaction of water with isocyanate must also be mentioned (Scheme 4 e). Because isocyanate is so active, it reacts with active or acidic hydrogen almost instantly. This reaction with water has

become the most important side reaction that should be avoided or minimized, except if a foam or high urea content is desired. The amine groups formed will further react with remaining isocyanate to produce urea groups. The carbon dioxide formed can be used to produce a PU foam. The net effect of this reaction on the ratio of reactants is the consumption of one unit of isocyanate and the formation of one amine group. Further reaction of the amine group with an isocyanate leads to the formation of an urea.This reaction has been exploited in the synthesis of polyureas. Isocyanates also react with carboxylic acids to yield an amide group and CO_2 (Scheme 4 f) and with other isocyanates to yield dimers or trimers (Scheme 4 g).

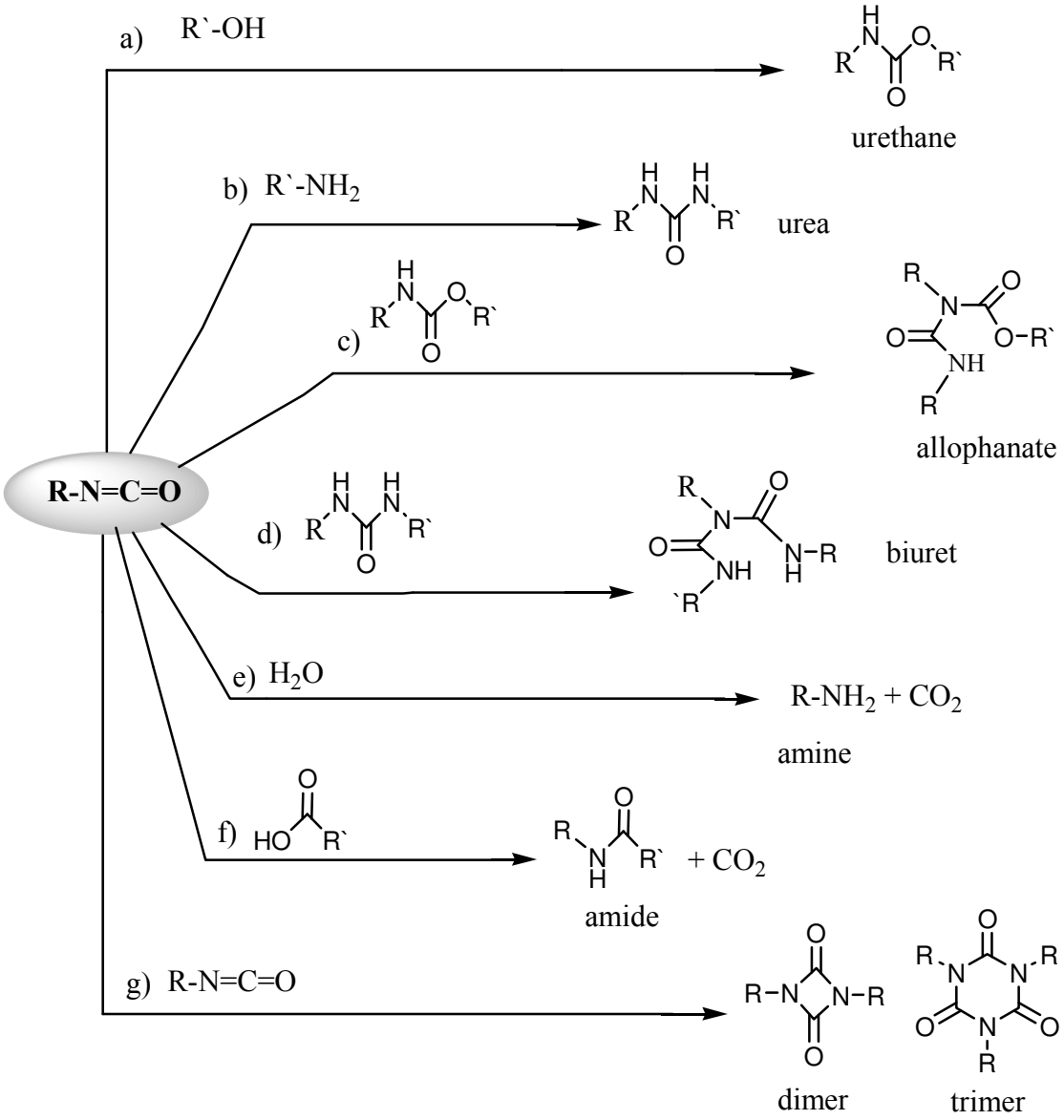

Scheme 4. Isocyanates side reactions involved in the synthesis of PUs.

The most important isocyanates used in PU manufacture are diisocyanates, containing two isocyanate groups per molecule (Figure 2) . These two functional groups work to join together by chemical reaction with two other molecules (polyol) to form a linear chain. Diisocyanate can be either aromatic or aliphatic. When the functionality is greater than two, a branch site is formed between the molecules, leading to network or crosslink formation.Whereas the diisocyanates used are usually commercial, polyols offer a wide range of possibilities; therefore, the properties of the final material strongly depend on the polyol.

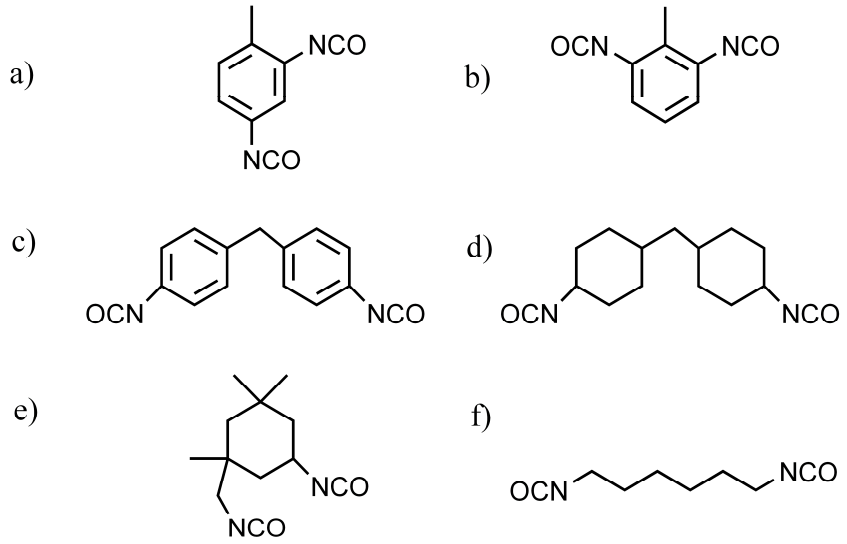

Figure 2. Typical diisocyanates used in the synthesis of PUs: a) 2,4-toluene diisocyanate (2,4-TDI), b) 2,6-toluene diisocyanate (2,6-TDI) c) 4,4`-methylene-bis(phenylisocyanate) (MDI), d) 4,4`-dicyclohexylmethane diisocyanate (DMDI), e) isophorone diisocyanate (IPDI), f) hexamethylene diisocyanate (HDI).

Such diversity of applications originates from the tailorable chemistry of polyurethanes, the chemical composition of polyurethanes can be tailored, by choosing different raw materials and processing conditions, to accommodate many specific requirements. All these raw materials come from petroleum but recently, chemical industry has paid intensive interest to the production of biobased polyols, mainly synthesized from vegetable oils.

Vegetable oil-based polyols

Most of polyols currently used for PUs synthesis are polyether polyols (75%), resulting from the reaction between a "starter" polyol and an alkylene oxide, both petrobased. Other polyols used for PUs synthesis are polyesters polyols (25%), obtained by step growth polycondensation between dicarboxylic acid and polyol in excess.[13] A first approach to increase the renewable content of polyurethanes consists in replacing the "starter" polyol by a biobased polyol from saccharides (sorbitol, sucrose) for the synthesis of partially biobased polyether polyols. However, it results in low renewable content polyurethanes. Therefore it is more interesting to work on prepolymers that account for higher percentage of renewable content. Polyether polyol could also be obtained by polycondensation of propane-1,3-diol coming from glycerin. Furthermore, biobased polyester polyols generally result from condensation of biobased dicarboxylic acids such as adipic or succinic acid with biobased polyols (propane-1,3-diol). Finally, another approach to obtain biobased polyols consists in the use of natural oils (vegetable or animal) i.e. the most abundant and cheapest renewable organic resources.

a) Epoxidation /oxirane ring opening

Most vegetable oil-based polyols are produced by the epoxidation of vegetable oils, followed by oxirane ring opening with proton donors (shown in A, Scheme 5). Vegetable oils are typically epoxidized by generating a peracid in situ from hydrogen peroxide and acetic or formic acid. This method results in sufficient yields of epoxidized oil (75–90%) and is used in most commercial processes. Recently, other epoxidation procedures have been introduced to further increase the yield of epoxy groups leading to higher functionality polyols and, also of current interest is the chemo-enzymatic epoxidation of vegetable oils, which is advantageous as the undesirable ring opening of the epoxide is completely suppressed.[14]

[13] Ionescu, M. Chemistry and technology of polyols for polyurethanes; Rapra Technology Limited. 2005.
[14] a) S.Z. Erhan, Industrial Uses of Vegetable Oils, AOCS Publishing, Urbana, 2005; b) U. Biermann, W. Friedt, S. Lang, W. Luhs, G. Machmuller, J. O. Metzger, M. Rusch gen. Klaas, H.J. Schafer, M.P. Schneider, Angew. Chem: 112, 2292-2310, 2000.

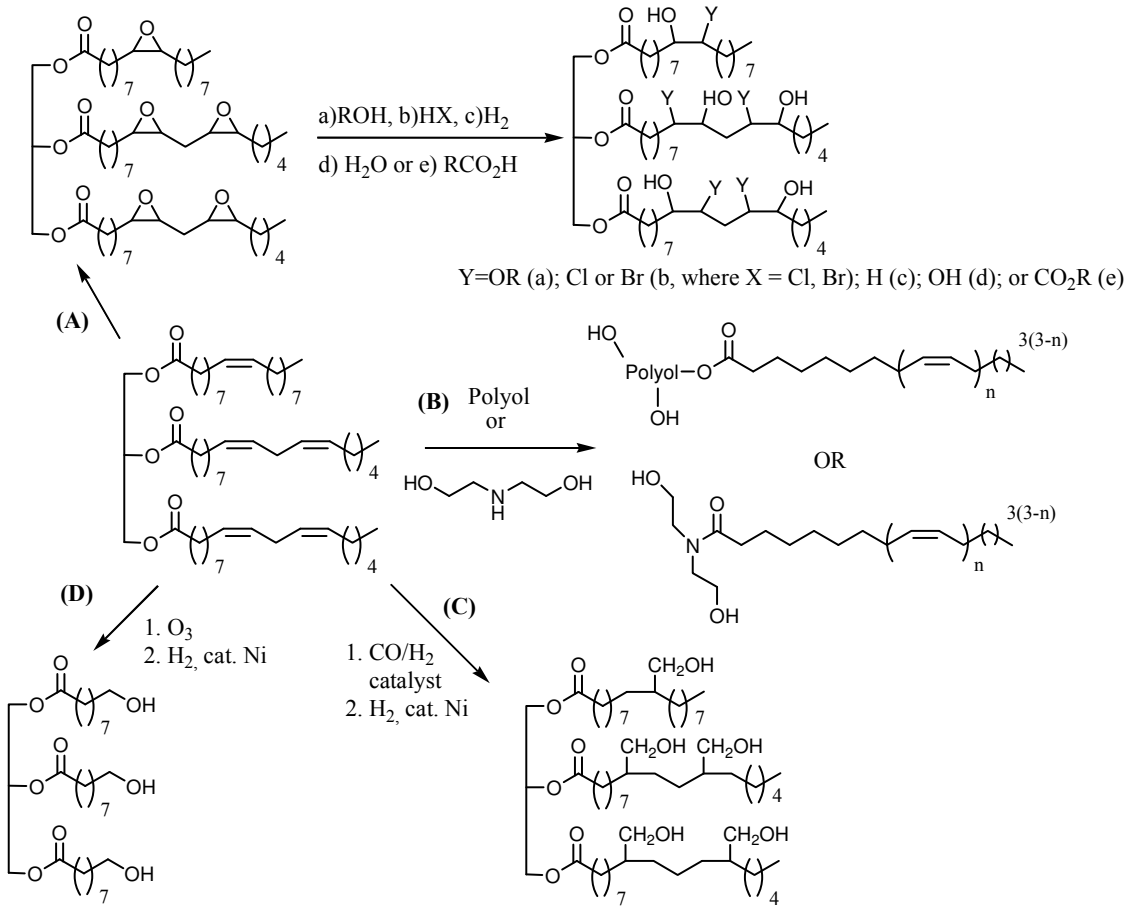

Scheme 5. The most common routes to vegetable oil-based polyols.

b) Transesterification/amidation

Two other common routes to synthesize vegetable oil-based polyols involve transesterification of vegetable oils with various polyols, or amidation, typically with diethanolamine, of vegetable oils (shown in B, Scheme 5). The most frequently used polyol is glycerol. The transesterification of vegetable oils with an excess of glycerol leads to the formation of monoglycerides in a single step and, therefore, has advantages economically.[15] Typically, the transesterification reaction is catalyzed by base, but enzymes have also been used as catalysts.[16] Interestingly, certain lipases can target the 1,3-positions of the glycerol backbone to give polyols containing only primary alcohols. Although enzymatic catalysts are appealing environmentally, their extremely high cost limits their use commercially.

[15] a) C. Lyon, V. Garrett, L. Goldblatt, J. Am. Oil Chem. Soc: 38, 262, 1961; b) N. Karak, R. Konwarh, B. Voit, Macromol. Mater. Eng: 295, 159-169, 2010.
[16] a) M.D. Bhabhe, V.D. Athawale, J. Appl. Polym. Sci: 69, 1451-1458, 1998, b) V.D. Athawale, K.R. Joshi, Eur. Coat. J: 6, 42-46, 2000. c) P.P. Kiatsimkul, G.J. Suppes, W.R. Sutterlin, Ind. Crops. Prod: 25, 202-209, 2007.

c) Hydroformylation/reduction

The hydroformylation/reduction of vegetable oils involves the addition of hydroxymethyl groups to the carbon-carbon double bonds in the fatty acid chains using a two-step procedure (shown in C, Scheme 5). In the first step, the vegetable oil is treated with syngas (a mixture of CO and H_2) in the presence of a catalyst to give aldehydes, which are then reduced with H_2 in the second step to yield hydroxyl groups. The most commonly used catalysts are simple cobalt carbonyl complexes, cobalt carbonyl complexes modified by tertiary phosphine/phosphite ligands, and tertiary phosphine/phosphite rhodium carbonyl species.[14] With hydroformylation/reduction, the hydroxyl functionality of the vegetable oil-based polyol is dependent on the number of carbon-carbon double bonds in the vegetable oil. Because of this, soybean oil is most commonly used as the starting material, but other oils, including safflower and linseed oils, have also been used.[17-20]

d) Ozonolysis/reduction

The ozonolysis/reduction of vegetable oils results in terminal primary hydroxyl groups (shown in D, Scheme 5). This method involves the efficient cleavage of the carbon-carbon double bonds present in the fatty acid chains to give, under the right conditions, shorter chain alcohols. In the first step, an ozonide is formed by treating a vegetable oil with ozone, which is then reduced by zinc to give an aldehyde, and further reduced with Raney nickel to the corresponding primary alcohol. The ozonide can also be treated with sodium borohydride to afford the primary alcohol directly. The ozonolysis procedure essentially removes half of each fatty acid chain, which is advantageous, because these dangling chains are not incorporated into the polyurethane and act as plasticizers to weaken the materials.

While the epoxidation/oxirane ring opening and hydroformylation/reduction methods can potentially give polyols with high functionality, the vegetable oil-based polyols obtained from ozonolysis/reduction have at most three hydroxyl groups. With

[17] a) T. Khoe, F. Otey, E. Frankel, J. Am. Oil Chem. Soc: 49, 615, 1972, b) A. Kaushik, P. Singh, Int. J. Polym. Anal. Charact: 10, 373-386, 2005.
[18] Z.S. Petrovic, I. Cvetkovic, D. Hong, X.M. Wan, W. Zhang, T.W. Abraham, J. Malsam, Eur. J. Lipid. Sci. Technol: 112, 97-102, 2010.
[19] A. Guo, D. Demydov, W. Zhang, Z.S. Petrovic, J. Polym. Environ: 10, 49-52, 2002.
[20] a) P. Kandanarachchi, A. Guo, Z.S. Petrovic, J. Mol. Catal. A: 184, 65-71 2002, b) Z.S. Petrovic, A. Guo, I. Javni, I. Cvetkovic, D.P. Hong, Polym. Int: 57, 275-281, 2008.

ozonolysis/reduction, the amount of saturated fatty acids contained in the vegetable oil is more important than the total number of carbon-carbon double bonds in the triglyceride.[21]

Fatty acid-based polyols

Fatty acids which can be easily isolated from oils are also attractive platform chemicals for polyurethane industry since they can be used as building blocks for the synthesis of polyols.[22] Fatty ester-based polyether polyols have been prepared and envisioned as a potential replacement for the commonly used petroleum-based polyether polyols, which are important building blocks for polyurethane applications.[23] As the structure in Scheme 6 indicates, the polyols can be obtained by the fluoroantimonic acid-catalyzed oligomerization of epoxidized methyl oleate, followed by controlled reduction of the ester groups to hydroxyl groups using lithium aluminum hydride.

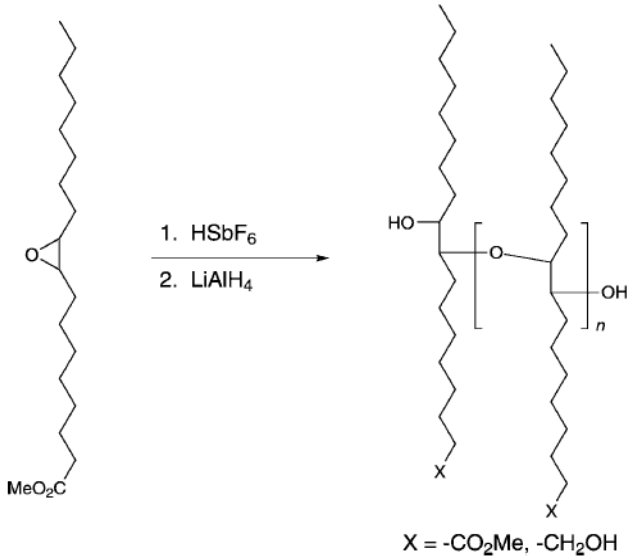

Scheme 6. Preparation of fatty ester-based polyether polyols.

Recently, ricinoleic and oleic acids were used as precursors for AB monomers synthesis leading to polyurethanes synthesis by direct polycondensation [24] (Scheme 7). This multi-step process goes through an azidation reaction with NaN_3 at 0°C for 1h. The

[21] Z.S. Petrovic, Polym. Rev: 48, 109-155, 2008
[22] G. Lligadas, J.C. Ronda, M. Galia, V. Cádiz, Biomacromolecules: 11, 2825-2835, 2010.
[23] a) G. Lligadas, J.C. Ronda, M. Galia, U. Biermann, J.O. Metzger, J. Polym. Sci. Poly. Chem: 44, 634-645, 2006, b) G. Lligadas, J.C. Ronda, M. Galia, V. Cádiz, Biomacromolecules: 8, 686-692, 2007.
[24] D.V. Palaskar, A. Boyer, E. Cloutet, C. Alfos, H. Cramail, Biomacromolecules: 11, 1202-1211. 2010.

next step consists of either a self condensation at 80°C for 24h, or by a transurethane reaction catalyzed by $Ti(OBu)_4$ at 130°C for 6h.

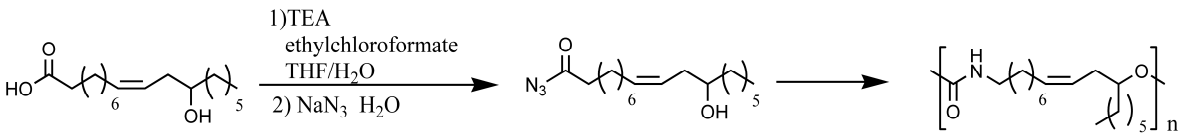

Scheme 7. Synthesis of AB monomer for polyurethanes synthesis by direct polycondensation.

Envisioning thermoplastic polyurethane applications, two linear diols, a saturated short-chain diol and an unsaturated long-chain diol, have been prepared from oleic acid.[25] The synthesis of the short-chain diol involves ozonolysis of oleic acid to give a saturated diacid, which is then reduced with lithium aluminum hydride to give the saturated short-chain diol. The unsaturated diol is formed by the self metathesis of oleic acid using Grubbs catalyst to give an unsaturated diacid, followed by reduction to the diol. This diol was reacted with different diisocyanates to obtain thermoplastic polyurethanes. It is noteworthy, that the polyurethane synthesized with a diisocyanate based in fatty acid presented similar properties to those from commercial ones.

The unique aromatic polyols are prepared through the palladium-catalyzed cyclotrimerization of alkyne fatty esters, followed by reduction of the ester groups with lithium aluminum hydride to give primary alcohols. The alkyne fatty esters are obtained from 10-undecenoic acid and oleic acid by bromination, dehybromination, and esterification.[26]

Fatty acid can dimerize and further be reduced into fatty diol dimers in order to confer high hydrophobic, stretching and chemical stability properties to polyurethane synthesized. Dimerization of fatty acids is a complex reaction realized at high temperature. The catalysts used are homogeneous such as ionic salts of alkali metals or heterogeneous (most currently used) such as clays (montmorillonite or bentonite) or aluminosilicates.[27] The synthesized dimers are reduced to yield fatty diols dimers (see Scheme 8).

[25] L. Hojabri, X. Kong and S.S. Narine, Biomacromolecules: 11, 911-918, 2010.
[26] G. Lligadas, J.C. Ronda, M. Galia, V. Cadiz, Biomacromolecules: 8, 1858-1864, 2007.
[27] P. Tolvanen, P. Maki-Arvela, N. Kumar, K. Eranen, R. Sjoholm, J. Hemming, B. Holmbom, T. Salmi, D.Y. Murzin, Appl. Catal. A: General: 330, 1-11, 2007.

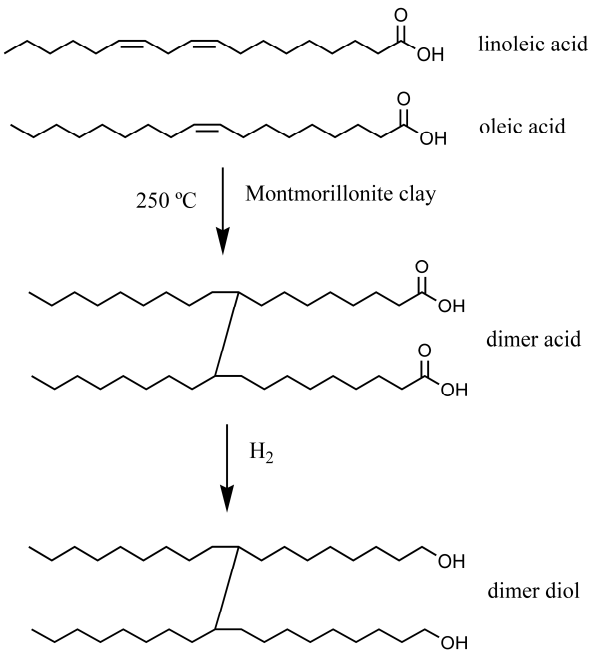

Scheme 8. Preparation and structure of dimeric fatty acid diols.

In the literature, limited attention has been paid to the preparation of long-chain or oligomeric diols with funtionality 2 (requirement for thermoplastic polyurethane formulations) using fatty acids as starting materials.[22] Dimerization of oleic acid and linoleic acids (Scheme 8), producing a complex mixture known as dimer acid, and consecutive reduction of carboxylate groups is a classical procedure for the synthesis of long-chain diol known as dimer diol. This methodology was originally introduced in the 1950s by General Mills Chemicals and Emery (currently, Cognis Corp.).[28] Dimer diol, dimer diol oligoethers and dimer diol oligocarbonates are comercially available. Fatty acid dimer based polymers have been thoroughly investigated for their biocompatibility, because, a natural fatty acid is extensively metabolized in the body and excreted mostly as carbon dioxide.[29]

The double bonds of fatty acids are electron-rich, which allows radical addition of various molecules. Thus, thiol-ene (TEC) and thiol-yne (TYC) coupling is an interesting functionalization method to prepare long-chain or oligomeric fatty acids-derived diols and triols for thermoplastic and thermostable polyurethane formulations.[30]

[28] a) E.M. Fisher, U.S. Patent 3, 157,681, 1964, b) L.D. Myers, C. Goebel, F.O. Barreto, U.S. Patent 2,955,121, 1960.
[29] J.P. Jain, M. Sokolsky, N. Kumar, A.J. Domb, Polym. Rev: 48, 156-191, 2008.
[30] G. Lligadas, J.C. Ronda, M. Galia, V. Cádiz, Polymers: 2, 440-453, 2010.

CHAPTER I

A green approach toward oleic and undecylenic acids-derived polyurethanes

A Green Approach toward Oleic and Undecylenic Acids-Derived Polyurethanes

R. J. González-Paz, C. Lluch, G. Lligadas, J. C. Ronda, M. Galià, V. Cádiz.
Departament de Química Analítica i Química Orgànica.
Universitat Rovira i Virgili.
Campus Sescelades.
c/Marcel.lí Domingo s/n.
43007 Tarragona. Spain.

Abstract

Naturally-occurring oleic and undecylenic acids were used as raw material for the synthesis of novel polyurethanes. The application of environmentally friendly thiol-ene additions to 10-undecenoate and oleate derivatives, was studied with the goal to obtaining renewable diols. The resulting monomers were then polymerized with 4,4′-methylenebis (phenylisocyanate), in DMF solution using tin (II) 2-ethylhexanoate as catalyst, to produce the corresponding thermoplastic polyurethanes (TPUs). Also, ultrasound irradiation has been tested to improve the polyurethane synthesis. Under these conditions TPUs were obtained in high yields (80-99%) with weight-average molecular weights in the 36-83 KDa range. The chemical structures of polyurethanes were assessed by FTIR and NMR spectroscopy. The thermal and mechanical properties of the synthesized TPUs have been studied and show a clear dependence on the structure of the parent diol. MTT test was carried out to asses the potential citotoxicitity of the prepared polyurethanes, indicating no cytotoxic response.

Journal of Polymer Science: Part A: Polymer Chemistry: 49, 2407–2416, 2011

Introduction

To date, a wide range of industrial materials such as solvents, fuels, synthetic fibers, and chemical products are being manufactured from petroleum resources. However, rapid depletion of fossil and petroleum resources is encouraging current and future chemists to orient their research toward designing safer chemicals, products, and processes from renewable feedstock with an increased awareness of environmental and industrial impact.[1]

Nature offers an abundance of opportunities for designing novel monomers and shaping structural and functional polymers in its wide variety of raw materials.[2] Presently their relative use for monomers and polymers synthesis compared to petrochemicals is small. Natural oils, such as vegetable oils provide interesting feedstock -triglyceride fatty acids- that beyond their use in food allow additional chemistry that yields either opportunities for replacing petrochemicals or may be directly used to synthesize bio-inspired materials.[3-6] Fatty acids have been used in various classes of biodegradable polymers but have been largely confined to polyanhydrides, polyesters, and poly(ester-anhydrides). In these polymers, fatty acid monomers obtained from natural sources were incorporated in the polymer backbone to obtain the desired properties.[7]

Vegetable oils are becoming extremely important as renewable resources for the preparation of polyols required for the polyurethane industry.[8] Polyols from natural oils, such as soybean, castor and palm oils are increasingly being viewed by industry as a viable alternative to hydrocarbon-based feedstocks. In sustainable materials, polyurethanes are currently prepared starting from renewable polyols, while the second partner, isocyanate, is mainly made from petroleum resources.[9,10] There is limited literature available concerning the synthesis of isocyanate compounds based on plant oils. Kusefoglu and Çayli reported two synthetic routes for the functionalization of soybean oil with isocyanate moieties[11] and both plant-based isocyanates were suitable for polyurethane preparation. On the other hand, recently Narine et al. have developed methodologies for the synthesis of isocyanates and polyols from vegetable oils and corresponding biobased polyurethanes entirely from lipid feedstock.[12] Moreover, concerning nonisocyanate methods for the preparation of polyurethanes derived from

plat oils, two methodologies have been described: the reaction of cyclic carbonates with amines[13] and the more recent self-condensation approach of AB-type monomers.[14]

Classically the reaction between a thiol and a double bond has received significant attention as candidate for many applications including coatings, adhesives, dental materials, and imprinting lithography. Resurgence over the past decades has occurred in response to the many benefits thiol-ene coupling presents for polymer synthesis: tolerance to many different reaction conditions/solvents, clearly defined reaction pathways/products, and facile synthetic strategies from a range of easily obtained starting materials.[15] Thus, thiol-ene chemistry has recently emerged as a powerful tool for synthetic chemistry and polymer functionalization that has the potential to fall within the realm of click chemistry.[16-18] The thiol-ene coupling makes use of the high nucleophilicity of the sulfhydryl moiety and proceeds under physiological conditions. The formed tioether linkage is very stable under physiological conditions and resists a strong basic or acidic environment and is also stable toward reducing agents; however, it is susceptible toward oxidizing agents. The robust nature of thiol-ene chemistry allows for the preparation of well-defined materials with few structural limitations and synthetic requirements.[19] While both heat and light have been used to generate radicals that initiate the thiol-ene radical chain process, the use of light has enormous advantages for small molecule synthesis, surface and polymer modification, and polymerization reactions. A vast array of work has been performed in an effort to understand and implement radical-mediated thiol-ene reactions, primarily focusing on the photo-initiated reactions. This large body of literature is detailed in very recent review articles.[20-23]

In the last decade, many authors have reported the use of vegetable oils as feedstock for UV-curable systems,[24-26] and although UV-curable chemistries based upon thiol-ene functionality offer many advantages,[27,28] only recently thiol-ene UV-curable coatings using vegetable oils is reported. [29]

In particular, thiol-ene click chemistry of fatty acid derivatives,[30,31] obtained from plant oils, is a promising route that can be used for the synthesis of novel chemical intermediates from renewable resources. Our research applies the thiol-ene click chemistry of unsaturated fatty acid ester derivatives with hydroxyl-functionalized thiols

for its ability to add hydroxyl functionality in lieu of double bounds. This methodology provides a green approach toward novel plant-derived diols.[32]

In this work we report UV-light mediated synthesis of four diols from oleic acid and 10-undecenoic acid derivatives. Oleic and 10-undecenoic acids are the major products of high oleic sunflower oil saponification and castor oil pyrolisis,[33] respectively. We will focus our discussion on the synthesis of monomer diols which have been used in the synthesis of polyurethanes, as well as characterization, and properties of the resulting polyurethanes.

Experimental Part

Materials

Methyl oleate (OLM) and methyl 10-undecenoate (UDM) were synthesized from oleic acid (90% Mallinckrodt) and 10-undecenoic acid (98%, Aldrich) following standard methods. The following chemicals were purchased from Aldrich and used as received: Lithium aluminum hydride, $LiAlH_4$ (95%), acetonitrile, allyl alcohol (>98%), 2,2-dimethoxy-2-phenylacetophenone (DMPA) (99%), 2-mercaptoethanol (99%), tin(II) 2-ethylhexanoate, and 4,4′-methylenebis(phenylisocyanate) (MDI). Tetrahydrofuran (THF) was distilled from sodium immediately before use, N,N-dimethylformamide (DMF) was dried with CaH_2 for 24 h and freshly distilled before use. Phosphate-buffered solution (PBS) of pH = 7.4 from Sigma was used as received. Thermanox (TMX) control disks were supplied by Labclinics S. L., and aqueous solutions of Triton X-100 were supplied by Aldrich. Tissue culture media, additives, and 3-(4,5-dimethylthiazol-2-yl)-2,5-diphenyltetrazolium bromide (MTT) were purchased from Sigma. The fetal bovine serum was obtained from Gibco, and L-glutamine, penicillin, and streptomycin from Sigma.

Synthesis of Allyl 10-Undecenoate (UDA)

To a 250-mL round-bottom flask, 40 g (0.213 mol) of 10-undecenoic acid, an excess of allyl alcohol 53 mL (0.778 mol), and p-toluensulphonic acid as a catalyst were added, and the mixture was refluxed and magnetically stirred for 8h. Once the reaction was completed, the mixture was washed with ethyl ether and 10% sodium bicarbonate

solution, dried over anhydrous magnesium sulphate and filtered. The solvent was evaporated off under reduced pressure. Finally, the product was distilled under vacuum (bp 110ºC at 0.45 mmHg) to afford pure allyl 10-undecenoate as viscous oil, in a 80 % yield.

^{1}H NMR ($CDCl_3$, TMS), δ(ppm)): 5.88 (m, -CH=C), 5.78 (m, C=CH), 5.33-5.21 (dd, C=CH_2), 5.00-4.90 (dd, CH_2=C), 4.56 (d, -OCH_2), 2.32 (t, -CH_2-CO-), 2.01 (m, CH-C$\underline{H}_2$-), 1.62 (m, -CH_2-), 1.33-1.28 (m, -CH_2-, 10 H).

^{13}C NMR ($CDCl_3$, δ(ppm)): 173.45 (s), 139.12 (d), 132.41 (d), 118.04 (t), 114.20 (t), 64.93 (t), 34.28 (t), 33.83 (t), 29.32 (t), 29.24 (t), 29.16 (t), 29.09 (t), 28.93 (t), 24.98 (t).

Synthesis of Allyl Oleate (OLA)

OLA was synthesized following the procedure described for UDA. The product was purified by column chromatography using as eluent hexane:ethyl acetate, 8:2, to afford pure allyl oleate as viscous oil, in a 80 % yield.

^{1}H RMN ($CDCl_3$, TMS, δ (ppm)): 5.88 (m, -CH=C), 5.35 (m, -HC=CH-, 2H), 5.25 (m, C=CH_2), 4.58 (d, -OCH_2), 2.37 (t, -CH_2-CO-), 2.01 (m, -C$\underline{H}_2$-CH=CH-, 4H), 1.62 (t, -C$\underline{H}_2$-CH_2-COO-), 1.38-1.22 (m, -CH_2-, 20 H), 0.93 (CH_3-).

^{13}CRMN ($CDCl_3$, TMS, δ (ppm)): 173.80 (s), 132.15 (d), 130.00 (d), 129.80 (d), 118.02 (t), 64,73 (t), 34,10 (t), 32,15 (t), 32.1 (t), 29.81 (t), 29.62 (t), 29.55 (t), 29.25 (t), 29.21 (t), 29.12 (t), 29.00 (t), 27.21 (t), 27.15 (t), 24.5 (t), 22.32 (t), 14.1 (q).

Synthesis of 3-(2-hydroxyethylthio) propyl 11-(2-hydroxyethylthio) undecanoate (UDA-diol): Thiol-Ene Coupling of UDA with 2-Mercaptoethanol

In a 25 mL flask 5.0 g (22 mmol) of allyl 10-undecenoate (UDA) reacted with 4,3 g (55 mmol) of mercaptoethanol. The radical initiator, DMPA, was added in the proportion 0,3% mol init./mol C=C. The amount of acetonitrile necessary to dissolve the photoinitiator was added. The reaction was carried out at room temperature, without deoxygenation, by irradiation with two 9 W UV-lamps (λ=365 nm). After few minutes a white solid precipitated. The completion of the reaction was confirmed by ^{1}H NMR by the completely disappearance of the double bond signals that appear in the region of 5-6

ppm. The mixture was crystallized from ether, filtered, washed with cold ether and hexanes, and dried under vacuum (yield 98%).

^{1}H NMR ($CDCl_3$, TMS, δ, ppm)): 4.15 (t, -OCH_2), 3.73 (t, -CH_2-OH), 3,70 (t, -CH_2-OH), 2.73 (t, $HOCH_2$-$C\underline{H}_2$-S-), 2.72 (t, $HOCH_2$-$C\underline{H}_2$-S-), 2.59 (t, -O-$(CH_2)_2$-$C\underline{H}_2$-S-), 2.51 (-CH_2-$C\underline{H}_2$-S), 2.29 (CH_2-COO-), 1.93 (m, -CH_2-), 1.59 (m, -CH_2-, 4H), 1.38-1.26 (m, -CH_2-, 12 H).

^{13}C NMR ($CDCl_3$, TMS, δ ppm)): 173.96 (s), 62.79 (t), 60.40 (t), 60.28 (t), 35.43 (t), 35.40 (t), 34.40 (t), 31.73 (t), 29.84 (t), 29.51 (t), 29.45 (t), 29.32 (t), 29.26 (t), 29.22 (t), 28.94 (t), 28.91 (t), 28.23 (t), 25.06 (t).

Synthesis of 3-(2-hydroxyethylthio) propyl 9- and 10-(2-hydroxyethylthio) octadecanoate as a mixture of isomers (OLA-diol): Thiol-Ene Coupling of OLA with 2-Mercaptoethanol.

OLA-diol was synthesized following the procedure described for UDA-diol but higher ratio of radical initiator was used (1.7% mol init./mol C=C). The product was purified by column chromatography using as eluent hexane:ethyl acetate, 1:1, to afford OLA-diol as viscous oil, in a 80 % yield.

^{1}H RMN ($CDCl_3$, TMS, δ(ppm)): 4,10 (t, -COO-CH_2), 3,66 (q, $HOCH_2$-), 3,63 (q, $HOCH_2$-), 2,67 (t, $HOCH_2$-$C\underline{H}_2$-S-), 2,65 (t, $HOCH_2$-$C\underline{H}_2$-S-), 2.53 (t, -O-$(CH_2)_2$-$C\underline{H}_2$-S-), 2,50 (m, -CH-S-), 2,23 (t, -CH_2-COO-), 1,85 (m, -O-CH_2-$C\underline{H}_2$-CH_2-S) 1.56–1.25 (m, -CH_2-, 28H), 0.81 (t, CH_3)

^{13}C RMN ($CDCl_3$, TMS, δ (ppm)): 174 (s), 62.55 (t) 60.50 (t), 60.25 (t), 45.80 (d) , 35.04 (t), 34.99 (t), 34.98 (t), 34.10 (t), 33.75 (t), 31.72 (t), 29.68 (t), 29.64 (t), 29.61 (t), 29.52 (t), 29.42 (t), 29.31 (t), 29.22 (t), 29.15 (t), 28.80 (t), 28.01 (t), 26.60 (t) 25.00 (t) 22.65 (t), 14.11 (q).

Synthesis of Methyl 11-(2-hydroxyethylthio) undecanoate (UDM-OH): Thiol-Ene Coupling of UDM with 2-Mercaptoethanol.

UDM-OH was synthesized following the procedure described for UDA-diol but in this case no radical initiator was used. The product was obtained as a white solid with 95 % yield.

^{1}H NMR ($CDCl_3$, TMS, δ (ppm)): 3.73 (t, HO-C<u>H$_2$</u> -CH_2-S–), 3.66 (s, -OCH_3), 2.73 (t, $HOCH_2$-C<u>H$_2$</u>-S-), 2.51 (t, -S-CH_2), 2.30 (t, -CH_2-COO), 1.63-1.27 (m, -CH_2-, 16H)

^{13}C NMR ($CDCl_3$, TMS, δ (ppm)): 174.51 (s), 60.44 (t), 51.59 (q), 35.36 (t), 34.22 (t), 31.80 (t), 29.86 (t), 29.52 (t), 29.45 (t), 29.32 (t), 29.28 (t), 29.23 (t), 28.93 (t), 25.05 (t)

Synthesis of Methyl 9- and 10-(2-hydroxyethylthio) octadecanoate as a mixture of isomers (OLM-OH): Thiol-Ene Coupling of OLM with 2-Mercaptoethanol.

OLM-OH was synthesized following the procedure described for UDA-diol but higher ratio of radical initiator was used (1.7% mol init./mol C=C). The product was obtained as viscous oil with 80 % yield.

^{1}H NMR ($CDCl_3$, TMS, δ (ppm)): 3.69 (t, HOC<u>H$_2$</u> -CH_2-S-), 3.66 (s, -OCH_3), 2.71 (t, $HOCH_2$ -C<u>H$_2$</u>-S-), 2.57 (m, -CH-S-), 2.29 (t, -CH_2-COO), 1.63-1.25 (m, -CH_2-, 28H), 0.87 (t, CH_3).

^{13}C NMR ($CDCl_3$, TMS, δ (ppm)): 174.53 (s), 60.89 (t), 51.64 (q), 45.95 (d) , 35.14 (t), 34.27 (t), 33.95 (t), 32.03 (t), 29.83 (t), 29.75 (t), 29.68 (t), 29.62 (t), 29.54 (t), 29.48 (t), 29.42 (t), 29.35 (t), 29.22 (t), 26.95 (t), 25.05 (t), 22.83 (t), 14.28 (q).

Synthesis of 11-(2-hydroxyethylthio) undecan-1-ol (UDM-diol)

A 250 mL, two-necked, round-bottom flask equipped with a Teflon-coated magnetic bar and a pressure-equalized dropping funnel was charged with $LiAlH_4$ (0.42 g, 0.011 mol) and anhydrous THF (15 mL) under argon. UDM-OH (3 g, 0.011 mol) dissolved in 15 mL of anhydrous THF was added slowly with stirring for 1 hour. 3x10 mL anhydrous THF were added as the viscosity increased. After 30 min., excess $LiAlH_4$ was decomposed by the addition of 20 mL of ethyl acetate dropwise, then a saturated 10% H_2SO_4 aqueous solution (60 mL) was added, the phases were separated, and the aqueous layer was extracted with ethyl acetate. The combined organic phase was washed with a saturated aqueous NaCl solution, dried over anhydrous magnesium sulphate, filtered, and the solvent was removed under reduced pressure. The solid product was recrystallized from heptane to obtain a white solid (yield 84 %).

^{1}H NMR ($CDCl_3$, TMS, δ (ppm)): 3.71 (t, $HOC\underline{H}_2$-CH_2-S-), 3.64 (t, $HOCH_2$-), 2.73 (t, $HOCH_2$ -$C\underline{H}_2$-S-), 2.51 (t, -S-CH_2-), 1.58 (m, -$C\underline{H}_2$-CH_2OH), 1.5 (m, -$C\underline{H}_2$-CH_2-S-), 1.37-1.25(m, -CH_2-, 14H).

^{13}C NMR ($CDCl_3$, TMS, δ (ppm)): 63.30 (t), 60.30 (t), 35.55 (t), 33.00 (t), 31.80 (t), 29.93 (t), 29.74 (t), 29.67 (t), 29.65 (t), 29.59 (t) 29.38(t), 29.02 (t), 25.93 (t).

Synthesis of 9- and 10-(2-hydroxyethylthio) octadecan-1-ol (OLM-diol)

OLM-diol was synthesized following the procedure described for UDM-diol. The product was dissolved in ethyl ether (5 mL) and crystallized (-20 ºC) with 75 % yield.

^{1}H NMR ($CDCl_3$, TMS, δ ppm)): 3.69 (t, $HOC\underline{H}_2$ -CH_2-S-), 3.66 (t, $HOCH_2$-), 2.72 (t, $HOCH_2$ -$C\underline{H}_2$-S-), 2.58 (m, -CH-S-), 1.58-1.25 (m, -CH_2-, 30H), 0.88 (t, -CH_3).

^{13}C NMR ($CDCl_3$,TMS, δ ppm)): 63.00 (t), 60.67 (t), 45.80 (d), 34.99 (t), 34.90 (t), 33.80 (t), 32.72 (t), 31.86 (t), 29.68 (t), 29.57 (t), 29.48 (t), 29.44 (t), 29.35 (t), 29.28 (t), 26.77 (t), 26.71 (t), 26.69 (t), 25,73 (t), 22.65 (t), 14.11 (q).

General Procedure for Polyurethanes Synthesis

To a dry 50 mL round-bottom flask were charged 12 mL of DMF, 6 mmol of diol (UDM-diol, OLM-diol, UDA-diol or OLA-diol), 6 mmol of MDI, and 2% w/w (with respect to MDI) of tin (II) 2-ethylhexanoate. The flask was immersed into a 50 ºC preheated silicone oil bath with a magnetically stirred. The reaction was continued for 24 h. and the polyurethanes were isolated as white solids by precipitation into diethyl ether. Purification of polyurethanes was carried out by dissolving the polymer in the minimum volume of chloroform or THF, and reprecipitation into diethyl ether. The pure polymers were dried under vacuum and stored in a dissecator until needed. Films were solution cast from DMF and dried at 50ºC for 1 day and then in a vacuum oven until constant weight.

Instrumentation

The FTIR espectra were recorded on a JASCO 680 FTIR spectrophotometer with a resolution of 2 cm^{-1} in the absorbance mode. An attenuated total reflection (ATR)

accessory with thermal control and a diamond crystal (Golden Gate heated single – reflection diamond ATR, Specac. Teknokroma) was used to determine FTIR spectra. ^{1}H 400 MHz, ^{13}C (100.5 MHz) NMR spectra were obtained using a Varian Gemini 400 spectrometer with Fourier transform, $CDCl_3$ as solvent and TMS as internal standards. Calorimetric studies were carried out on a Mettler DSC821e and DSC822e thermal analyzer using N_2 as a purge gas (20 ml/min) at scanning rate of 10ºC/min. Thermal stability studies were carried out on a Mettler TGA/SDTA851e/LF/1100 with N_2 as a purge gas. The heating rate in the TGA dynamic mode was 10ºC/min. Isothermal measurements were carried out at 240 ºC, 250 ºC and 260 ºC. Degradation kinetic of polymers was studied using TGA with experimental data being processed using the Flynn method which includes three isothermal and one dynamic TGA curves.[34] This method provides the activation energy dependence with temperature. Size exclusion chromatography (SEC) analysis was carried out with an Agilent 1200 series system equipped with an Agilent 1100 series refractive-index detector. THF was used as an eluent at a flow rate of 1.0 mL/min.

Mechanical properties were measured using a dynamic mechanical thermal analysis (DMTA) apparatus (TA DMA 2928) in the controlled force-Tension Film mode. The tensile essays were performed on rectangular films (5 x 3 x 0,2 mm^3) measuring the strain while applying a ramp of 3 N/min. at 35ºC. A preload force of 0.01 N and a soak time of 5 min. were used. Sonication techniques: The main sources of ultrasound used were a Branson 2510 horn system, operating at 42 KHz and used in the usual configuration whereby the horn was immersed to a depth of about 1.5 cm in the reaction mixture. Thermostatting around ambient temperature was achieved to ± 1 ºC by water bath surrounding the reaction vessel.

Hydrolytic degradation assays

Films of aliphatic polyurethanes with a thickness of approximately 200 μm, were prepared by casting at room temperature from a solution in THF. The films were cut into 10 mm diameter, 20 to 30 mg weight disks, which were dried under vacuum at 50 ºC to constant weight. For incubation, samples were immersed in vials containing 10 mL of the sodium phosphate buffer (pH 7.4) and experiments were carried out at temperature of 60 ºC. After incubation for the scheduled period of time, samples were

removed, rinsed thoroughly with water and dried to constant weight. Sample weighing and SEC measurements were used to follow the evolution of the hydrolytic degradation.

Biocompatibility of Polymers

The negative control used was tissue culture plastic, Thermanox (TMX), and the positive control (toxic agent) was a 0.5% aqueous solution of Triton X-100. Disks of 10 mm diameter and 1 mm thickness of the polymers, and the controls were used for direct and indirect biocompatibility experiments. The polymers were tested in cytotoxicity assay. All specimens were sterilized with ethylene oxide. The cells used in the primary cell culture were human fibroblasts and were cultured at 37 °C. The culture medium was Dubelcco's modified eagle medium (DMEM), rich in glucose, modified with HEPES (Sigma) and supplemented with 10% fetal bovine serum, 200 mM L-glutamine, 100 units/mL penicillin, and 100 μg/mL streptomycin. The culture medium was changed at selected time intervals with care to cause little disturbance to culture conditions.

MTT Assay for Polymers

TMX, Triton, and disks of copolymers were set up in 5 mL of DMEM, FCS-free. They were placed on a roller mixer at 37 °C, and the medium was removed at different time periods (1, 2, and 7 days) and replaced with another 5 mL of fresh medium. All the extracts were obtained under sterile conditions. Human fibroblasts were seeded at a density of 11 x 10^4 cells/mL in complete medium in a sterile 96-well culture plate and incubated to confluency. Then, the medium was replaced with the corresponding eluted extract and incubated at 37 °C in a humidified air with 5% CO_2 for 24 h. A solution of MTT was prepared in warm PBS and filtered before use. MTT, 10 μL, was added to all wells to give a final concentration of 0.5 mg/mL, and the plates were incubated at 37 °C, 5% CO_2 for 4 h. Excess medium and MTT were removed, and 100 μL of dimethyl sulfoxide (DMSO) was added to all wells in order to dissolve the MTT taken up by the cells. This was mixed for 10 min, and the absorbance was measured with a Biotek ELX808 IU plate reader, using a test wavelength of 570 nm and a reference wavelength of 630 nm. The cell viability was calculated from equation 1:

$$\text{Relative cell viability} = 100 \times (OD_S - OD_B)/OD_C \qquad \text{(Eq. 1)}$$

where OD_S, OD_B and OD_C are the optical density of formazan production for the sample, blank (DMEM without cells), and control (Tween solution in free serum supplemented DEMM), respectively. Results were normalized with respect to a negative control (TMX = 100%) and statistically tested with ANOVA ($p < 0.05$).

Results and discussion

Synthesis of Allyl 10-Undecenoate (UDA) and Allyl Oleate (OLA)

The synthesis of allyl ester of 10-undecenoic acid (UDA) was carried out by refluxing 10-undecenoic acid, which is the major product of castor oil pyrolysis,[33] with an excess of allyl alcohol and using 2% *p*-toluenesulfonic acid as catalyst, for 6-8 h (Scheme 1). The ^{1}H NMR spectrum of the product corresponded to the expected structure. The five allyl protons resonate at 5.88, 5.27, and 4.56 ppm, whereas the three protons of the vinyl group resonate at 5.78 and 4.95 ppm. Their resonance intensity ratios were in excellent agreement with their proton number ratios. Although allyl alcohol is a large-scale industrial chemical, presently produced from propene, it is worth mentioning here that UDA is potentially a 100% biomass-derived monomer. Allyl alcohol can be easily obtained from glycerol, the main byproduct in the triglyceride transesterification process for biodiesel manufacture.[35] Alternatively, synthetic procedures for allyl esters starting from fatty acids and glycerol are also available in the literature.[36]

The synthesis of allyl oleate (OLA) was carried out in a similar way than allyl 10-undecenoate but using oleic acid as fatty acid. Also in this case, the ^{1}H NMR spectrum of the product confirmed the expected structure, showing together with the five allyl protons a multiplet at 5.35 ppm corresponding to the two olefinic protons of the central double bond.

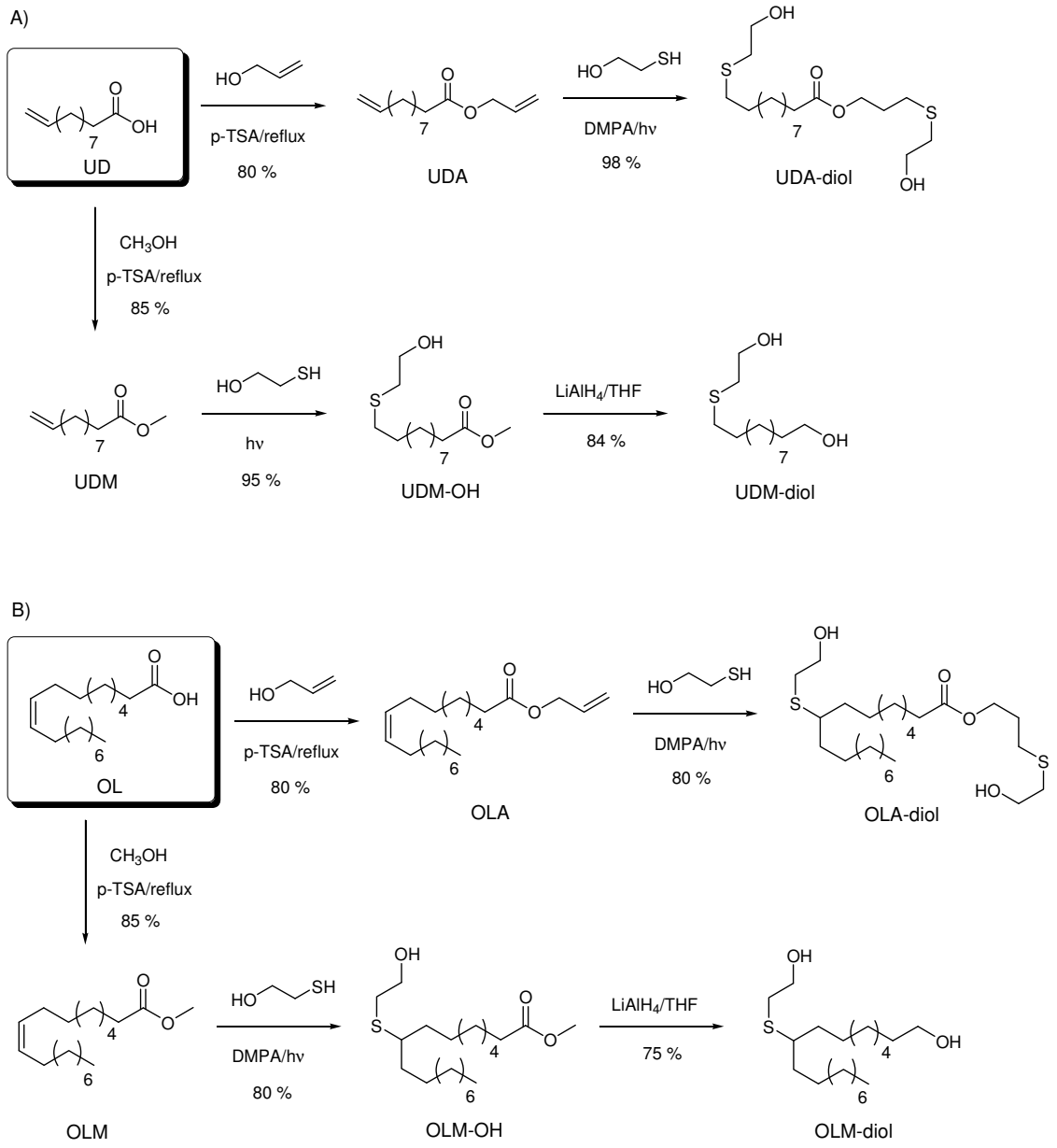

Sheme 1. Synthetic procedure for the preparation of diols

Reactivity of Undecenoates and Oleates toward Thiol Addition.

The thiol-ene coupling mechanism has been extensively studied and is known to follow a radical mechanism, in which the addition of a thiyl radical to a double bond is followed by chain transfer to thiol.[37] The thiol-ene addition product is formed, with anti-Markovnikov orientation, with the concomitant generation of a new thiyl radical. Possible termination reactions involve typical radical-radical coupling processes.

$$RS^{\cdot} + CH_2{=}CHR' \rightarrow R\text{-}SCH_2\text{-}\dot{C}HR' \quad (1)$$

$$R\text{-}SCH2\text{-}\dot{C}HR' + HSR \rightarrow RSCH_2\text{-}CH_2R' + RS^{\cdot} \quad (2)$$

Reactivity in the radical thiol-ene reaction can vary considerably depending on the chemical structure of the ene and thiol components. UDA is a monomer with allylic and vinylic different double bond end groups and OLA is a diolefinic monomer with allylic and internal double bonds. It is logical that the chemical structure of an alkene can significantly affect its reactivity in thiol-ene reactions because of differences in the steric strain and ene susceptibility to thiyl attack and subsequent hydrogen abstraction. It is well known that terminal alkenes react very rapidly and irreversible with thiols, achieving complete conversions in few minutes.[38,39] The relative reactivity of two UDA end groups toward photoinitiated radical addition with 2-mercaptoethanol and in presence of DMPA as photoinitiator was studied, finding that allylic and vinylic chain ends exhibit different reactivity toward thiol addition (about 1.8 less the former against the latter).[32] Presumibly, this is due to the presence of an electron-withdrawing group that destabilize the radical intermediate.

Generally, terminal enes are significantly more reactive towards hydrothiolation compared to internal enes. Thus, Hoyle et *al*. reported that 1-hexene is 8 x more reactive than *trans*-2-hexene and 18 x more reactive than *trans*-3-hexene, clearly highlighting that steric effects are important when considering reactivity.[15] However, these differences in reactivity are not due entirely to steric effects. As reported previously,[40-43] thyil radical addition to *cis* C=C bonds is reversible and is accompanied with an isomerisation process*, i.e*. thyil radicals can be employed as means of converting *cis* C=C bonds to *trans* C=C bonds with high efficiency. A detailed analysis of the ^{1}H NMR spectra during the 2-mercaptoethanol addition to methyl oleate (OLM) confirmed this process takes place. As shown in Figure 1a, pure OLM double bond with *cis* configuration gives signal (**a)** at around 5.33 ppm. After 5 min (37% conversion) a new signal (**b**) appears at 5.36 ppm, which is attributed to the chemical shift characteristic of C=C with *trans* configuration. The appearance of this signal confirms that under these conditions, the addition of a thiyl radical to methyl oleate is a reversible process that generates a more thermodynamically stable *trans* double bond. After 30 min, at the point of 50% conversion the signal of *trans* is higher than the *cis* and at the point of 72 % conversion (60 min) only practically the signal of trans ene is remaining. This signal

completely disappears after 120 min. This insertion-isomerization-elimination reaction sequence is also responsible of the reduced reactivity observed for OLM

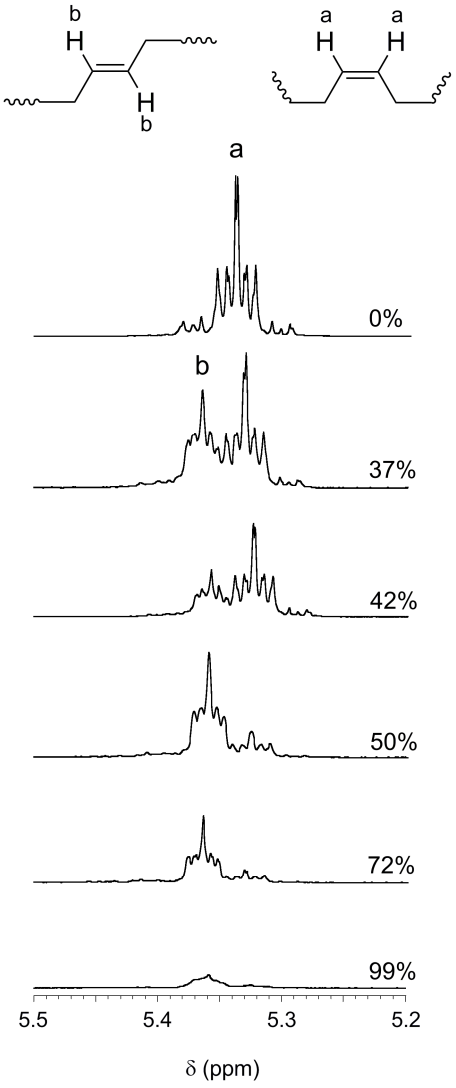

Figure1. Expansion of the 400 MHz ^{1}H NMR spectra during the photoinitiated thiol-ene coupling between 2-mercaptoethanol and methyl oleate.

Following the above considerations both allyl and methyl undecenoates were reacted with 2-mercaptoethanol to yield UDA-diol and UDM-diol respectively. Also both allyl and methyl oleates yielded OLA-diol and OLM-diol following the procedure described for UDA-diol, but with higher ratio of radical initiator. (Scheme 1).

The evolution of the oleic acid (OL) to OLA-diol could be followed by ^{1}H NMR (Figure 2). The spectrum (A) of the initial oleic acid shows the characteristic signals of the internal C=C at 5.35 ppm. The formation of allyl oleate (spectrum B) is observed for

the peaks arising from the methylene next to terminal C=C at 4.58 ppm and the new peaks in the olefinic zone at 5.27 and 5.88 ppm corresponding to protons of terminal C=C. The success of the thiol-ene coupling to yield OLA-diol (spectrum C) was noted from the appearance signals at about 2.4 and 2.6 ppm corresponding to the new formed carbon-sulfur bonds. More evidence of successful coupling was obtained from the complete disappearance of signals corresponding to alkene protons.

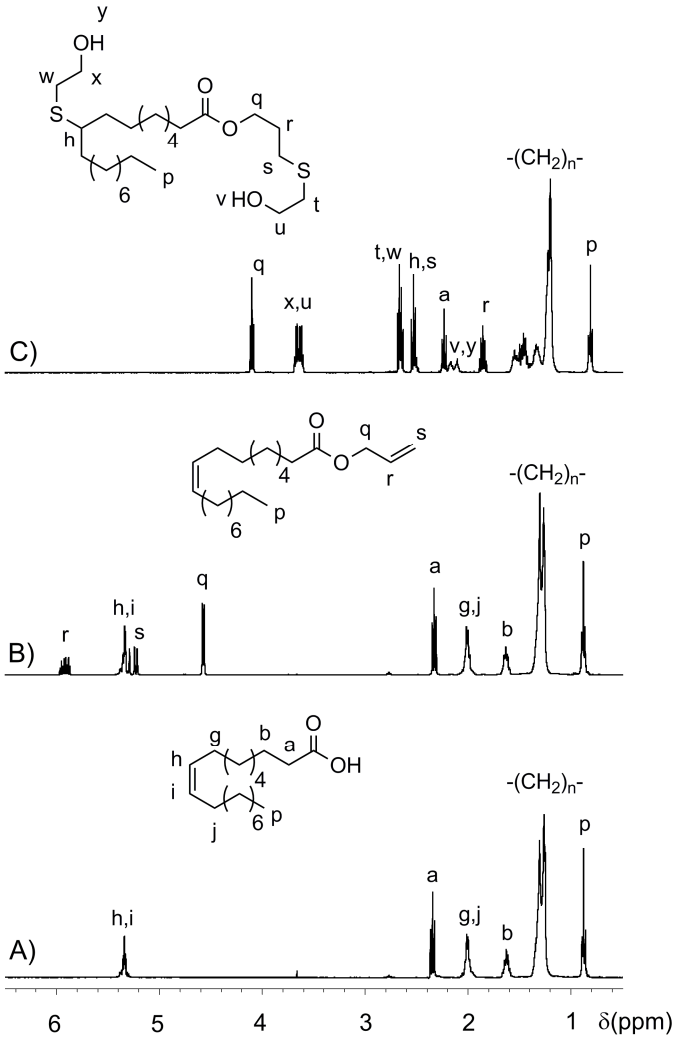

Figure 2. ^{1}H NMR spectra of (A) OL; (B) OLA; and (C) OLAdiol

Results obtained in the synthesis of polyurethanes studied in this work as well as some characterization data are given in Table 1. The synthesized undecylenic and oleic acids based diols (UDM-diol, UDA-diol, OLM-diol and OLA-diol) were polymerized with MDI in DMF solution at 50 ºC for 24 h using tin (II) 2-ethylhexanoate as catalyst. Under these conditions the reaction proceeded in one step and isolation and purification of the polyurethanes (PUs) were carried out by solution-precipitation cycles and

subsequent drying under vacuum; yields were in the 80-99% range. Weight-average molecular weights of polyurethanes were in the 36-83 KDa range. Polydispersities oscilated between 2.2 and 1.9 with perceivable differences between those with and without ester groups in the polymer chain. In the case of polyurethane obtained with ultrasound irradiation the polydispersity was lower.

Table1. Polycondesation Results and Some Properties of PUs

PU	Diol	T (ºC)	t (h)	Yield (%)	SEC [c] M_n (g/mol)	SEC [c] M_w (g/mol)	M_w/M_n	Solubility [d] H_2O	DMSO	$CHCl_3$	THF
PU1[a]	UDM	50	24	99	83,293	188,670	2.1	-	+	-	+
PU2[a]	OLM	50	24	80	36,340	84,050	2.2	-	+	+	+
PU3[a]	UDA	50	24	99	50,930	96,310	1.9	-	+	+	+
PU3[b]	UDA	40	7	99	71,210	120,820	1.6	-	+	+	+
PU4[a]	OLA	50	24	92	61,860	120,020	1.9	-	+	+	+

[a] Polycondensation reaction carried out in DMF by conventional heating.

[b] Polycondensation reaction carried out in DMF by ultrasound irradiation (42 kHz).

[c] Number and average molecular weights determined by GPC in THF against PS standards.

[d] Solubility at 25 ºC: + soluble, - insoluble.

The chemical structures of polyurethanes were assessed by FTIR and NMR spectroscopy. Characteristic IR absorption bands of main chains were observed. Thus, the C=O stretching bands arising from ester and urethane at 1728 and 1701 cm^{-1} respectively, the NH stretching band appearing at around 3320 cm^{-1} and NH bending band at 1532 cm^{-1} and the stretching band of C=C of aromatic ring. ^{1}H and ^{13}C NMR spectra were in all cases in full concordance with the expected chemical structures of polyurethanes.

The solubility of the polyurethanes is collected in Table 1 for a set of representative solvents evidencing that these compound have high solubility in all solvents except in water. Only PU1 showed no solubility in $CHCl_3$.

The effect on thermal transitions Tg and Tm arising from the different precursor fatty acid units in the polyurethane chain was investigated by DSC. Polyurethanes samples were quenched from the melt to make clear the observation of the glass transition. Tg values measured in such DSC traces are given in Table 2. Tm values were measured on the heating DSC traces recorded polyurethanes samples coming directly from the synthesis and are also given in Table 2. PU1 and PU3 derivatives from undecylenic acid showed higher crystallinity than PU2 and PU4 derivatives from oleic acid. This can be related to the presence of pendant chains in PU2 and PU4, that difficult the packing.

Table 2. Thermal Properties of PUs

	DSC					TGA (ºC)		E_a (J/mol)		
	T_g (ºC)	Tm_1 (ºC)	ΔH_1 (J/g)	Tm_2 (ºC)	ΔH_2 (J/g)	$T_{5\%}$	T_{max}	240ºC	250ºC	260ºC
PU1	56	115	17	141	19	274	293/361/463	116	94	97
PU2	28	104	3	-	-	277	284/356/463	151	158	141
PU3	20	124	42	-	-	269	294/362/462	60	71	59
PU4	8	-	-	-	-	290	301/362/459	125	110	127

Previously it was reported that the rates of reaction in the preparation of polyurethanes from H_{12}MDI and different aliphatic diols, can be accelerated by the use of high intensity ultrasound.[44] The source of the effect seems to be related to local heating around collapsing cavitation bubbles together with the enhanced mass transfer caused by the fluid motion but it was likely that an effect took place to modify the mode of action of the catalysts in these systems. Hence, we carried out one experience of polymerization of UDA-diol under ultrasonic irradiation. The results shown in Figure 3 and Table 1 allow confirm that sonochemical reaction proceeded faster in the early stages and led to higher molecular weight polyurethane compared to polyurethane obtained by conventional thermal polymerization.

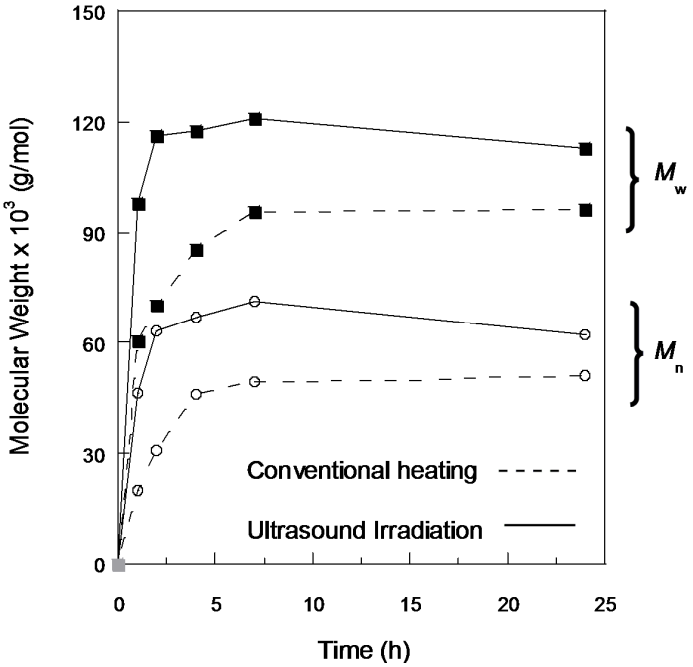

Figure 3. Evolution of Mn and Mw versus time under conventional heating and ultrasound irradiation of PU3´.

The hydrolytic degradability of polyurethanes was evaluated by incubation assays. Neither weight loss nor molecular weight decrease were observed after six months. These results are in agreement with the hydrophobic character of all synthesized polyurethanes.

The thermal stabilities of polymers were investigated with TGA in nitrogen stream and the results are collected in Table 2. All polyurethanes showed three degradation stages and the derivative of the weight loss versus temperature showed three peaks centered at ca. 300 ºC, 360 ºC, and 460 ºC. The range of temperatures of the first stage suggests that degradation starts at urethane linkages, which takes place through the dissociation to isocyanate and alcohol, the formation of primary amines and olefins, or the formation of secondary amines.[45]

Degradation kinetic studies for the temperature region of 240-260 were carried out. Figure 4 shows the dependence of degradation times in nitrogen upon conversion at three different temperatures. Activation energies calculated from the slope of isothermal curves are collected in Table 2. As can be seen, activation energies show dependence on the chemical structure of polyurethanes, being lower for ester group-containing

polyurethanes PU3 and PU4, which should influence the initial degradation step (below 10% conversion) becoming the degradation process more complex.

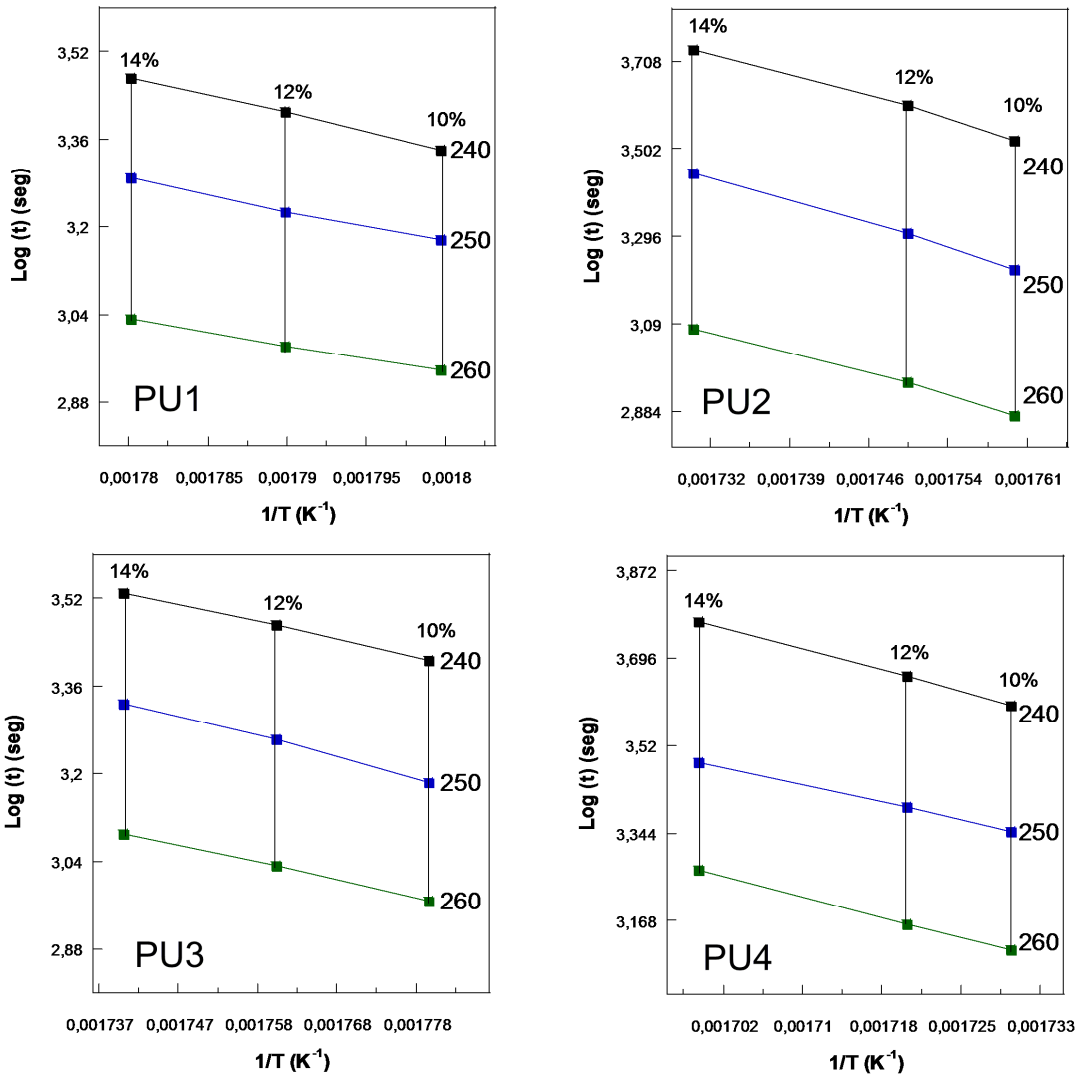

Figure 4. Dependence of degradation times in nitrogen on conversion at three temperatures for the polyurethanes.

Mechanical properties of polyurethanes including tensile strength, modulus, and elongation at break were evaluated from stress-strain curves (Figure 5). PU4 and PU2 samples show a smooth transition in their stress–strain behaviour similar to lightly crosslinked amorphous rubbers. The stress-strain behaviour of PU1 and PU3 samples is different showing a yield point as a result of the presence of crystalline domains in these samples which act increasing the rigidity of the material.

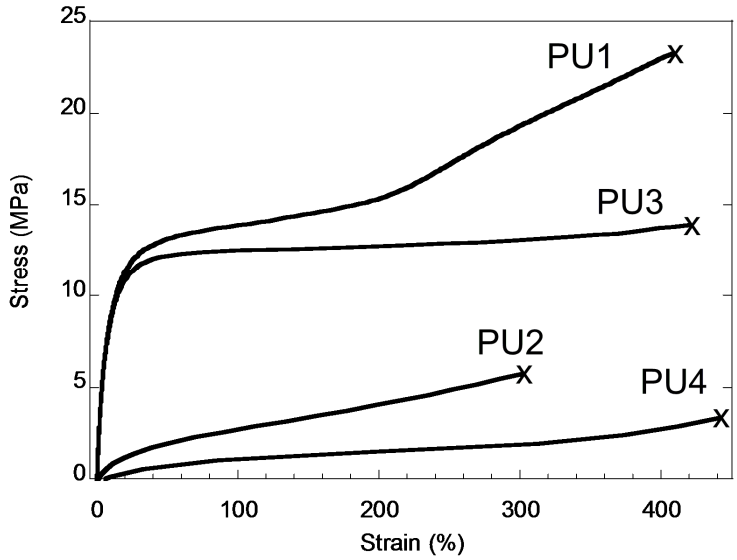

Figure 5. Stress–strain curves of the polyurethanes.

Cytotoxicity of polyurethanes was evaluated using the MTT assay for testing the toxicity of eluates. Figure 6 shows that cell viability was not affected by the presence of extracts from any polyurethane systems within seven days, reaching values higher than 85% of the control TMX in all polymers. These initial cytotoxicity tests indicates that these materials are promising for biomedical purposes, however, further testing is required to ascertain whether they are biocompatible.

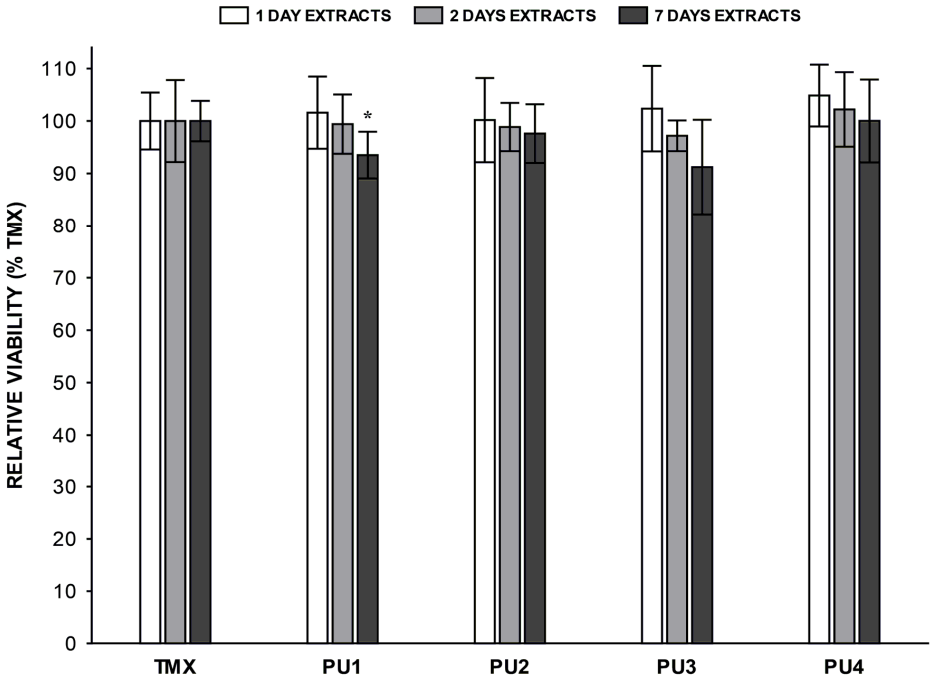

Figure 6. MTT cytotoxicity results for control TMX and polyurethanes. Results are the mean ± standard deviation. Statistical analysis (n = 12) of each polymer was performed with respect to TMX at a significance level of *$p < 0.05$.

Conclusions

In this study we describe a novel route to obtain diols derived from fatty acids. The application of thiol-ene additions to 10-undecenoate and oleate derivatives was carried to obtain the required monomers. The resulting monomers were then polymerized with 4,4′-methylenebis (phenylisocyanate), in DMF solution using tin (II) 2-ethylhexanoate as catalyst, to produce the corresponding thermoplastic polyurethanes. Ultrasound irradiation has been proved to improve the polyurethane synthesis. The thus prepared polyurethanes were characterized and revealed good thermal and mechanical properties, making them possible candidates for the substitution of petroleum based materials. MTT test was carried out to asses the potential citotoxicitity of the prepared polyurethanes, indicating no cytotoxic response which indicates that these materials are promising for biomedical purposes.

Acknowledgements

The authors express their thanks to CICYT (Comisión Interministerial de Ciencia y Tecnología) (MAT2008-01412) for financial support for this work and to J. Parra for cytotoxicity assays.

References

[1] Koopmans, R. J. Soft Matter 2006, 2, 537-543.

[2] Gandini, A.; Belgacem, M. N. Monomers, Polymers and Composites from Renewable Resources; Elsevier: Oxford, UK, 2008.

[3] Meier, M. A. R.; Metzger, J. O.; Schubert, U. S. Chem Soc Rev 2007, 36, 1788–1802.

[4] Güner, F. S.; Yagci, Y.; Erciyes, A. T. Prog Polym Sci 2006, 31, 633–670.

[5] Sharma, V. ; Kundu, P.P. Prog Polym Sci 2006, 31, 983-1008; 2008, 33, 1199-1215.

[6] Biermann, U.; Friedt, W.; Lang, S.; Lühs, W.; Machmüller, G.; Metzger, J.O.; Klaas, M. Rüsch gen.; Schäfer, H.J.; Schneider, M.P. Angew Chem Int Ed 2000, 39, 2206-2224.

[7] Jain, J. P.; Sokolsky M.; Kumar, N.; Domb, A. J Polym Rev 2008, 48, 156-191.

[8] Lligadas, G.; Ronda, J. C.; Galià, M; Cádiz V. Biomacromolecules 2010, 11, 2825-2835.

[9] Petrovic, ZS. Polym Rev 2008, 48, 109-155.

[10] Lligadas, G.; Ronda, J. C.; Galià, M.; Biermann, U.; Metzger, J. O. J Polym Sci Part A: Polym Chem 2006, 44, 634-645; Lligadas, G.; Ronda, J. C.; Galià, M; Cádiz V. Biomacromolecules 2006, 7, 2420-2426; Biomacromolecules 2007, 8, 686-692; Biomacromolecules 2007, 8, 1858-1864.

[11] Çayll, G.; Küsefoglu, S. J Appl Polym Sci 2008, 109, 2948-2955; J Appl Polym Sci 2010, 116, 2433-2440.

[12] Hojabri, L.; Kong, X.; Narine, S.S. Biomacromolecules 2009, 10, 884-891; Biomacromolecules 2010, 11, 911-918.

[13] Tamami, B.; Sohn, S.; Wilkes, G. L. J Appl Polym Sci 2004, 92, 883-891.

[14] Palaskar, D. V.; Boyer, A.; Cloutet, E.; Alfos, C.; Cramail, H. Biomacromolecules 2010, 11, 1202-1211.

[15] Hoyle C. E.; Lee, T. Y.; Roper, T. J Polym Sci Part A: Polym Chem 2004, 42, 5301-5338.

[16] Hoyle, C. E.; Lowe, A. B.; Bowman, C. N. Chem Soc Rev 2010, 39, 1355-1387.

[17] Killops, K. L.; Campos, L. M.; Hawker, C. J. J Am Chem Soc 2008, 130, 5062-5064.

[18] Campos, L. M.; Killops, K. L.; Sakai, R.; Paulusse, J. M. J.; Damiron, D.; Drockenmuller, E.; Messmore, B. W.; Hawker, C. J. Macromolecules 2008, 41, 7063-7070.

[19] Kade, M. J.; Burke, D. J.; Hawker, C. J. J Polym Sci Part A: Polym Chem 2010, 48, 743-750

[20] Hoyle C. E.; Bowman, C. N. Angew Chem Int Ed 2010, 49, 1540-1573.

[21] Lowe, A. B. Polym Chem 2010, 1, 17-36

[22] Van Dijk, M.; Rijkers, D. T. S.; Liskamps, R. M. J.; Van Nostrum, C. F.; Hennick, W.E. Bioconjugate Chem 2009, 20, 2001-2016.

[23] Dondoni, A. Angew Chem Int Ed 2008, 47, 8995-8997.

[24] Yu, X. E.; Homan, J. G.; Connor, T.J., Cooper, S.L. J Appl Polym Sci 1991, 43, 2249-2257.

[25] Crivello, J. V.; Narayan, R.; Sternstein, S. S. J Appl Polym Sci 1997, 64, 2073-2087.

[26] Crivello, J. V.; Chakrapani, S. J. J Macromol Sci Part A 1998, 35, 1-20.

[27] Carioscia, J. A.; Stansbury, J. W.; Bowman, C. N. Polymer 2007, 48, 1526-1532.

[28] Phillips, J. P.; Mackey, N. M.; Confait, B. S., Heaps, D. T.; Deng, X.; Todd, M. L.; Stevenson, S.; Zhou, H.; Hoyle C. E. Chem. Mater 2008, 20, 5240-5245.

[29] Black M.; Rawlins, J. W. Eur Polym J 2009, 45, 1433-1441.

[30] Samuelsson, J.; Jonsson, M.; Brinck, T.; Johansson, M. J Polym Sci Part A: Polym Chem 2004, 42, 6346-6352.

[31] Türünç, O.; Meier M. A. R. Macromol Rapid Commun 2010, 31, 1822-1826.

[32] Lluch, C.; Ronda, J. C.; Galià, M; Lligadas, G.; Cádiz V. Biomacromolecules 2010, 11, 1646-1653.

[33] Van der Steen, M.; Stevens, C. V. ChemSusChem 2009, 2, 692-713.

[34] Flynn, J. H.; Wall, L. A. J Polym Sci part B: Polym Lett 1966, 4, 323-328

[35] Arceo, E.; Marsden, P.; Bergman, R. G.; Ellman, J. A. Chem Commun 2009, 23, 3357-3359.

[36] Eras, J.; Escribà, M.; Villorbina, G.; Oromí-Farrús, M.; Balcells, M.; Canela, R. Tetrahedron 2009, 65, 4866-4870.

[37] Jacobine, A. F. Thiol-ene Photopolymerization in Radiation Curing. In Polymer Science and Technology; Fouassier, J. P., Rabek, J. F., Eds.; Chapman and Hall: London, 1993; Vol. 3.

[38] Roper, T. M.; Guymon, C. A.; Jönsson, E. S.; Hoyle, C. E. J Polym Sci Part A: Polym Chem 2004, 42, 6283-6298.

[39] Walling, C.; Helmreich, W. J Am Chem Soc 1959, 81, 1144-1148.

[40] Chatgilialoglu, C.; Samadi, A.; Guerra, M.; Fischer, H., ChemPhysChem 2005, 6, 286-291.

[41] Chatgilialoglu, C.; Altieri, A.; Fischer, H. J Am Chem Soc 2002, 124, 12816-12823.

[42] Ferreri, C.; Samadi, A.; Sassatelli, F.; Landi, L.; Chatgilialoglu, C. J Am Chem Soc 2004, 126, 1063-1072.

[43] Claudino, M.; Johansson, M.; Jonsson, M. Eur Polym J 2010, 46, 2321-2332.

[44] Price, G. J. Ultrason Sonochem 2003, 10, 277-283.

[45] Levchik, S. V.; Weil, E. D. Polym Int 2004, 53, 1585.

CHAPTER II

Thiol-yne reaction on alkyne-derivatized fatty acids: biobased polyols and cytocompatibility of derived polyurethanes

Thiol-yne Reaction on Alkyne-derivatized Fatty Acids: Biobased Polyols and Cytocompatibility of derived Polyurethanes

Rodolfo J. González-Paz, Gerard Lligadas, Juan C. Ronda, Marina Galià, Virginia Cádiz.
Departament de Química Analítica i Química Orgànica.
Universitat Rovira i Virgili.
Campus Sescelades.
c/Marcel.lí Domingo s/n.
43007 Tarragona, Spain.

Abstract:

With the goal of obtaining renewable diols and polyols for polyurethane (PU) technology, thiol-yne coupling reaction was applied to alkyne-derivatized fatty acids derived from naturally occurring oleic and 10-undecenoic acids. The resulting monomers were then polymerized with 4,4'-methylenebis(phenylisocyanate) to produce the corresponding PUs. The chemical structures, thermal and mechanical properties of the synthesized PUs have been evaluated by FTIR and NMR spectroscopy, DSC, TGA and tensile tester respectively. Moreover, the biocompatibilities of the synthesized PUs with human osteoblast-like cell line (MG63) have also been evaluated for tissue engineering purpose.

Introduction

Polyurethanes (PUs), which can be perfectly tailored by the right choice of isocyanates and polyols, became one of the most dynamic groups of polymers, exhibiting versatile properties suitable for use in practically all the fields of polymer applications.[1] However, in ages of achieving greater awareness of sustainable development, is time to move toward a more sustainable PU technology.

Nowadays, the general strategy that is being used to increase the sustainability of PUs consists in replacing the conventionally used petroleum-based monomers, i.e. isocyanates and polyols, by biobased starting products.[2,3] Although the history of PU technology is strongly linked to renewable resources, plant oils, fatty acids and derivatives have recently attracted significant interest for the production of polyols and isocyanates leading to PUs partially or entirely from lipid feedstock.

Taking into account that the use of alternative renewable resources is only one of the *12 Principles of Green Chemistry* that contributes to sustainability in chemistry,[4] the contribution of this technology to sustainable development must go further than simply exploit biomass. In this context, if the synthesis of a particular polyol or isocyanate is a tedious, inefficient, and expensive process, a significant portion of the benefit provided by PU technology is lost. Therefore, there is no doubt that actual research in this field is moving to a more efficient chemical transformations exemplified by click chemistry reactions.[5] Thiol-ene coupling (TEC) has become an outstanding synthetic tool, owing to its special features such as chemoselectivity, versatility, and the absence of any need for metal catalysts.[6,7] Our group and others recently applied thiol-ene click chemistry to plant oils and fatty acids.[8] Special attention has been paid to TEC with hydroxyl-functionalized thiols as an efficient methodology to prepare a variety of plant-derived diols and polyols.

In this paper, we used the thiol-yne radical coupling (TYC), which can be considered as a sister reaction to the radical TEC, to functionalize with hydroxyl functional groups alkyne-derivatized oleic and 10-undecenoic fatty acids, which are the major products of high oleic sunflower oil saponification and castor oil pyrolysis, respectively. The radical-mediated addition of a thiol to an yne has been known since the first half of the last century.[9,10] As with the TEC, the thiol-yne addition, in general proceeds rapidly under a variety of experimental conditions selectively yielding the mono- or bis-addition products. In the case of the double addition products formed under radical conditions, the reaction of two equivalents of thiol with an alkyne is itself a two-step process (Scheme 1).

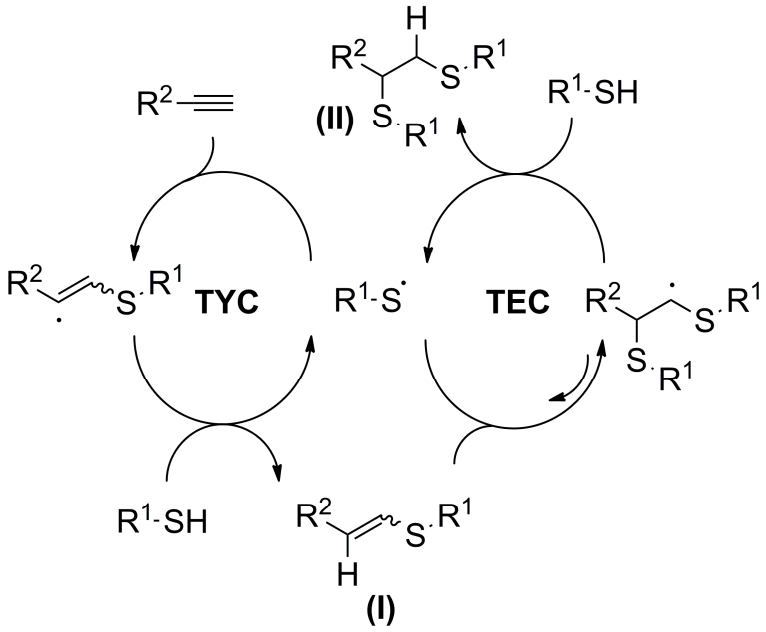

Scheme 1. Sequential addition and hydrogen abstraction steps of primary alkyne and the subsequent vinyl sulfide during a thiol-yne coupling.

The first step involves the addition of thiol to the C≡C triple bond to yield an intermediate vinyl thioether (I) that subsequently undergoes a second, formally TEC reaction with an additional thiol, yielding the 1,2 double-addition product (II) as the sole product in quantitative yield.[10] While the TYC is well-documented in the fields of organic[11] and organometallic chemistry, it has been essentially overlooked in the polymer/materials field. However, a breakthrough has actually been developed in a group of very recent papers where the authors exploited the TYC in the field of polymer chemistry.[12]

Here, TYC double addition using a hydroxyl-functionalized tiol was used as a key step to introduce two primary hydroxyl groups into fatty acid chains. We will focus our discussion on the synthesis of four new plant oil-derived PU precursors, two diols and two triols, as well as the thermal, mechanical and surface properties characterization of the derived linear and crosslinked PUs. Since biobased polymers offer the advantage of being similar to biological macromolecules, for which the biological environment is prepared to recognize and deal with metabolically, we have also evaluated the biocompatibility of the synthesized PUs with human osteoblast-like cell line MG63 for tissue engineering purpose in orthopaedic and trauma surgery. Despite being a tumour

cell line, MG63 cells exhibit many osteoblastic traits, which are characteristic of bone-forming cells.

Experimental Part

Materials

The following chemicals were obtained from the sources indicated and used as received: Oleic acid, 10-undecenoic acid, and trimethylorthoformate (98%), bromine (99%), Amberlist 15, lithium aluminum hydride (95%), acetonitrile, 2,2-dimethoxy-2-phenylacetophenone (DMPA, 99%), 2-mercaptoethanol (99%) and 4,4′-methylenebis(phenylisocyanate) (MDI) (Aldrich), and potassium hydroxide (90%) (Scharlau).

Tetrahydrofuran (THF) was distilled from sodium immediately before use and N,N-dimethylformamide (DMF) was dried with CaH_2 for 24 h and freshly distilled before use.

Synthesis of 10-Undecynoic Acid (UDY).

A 1000 mL, two-necked, round bottom flask provided with a Teflon-coated magnetic bar and a pressure equalized dropping funnel was charged with 46 g (0.25 mol) of 10-undecenoic acid and 500 mL of diethyl ether. The flask was cooled in an ice/water bath, the solution was stirred magnetically, and 48 g (0.3 mol) of bromine was added during a period of 1 h. The mixture was allowed to warm up gradually to room temperature, and after stirring overnight, the solvent and the excess of bromine were removed under reduced pressure. The brown liquid dibromo acid was transferred to a 2 L round-bottomed flask containing 800 mL of n-propanol, and a solution of 120 g of potassium hydroxide in 140 mL of water was added. After heating at reflux temperature for 15 h, 1.5L of water was added and the reaction mixture neutralized with HCl 2N. The product was extracted with several portions of diethyl ether, dried with anhydrous magnesium sulfate, and concentrated under reduced pressure. The residue was distilled under reduced pressure (0.85 mmHg) and the fraction at 122-134 °C was collected. The

product that solidifies on cooling was recrystallized twice from hexanes to obtain a white solid (yield 70%, mp 41-42 °C).

^{1}H NMR ($CDCl_3$/TMS, δ, ppm): 1.24-1.33 (m, 8H), 1.44 (m, 2H), 1.55 (m, 2H), 1.88 (s, 1H), 2.11 (m, 2H), 2.23 (t, 2H), 11.81 (s, 1H).

Synthesis of 9-Octadecynoic Acid (OLY).

9,10-Dibromooctadecanoic acid was obtained using a similar procedure as described above starting from 58 g (0.23 mol) of oleic acid, but dehydrobromination was carried out using a solution of potassium hydroxide (112 g, 2 mol), 50 mL of water, and 400 mL of ethylene glycol monoethylether. The product was distilled under reduced pressure (0.5 mmHg), and the fraction at 196-200 °C was collected. The product solidifies on cooling and was recrystallized from hexane to obtain a white solid (yield 37%).

^{1}H NMR ($CDCl_3$/TMS, δ, ppm): 0.86 (t, 3H), 1.23-1.67 (m, 22H), 2.11 (m, 4H), 2.29 (t, 2H), 11.62 (s, 1H).

Synthesis of Methyl 10-Undecynoate (UDYM) and Methyl 9-Octadecynoate (OLYM).

A 500 mL round-bottomed flask was charged with 54.7 g (0.3 mol) of UDY, 200 mL of methanol, 17 mL (15.9 g, 0.15 mol) of trimethyl orthoformate, and 2 g of Amberlist 15. The mixture was heated under reflux for 4 h, the resin was filtered, and 200 mL of diethyl ether was added. The solution was washed twice with water, dried with anhydrous magnesium sulfate, and the diethyl ether removed under reduced pressure. Methyl 10-undecynoate was purified by fractionated distillation (4 mmHg, 96-98 °C) (yield 87%).

^{1}H NMR ($CDCl_3$/TMS, δ, ppm): 1.24-1.33 (m, 8H), 1.44 (m, 2H), 1.55 (m, 2H), 1.88 (s, 1H), 2.11 (m, 2H), 2.23 (t, 2H), 3.59 (s, 3H).

Methyl 9-octadecynoate was prepared by the same procedure starting from 42 g (0.15 mol) of OLY. The product was purified by fractionated distillation (0.5 mmHg, 125-130 °C) (yield 93%).

^{1}H NMR ($CDCl_3$/TMS, δ, ppm): 0.86 (t, 3H), 1.23-1.67 (m, 22H), 2.11 (m, 4H), 2.29 (t, 2H), 3.65 (s, 3H).

Synthesis of Methyl 9,10-bis(2-hydroxyethylthio)octadecanoate (OLYM-diol).

In a 25-mL flask, 5.0 g (17 mmol) of OLYM was reacted with 5.3 g (57 mmol) of mercaptoethanol. The radical initiator, DMPA, was added in the proportion of 3.4 % mol init./mol C≡C. The amount of acetonitrile necessary to dissolve the photoinitiator was added. The reaction was carried out at room temperature, without deoxygenation, by irradiation with two 9 W UV lamps (λ= 365 nm). After 1 h the completion of the reaction was confirmed by ^{1}H NMR by the complete disappearance of the adjacent hydrogens to internal triple bond signals that appear at 2.15 ppm. The product was purified by column chromatography using hexane:ethyl acetate, 1:1, as eluent, to afford pure OLYM-diol as viscous oil, in a 93% yield.

^{1}H NMR [$CDCl_3$, TMS, δ, (ppm)]: 3.71 (t, -CH_2-OH, 4H), 3.65 (s, -OCH_3), 2.86 (m,-CH-, 2H), 2.70 (t,-CH_2-S-,4H) 2.29 (t, -CH_2-COO), 1.6 (m,-$C\underline{H_2}$-CH-,4H) 1.58 (m, -$\underline{CH_2}$-CH_2-COO,2H) 1.30- 1.26 (m, -CH_2-, 20H) 0.85 (t, -CH_3,)

^{13}C NMR [$CDCl_3$, TMS, δ, (ppm)]: 174.33 (s), 61.32 (t), 60.99 (t), 53 (q), 51.65 (d), 51.56 (d), 36.38 (t), 35.24 (t), 34.1 (t), 33.13 (t), 31.8 (t), 29.45 (t), 29.25 (t), 29.22 (t), 29.20 (t), 29.10 (t), 29.05 (t), 29 (t), 28.05 (t), 27.83 (t), 24.81 (t), 22.62 (t), 14.07 (q).

Synthesis of Methyl 10,11-bis(2-hydroxyethylthio) undecanoate (UDYM-diol).

UDYM-diol was synthesized following the procedure described for OLYM-diol starting from 2.6 g (13 mmol) of UDYM. In this case no radical initiator was used. The product was obtained as viscous oil with 96% yield.

^{1}H NMR [$CDCl_3$, TMS, δ, (ppm)]: 3.74 (t,-CH_2-OH, 4H) 3.65 (s,-OCH_3), 2.78-2.73 (m,-CH_2-S-,4H,-S-$\underline{CH_2}$-CH-,2H,-S-CH,1H), 2.29 (t,-CH_2-COO,2H), 1.6 (m,-C$\underline{H_2}$-CH-,2H) 1.56 (m,-$\underline{CH_2}$-CH_2-COO,2H) 1.30-1.26 (m,-CH_2-,10H).

^{13}C NMR [$CDCl_3$, TMS, δ, (ppm)]: 174.38(s), 61.04(t), 60.77(t), 51.48(q), 46.34 (d), 38.27 (t), 36.12 (t), 34.32 (t), 34.06 (t), 29.28 (t), 29.20 (t), 29.11(t), 29.03(t), 26.74(t), 24.87(t).

Synthesis of 10,11-bis(2-hydroxyethylthio)undecanol (UDYM-triol).

A 250-mL, two-necked, round-bottom flask equipped with a Teflon-coated magnetic bar and a pressure-equalized dropping funnel was charged with a solution of $LiAlH_4$ (0.3 g, 7.8 mmol) in anhydrous THF (15 mL) under argon. UDYM-diol (1.9 g, 5.3 mmol) dissolved in 10 mL of anhydrous THF was added slowly with stirring for 1 h. Anhydrous THF (2 x 10 mL) was added as the viscosity increased. After 30 min, the excess of $LiAlH_4$ was decomposed adding 25 mL of ethyl acetate dropwise, then a saturated 10% H_2SO_4 aqueous solution (50 mL) was added, the phases were separated, and the aqueous layer was extracted with ethyl acetate. The combined organic phase was washed with a saturated aqueous NaCl solution, dried over anhydrous magnesium sulfate, filtered, and the solvent was removed under reduced pressure. The producte was purified by column chromatography using hexane:ethyl acetate, 4:5, as eluent, to afford pure UDYM-triol as viscous oil, in a 89% yield.

^{1}H NMR [$CDCl_3$, TMS, δ, (ppm)]: 3.74 (t,-CH_2-OH, 4H) 3.63 (t,-CH_2-OH,2H), 2.78-2.73 (m,-CH_2-S-,4H,-S-$\underline{CH_2}$-CH-,2H,-S-CH,1H), 1.6 (m,-C$\underline{H_2}$-CH-,2H) 1.56 (m,-$\underline{CH_2}$-CH_2-OH,2H) 1.30-1.26 (m,-CH_2-,12H).

^{13}C NMR [$CDCl_3$, TMS, δ, (ppm)]: 62.84(t), 61.17(t), 60.91(t), 46.32 (d), 38.32 (t), 35.92 (t), 34.19 (t), 34.12 (t), 32.63 (t), 29.31 (t), 29.29(t), 29.27(t), 29.26(t), 26.68(t), 25.65(t).

Synthesis of 9,10-bis(2-hydroxyethylthio)octadecanol (OLYM-triol).

OLYM-triol was synthesized following the procedure described for UDYM-triol starting from 2 g (4.5 mmol) of OLYM-diol. The product was obtained as viscous oil with 88 % yield.

^{1}H NMR [$CDCl_3$, TMS, δ, (ppm)]: 3.71 (t, -CH_2-OH, 4H), 3.63 (t, -CH_2-OH,2H) 2.86 (m, -CH-, 2H), 2.70 (t,-CH_2-S-,4H), 1.6 (m,-C$\underline{H_2}$-CH-,4H) 1.58 (m,-$\underline{CH_2}$-CH_2-OH,2H), 1.30- 1.26 (m, -CH_2-, 20H) 0.85 (t, -CH_3,).

^{13}C NMR [$CDCl_3$, TMS, δ, (ppm)]: 65.03 (t), 62.76 (t), 61.05 (t), 51.96 (d), 51.70 (d), 37.125 (t), 37.123 (t), 32.58 (t),32.08 (t), 31.83 (t), 29.53 (t), 29.49 (t), 29.44 (t), 29.38 (t), 29.33 (t), 29.26 (t), 29.09 (t), 28.03 (t), 25.57 (t), 23.84 (t), 22.62 (t),14.08 (q).

Synthesis of Linear Polyurethanes.

A dry 50 mL round-bottom flask was charged with 12 mL of anhydrous DMF, 6 mmol of diol (UDYM-diol and OLYM-diol), 6 mmol of MDI, and 2%, w/w (with respect to MDI) of tin (II) 2-ethylhexanoate. The flask was immersed into a 50 ºC preheated silicone oil bath with magnetic stirring. The reaction was continued for 24 h, and the PUs were isolated as white solids by precipitation into diethyl ether. Purification of PUs was carried out by dissolving the polymer in the minimum volume of chloroform or THF and reprecipitation into diethyl ether. The pure polymers were dried under vacuum and stored in a desiccator until needed. Films were solution cast from THF and dried at 50 ºC for 1 day and then in a vacuum oven until constant weight.

Synthesis of Crosslinked Polyurethanes.

Triol (UDYM-triol and OLYM-triol) was dissolved in anhydrous THF (50% solution) under argon atmosphere, heated at 55°C and added to a 50% solution of MDI in THF (55 ºC) under argon atmosphere. The solution was homogenized and casted over silanized glass preheated at 50°C. The polyurethane was cured at 50 °C overnight and at 110 °C for 6 hours.

Instrumentation.

The FTIR espectra were recorded on a JASCO 680 FTIR spectrophotometer with a resolution of 2 cm^{-1} in the absorbance mode. An attenuated total reflection (ATR) accessory with thermal control and a diamond crystal (Golden Gate heated single – reflection diamond ATR, Specac. Teknokroma) was used to determine FTIR spectra. ^{1}H 400 MHz and ^{13}C (100.5 MHz) NMR spectra were obtained using a Varian Gemini 400 spectrometer with Fourier transform, $CDCl_3$ as solvent and TMS as internal standards. Size exclusion chromatography (SEC) analysis was carried out with an Agilent 1200 series system equipped with an Agilent 1100 series refractive-index detector. THF was used as an eluent at a flow rate of 1.0 mL/min.

Calorimetric studies were carried out on a Mettler DSC821e and DSC822e thermal analyzer using N_2 as a purge gas (20 ml/min) at scanning rate of 10ºC/min. Thermal stability studies were carried out on a Mettler TGA/SDTA851e/LF/1100 with N_2 as a purge gas. The studies were performed in the 30-800 ºC temperature range at a heating rate in the of 10ºC/min. Tensile properties of the studied samples were measured by means of a mechanical tester MTS Qtest/10 Elite Controller, at a crosshead speed of 2 mm/min, at room temperature. The specimens were cut in rectangular films with approximate dimensions 10/5/0.4 mm (length/width/thickness). At least three specimens of each sample have been used. The wettability of the samples was evaluated by contact angle measurements using CAM 200 KSV Instrument, equipped with Tetha software. Static contact angle measurements were carried out adding a drop 5µl-drops of distilled water by a motor driving syringe at room temperature on three different samples of each material and at least five measurments for each sample, obtaining final presented data a final average value. The morphology of cells was observed using a LEO 1430VP SEM Equipment, the cell-cultured samples were washed twice in 0.15 M cacodylate buffer (Sigma) and fixed for 30 min at 4 ºC with Karnowsky solution (2% paraformaldehyde and 2.5 % glutaraldehyde in 0.15M cacodylate buffer, pH 7.2-7.4, Sigma), dehydrated in increasing EtOH (Sigma) concentrations, dried and coated with a conductive thin gold film, before SEM examination.

Cell culture.

Synthesized PUs were examined as scaffolds for growth of MG63 osteoblast cells. Cells were cultured in Dulbecco's modified Eagle's medium enriched with 10% fetal bovine serum (FBS), glutamine (2mM), penicillin (100 U/ml) and streptomycin (100 μg/ml) (Euroclone, Italy). Cells were maintained at 37° C in a humidified atmosphere with 5% CO_2. The cells were seeded at a density of $10^5 x cm^2$ on the PUs surface. Cell adhesion and viability were assayed by a colorimetric MTS assay after 24 h. The morphology of cell attachment on the scaffolds was observed by scanning electronic microscopy.

MTS assay and cell attachment.

To evaluate cell viability, MTS assay was performed. Cells were cultured on different surfaces for 24 hours. A [3-(4,5-dimethylthiazol-2-yl)-5-(3-carboxymethoxyphenyl)-2-(4-sulfophenyl)-2H-tetrazolium, inner salt (MTS) solution was added to culture medium. After 3 h, culture medium was removed and the solution was read in UV-VIS spectroscopy (V-630 UV-Vis Spectrophotometer, Jasco, USA) at 490 nm. The absorbance was directly proportional to viable cells amount.

To study the morphology of cell attachment, the 24 h cell-cultured PU films were washed twice in 0.15M cacodylate buffer and fixed for 30 minutes at 4°C with Karnowsky solution (2% paraformaldehyde and 2.5% gluteraldehyde in 0.15M cacodylate buffer, pH 7.2-7.4). Following fixation, samples were treated for 30 minutes with 1% osmium tetroxide in 0.15M cacodylate buffer solution. Samples were then dehydrated with graded ethanol (from 50% to 100%), soaked for 30 minutes in hexamethyldisilazane. Completely dried samples were sputter-coated with gold-palladium and observed using scanning electron microscopy (SEM, Leo 1450VP, LeoCo.LTD). Images were collected at different magnifications.

Results and Discussion

Synthesis of Biobased Polyols

Whilst alkenic fatty acids occur abundantly in nature, alkynic fatty acids are rare. However, alkynic fatty derivatives can be obtained in acceptable yields from the corresponding fatty acids by bromation, dehydrobromination from alkenic fatty acids, using well-established procedures.[13] In this study, 10-undecynoic acid (UDY) and 9-octadecynoic acid (OLY) were prepared by dehydrobromination of the corresponding 10-undecenoic and 9-octadecenoic acid derivatives (Scheme 2).

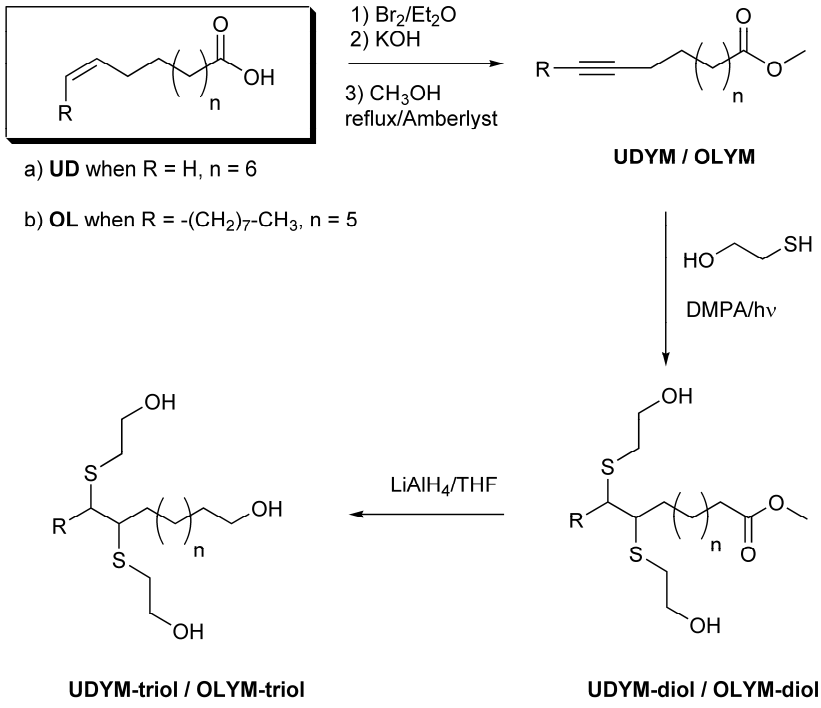

Scheme 2. Synthesis of fatty acid derived polyols starting from 10-undecenoic (UD) and oleic (OL) acids.

The double elimination reaction of 9-octadecenoic acid derivative was carried out using a mixture of ethylene glycol monoethylether and water as a solvent obtaining the expected product in moderate yield.[14] Applying the same conditions to 10-undecenoic acid derivative, 9-undecynoic acid was isolated as a major product due to isomerization of the terminal triple bond. Using a mixture of n-propanol and water to

decrease the reaction temperature, isomerization did not take place an UDY was isolated with 70% yield.

Photoinitiated thiol-yne addition was selected as a key reaction step to functionalize both alkyne-derivatized fatty acids with hydroxyl moieties. Commercial 2-mercaptoethanol was used as a functional thiol and our objective was the 1,2 double addition to the alkyne-derivatized fatty acid. Initially, the kinetics of the coupling between 10-undecynoic acid and 9-octadecynoic acid methyl esters with 2-mercaptoethanol were studied. Reactions were carried out at room temperature under UV-light with/without 2,2-dimethoxy-2-phenylacetophenone (DMPA) as photoinitiator using an excess of thiol (3 equiv. relative to triple bond). Figure 1 compares the C≡C conversion, measured by ^{1}H NMR spectroscopy, as a function of time. Following the same trend observed during the thiol additions to terminal and internal enes, thiol-yne addition to terminal yne is faster reaching complete conversion after 5 min. Moreover, it can even proceed to complete conversion in absence of radical initiator with longer reaction times.

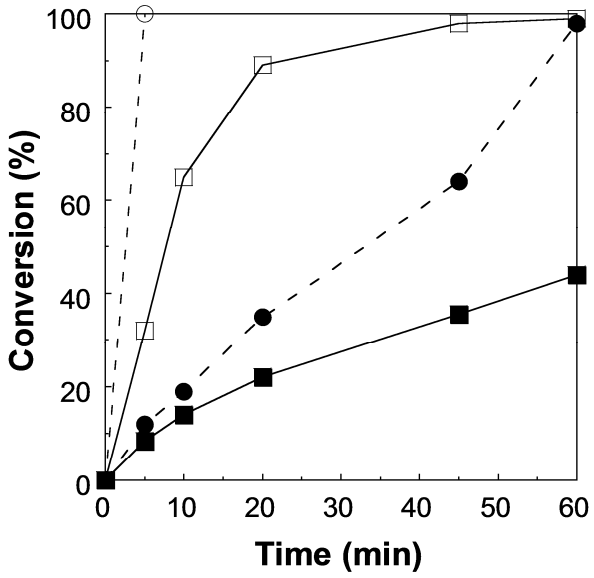

Figure 1. Kinetic plots for the TYC between 2-mercaptoethanol and (○) UDYM and (□) OLYM in the presence of photoinitiator DMPA, and (●) UDYM and (■) OLYM in absence of photoinitiator.

Optimized reaction conditions were applied to UDYM and OLYM to prepare UDYM-diol and OLYM-diol respectively (Scheme 2). Both diols were obtained in high

yields as viscous oils. The evolution of OLYM to the corresponding diols could be followed by ^{1}H NMR. Figure 2A of the initial OLYM shows the characteristic signal *e*/*f* corresponding to methylenes alpha to internal C≡C. The structure of OLYM-diol was confirmed by the disappearance of this signal and the appearance of signals corresponding to mercaptoethanol attached units (Figure 2B). UDYM-diol and OLYM-diol were used as starting materials for the preparation of biobased triols UDYM-triol and OLYM-triol by reduction of methyl ester groups using $LiAlH_4$ as reducing agent (Scheme 2). Spectrum (C) in Figure 2 shows how after reduction of OLYM-diol, signals *a* of methyl ester disappears whereas a new signal *z* corresponding to the newly formed methylol group appears.

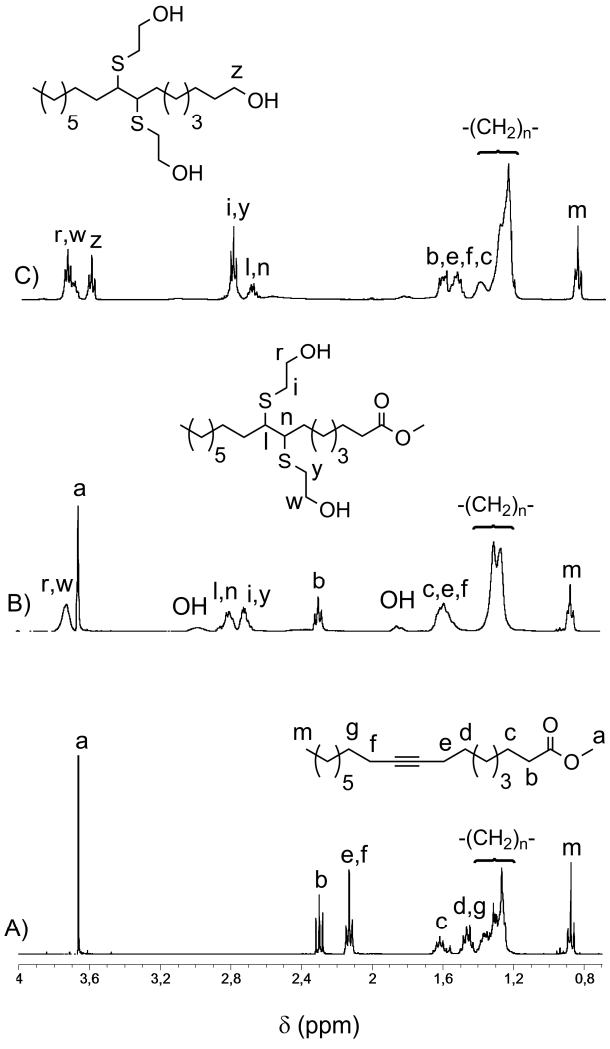

Figure 2. ^{1}H NMR spectra (400 MHz, $CDCl_3$) of: A) OLYM, B) OLYM-diol, and C) OLYM-triol.

Polyurethane Synthesis

UDYM-diol and OLYM-diol were combined with MDI in DMF solution at 50ºC for 24h using tin (II) 2-ethylhexanoate as catalyst. PUs were isolated and purified by two solution-precipitation cycles and subsequent drying under vacuum. The chemical structures of the corresponding linear PUs were assessed by FTIR and NMR spectroscopy. Characteristic IR absorption bands of main chains were observed. Thus, the C=O stretching and NH stretching and bending bands arising from urethane linkages appear at 1701 cm^{-1}, 3320 cm^{-1} and 1532 cm^{-1} respectively. Moreover, the C=O stretching band of dangling methyl ester groups appear at 1730 cm^{-1}. ^{1}H and ^{13}C NMR spectra were in all cases in full concordance with the expected chemical structures of PUs. Table 1 shows the molecular weight and polydispersity of the PUs synthesized. OLYM-diol combined with MDI produced a PU with number-average molecular weight of 48 kDa. However, under the same condicions UDYM-diol produced a PU with molecular weight lower than expected. The latter might be attributed to the higher hygroscopicity of this diol. The presence of water would consume isocyanates and lead to a decrease in the [NCO]/[OH] ratio, resulting in a lower molecular weight. In fact, PU1 showed a peak at 1650 cm^{-1} in the FTIR spectra, which arose from the stretching of urea carbonyl groups. The solubility of both PUs is also collected in Table 1 for a set of representative solvents evidencing that these PUs have high solubility in all solvents except in water.

Table 1. Polycondensation results and solubility of thermoplastic PUs

			SEC [a]		Solubility [b]			
	Diol	Yield (%)	M_n (g/mol)	M_w/M_n	H_2O	DMSO	$CHCl_3$	THF
PU1	UDYM-diol	94	18,200	1.5	-	+	+	+
PU2	OLYM-diol	96	48,230	1.7	-	+	+	+

[a] Number molecular weight determined by SEC in THF against polystyrene standards.

[b] Solubility at 25ºC: + soluble, - insoluble.

UDYM- and OLYM-triols were used to prepare PU thermosets by reaction with MDI in solution of THF. Both triols showed an excellent compatibility with the MDI suspension leading to homogeneous systems before the curing cycle. FTIR analysis was used to confirm complete curing after curing cycle, by the disappearance of the band at 2240 cm^{-1} corresponding to the –N=C=O stretching of the isocyanate group and the appearance of the characteristic absorbances of urethane linkages.

Thermal, Mechanical and Contact Angle Properties

The thermal analysis of PU samples was studied by DSC and TGA. The Tg values of PUs are presented in Table 2. Linear PU formulations, showed Tg's below room temperature, 15ºC for PU1 and 20ºC for PU2, and no crystallinity was observed. As expected, crosslinked PUs showed higher Tg than linear systems. DSC analysis of crosslinked PU3 and PU4 showed Tg values of 42ºC and 59ºC, respectively. Due to the presence of dangling chains in linear and crosslinked OLYM-derived PU systems, higher Tg values would be expected for UDYM-derived PUs. However, Mn data (Table 1) may explain the opposite observed trend.

Table 2. Thermal and mechanical properties of linear and crosslinked PUs

		DSC	TGA	Tensile Properties		
	Polyol	Tg (ºC)	$T_{5\%}$	E [a] (MPa)	σ [b] (MPa)	ε [c] (%)
PU1	UDYM-diol	15	258	0.054	0.035	1693
PU2	OLYM-diol	20	261	0.014	3	965
PU3	UDYM-triol	42	245	143	488	10
PU4	OLYM-triol	59	245	89	378	12

[a] Young's Modulus

[b] Stress at break

[c] Strain at break

The thermal stability of PUs was investigated with TGA in a nitrogen stream and data are collected in Table 2. The thermograms showed three main degradation stages and the derivative of the weight loss versus temperature showed three peaks centered at about 250, 350 and 450 ºC. The first degradation step can be associated to the decomposition of urethane linkages.

Tensile properties of synthesized PUs were investigated at 50 mm gauge length, 0.4 mm thick samples at the extension rate 2 mm/min. Tensile properties are reported in Table 2. Thermoplastic PUs show a behaviour similar to lightly crosslinked amorphous rubbers with low modulus and smooth transition in their stress-strain behaviour. It is important to notice the high elongation at break values: 1693 % for PU1 and 965 % for PU2, reached by both PUs. On the other hand, crosslinked PUs show higher Young modulus. However, PU3 and PU4 Young modulus values of 143 MPa and 89 MPa respectively indicate that crosslinked PUs are rather soft.

Hydrophilicity/hydrophobicity balance strongly affects the biocompatibility of materials. Polyurethanes prepared from vegetable oils are expected to exhibit a non-wetting surface due to the hydrophobic nature of triglycerides. Contact angle measurements (Figure 3) demonstrated the high hydrophobicity of the synthesized PUs. Linear systems PU1 derived from UDYM-diol exhibited contact angle of 94.7º. Compared to the non-branched material, PU2 with dangling aliphatic chains is conjectured to be more hydrophobic and therefore exhibit a larger contact angle. In fact, the angle measured for the branched linear polyurethane PU2 derived from OLYM-diol is slightly higher (97.2º). Crosslinked PUs derived from UDYM-triol and OLYM-triol were more hydrophilic showing contact angle values of 85.6º and 87.3º, respectively. These results agree with the increase of the urethane content in the final network.

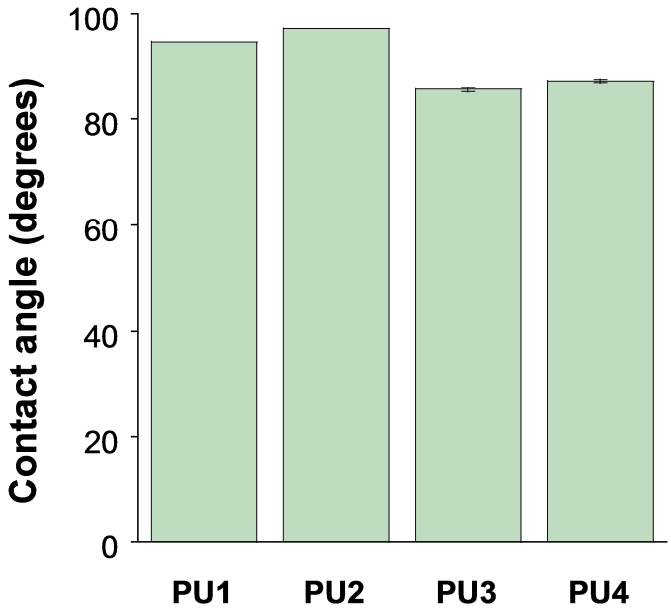

Figure 3. Contact angle values for PUs.

Cell Compatibility

PUs have found numerous applications as scaffolds in tissue engineering. Bone repair, for example, is an attractive and natural target for tissue engineering, as bone regeneration is needed for the therapy of numerous serious clinical indications. The use of PUs as bone grafts and bone substitute materials in orthopedic medicine is well known. The osteoblast cell line MG63 was used to evaluate the biocompatibility of the PUs. These cells are derived from a human osteosarcoma and express a number of features characteristics of osteoblasts.[15] The cytotoxicity of PUs was evaluated by examining MG63 cell responses to their surfaces over a period of 24h at 37ºC. Cell viability based upon intact metabolic activity was monitored using a MTS assay, which was frequently applied to screen the polymer cytotoxicity for its reliability and sensibility. Figure 4 shows cell viability of MG63 osteoblastic-like cells cultured on the PU specimens and under control conditions (absence of materials, standard plastic culture plates), evaluated by MTS reduction. Compared to the control culture, PUs do not show significant cytotoxicity against cells reaching values higher to 75 % in all cases. No significant differences were observed between linear and crosslinked systems or PUs derived from oleic and 10-undecenoic acid.

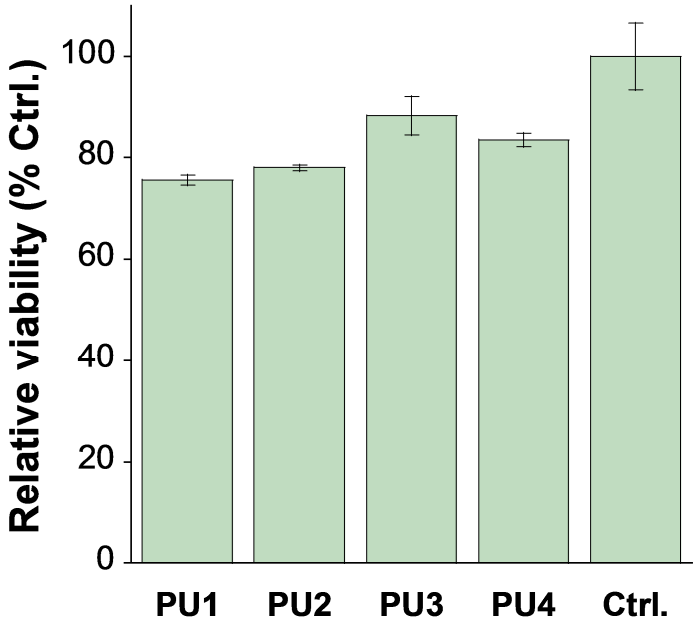

Figure 4. MTS cytotoxicity results for control and PUs.

Cell morphology on the various polymer surfaces was analyzed by SEM. As can be seen in Figure 5, cells successfully attached to all samples after 24 h. In agreement with MTS data, best results were obtained for crosslinked PU3. PU3 also showed the highest hydrophilic character according contact angle measurements. Cells were well attached and spread out, displaying a flat configuration and normal morphology. Moreover, neighbor cells connected with each other through cytoplasmatic extensions. Overall, mostly rounded morphologies were observed in PU1, PU2 and PU4.

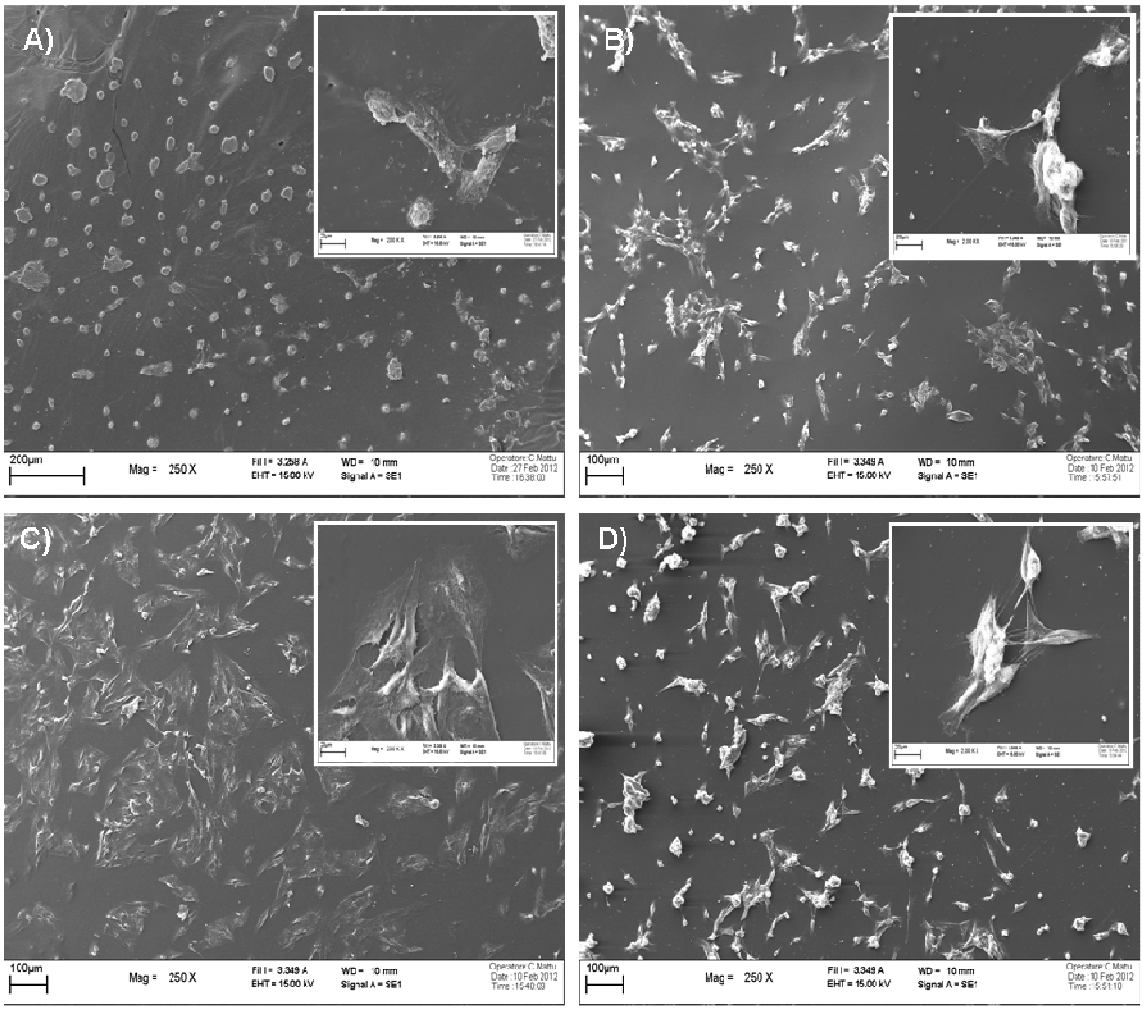

Figure 5. Scanning electronic micrographs of MG63 cells cultured on PUs: A) PU1, B) PU2, C) PU3, and D) PU4.

Conclusions

In this study we describe a novel route to obtain diols derived from fatty acids. The application of thiol-yne additions to 10-undecenoate and oleate derivatives was carried to obtain the required monomers. The resulting monomers were then polymerized with MDI to produce the corresponding thermoplastic and thermosetting polyurethanes. The thus prepared polyurethanes were characterized and revealed good thermal and mechanical properties. Cytocompatibility of the PUs was investigated in terms of cell attachment of an osteoblastic cell line. Based on these obtained results, we anticipate that these PUs will be useful as polymeric scaffolds for tissue engineering.

Acknowledgements

The authors express their thanks to CICYT (Comisión Interministerial de Ciencia y Tecnología) (MAT2011-24823) for financial support for this work and to Prof. G. Ciardelli and Dr. F. Boccafoschi for cytocompatibility assays.

References

[1] Woods, G. The ICI Polyurethanes Book, 2nd ed..; Wiley Interscience, John Wiley & Sons: New Cork, NY, 1990.

[2] Lligadas, G.; Ronda, J.C.; Galià, M.; Cádiz, V. Biomacromolecules 2010, 11, 2825-2835.

[3] Desroches, M.; Escouvois, M.; Auvergne, R.; Caillol, S.; Boutevin, B. Polym. Rev. 2012, 52, 38-79.

[4] Anastas, P. T., Warner, J. C. In Green Chemistry: Theory and Practice, Oxford University Press Inc.: New York, NY, 1998.

[5] Kolb, H. C.; Finn, M. G.; Sharpless, K. B. Angew. Chem. Int. Ed. 2001, 40, 2004-2021

[6] Dondoni, A. Angew. Chem. Int. Ed. 2008, 47, 8995-8997.

[7] Kade, M. J.; Burke, D. J.; Hawker, C. J. J. Polym. Sci., Part A: Polym. Chem. 2010, 48, 743–750.

[8] Samuelsson, J.; Jonsson, M.; Brinck, T.; Johansson, M. J. Polym. Sci., Part A: Polym. Chem. 2004, 42, 6346–6352; Claudino, M.; Johansson, M.; Jonsson, M. Eur. Polym. J., 2010, 46, 2321–2332; Bantchev, G. B.; Kenar, J. A.; Biresaw, G.; Han, M. G. J. Agric. Food Chem. 2009, 57, 1282–1290; Lluch, C.; Ronda, J. C.; Galià, M.; Lligadas, G.; V. Cádiz, Biomacromolecules, 2010, 11, 1646–1653; Turunc, O.; Meier, M. A. R. Macromol. Rapid Commun., 2010, 31, 1822–1826; Turunc, O.; Meier, M. A. R., Green Chem., 2011, 13, 314–320; Lluch, C.; Lligadas, G.; Ronda, J. C.; Galià, M.; Cádiz, V. Macromol. Rapid Commun., 2011, 32, 1343–1351; Gonzalez- Paz, R. J.; Lluch, C.; Lligadas, G.; Ronda, J. C.; Galià, M.; Cádiz, V. J. Polym. Sci., Part A: Polym. Chem. 2011, 49, 2407–2416; Desroches, M.; Caillol, S.; Lapinte, V.; Auverge, R.; Boutevin, B. Macromolecules 2011, 44, 2489-2500; Desroches, M.; Caillol, S.; Auverge, R.;

Boutevin, B.; David, G. Polym. Chem. 2012, 3, 450-457; Palaskar, D. V.; Boyer, A.; Cloutet, E.; Le Meins, J-F.; Gadenne, B.; Alfos, C.; Farcet, C.; Cramail, H. J. Polym. Sci., Part A: Polym. Chem. 2012, 50, 1766-1782.

[9] Bader, H.; Cross, L. C.; Heilbron, I.; Jones, E. R.H. Chem. Soc. J. 1949, 1, 619-623

[10] Sauer, J.C. J. Am. Chem. Soc. 1957, 79, 5314-5315.

[11] Minozzi, M.; Monesi, A.; Nanni, D.; Spagnolo, P.; Marchetti, N.; Massi, A. J. Org. Chem. 2011, 76, 450-459.

[12] Fairbanks, B.D.; Scott, T.F.; Kloxin, C.J.; Anseth, K.S.; Bowman, C.N. Macromolecules, 2009, 42, 211-217; Chan, J.W.; Hoyle, C.E.; Lowe, A.B. J. Am. Chem. Soc. 2009, 131, 5751-5753; Hensarling, R.M.; Doughty, V.A.; Cjan, J.W.; Patton, D.L. J. Am. Chem. Soc. 2009, 131, 14673-14675; Konkolewicz, D.; Gray-Weale, A.; Perrier, S. J. Am. Chem. Soc. 2009, 131, 18075-18077; Chan, J.W.; Zhou, H.; Hoyle, C.E.; Lowe, A.B. Chem. Mater. 2009, 21, 1579-1585; Yu, B.; Chan, J.W.; Hoyle, C.E.; Lowe, A.B. J. Polym. Sci. Part A: Polym. Chem. 2009, 47, 3544-3557; Fairbanks, B.D.; Sims, E.A.; Anseth, K.S.; Bowman, C.N. Macromolecules, 2010, 43, 4113-4119; Chan, J.W.; Shin, J.; Hoyle, C.E.; Bowman, C.N.; Lowe, A.B. Macromolecules, 2010, 43, 4937-4942; Hoogenboom, R. Angew. Chem. Int. Ed. 2010, 49, 3415-3417; Huynh, V.T.; Chen G.; Souza, P; Stenzel, M.H. Biomacromolecules, 2011, 12, 1738-1751; Liu, J.; Lam, J.W.Y.; Jim, C.K.W.; Ng, J.C.Y.; Shi, J.; Su, H.; Yeung, K.F.; Hong, Y.; Faisal, M.; Yu, Y.; Wong, K.S.; Tang, B.Z. Macromolecules, 2011, 44, 68-79.

[13] Vogel's Textbook of Practical Organic Chemistry, 5th ed.; Furniss, B. S., Hannaford, A. J., Smith, P. W. G., Tatchell, A. R., Eds.; Longman Scientific & Technical: Harlow, 1989.

[14] Lligadas, G.; Ronda, J.C.; Galià, M.; Cádiz, V. Biomacromolecules 2007, 8, 1858-1864.

[15] Clover, J.; Gowen, M. Bone 1994, 15, 585-591.

CHAPTER III

Thiol-yne reaction on alkyne-derivatized fatty acids: thiol- reactive linear polyurethanes

Thiol-yne Reaction of Alkyne-derivatized Fatty Acids: Thiol-Reactive Linear Polyurethanes

Rodolfo J. González-Paz, Gerard Lligadas, Juan C. Ronda, Marina Galià, Virginia Cádiz.
Departament de Química Analítica i Química Orgànica.
Universitat Rovira i Virgili, Campus Sescelades.
c/Marcel.lí Domingo s/n, 43007 Tarragona, Spain.

Polyurethanes (PU's) are a versatile class of polymers used in todays in practically all the fields of polymer applications.[1] PUs which can be perfectly tailored by the right choice of diisocyanates, diols or polyols and catalyst, became one of the most dynamic groups of polymers, exhibiting versatile properties suitable for use in medicine, construction, automotive, flooring and sports.[2] In ages of achieving greater awareness of sustainable development, PU technology is progressively moving towards environmentally friendly chemicals and processes. The general strategy that is being used to increase the sustainability of PUs consists in replacing the conventionally used petroleum-based monomers, i.e. isocyanates and polyols, by biobased starting products.[3,4] Although the history of PU technology is strongly linked to renewable resources, plant oils, fatty acids and derivatives have recently attracted significant interest for the production of polyols and isocyanates leading to PUs partially or entirely from lipid feedstock.

Recently, much attention is paid to the development of functional polymers, including PUs, as these materials would lead to new applications that can broaden the classical market. A broad palette of functional groups including hydroxyl, ester, and amino groups has been directly introduced into linear PUs by using a functional building block. Nevertheless, careful attention must always be paid toward the inertness of the introduced functional groups during the PU synthesis. Thus, usually tedious protection/deprotection steps are required. On the other hand, functionalization strategies of PUs are moving to functional groups that may be involved in an efficient chemical transformations exemplified by click chemistry reactions with high yields and with little or no byproduct.[5] The combination of polyurethanes and click chemistry was

explored by Fournier et al. [6]In this case, the most popular reaction of the chemical concept click chemistry, the highly efficient, regioselective and orthogonal copper(I) catalyzed alkyne-azide cycloaddition reaction, was used to functionalize alkyne containing linear PU chains, as well as in films and foams, with a range of azide containing molecules. Recently, efforts have been made to the application of suitable metal-free click reactions to the functionalization of linear PUs. A maleimide containing diol was incorporated in different ratios into the PU backbone and subsequently coupled with several functional thiols, via the efficient metal-free thiol-maleimide coupling reaction. In this case, classical drawbacks associated to copper(I) catalyzed alkyne-azide cycloaddition reactions such as undesired coloring and safety concerns with low molecular weight azides are avoided.[7]

Our group and others have widely applied thiol-ene (TEC) and more recently thiol-yne (TYC) to plant oils, fatty acids and derivatives paying special attention to the preparation of biobased diols and polyols.[8] TEC and TYC have become an outstanding synthetic tools, owing to its special features such as chemoselectivity, versatility, and the absence of any need for metal catalysts.[9,10] The TYC, whose discovery dates back to the mid-1900s,[11] serves to introduce two thiol fragments across a carbon-carbon triple bond. Notably, the thiol-yne reaction can be photoinitiated in the UV-visible range (254-470 nm) and proceeds at room temperature with high efficiency in the presence of oxygen/water. Recently, Lo Conte et al. demonstrated for small molecules[12] and later more complex and biologically relevant molecules[13] that the photoinduced hydrothiolation of the triple bonds can be carried out by the sequential addition of two different thiols. Thus, under suitable reaction conditions the vinyl sulphide intermediate formed by addition of a first thiol can be trapped by a second and different thiol via a thiol-ene type coupling.

The aim of the present work was to synthesize and functionalize thiol-reactive linear polyurethanes from renewable feedstock. To achieve this goal, a vinyl sulphide-containing diol has been synthesized from 10-undecynol, a 10-undecenoic acid derivative which is the major product of castor oil pyrolysis, and 2-mercaptoethanol. 10-undecynol was prepared by reduction of 10-undecinoic acid methyl ester, which was prepared by successive bromation, dehydrobromination of the corresponding alkenic fatty acid. The further reaction of vinyl sulphide-containing diol with MDI to synthesize

linear PU bearing functionalities precisely located on the main chain was carried out. Finally, the PU was functionalized with 7-mercapto-4-methylcoumarin as fluorescent tag.

Reaction conditions were optimized to allow only one equivalent of 2-mercaptoethanol to add to the alkyne-fatty alcohol. Thus, coupling between the two components was carried out using different alkyne/thiol molar ratios under thermal and photoinitiated conditions as summarized in Table 1. Reactions preformed under the thermal conditions (80ºC) were carried out using AIBN as a radical initiator, whereas photoinduced reactions were carried out at room temperature under UV irradiation (365 nm) using DMPA as a photoinitiator. All reactions were performed for 15 min. The highest amount of vinyl sulphide diol was obtained using 10 % mol AIBN as a thermal initiator and a slight excess of thiol. Lower amounts of initiator lead to a significant % of unreacted alkyne. Vinyl sulphide-containing diol was isolated by column chromatography as a mixture of *E* and *Z* isomers.

Table 1. Reaction conditions for the monoaddition of 2-mercaptoethanol to 10-undecynol.

Radical Initiator	Molar Ratio Alkyne : Thiol : Initiator	Unreacted Alkyne (%)	Monoadition product (%)	Diadition product (%)
-	1 : 1 : 0	100	-	-
-	1 : 2 : 0	80	3	17
DMPA	1 : 0.25 : 0.005	60	19	21
DMPA	1 : 0.5 : 0.005	47	26	25
DMPA	1 : 0.25 : 0.036	58	19	23
DMPA	1 : 0.5 : 0.036	38	30	32
DMPA	1 : 1 : 0.036	26	27	47
AIBN	1 : 1 : 0.05	32	38	30
AIBN	1 : 1 : 0.1	7	65	28
AIBN	1 : 1.05 : 0.1	2	80	18
AIBN	1 : 1.1 : 0.1	3	60	37
AIBN	1 : 1.15 : 0.1	3	51	46

Figure 1 shows the ^{1}H and ^{13}C NMR spectra of the isolated product with all the assignments. The presence of the vinyl thioether intermediate was confirmed by the presence of two sets of signals between 5.5-6.0 ppm corresponding to the *E* and *Z,* C-C double bond protons. Signals b/b' and e/e' also appear splited into two signals due to the presence of both isomers. The unequivocal assignments could be carried out using 2-D NMR gHSQC experiments. Thus, it could be proved that whereas ^{1}H NMR spectrum shows protons d/d' more shielded than c/c', the corresponding carbons showed inverse trend in ^{13}C NMR spectrum.

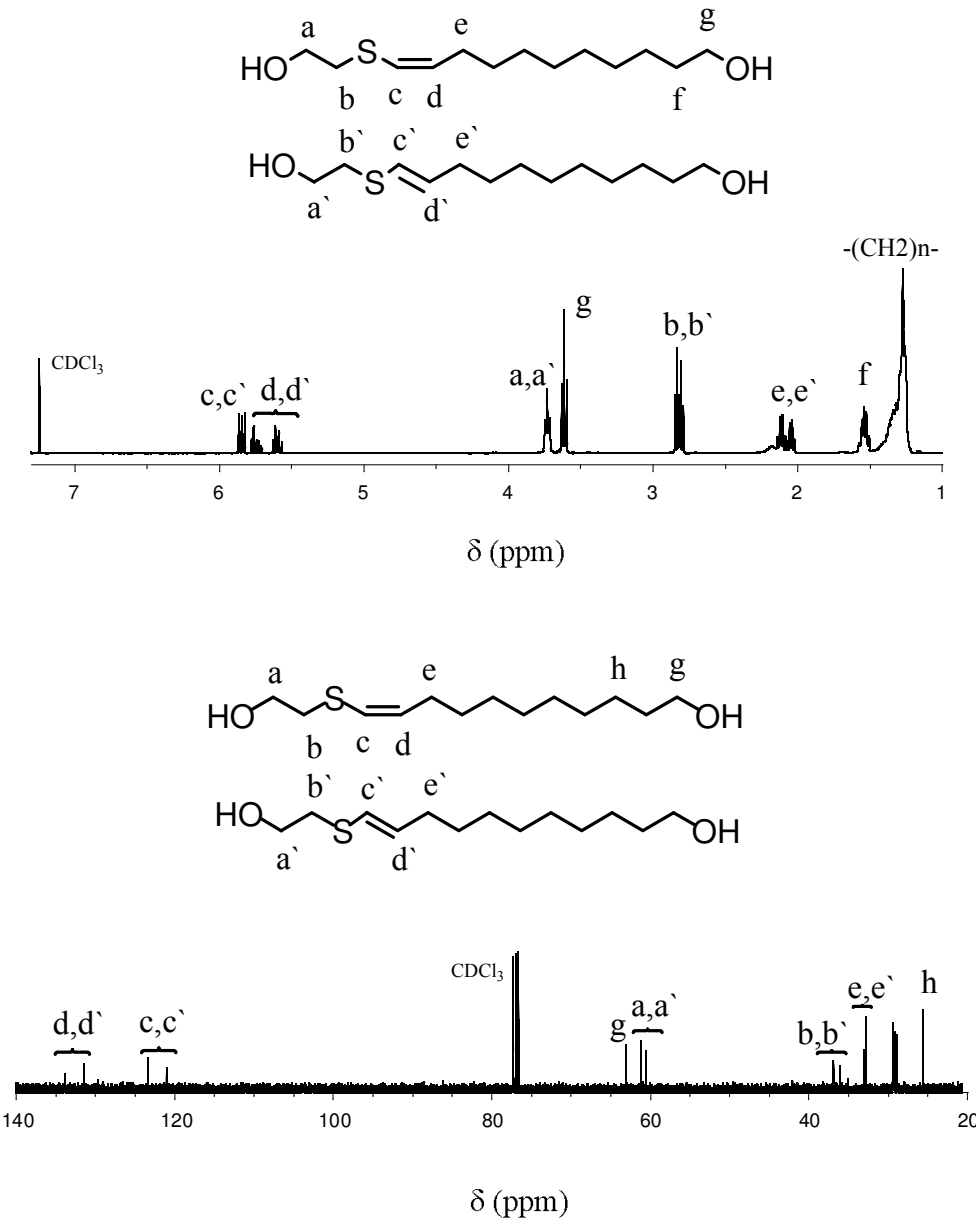

Figure 1. ^{1}H and ^{13}C NMR spectra of UDEM-diol.

The synthesis of a vinyl sulphide-containing linear PU was performed using an equimolar amount of MDI in DMF at 50ºC for 12h in the presence of 2%, w/w (with respect to MDI) of tin (II) 2-ethylhexanoate. PU was isolated quantitatively by two precipitations in diethyl ether and finally dried under vacuum overnight prior to further characterization. Figure 2 shows the ^{1}H NMR spectrum of the synthesized PU. The resonance of C-C double bond protons appears at around 6 ppm proving that the functionalized diol has been incorporated into the polymer without any side reaction.

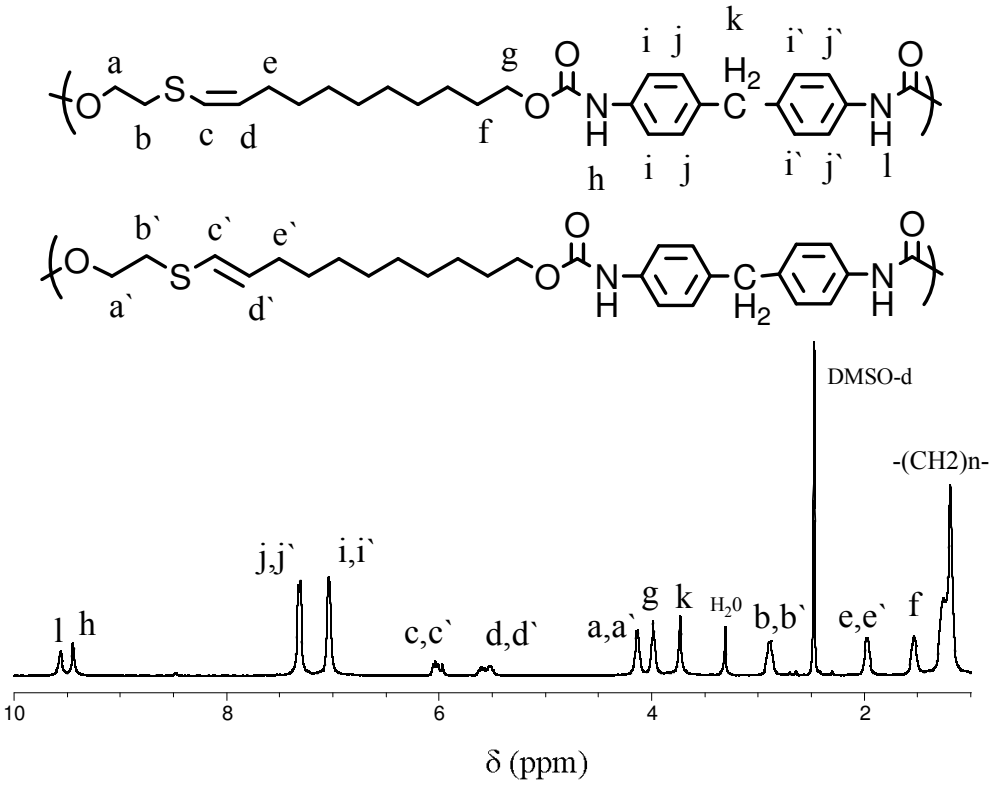

Figure 2. ^{1}H NMR spectra of PU.

Molecular weight by SEC and solubilities of the PU were studied and results are summarized in Table 2. Molecular weight of 66,100 Da was obtained using polystyrene standards as a reference. Synthesized PU was soluble in all tested solvents excepting water and $CHCl_3$.

Table 2. Polycondensation results and some properties of PU.

			SEC [a]			Solubility [b]			
T (ºC)	t (h)	Yield (%)	M_n (g/mol)	M_w (g/mol)	M_w/M_n	H_2O	DMSO	$CHCl_3$	THF
50	12	99	66,100	140,120	2.1	-	+	-	+

[a] Number and average molecular weights determined by GPC in THF against PS standards.

[b] Solubility at 25 ºC: + soluble, - insoluble.

Thermal and mechanical properties were studied by DSC, TGA, and DMTA (Table 3). PU showed a glass transition temperature (T_g) at 65 ºC and a melting process at 132 ºC. 5% Weight loss temperature under nitrogen atmosphere at around 300 ºC was observed as expected for PU-type polymer. Concerning mechanical properties, PU showed a typical behaviour of semicrystalline polymer. Tensile strength and elongation at break were evaluated from stress-strain curve shown in Figure 3.

Table 3. Thermal and mechanical properties of PU

DSC			TGA (ºC)		Mechanical Properties	
T_g (ºC)	T_{m1} (ºC)	ΔH_1 (J/g)	$T_{5\%}$	T_{max}	σ_{max} (MPa)	ε_{max} (%)
65	132	24	298	351/470	27	400

PUs containing vinyl sulphide groups in the main chain are expected to be highly thiol reative. Vinyl-sulphide PU was studied in THF solution using a 7-mercapto-4-methylcoumarin (Cm-SH) as a fluorescent probe using DMPA as a photoinitiator. The success of the polymer modification was assessed by ^{1}H NMR analysis. Figure 4 shows how after irradiation at 365 nm for 2 h signals corresponding to the C-C double bonds completely disappeared and new signal corresponding to coumarin moiety appeared.

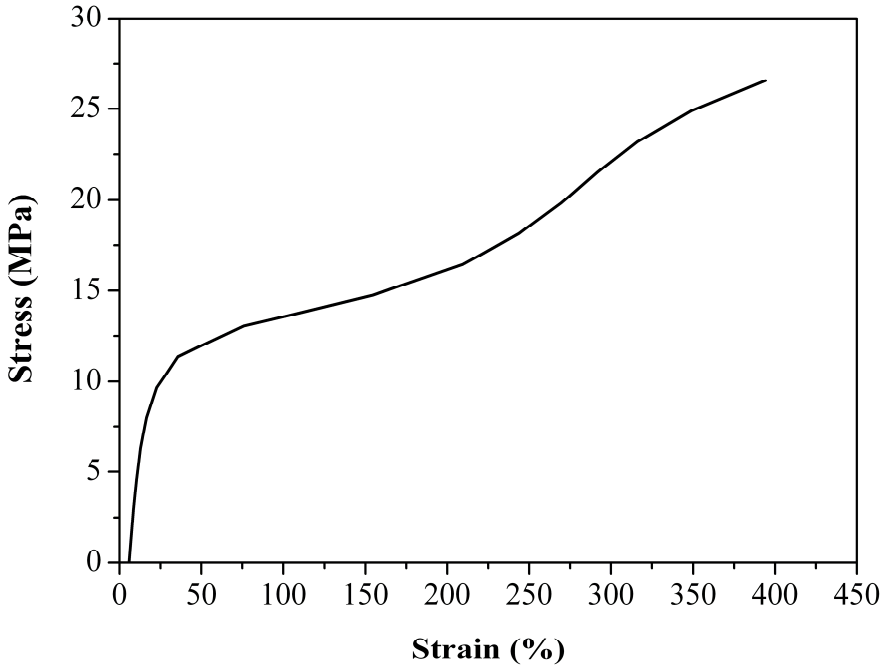

Figure 3. Stress-strain curve of the PU

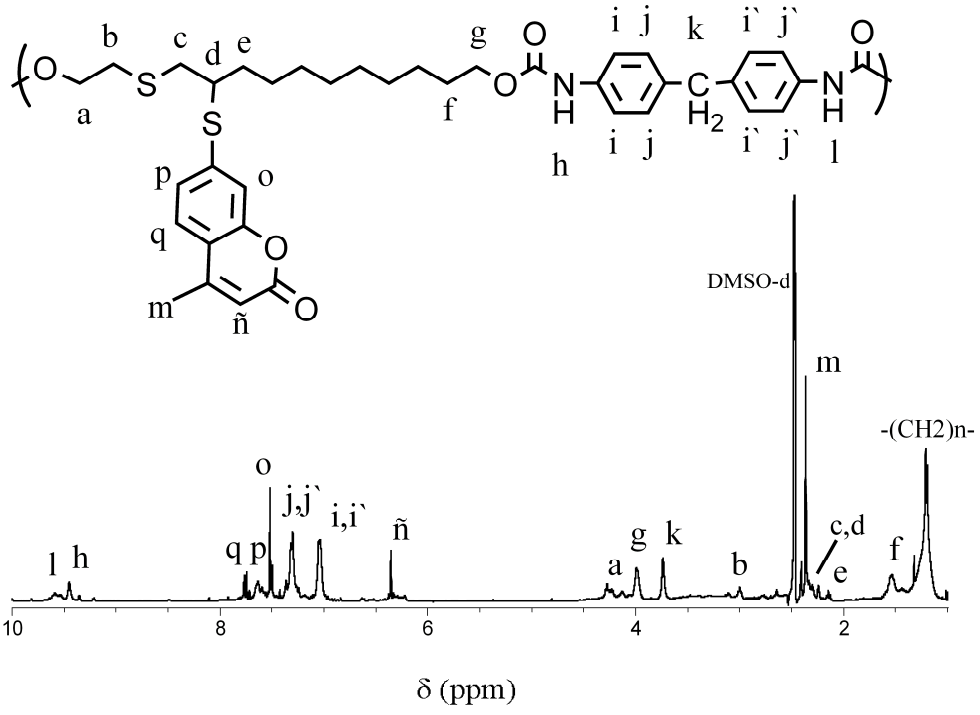

Figure 4. ^{1}H NMR spectra of PU-Cm.

The incorporation of coumarin moiety to PU was assessed by fluorescence spectroscopy. Figure 5a shows the emission spectrum of Cm-SH solution after excitation at 358 nm. The emission band presents a maximum at 400 nm. When emission fluorescence spectrum of the modified PU was recorded in the same experimental conditions, a new emission band appears at 531 nm and the maximum of the initial band is shifted to 416 nm, which is indicative that the emission of coumarin is produced in a different chemical environment (Figure 5b). Considering that initial PU shows a lower emission band at 460 nm is possible to conclude that coumarin moiety has been linked to PU main chain.

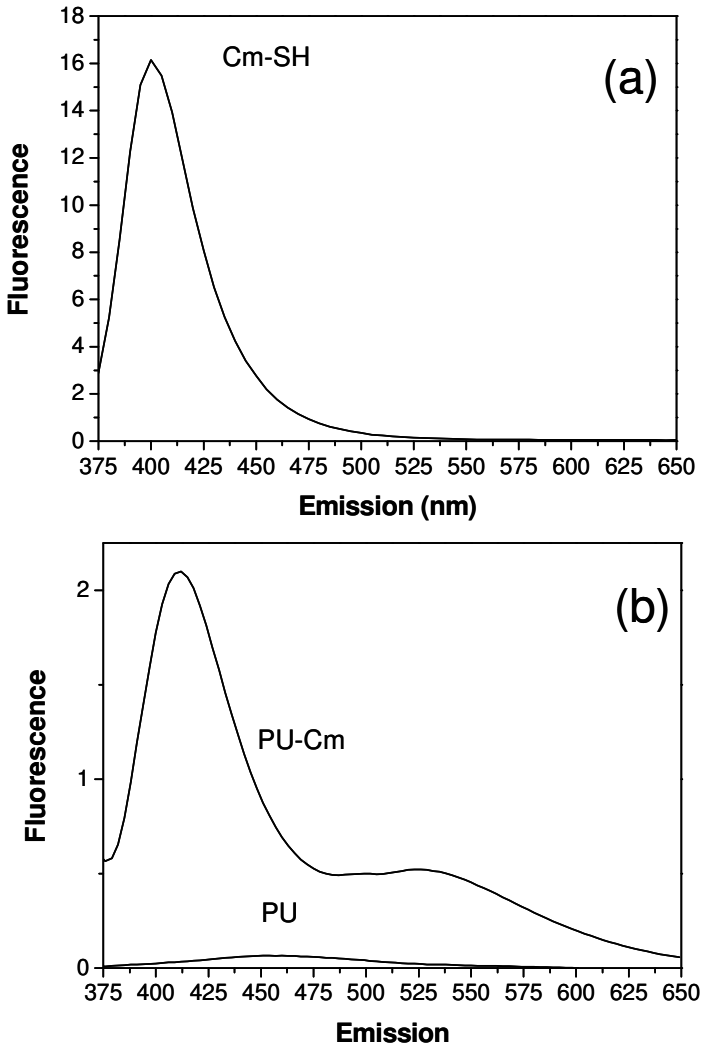

Figure 5. Fluorescence spectrum of the (a) Cm-SH, (b) PU and PU-Cm in DMF solution with excitation (λ_{exc}) at 358 nm.

In view of these results this technique was used to study the surface modification of synthesized vinyl-sulphide PU in the search of thiol-reactive PU scaffolds. The surface modification of synthesized vinyl-sulphide PU was studied using a Cm-SH as a fluorogenig tag.[14] PU films were prepared by casting from DMF solution. PU films were immersed into a acetonitrile solution containing 1.9% (m/V) of fluorescent thiol and 0.2% (m/V) of DMPA. UV irradiation was used to initiate the chemical modification. PU functionalization was characterized by fluorescence spectroscopy.

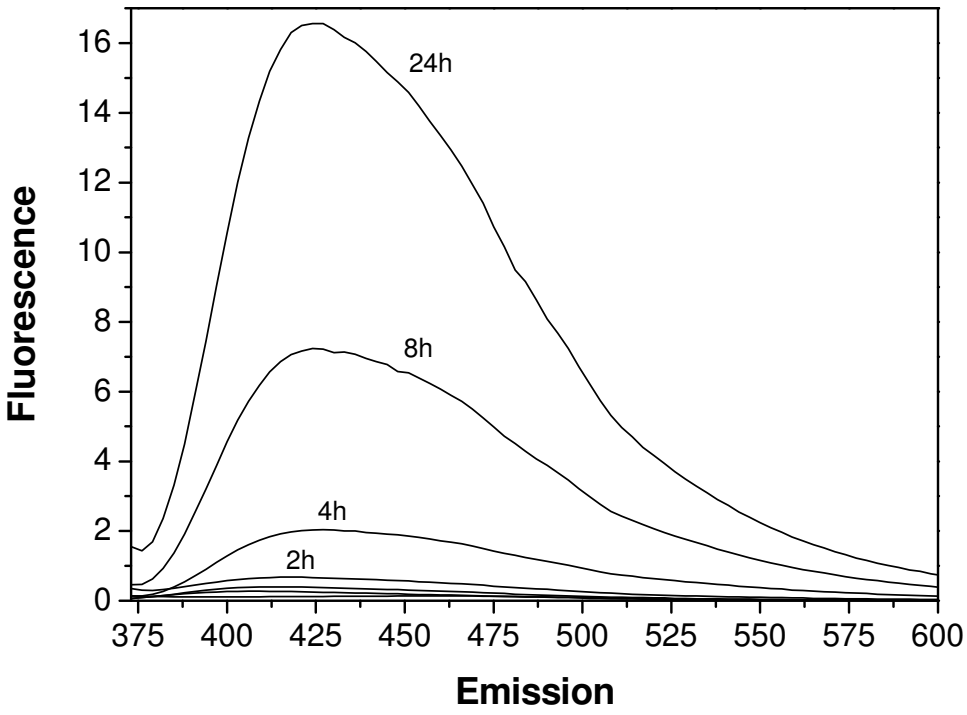

Figure 6. Fluorescence spectrum of the PU films with excitation (λ_{exc}) at 358 nm upon increasing additions of Cm-SH on the PU surface at different reaction times.

Figure 6 shows the emission spectrum of the PU films with excitation at 358 nm upon increasing thiol-ene additions of Cm-SH on the PU surface at different reaction times. As the reactions proceed, the intensities of the emission spectra (425 nm) increased, with sufficient sensitivity to monitor the thiol-ene addition of Cm-SH to vinyl sulphide groups present on PU surface.

Nowadays[15] this behavior may be exploited in biomedical applications since these fluorescence-sensitive polymers not only facilitate the delivery of therapeutic

agents but also allow to monitoring of the degradation profile of implants over time by fluorescence imaging.

Experimental Part

Materials

The following chemicals were obtained from the sources indicated and were used as received: 10-undecenoic acids, trimethylorthoformate 98% (from Fluka), potassium hydroxide (90%, Scharlau), Amberlist 15, lithium aluminum hydride ($LiAlH_4$, 95%), 2,2-dimethoxy-2-phenylacetophenone (DMPA, 99%), 2,2`-azobis(2-methylpropionitrile) (AIBN, 99%), 2-mercaptoethanol (99%), tin(II) 2-ethylhexanoate, 4,4′-methylenebis(phenylisocyanate) (MDI), 7-mercapto-4-methylcoumarin (Cm-SH) and bromine (from Aldrich).

Tetrahydrofuran (THF) was distilled from sodium immediately before use, N,N-dimethylformamide (DMF) was dried with CaH_2 for 24 h and freshly distilled before use. Other solvents were purified by standard procedures.

Synthesis of 10-Undecynoic Acid.

A 1000 mL, twonecked, round bottom flask provided with a Teflon-coated magnetic bar and a pressure equalized dropping funnel was charged with 46 g (0.25 mol) of 10-undecenoic acid and 500 mL of diethyl ether. The flask was cooled in an ice/water bath, the solution was stirred magnetically, and 48 g (0.3 mol) of bromine was added during a period of 1 h. The mixture was allowed to warm up gradually to room temperature, and after stirring overnight, the solvent and the excess of bromine was removed under reduced pressure. The brown liquid dibromo acid was transferred to a 2 L round-bottomed flask containing 800 mL of n-propanol, and a solution of 120 g of potassium hydroxide in 140 mL of water was added. After heating at reflux temperature for 15 h, 1.5L of water was added and the reaction mixture neutralized with HCl 2N. The product was extracted with several portions of diethyl ether, dried with anhydrous

magnesium sulfate, and concentrated under reduced pressure. The residue was distilled under reduced pressure (0.85 mmHg) and the fraction at 122-134 °C was collected. The product that solidifies on cooling was recrystallized twice from hexanes to obtain a white solid (yield 70%, mp 41-42 °C).

^{1}H NMR ($CDCl_3$,TMS, δ, ppm): 1.24-1.33 (m, 8H, -CH_2-), 1.44 (m, 2H, , -$\underline{CH_2}$-CH_2-C≡CH), 1.55 (m, 2H, -$\underline{CH_2}$-CH_2-COOH), 1.88 (s, 1H, -C≡CH), 2.11 (m, 2H, -CH_2-C≡CH), 2.23 (t, 2H, -CH_2-COOH), 11.81 (s, 1H, -COOH).

^{13}C NMR (CDCl3, δ, ppm): 180.67 (s), 84.89 (s), 68.31 (d), 34.27 (t), 29.30 (t), 29.19(t), 29.01(t), 28.65(t), 28.50(t), 24.79 (t), 18.55 (t).

Synthesis of Methyl 10-Undecynoate.

A 500 mL round-bottomed flask was charged with 54.7 g (0.3 mol) of 10-undecynoic acid, 200 mL of methanol, 17 mL (15.9 g, 0.15 mol) of trimethyl orthoformate, and 2 g of Amberlist 15. The mixture was heated at reflux temperature for 4 h, resin was filtered, and 200 mL of ether was added. The solution was washed twice with water and dried with anhydrous magnesium sulfate, and the ether was removed under reduced pressure. Methyl 10-undecynoate was purified by fractionated distillation (4 mmHg, 96-98 °C) (yield 87%).

^{1}H NMR ($CDCl_3$,TMS, δ, ppm): 1.24-1.33 (m, 8H, -CH_2-), 1.44 (m, 2H, -$\underline{CH_2}$-CH_2-C≡CH), 1.55 (m, 2H, -$\underline{CH_2}$-CH_2-$COOCH_3$), 1.88 (t, 1H, -C≡CH), 2.15 (m, 2H, -CH_2-C≡CH), 2.28 (t, 2H, -CH_2-$COOCH_3$), 3.65 (s, 3H, -$COOCH_3$).

^{13}C RMN (CDCl3,TMS, δ, ppm): 18.49 (t), 25.02 (t), 29.30 (t), 29.19(t), 29.01(t), 28.65(t), 28.50(t) , 34.18 (t), 51.57 (q), 68.26 (d), 84.78 (s), 174.38 (s).

Synthesis of 10-Undecynol.

A 250-mL, two-necked, round-bottom flask equipped with a Teflon-coated magnetic bar and a pressure-equalized droppingfunnel was charged with LiAlH4 (0.3 g, 7.8 mmol) and anhydrous THF (15 mL) under argon. Methyl 10-Undecynoate (1.9 g,

5.3 mmol) dissolved in 10 mL of anhydrous THF was added slowly with stirring for 1 h. Anhydrous THF (2 x 10 mL) was added as the viscosity increased. After 30 min, excess $LiAlH_4$ was decomposed by the addition of 25 mL of ethyl acetate dropwise, then a saturated 10% H_2SO_4 aqueous solution (50 mL) was added, the phases were separated, and the aqueous layer was extracted with ethyl acetate. The combined organic phase was washed with a saturated aqueous NaCl solution, dried over anhydrous magnesium sulfate, filtered,and the solvent was removed under reduced pressure. The producte was purified by vacuum distillation (140-142 ° C, 0.85 mm Hg), to afford pure UDYM-diol in a 89% yield.

^{1}H NMR [$CDCl_3$, TMS, δ, (ppm)]: 3.62 (t, -CH_2-OH,2H), 2.15 (t, -$\underline{CH_2}$-C≡CH, 2H), 1.91 (s,-C≡CH, 1H), 1.58 (m,-$\underline{CH_2}$-CH_2-OH,2H), 1.53- 1.26 (m,-CH2-, 12H).

^{13}C NMR [$CDCl_3$,TMS, δ, (ppm)]: 85.12 (s), 69.12 (d), 65.22 (t), 34.22 (t), 29.76 (t), 29.66 (t), 29.32 (t), 29.11 (t), 28.75 (t), 26.13 (t), 19.13 (t).

General procedures for the 2-mercaptoethanol monoaddition to 10-undecynol under thermal and photoinduced conditions

Thermal initiation. 10-Undecynol and 2-mercaptoethanol were introduced in different molar ratios (see Table 1) into a round-bottoned flask with magnetic stirrer. The radical initiator, AIBN, was added in the proportion of 5 or 10 % mol init./mol C≡C with the amount of toluene necessary to dissolve the thermoinitiator and stirred at 80ºC for 15min.

Photoinduced initiation. 10-Undecynol and 2-mercaptoethanol were introduced in different ratios (see Table 1) into a round-bottoned flask with magnetic stirrer. After the addition of DMPA, (0.5 or 3.6 % mol init./mol C≡C) with the amount of toluene necessary to dissolve the photoinitiator, the flask was placed onto a magnetic stirrer equipped with UV lamps (365nm, 18W) and stirred at room temperature for 15min.

Synthesis of 11-(2-hydroxyethylthio)undecenol (UDEM-diol).

In a 25-mL flask, 5.0 g (29.7 mmol) of 10-undecynol reacted with 2.44 g (31.19 mmol) of 2-mercaptoethanol. The radical initiator, AIBN, was added in the proportion of 10 % mol init./mol C≡C. The amount of toluene necessary to dissolve the thermoinitiator was added (0.06 ml). The reaction was carried out at room temperature, without deoxygenation, by heating at 80ºC. After 15 min the monoaddition reaction was confirmed by ^{1}H NMR by the appearance of the hydrogens corresponding to the doble bond signals that appear between 5.59-5.87 ppm. The producte was purified by column chromatography using hexane:ethyl acetate, 3:7, as eluent, to afford pure UDEM-diol as viscous oil, in a 98% yield.

^{1}H NMR [$CDCl_3$, TMS, δ, (ppm)]: 5.83-5.87 (m,-S-C<u>H</u>=CH-,2H,c,c`), 5.59-5.76 (dm,-S-CH=C<u>H</u>-,2H,d,d`), 3.73 (t, HO-C<u>H</u>$_2$-CH$_2$-S-,4H,a,a`), 3.62 (t, -CH$_2$-OH,4H), 2.82 (m, HO-CH$_2$-C<u>H</u>$_2$-S-,4H,b,b`) 2.10 (dq, -S-CH=CH-C<u>H</u>$_2$-, 4H,e,e`), 1.58 (m,-<u>CH</u>$_2$-CH$_2$-OH,2H), 1.39- 1.26 (m,-CH2-, 24H).

^{13}C NMR [$CDCl_3$, TMS, δ, (ppm)]: 134,02 (d), 131,92 (d), 123,51 (d) 121,51 (d), 63,12 (dt) 61,32 (t), 60,57 (t), 37,12 (t), 36,03 (t) 34.22 (t), 33,11 (t), 32,72 (t), 29.62 (t), 29.51(t), 29.42(t), 29.40 (t), 29.30 (t), 29.24(t), 29.11 (t), 28.95 (t),28.93(t), 28.81 (t), 28.82(t), 25,6 (dt).

Synthesis of Polyurethane.

A dry 50 mL round-bottom flask was charged with 6 mL of DMF, 4.06 mmol of diol (UDEM-diol), 4 mmol of MDI, and 2%, w/w (with respect to MDI) of tin (II) 2-ethylhexanoate. The flask was immersed into a 50 ºC preheated silicone oil bath with magnetic stirring.The reaction was continued for 12 h, and the PUs were isolated as white solids by precipitation into diethyl ether. Purification of PUs was carried out by dissolving the polymer in the minimum volume of chloroform or THF and reprecipitation into diethyl ether. The pure polymers were dried under vacuum and stored in a desiccator until needed. Films were solution cast from DMF and dried at 50 ºC for 1 day and then in a vacuum oven until constant weight.

Solution modification

In a 25 mL flask 0.1 g (0.2 mmol) of polyurethane reacted with 0.08 g (0,4 mmol) of 7-mercapto-4-methylcoumarin. The radical initiator, DMPA, was added in the proportion 10% mol init./mol C=C. The amount of tetrahydrofuran necessary to dissolve the polyurethane was added (2 ml). The reaction was carried out at room temperature, without deoxygenation, by irradiation with two 9 W UV-lamps (λ=365 nm). The completion of the reaction was confirmed after 2 h by ^{1}H NMR by the completely disappearance of the vinyl sulphide signals that appear in the region of 5.5-6 ppm. The resulting polyurethane was precipitated in toluene and dried under vacuum (yield 98%). The emission spectra of the Cm-SH, PU and PU-Cm solution were measured with excitation waveleng of 358 nm. Samples of 5 mg were disolved in 1ml of DMF for fluorescence spectroscopy measurements.

Surface modification

Six PU samples of 0,7 x 0,7 x 0,02 cm^2 reacted with 7-mercapto-4-methylcoumarin (PU/Cm-SH, 1/2) in a 25 mL flask. The radical initiator, DMPA, was added in the proportion 10% mol init./mol C=C. The amount of acetonitrele necessary to dissolve the Cm-SH was added (4 ml). The reaction was carried out at room temperature, without deoxygenation, by irradiation with two 9 W UV-lamps (λ=365 nm). The thiol-ene addition of Cm-SH on PU surface was followed by fluorescence at different times (30 min, 1, 2, 4, 8 and 24 h). The emission spectra of the PU films were measured with excitation wavelength of 358 nm. The resulting PU films were extensively washed with acetonitrile to remove the residual unreacted Cm-SH on the surface at different times.

Instrumentation

^{1}H (400 MHz) and ^{13}C (100.5 MHz) NMR spectra were obtained using a Varian Gemini 400 spectrometer with Fourier transform, DMSO and $CDCl_3$ as solvents and TMS as internal standards.

Calorimetric studies were carried out on a Mettler DSC821e and DSC822e thermal analyzer using N_2 as a purge gas (20 ml/min) at scanning rate of 10ºC/min. Thermal stability studies were carried out on a Mettler TGA/SDTA851e/LF/1100 with N_2 as a purge gas (100ml/min). The studies were performed in the 30-800 ºC temperature range at a heating rate in the of 10ºC/min.

Mechanical properties were measured using a dynamic mechanical thermal analysis (DMTA) apparatus (TA DMA 2928) in the controlled force-Tension Film mode. The tensile essays were performed on rectangular films (5 x 2 x 0,2 mm^3) measuring the strain while applying a ramp of 3 N/min. at 35ºC. A preload force of 0.01 N and a soak time of 5 min. were used.

Size exclusion chromatography (SEC) analysis was carried out with an Agilent 1200 series system equipped with an Agilent 1100 series refractive-index detector. THF was used as an eluent at a flow rate of 1.0 mL/min. Fluorescent measurements were performed with a AMINCO-BOWMAN fluorescence spectrophotometer.

Acknowledgements

The authors express their thanks to CICYT (Comisión Interministerial de Ciencia y Tecnología) (MAT2011-24823) for financial support for this work.

References

[1] Thomson, T. Polyurethanes as specialty chemicals: principles and applications,CRC Press, Boca Raton 2005.
[2] Chattopadhyay, D.K.; Raju, K.V.S.N. Prog. Polym. Sci. 2007, 32, 352-418.
[3] Lligadas, G.; Ronda, J.C.; Galià, M.; Cádiz, V. Biomacromolecules 2010, 11, 2825-2835.

[4] Desroches, M.; Escouvois, M.; Auvergne, R.; Caillol, S.; Boutevin, B. Polym. Rev. 2012, 52, 38-79.

[5] Kolb, H. C.; Finn, M. G.; Sharpless, K. B. Angew. Chem. Int. Ed. 2001, 40, 2004-2021

[6] Fournier, D.; Du Prez, F. E. Macromolecules 2008, 41, 4622-4630.

[7] Billiet, L.; Gok, O.; Dove, A. P.; Sanyal, A.; Nguyen, L-T. T.; Du Prez, F. E. Macromolecules 2011, 44, 7874-7878.

[8] Samuelsson, J.; Jonsson, M.; Brinck, T.; Johansson, M. J. Polym. Sci., Part A: Polym. Chem. 2004, 42, 6346–6352; Claudino, M.; Johansson, M.; Jonsson, M. Eur. Polym. J., 2010, 46, 2321–2332; Bantchev, G. B.; Kenar, J. A.; Biresaw, G.; Han, M. G. J. Agric. Food Chem. 2009, 57, 1282–1290; Lluch, C.; Ronda, J. C.; Galià, M.; Lligadas, G.; V. Cádiz, Biomacromolecules, 2010, 11, 1646–1653; Turunc, O.; Meier, M. A. R. Macromol. Rapid Commun., 2010, 31, 1822–1826; Turunc, O.; Meier, M. A. R., Green Chem., 2011, 13, 314–320; Lluch, C.; Lligadas, G.; Ronda, J. C.; Galià, M.; Cádiz, V. Macromol. Rapid Commun., 2011, 32, 1343–1351; Gonzalez-Paz, R. J.; Lluch, C.; Lligadas, G.; Ronda, J. C.; Galià, M.; Cádiz, V. J. Polym. Sci., Part A: Polym. Chem. 2011, 49, 2407–2416; Gonzalez-Paz, R. J.; Lligadas, G.; Ronda, J. C.; Galià, M.; Cádiz, V. Polym. Chem. 2012, 3, 9, 2471-2478; Desroches, M.; Caillol, S.; Lapinte, V.; Auverge, R.; Boutevin, B. Macromolecules 2011, 44, 2489-2500; Desroches, M.; Caillol, S.; Auverge, R.; Boutevin, B.; David, G. Polym. Chem. 2012, 3, 450-457; Palaskar, D. V.; Boyer, A.; Cloutet, E.; Le Meins, J-F.; Gadenne, B.; Alfos, C.; Farcet, C.; Cramail, H. J. Polym. Sci., Part A: Polym. Chem. 2012, 50, 1766-1782.

[9] Dondoni, A. Angew. Chem. Int. Ed. 2008, 47, 8995-8997.

[10] Kade, M. J.; Burke, D. J.; Hawker, C. J. J. Polym. Sci., Part A: Polym. Chem. 2010, 48, 743–750.

[11] Bader, H.; Cross, L. C.; Heilbron, I.; Jones, E. R.H. Chem. Soc. J. 1949, 1, 619-623

[12] Lo Conte, M.; Pacifico, S.; Chambery, A.; Marra, A.; Dondoni, A. J. Org. Chem. 2010, 75, 4644-4647

[13] Lo Conte, M.; Staderini, S.; Marra, A.; Sanchez-Navarro, M.; Davis, B. G.; Dondoni, A. Chem. Comm. 2011, 47, 11086-11088.

[14] Gonzalez-Bejar, M.; Frenette, M.; Jorge, L.; Scaiano, J.C. Chem. Commun. 2009, 3202-3204.

[15] Nagarajan, S.; Boreddy Siva Rami Reddy, Tsibouklis, J. Eur. Polym. J. 2012, 48, 1357-1360.

To be submitted

SECOND PART

Biocompatibility of polyurethanes and functionalization strategies

BIOCOMPATIBILITY OF POLYURETHANES

Introduction

In the last 50 years, the development and the conception of biomaterials used for the construction of prostheses and medical devices has expanded very rapidly. A wide variety of biomaterials are now commonly implanted in the human body for the treatment of various diseases such as heart failure, atherosclerotic diseases, aortic aneurysm, ear dysfunction and cataracts. They are also used to augment tissue, namely, bone, muscle, skin and breast either after trauma or for cosmetic reasons. Biomaterials are the basic constituents of prostheses or implants which are designed to restore and support functions of organs and tissues as well as substitute and consolidate tissue, ligamentous, articular and osseous structures. They also can be used to stimulate the repair and healing of nerves, tissues and wounds in a precise and predetermined timeframe or for a period of time exceeding the life expectancy of the recipient.

Biomaterials must exhibit mechanical, physical, or electrical properties for their application. Surface properties are also important and should be accounted by any investigator. Surface characteristics that should be considered are hydrophilicity, charge, polarity and energy, heterogenous distribution of functional groups, wettability, water absorption and chain mobility. As well, morphological or topographical aspects including texture, smoothness and roughness should be accounted for.

However, all these properties may be modified under a physiological environment because they will be subjected to the following components: the duration of implantation, the temperature of the body and the pathological conditions at the implant site. Biomaterials must maintain their biostability and biofunctionality during implantation in order to avoid graft failure. In other words, the function of the organ or tissue must be guaranteed and the materials must maintain their mechanical, chemical and structural properties for long-term use. Finally, any biomaterial should not induce any deleterious reactions or disturb the biological environment.

Definitions of Biocompatibility

The selection of the materials used in the construction of prostheses and implants is basically focussed on their ability to maintain mechanical, chemical and structural integrity and on various characteristics which allow this function to substitute any organ or tissue properly and exhibit safe, effective performance within the body. For a number of years, biocompatibility has been defined as the ability of a material to perform with an appropriate host response in a specific application.[1]

Biocompatibility is by no means a measurable entity. In fact, biocompatibility is a complex notion which has to be interpreted as a series of events or interactions happening at the tissue/material interface whose outcome must be satisfactory or optimal. One may simulate observing the biocompatibility of a material by comparing its behaviour to reference materials in standardized experimental conditions.

By 2008, David F. Williams published a review[2] called "On the mechanisms of biocompatibility", which re-define the concept of biocompatibility: "Biocompatibility refers to the ability of a biomaterial to perform its desired function with respect to a medical therapy, without eliciting any undesirable local or systemic effects in the recipient or beneficiary of that therapy, but generating the most appropriate beneficial cellular or tissue response in that specific situation, and optimising the clinically relevant performance of that therapy."

Moreover, a particular concept about biocompatibility of tissue engineering scaffolds is defined as: "The biocompatibility of a scaffold or matrix for a tissue engineering product refers to the ability to perform as a substrate that will support the appropriate cellular activity, including the facilitation of molecular and mechanical signalling systems, in order to optimise tissue regeneration, without eliciting any undesirable local or systemic responses in the eventual host".

[1] D.F. Williams. Definitions in biomaterials. Amsterdam: Elsevier; 1987.
[2] D.F. Williams, Biomaterials: 29, 2941–2953, 2008.

Tissue engineering scaffolds

Biocompatible polymers are extensively investigated for applications in tissue and organ repair. With the increasing interest in engineering various tissues for the treatment of many types of injuries and diseases, a wide variety of degradable polymers with desirable mechanical, degradation, and cytophilic properties are needed. Thus, tissue engineering has been defined conceptually as: The persuasion of the body to heal itself, through the delivery to the appropriate sites of molecular signals, cells and/or supporting structures.[3]

In recent decades, tissue engineering has emerged as an alternative method for the regeneration of tissues and restoration of organs function through implantation of cells/tissues grown outside the body or stimulating cell to grow into an implanted matrix.[4] While initial biomaterials were commonly inert, biomaterial research then focused on bioactive materials that elicit action and reaction in the biological environment. Today, there is a move to new generation of materials to repair or replace diseased or damaged tissues, using scaffolds in which cells can be seeded usually before implantation. The materials and scaffold can stimulate specific cellular response at the molecular level; they are also biodegradable and can be tailored to suit specific tissues. Ideally, the living tissue construct is functionally, structurally and mechanically equal to the tissue it has been designed to replace.[5]

There are a number of materials used for tissue engineering application; the materials can be subdivided into natural materials and synthetic materials. Examples of natural materials include collagen, glycosaminoglycans (GAGs), chitosan and alginates.[6] The advantages of natural materials are that they have low toxicity and a low chronic inflammatory response. They can be combined into a composite or blend with other natural or synthetic materials (thus possessing the mechanical strength of the synthetic material as well as the biocompatibility of the natural material) and can be degraded by naturally occurring enzymes. However, disadvantages include poor

[3] D.F. Williams. The Williams dictionary of biomaterials. Liverpool: Liverpool University Press, 1999.
[4] A. Vats, N.S. Tolley, J.M. Polak, , J.E. Gough, Clin. Otolaryngol: 28, 165-172, 2003.
[5] E. Eybl, M. Grimm, M. Grabenwoger, P. Bock, M. M. Muller, E. Wolner, J. Thorac. Cardiovasc. Surg: 104, 3, 763-769,1992.
[6] a) J.E. Gough, , C.A. Scotchford, S. Downes, J. Biomed. Mater. Res: 61, 1, 121-130, 2002, b) S. Van Vlierberghe, P. Dubruel, E. Schacht, Biomacromolecules: 12, 1387–1408, 2011, c) C. Charbonneau, J.C Ruiz, P. Lequoy, M.J Hebert, G. De Crescenzo, M. R. Wertheimer, S. Lerouge, Macromol. Biosci: 2012, DOI: 10.1002/mabi.201100447.

mechanical strength as well as a complex structure and, hence, manipulation becomes more difficult. They can easily be denatured and often require chemical modification, which can lead to toxicity. Examples of synthetic materials include the biodegradable polymers such as polyglycolide (PGA), polylactide (PLA), polyurethanes (PUs) and polylactide-co-glycolide (PLG), non degradable polymers such as polytetrafluoroethylene (PTFE), nylon and polyethylene terephthalate (PET); bioceramics such as tricalcium phosphate (TCP) and hydroxyapatite (HA).[7]

Techniques or functionalization strategies used to manufacture biomaterials into scaffolds are dependent on the properties of the material and its intended application. Scaffolds may be composed of polymers, metals, ceramics, composites or blends. It is important to select a material that closely matches the properties of the tissue that it is to replace. For example, biomaterials intended to replace soft tissues such as skin, breast, eye, blood vessels and heart valves tend to be composed of natural and synthetic polymers. Replacement of hard tissues such as bone and dentine tends to use metals, bioceramics, composites or blends and polymers.[8]

Biomedical applications of polyurethanes

During the past few decades, PUs have been widely used for biomedical applications such as vascular prostheses, catheters ans for skin and bone regeneration. In these applications PU scaffolds demostrate to support cell in-growth and tissue remodeling.[9] PUs exhibit many excellent properties for biomedical applications. For instance, one of the characteristic properties of PUs is their mechanical flexibility combined with high tear strength, which can be achieved because of PUs chemical versatility. These desirable properties attract the attention of developers of biomedical devices.

---

[7] a) C.K. Breuer, B. A. Mettler, T. Anthony, V. L. Sales, F. J. Schoen, J. E. Mayer, Tissue Eng: 10, 1725-1736, 2004, b) H.P. Wiesmann, U. Joos, U. Meyer, Int. J. Oral Maxillofac. Surg: 33, 523-30, 2004, c) R.Z. LeGeros, Clin. Orthop. Relat. Res: 395, 81-98, 2002. d) J.C. Fricain, P. L. Granja, M. A. Barbosa, B. De Jeso, N. Barthe, C. Baquey, Biomaterials: 23, 971-980, 2002, e) K.F. Leonga, C.K. Chua, N. Sudarmadjia, W.Y. Yeong, J. Mech. Behav. Biom. Mat: 1, 140-152, 2008.

[8] a) A. Vats, N.S. Tolley, J.M. Polak, J.E. Gough, Clin. Otolaryngol: 28, 165-172, 2003, b) T.W. Wang, H.C. Wu, Y.C. Huang, J.S. Sun, F.H. Lin, Artif. Organs: 30, 141-149, 2006, d) C. Danielsson, S. Ruault, M. Simonet, P. Neuenschwander, P. Frey, Biomaterials: 27, 1410-1415, 2006, e)M. Yaszemski, D.J. Trantolo, K.U. Lewandrowski, V. Hasirci, D.E. Altobelli, D.L. Wise, Biomaterials in Orthopedics, Marcel Dekker Inc., New York-Basel, USA-Switzerland, 2004.

[9] a) S.A. Guelcher, Tissue Eng. Part B: 14, 3-17, 2008, b) J.P. Santerre, K. Woodhouse, G. Laroche, R.S. Labow, Biomaterials: 26, 7457-7470, 2005.

In 1958, PU materials were first introduced in biomedical applications; Pangman described a composite breast prosthesis covered with a polyester-urethane foam.[10] In the same year, Mandrino and Salvatore also used a rigid polyester-urethane foam called Ostamer™ for in situ bone fixation.[11] Three years later, the application of polyester-urethane (Estane®) was proposed by Dreyer et al to be used as components for heart valves and chambers, and aortic grafts.[12] In the mid-1960s, Cordis Corp. started to commercialize polyester-urethane diagnostic catheters.[13] In 1954, textile chemists at DuPont developed Lycra® spandex as a high-performance alternative to natural rubber in elastic thread. It was first introduced as a biomaterial in 1967 by Boretos and Pierce who obtained the polymer in solution directly from the DuPont spinning line that produced Lycra spandex yarn. This material was first used as the elastomeric components of a cardiac assist pump and its arterial cannulae.[14] The year 1971 marked the arrival of the earliest PU specifically designed for medical use; Avcothane-51™, a PU/silicone hybrid, was invented by AVCO-Everett Research Laboratory. In 1972, Biomer™, a version of Lycra® T-126 produced by Ethicon Corp. under a license from Dupont, was made available. Avcothane and Biomer were regarded as the first 'real' biomedical PUs and have been studied intensively. Avcothane was used clinically in the first intra-aortic balloon pump, starting in about 1971, and is still in clinical use today (see Table 1). Biomer® components were used in the 'Jarvik Heart' in 1982, the first artificial heart used for implantation. From that time, the research of PUs in biomedical applications has been intensive, and currently PUs have been applied in a number of biomedical tissue engineering areas such as pacemaker lead insulators, heart valves, breast implants, vascular prostheses, scaffolds for skin and bone regeneration, etc.[15]

[10] a) W.J. Pangman., Compound prosthesis, USA, 1965, b) W.J. Pangman, Compound prosthesis device, USA, 1958.
[11] a) M.P. Mandarino, J.E. Salvatore, Am. J. Surg: 4, 442-446, 1959, b) M.P. Mandarino, J.E. Salvatore, J.E., Surg. Forum: 9,762-765, 1958, c) M.P. Mandarino, Surg. Clin. North. Am: 40, 243-251, 1960, d) M.P. Mandarino, J.E. Salvatore, J.E. Arch. Surg: 80, 623-627, 1960.
[12] a) B. Dreyer, T. Akutsu, W.J. Kolff, J. Appl. Physiol: 14, 475-478, 1959, b) B. Dreyer, T. Akutsu, W.J. Kolff, J. Appl. Physiol: 15, 18-22, 1960.
[13] L. Pinchuk, J. Biomater. Sci. Polym. Ed: 6, 3, 255-267, 1994.
[14] a) J.W. Boretos, D.E. Detmer, J.H. Donachy, J. Biomed. Mater. Res: 5, 373-387, 1971, b) J.W. Boretos, W.S. Pierce, J. Biomed. Mater. Res: 2, 121-130, c) E. Bezon, J.A. Barra, A. Karaterki, J. Braesco, J.C. Pillet, P. Mondine, Chirurgie, 121, 447-452, 1996.
[15] P.Vermette, H.J. Griesser, G. Laroche, R. Guidoin, Polyurethanes in Biomedical Applications, Landes Bioscience Press, Texas, USA. 2001.

Table 1. Some comercial polyurethanes for biomedical applications

Trade Name	Composition	Notes and Applications	Processing
Cardiothane® (Avcothane-51™)	MDI / PDMS	Thermoplastic aromatic polyetherurethane polydimethylsiloxane copolymer	Solution casting
Biomer™	MDI / Water	Thermoplastic aromatic polyether-urethane-urea	Extrusion
Estane®	No available information	Thermoplastic polyester-urethane Catheters	Extrusion Melt coating
Biothane®	MDI / Castor oil-based polyols	Thermoset aromatic polyether-urethane Catalyst as additives	Solution casting
Tecoflex®	HMDI	Thermoplastic aliphatic polyether-urethane Blood pump diaphragms,wound dressings	Inyection molding
ChronoFlex®	HMDI /PC/BD	Thermoplastic aliphatic polycarbonate-urethane, butane diol as chain extender.	Solvent casting

Degradation of PUs in biomedical devices

Generally, the degradation of PUs in tissue environment follows bulk degradation mechanism.[15] Once PUs are implanted, there are several factors that contribute to their degradation, including hydrolysis, stress cracking, oxidation and enzymes. For example, the aliphatic ester linkages in polyester-urethanes are easy to be hydrolyzed into small molecules.[16] Biodegradable PU elastomers have been synthesized from MDI by controlling the frequency of ester linkages in the backbone, thereby promoting degradation to noncytotoxic fragments smaller than 2000 Da that are eliminated from body.[17] Polyether-urethane materials are known to be susceptible to a degradation phenomenon involving crack formation and propagation.[18] This happened in areas of devices where the stress level on the polymer is relatively high. Moreover, the residual polymer surface stress introduced during fabrication of the device can also cause the environmental stress cracking. The enzymatic degradation is in the physiological environment another PUs degradation form. Even though the enzymes are designed for highly specific interactions with particular biological substrates, some appear capable of recognizing and acting upon 'unnatural' substrates including PUs.[19] It is found that enzymes are capable of altering polymer structure and there are some models for the biodegradation by enzymes attack.[20] The differences in PUs chemistry

[16] K. Stokes, R. McVenes, J.M. Anderson, J. Biomater. Appl: 9, 321-354, 1995.
[17] a) E. Liljensten, K. Gisselfaelt, B. Edberg, H. Bertilsson, P. Flodin, A. Nilsson, A. Lindahl, L. Peterson, J. Mater. Sci. Mater. Med: 13, 351-359, 2002, b) K. Gisselfaelt, B. Edberg, P. Flodin, Biomacromolecules: 3, 951-958, 2002.
[18] R.E. Phillips, M.C. Smith, R.J. Thoma, J. Biomater. Appl: 3, 207-227, 1988.
[19] R. Smith, C. Oliver, D.F. Williams, J. Biomed. Mater. Res: 21, 991-1003, 1987.
[20] J.P. Santerre, D.G. Duguay, R.S. Labow, J.L. Brash, Am. Chem. Soc. Symp. Ser: 602, 352-370, 1995.

appear to stimulate the synthesis and release of the enzymatic activities from cells that cause their degradation.[21] Lipids can strongly interact with some enzymes.[22] Page et al[23] reported that most of enzymes are released, frequently within 4-6 hours, and in large quantities. The enzyme released appeared to include lipase, acid hydrolases, such as cathepsins, glycosidases, acid phosphatases, aryl sulfatase and others. Depending on the formulation, PUs may posses one or several types of vulnerable chemical groups that may be available for cleavage by hydrolitic enzymes. These may include urethane, ester, urea, and carbonate groups. Oxidative enzymes are likely to attract primarily the C-H bond adjacent to an ether or thioether linkages; these groups are known to be vulnerable to oxidative attack. Furthermore, all these degradation phenomena mentioned above are closely related to the surface of PUs.[15]

SURFACE PROPERTIES AND MODIFICATIONS

The communication of an implant with the host system first takes place via the surface. This initial, direct contact between the living tissues in the body and surface is a major determinant for the rejection or acceptance of a foreign device. Since materials interact with environment through their interfaces, both the kind and the strength of such interactions are largely dependent on the surface properties of the materials. While a material is in contact with a biological environment, the surface chemistry and topography of the material are important parameters that may influence protein adsorption, cell interaction, and ultimately the host response.[24] Moreover, as degradation generally proceeds from the surface into the bulk, the chemical composition of the surface layers affect the rates and mechanism of biodegradation.

It has been well known that the interactions between cells and their enviroments are mediated by the “bio-recognition processes”, the specific binding of the receptors on cell surface with their corresponding ligands or bioactive molecules (see Figure 1). Controlling cell-material surface interactions is an important goal for the development of tissue-engineered products. However, influencing even the most fundamental cellular

[21] L.A. Matheson, J.P. Santerre, R.S. Labow, J. Cell. Physiol: 199, 8-19, 2004.
[22] P. Vermette, G.B. Wang, J.P. Santerre, J. Thibault, G. Laroche, J. Biomater Sci. Polym. Edn : 10, 729-749, 1999.
[23] R.C. Page, P. Davies, A.C. Allison, Int. Rev. Citol: 52, 119-157, 1978.
[24] H. Chen, L. Yuan,W. Song, Z. Wu, D. Li, Prog. Polym. Sci: 33, 1059-1087, 2008.

functions (such as adhesion or migration, Figure 1) requires an ability to link and utilize concepts from a variety of scientific/engineering and biomedical disciplines.[25]

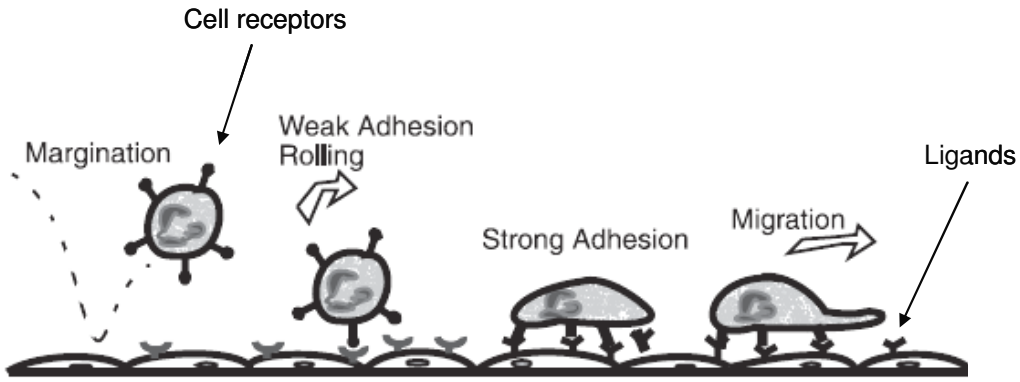

Figure 1. "Bio-recognition processes". The cell-surface receptors are enlarged to show and emphasize the importance of cell-ligands adhesive contacts in cell-materials surfaces interactions.

When foreign materials come into contact with body fluid or cell culture medium, the initial response is protein adsorption a top the materials' surfaces. Thus, the materials interact with the cells through the adsorbed protein layer. The composition and structure of this protein layer play critical roles in determining subsequent cell behaviors. Based on the understanding of the dominance of the biorecognition process on cell behaviors, two main strategies in surface engineering of materials are often employed. Firstly, the material surface properties such as chemical composition, hydrophilicity/hydrophobicity balance, surface charge and roughness, etc, (Table 2)[25] are modulated to a state that the adsorbed proteins can maintain their normal bioactivities. This method, however, cannot induce specific cell behaviors due to the nonspecific protein absorption. The second strategy is to directly immobilize certain bioactive molecules on the material surfaces to induce specific cellular responding.[26]

[25] K.C. Dee, D.A. Puleo, R. Bizius, An introduction to tissue-biomaterial interactions, John Wiley & Sons, Inc., Hoboken, New Jersey, p.xviii, p.38, p.149-160, 2002.
[26] Z. Ma, Z. Mao, C. Gao, Colloids Surf. B: Biointerfaces: 60, 137-157, 2007.

Table 2. Properties of surfaces and proteins that affect their interactions.

Feature	Effect
Morphology	Greater texture exposes more surface area for interaction with proteins.
Composition	Chemical makeup of a surface will determine the types of intermolecular forces governing interaction with proteins
Hydrophobicity	Hydrophobic surfaces tend to bind more proteins
Heterogeneity	Nonuniformity of surface characteristics results in domains that can interact defferently with proteins
Potential	Surface potential will influence the distribution of ions in solution and interaction with protein
Protein size	Large molecules can have more site of contact with the surface
Protein charge	Molecules near their isoelectric point generally adsorb more readily
Protein structure	Less stable proteins, such as those with less intramolecular cross-linking, can unfold to a greater extend and form more contacts points with the surface.

The major methods of immobilizing a bioactive compound to a polymeric surface are adsortion via electrostatic interactions, affinity interactions and covalent attachment (Figure 2). Non-covalent adsorption is sometimes desirable, as in certain drug delivery applications.[27] It is also appropriate in the case of regenerable antimicrobial textiles.[28] However, covalent immobilizations offer several advantages by providing the most stable bond between the compound and the functionalized polymer surface. In the biomedical field, a covalent immobilization can be used to extend the half-life of a biomolecule, prevent its metabolism or allow for continued bioactivity of in-dwelling devices (as in vascular devices, shunts, or catheters).[29]

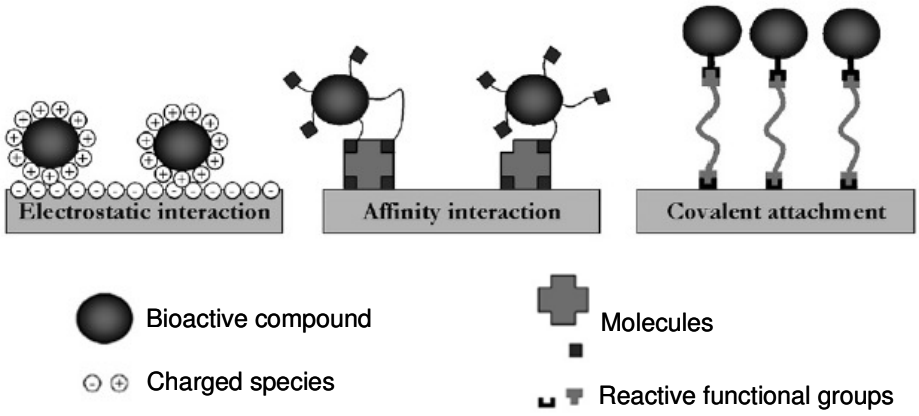

Figure 2. Mechanisms of immobilization.

[27] T. Richey, H. Iwata, H. Oowaki, E. Uchida, S. Matsuda, Y. Ikada, Biomaterials: 21, 1057-1065, 2000.
[28] G. Sun, X.J. Xu,Text. Chem. Color: 30, 26-30, 1998.
[29] I.S. Alferiev, J.M. Connolly, S.J. Stachelek, A. Ottey, L. Rauova, R.J. Levy, Biomacromolecules: 7, 317-322, 2006.

Techniques in surface modification

Wet chemical

In wet chemical surface modification, a material is treated with liquid reagents to generate reactive functional groups on the surface. This classical approach to surface modification does not require specialized equipment and thus can be conducted in most laboratories. It is also more capable of penetrating porous three-dimensional substrates than plasma and other energy source surface modification techniques,[30] and allows for "in situ" surface functionalization of microfluidic devices. Chromic acid and potassium permanganate in sulfuric acid have been used to introduce reactive oxygen-containing moieties to PE and PP.[31] Concentrated sodium hydroxide and sulfuric acid have been used to generate carboxylic acid groups by base and acid hydrolysis of PMMA.[32] Methyl ester side chains of PMMA also have been reduced to hydroxyls by treatment in lithium aluminum hydride in ether.[33] Primary amines have been introduced to poly(ester-urethane) (PU), PLA, and PLGA by aminolysis using various diamines including 1,6-hexanediamine, ethylenediamine, and N-aminoethyl-1,3-propanediamine, as well as lithiated diamines.[34] One problem of the hydrolisis/aminolysis method is the molecular weight of the polymer will be partially sacrificed, thus the reaction conditions should be well controlled.

Lastly, PTFE surfaces have been modified by refluxing with elementary sodium in toluene to generate double bonds, followed by an 8 h oxidation at 120 ºC in a 1:1 mixture of trifluoroacetic acid and hydrogen peroxide (38%) which improved membrane wetting and allowed immobilization of the enzyme alliinase.[35] Unfortunately, these wet chemical methods are non-specific, producing a range of oxygen-containing functional groups. In addition, those which target modification of

[30] X.H. Liu, P.X. Ma, Ann. Biomed. Eng: 32, 477-486, 2004.
[31] a) J.C. Eriksson, C.G. Golander, A. Baszkin, L. Terminassiansaraga. J. Colloid. Interface. Sci: 100, 381-392, 1984, b) E. Sheng, I. Sutherland, D.M. Brewis, R.J. Heath. J. Adhes. Sci. Technol: 9, 47-60, 1995.
[32] L. Brown, T. Koerner, J.H. Horton, R.D. Oleschuk. Lab. Chip: 6, 66-73, 2006.
[33] J.Y. Cheng, C.W. Wei, K.H. Hsu, T.H. Young, Sens. Actuators B: 99, 186-196, 2004.
[34] a) Y.B. Zhu, C.Y. Gao, T. He, J.C. Shen, Biomaterials: 25, 423-430, 2004, b) Y.B. Zhu, C.Y. Gao, Y.X. Liu, J.C. Shen, J. Biomed. Mater. Res. Part A: 69A, 436-443, 2004, c) T.I. Croll, A.J. O'Connor, G.W. Stevens, J.J. Cooper-White. Biomacromolecules: 5, 463-473, 2004.
[35] J. Glodek, P. Milka, I. Krest, M. Keusgen, Sens. Actuators B: 83, 82-89, 2002.

polymer side chains (as in PMMA ester modification) depend on side chain surface orientation. The degree of surface functionalization may therefore not be repeatable between polymers of different molecular weight, crystallinity, or tacticity. These wet chemical methods also can generate hazardous chemical waste and can lead to irregular surface etching .[36]

Ionized gas treatment

Plasma is a high energy state of matter, in which a gas is partially ionized into charged particles, electrons, and neutral molecules.[37] Plasma can provide modification of the top nanometer of a polymer surface without using solvents or generating chemical waste and with less degradation and roughening of the material than many wet chemical treatments.[38] The type of functionalization imparted can be varied by selection of plasma gas (Ar, N_2, O_2, H_2O, CO_2, NH_3) and operating parameters (pressure, power, time, gas flow rate). The gas is energized using techniques such as radio-frequency energy, microwaves, alternating current or direct current. The energetic species in a gas plasma include ions, electrons, radicals, metastables, and photons in the short-wave ultraviolet (UV) range.

Surfaces in contact with gas plasmas are bombarded by these energetic species and their energy is transferred from the plasma to the solid as shown in Figure 3. These energy transfers are dissipated within the solid by a variety of chemical and physical processes as schematically illustrated in Figure 4, to result in the surface modification. A wide variety of parameters can directly affect the chemical and physical characteristics of a plasma and subsequently affect the surface chemistry obtained by plasma modification. Processing parameters, such as gas types, treatment power, treatment time and operating pressure, can be varied by the user; and system parameters, such as electrode location, reactor design, gas inlets and vacuum, are set by the design of the plasma equipment. This wide range of parameters offers greater control over the plasma process than that offered by most high-energy radiation processes. Other advantages of this technology include low environmental impact; no

[36] S. Desai, R.P. Singh, Surface modification of polyethylene. In: Albertsson AC, editor. Long-term properties of polyolefins. New York: Springer: p. 231-293, 2004
[37] A. Dinklage, T. Klinger, G. Marx, L. Schweikhard. Plasma physics. New York: Springer; 2005.
[38] a) C.M. Chan, T.M. Ko, H. Hiraoka, Surf. Sci. Rep: 24, 3-54, 1996. b) M. Ozdemir, C.U. Yurteri, H.Sadikoglu, Crit. Rev. Food Sci: 39, 457-577, 1999.

line-of-sight problem compared with electron-beam, laser or UV radiation; and the surface modification is fairly uniform over the whole surface. In addition, although gas plasma treatments are typically carried out in a batch process, continuous on-line treatment of fibres, tubing membranes, fabrics and films, is also common. In many cases, a custom-designed reactor is necessary to maintain a high level of throughput and maximize the economic feasibility of the process.

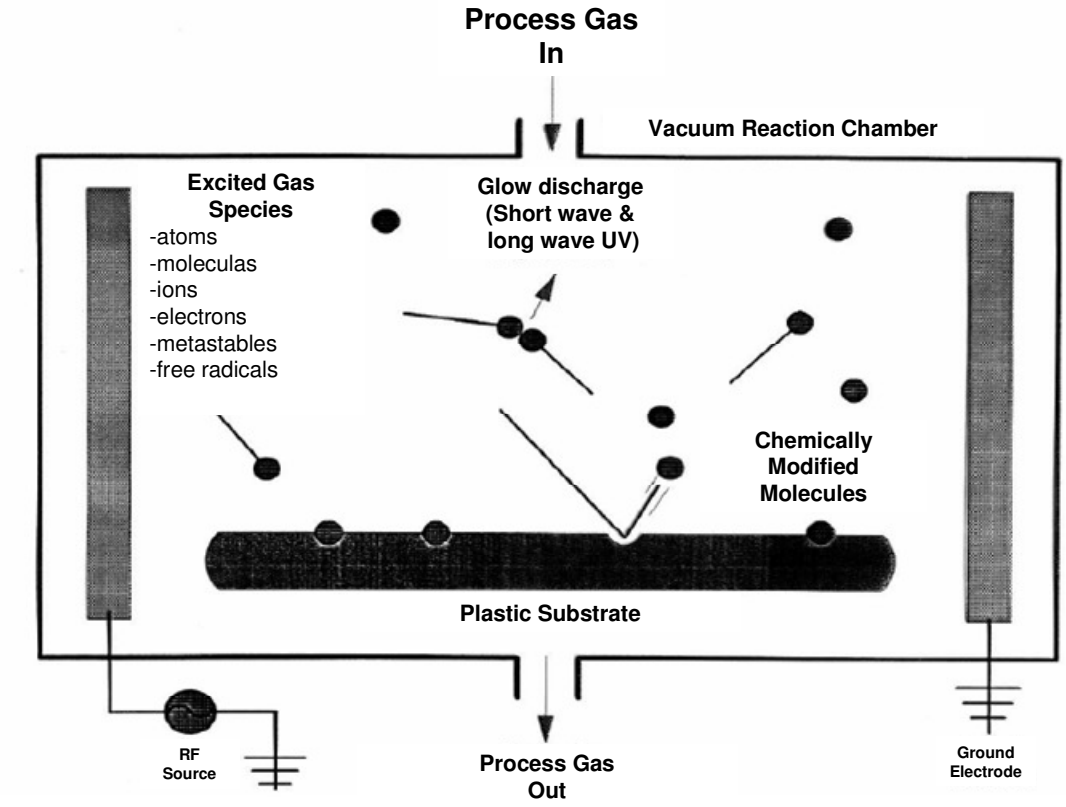

Figure 3. Schematic of plasma surface modification within the plasma reactor

As well as some disadvantages:

- Plasma treatments must be carried out in vacuum.

- The optimal parameters for one system usually cannot be adopted for another system, as there are many parameters involved to optimize conditions, including time, temperature, power, gas composition/flow/ pressure, orientation of reactor and distance of substrate from plasma source.

- It is very difficult to control precisely the amount of a particular function group formed on the surface.

- It should be noted that in addition to the monomers and gases intentionally introduced to the plasma chamber, latent chemicals from prior users may be present thus posing a risk of contamination. The plasma chamber should therefore be adequately cleaned, before introducing polymers for surface modification.

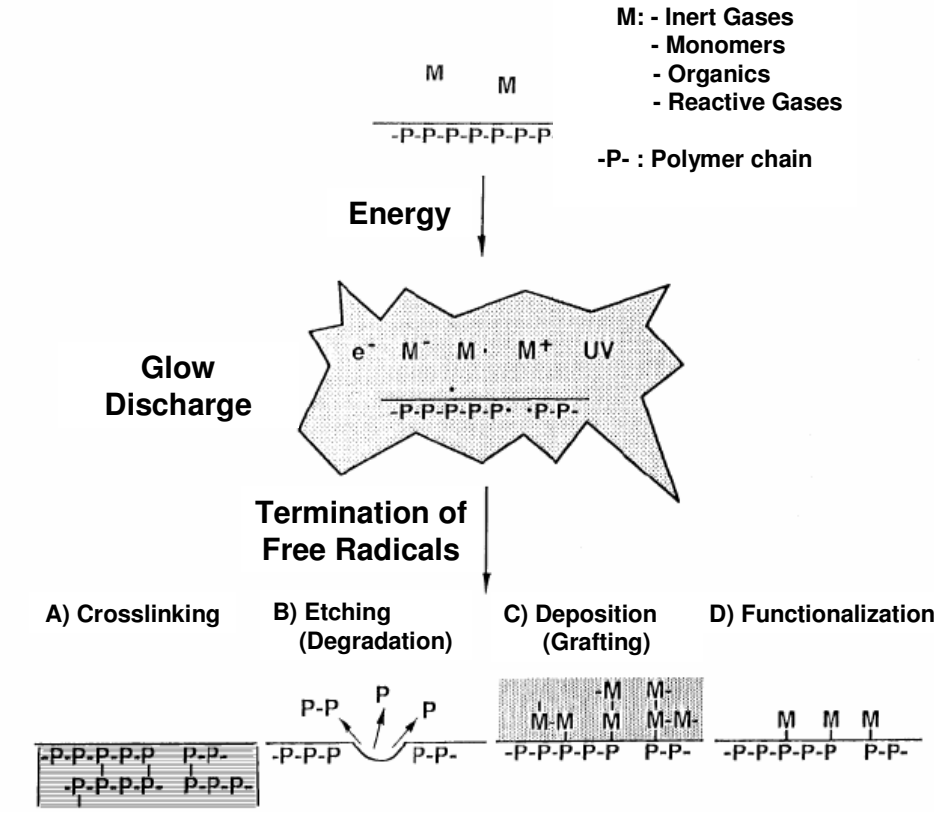

Figure 4. Schematic of the reaction mechanisms of plasma surface modifications

If initial surface functionalization does not generate enough surface reactive groups, or if the bioactive compound loses activity when linked directly to the hydrophobic polymer surface, it may be necessary to graft an intermediary (tether molecules) between the surface and the bioactive compound. There are many factors which influence the effect of the tether molecule on biomolecule activity, as illustrated in Figure 5. Factors such as structure–function relationships, location of functional groups available for conjugation, and the impact of binding the bioactive compound to a hydrophobic substrate must be considered. A thorough understanding of the bioactive

compound of interest is therefore critical in selecting which intermediary to utilize, if any.

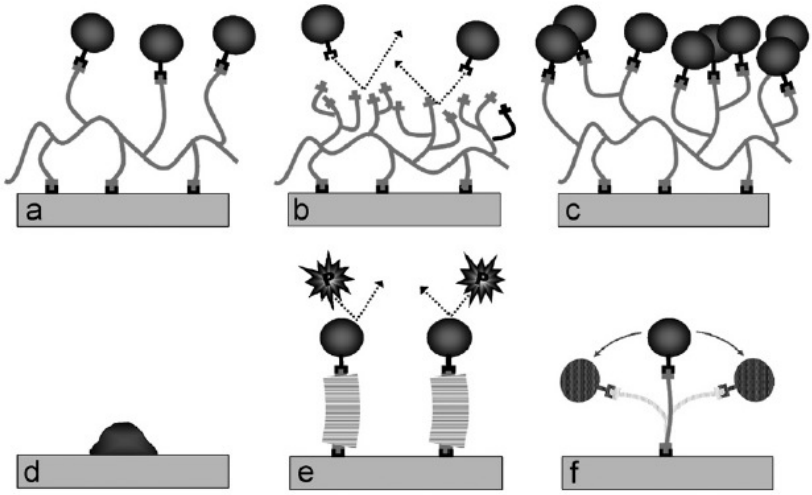

Figure 5. Effect of tether molecule on bioactivity: (a) increased biomolecule immobilization due to branched spacer molecule, (b) reduced biomolecule immobilization due to overfunctionalization of surface, (c) reduced bioactivity due to overcrowding of bioactive compounds, (d) surface induced denaturation, (e) reduced nonspecific adsorption of proteins due to hydrophilic spacer, (f) increased mobility due to spacer molecule.

Acrylic acid has been graft polymerized to polymer surfaces to generate surface carboxylic acids.[39] By using such a polyfunctional agent, one can increase the number of reactive sites available on a surface for immobilization of bioactive compounds (Figure 5a). For example, grafting poly(ethylenimine) to a surface onto which PEG is attached results in a high PEG density resulting in reduced protein adhesion.[40] The major risk in utilizing a highly branched tether is overcrowding, which may have dual impact. After a certain point, continuing to increase the number of reactive functional groups in a given area may lead to overcrowding of the functional groups which may reduce the immobilization of bioactive compounds (Figure 5b). In addition, if bioactive compounds are overcrowded on a surface, they may be sterically hindered, thus reducing bioactivity (Figure 5c).

[39] a) Y.J. Kim, I.K. Kang, M.W. Huh, S.C. Yoon. Biomaterials: 21, 121-130, 2000, b) Z.Y. Cheng, S.H. Teoh, Biomaterials: 25, 1991-2001, 2004.
[40] a) P. Kingshott, J. Wei, D. Bagge-Ravn, N. Gadegaard, L. Gram, Langmuir: 19, 6912-6921, 2003. b) K. Holmberg, F. Tiberg, M. Malmsten, C. Brink, Colloid Surface A: 123, 297-306, 1997.

Surface characterization

The traditional methods used to analyze the bulk structure of the materials are not suitable for surface determination. Unfortunately, one technique is not capable of providing all the needed information; therefore surface characterization requires the use of multiple analytical methods.[25] Surface analytical techniques provide information about the outermost one to ten atomic layers of a material. Characterization of a material's surface properties is needed to relate important surface characteristics to biological responses.

Spectroscopic and microscopic analyses

X-ray photoelectron spectroscopy (XPS). XPS, or Electron Spectroscopy for Chemical Analysis (ESCA), determines the atomic composition of a solid`s top several nanometers and is based on the process of photoemission. On irradiation of a sample with a beam of monochromatic X rays, the X rays penetrate the surface and transfer energy to valence and core level electrons in the sample. If sufficient energy is transferred, electrons will be ejected from the surface. A simple energy balance describes this process:

$$E_b = h_v - E_k$$

where E_b is the binding energy of the emitted electron, h_v is the energy of the incident X rays, and E_k is the kinetic energy of the ejected electrons. The detectors in XPS instruments measure the number and kinetic energy of emitted photoelectrons. Then, because h_v is known, the binding energy can be calculated. An XPS spectrum represents the photoelectron energy distribution. Because the core electrons of each element have characteristic binding energies, the peaks in the XPS spectra allow identification of all elements, except H and He. Additionally, because the electron binding energy is determined by the local chemical environment as well as the type of atom, shifts in the peaks can be used to obtain information about the chemical bonding state of atoms. Although X rays can penetrate materials to depths of 1 μm, XPS provides information about the outermost 5–75 A˚ of a material's surface. This is because photoelectrons

originating deeper in the sample lose energy in inelastic collisions and/or do not have sufficient energy to be emitted from the sample.

Scanning electron microscopy (SEM) / Energy-dispersive X-ray spectroscopy (EDS). In SEM, a beam of relatively high-energy electrons is scanned across the sample's surface. The primary electrons penetrate the surface and transfer energy to the material in a manner analogous to the way X rays and ions act in XPS. In SEM, the incident electrons transfer sufficient energy for electrons (secondary electrons) to be emitted from the sample. The intensity of the secondary electrons primarily depends on the topography of the surface. By scanning the electron beam across the samples and determining the current generated from secondary electrons, images of the surface are obtained. Thus, in contrast to the methods described previously, which provide surface chemical information, SEM generally gives images reflecting surface topography.

More specific chemical information can be obtained with complementary techniques such as energy- or wavelength-dispersive X-ray analysis (EDS). The basis of these methods is the emission of X rays following ejection of secondary electrons. Because the primary electrons penetrate micrometers into the material and therefore eject secondary electrons from deeper in the material, SEM and the dispersive X-ray analysis techniques are not as surface sensitive as XPS. Also, nonconductive samples, such as polymers and biological materials, must be coated with a conductive film to prevent buildup of negative charge in the sample.

Fourier transform infrared spectroscopy (FTIR). FTIR uses infrared radiation to determine the chemical functionalities present in a sample. When an infrared (IR) beam hits a sample, chemical bonds stretch, contract, and bend, causing it to absorb IR radiation in a defined wavenumber. In attenuated total reflectance (ATR) FTIR, the incident IR beam first passes through a Zn, Se, Ge, or diamond crystal, improving the surface sensitivity of the technique. The resulting plot is of absorbance (or transmittance) versus wavenumber. Sampling depth is dependent on the infrared transmitting crystal used to internally reflect the incident IR beam as well as the refractive index of the sample, and is on the order of microns. Although ATR-FTIR has a relatively deep sampling depth, it does not require ultra high vacuum conditions, as do XPS and EDS, and an analysis can therefore be conducted in less than ten minutes.

Non-spectral methods

Contact angle. Surface atoms and molecules are in different environment compared with their bulk counterparts, they are subjected to intermolecular attraction from one side only. The energy of the surface, which is directly related to its wettability, is an useful parameter that has often correlated strongly with biological interaction. Unfortunately, there are not direct methods to measure surface energy or surface tension of solids. However, a number of indirect empirical and semiempirical methods have been developed based on contact angle measurements.[41]

Water contact angle measures surface hydrophilicity by measuring how much a droplet of water spreads on a surface. The lower the contact angle, the more hydrophilic the surface is. As a surface becomes more oxidized, or has more ionizable groups introduced to it, hydrogen bonding with the water becomes more facile and the droplet spreads along the hydrophilic surface, resulting in a lower contact angle.

Dye assays or Colorimetric methods. ATR-FTIR, XPS are powerful techniques to understand surface chemistry qualitatively or quantitatively. A complement approach to measure the amount of surface functional groups on a polymer surface is colorimetric method, particularly when a large amount of functional groups exist on the surface. The main disadvantage of the colorimetric methods, however, is that they are far less sensitive than XPS, thus is only useful when a large amount of surface functional groups are present. Further, when the colorimetric method is based on ion exchange mechanism, functional groups have to be subjectively assumed to be able to bind equal molar amount of dye molecules. A method to determine surface carboxyl density is toludine blue (TBO) colorimetry.[42] TBO is a positively charged molecule that can combine with a carboxyl group in alkaline solution to form a stable electrostatic complex through ion exchange mechanism, as shown in Figure 6. The TBO molecules immobilized on surface can be detached by dissolving in acetic acid or other organic solvents. The amount of the -COOH groups can be calculated by the assumption that they combine with TBO stoichiometrically.

[41] C.M. Chan, Contact angle measurement, Munich, Hanser Publishers, 1994.
[42] E. Uchida, Y. Uyama, Y. Ikada, Langmuir: 9, 1121-1124, 1993.

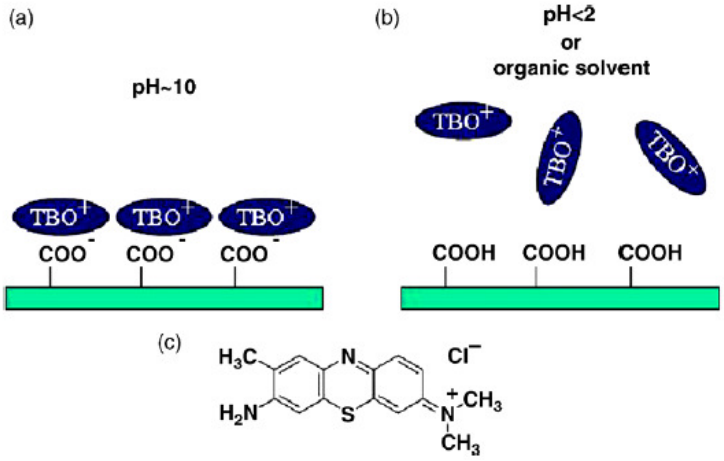

Figure 6. Quantitative analysis of –COOH group on material surface: (a) in basic solution (pH~10), positively charged TBO form complex with $–COO^-$, (b) in acídica solution (pH < 2) or organic solvents, the TBO molecules are released from the material surface; (c) molecular structure of TBO.

Similarly, methyl orange (MO) is a negatively charged dye and can combine with positively charged amino groups on material surface under acidic condition by ion exchange mechanism, as shown in Figure 7.[43]

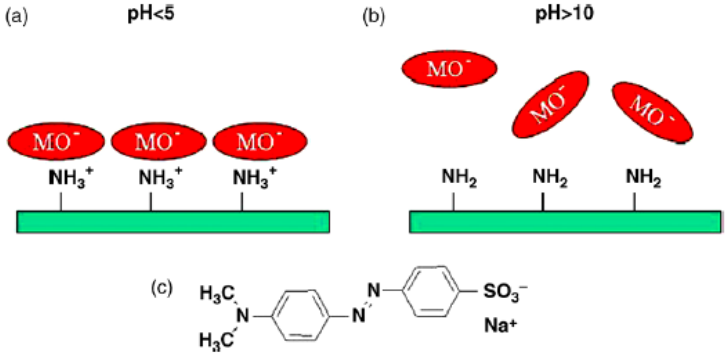

Figure 7. Quantitative analysis of amino group on material surface. (a) In acidic solution (pH~5), negatively charged MO form complex with $–NH_3^+$; (b) in basic solution (pH > 10) or organic solvents, the MO molecules are released from the material surface; (c) molecular structure of MO.

[43] A. Hartwig, M. Mulder, C.A. Smolders, Adv. Colloid. Interface Sci: 52, 65-78, 1994.

CHAPTER IV

Study on the interaction between gelatin and polyurethanes derived from fatty acids

Study on the Interaction between Gelatin and Polyurethanes derived from Fatty Acids

R. J. González-Paz[1], G. Lligadas[1], J. C. Ronda[1], M. Galià[1], A. M. Ferreira[2], F. Boccafoschi[3], G. Ciardelli[2,4], V. Cádiz[1].

[1]Department of Analytical and Organic Chemistry, Rovira i Virgili University, Campus Sescelades, Marcel.lí Domingo s/n, 43007 Tarragona, Spain.

[2]Department of Mechanical and Aerospace Engineering, Politecnico di Torino, Corso Duca degli Abruzzi, 24, 10129, Turin, Italy.

[3]Department of Clinical and Experimental Medicine, Università del Piemonte Orientale, Via Solaroli, 17, Novara, Italy.

[4] CNR-IPCF UOS Pisa Via Moruzzi 1, 56124 Pisa, Italy

Summary:

In this study, gelatin was blended to proprietary non-cytotoxic polyurethanes (PU) derived from vegetable oils with different weight ratios, as material for the preparation of novel biomedical products. The PU/Gelatin blends were characterised for their morphology through scanning electron microscopy. Mechanical and thermal properties, chemical interactions between components, degradation behavior, surface properties, cell adhesion and bioactivity were investigated as a function of the protein content. Higher blend miscibility was observed for the amorphous PUs, derived from oleic acid.Properties of PU/Gelatin films were strongly influenced by the concentration of gelatin in the films. Gelatin enhanced the hydrophilicity, bioactivity and cell adhesion of PUs.

Introduction:

Polyurethanes (PUs) are used in a wide variety of product applications in view of their extensive structure/property diversity such as excellent mechanical properties, elasticity and flexibility, high elongation and good biocompatibility.[1-5] During the past few decades, PUs have been widely used for biomedical applications such as vascular protheses, catheters and for skin and bone regeneration.[6] In these applications PU scaffolds demonstrated to support cell in-growth and tissue remodeling.[7-15]

Vegetable oils are abundant biological materials and are used to obtain bio-based PUs because of their numerous advantages: low toxicity, inherent biodegradability, high purity and non cytotoxic response. By modifying the chemical structure, these polymers will show different physical, chemical, and thermal properties and can become rigid or flexible, biostable or biodegradable and cytocompatible or bioactive. [16-21]

Blending has acquired importance in improving the performance of polymeric materials. It has become an economical and versatile way to obtain materials with a wide range of desirable properties. In order to ensure the homogeneity of the blends at microscopic level, resulting in superior material properties, it is necessary to reduce the interfacial tension between the two constituent materials.[22]

Blends of synthetic and natural polymers as proteins have been used in the last decades to develop new materials, the so-called ‘‘bioartificial polymeric materials’’. Their capability of combining good physical and mechanical properties with biocompatibility characteristics was used with the purpose of making new materials for biomedical applications.[23-27]

The combination of proteins with synthetic polymers should promote and stimulate enhanced cell and tissue compatibility of the synthetic matrix.[28] In general, all biological interactions (e.g. between cells, cells and extracellular matrix) are mediated by specific biorecognition involving cell receptors which show high-affinity to specific ligands. These ligands may be introduced into biomaterials by adsorption of extracellular matrix proteins on to a synthetic polymer. To engineer a cell-biomaterial interaction, it is necessary to understand the protein adsorption mechanism on a surface.

The primary interaction between a protein and a substrate upon which it adsorbs is the hydrophobic effect. Hydrophobic surfaces tend to adsorb large amount of proteins with respect to hydrophilic ones. Secondary interactions involved in protein adsorption are electrostatic forces, resulting from opposite charges on a protein and the interacting surface.[29,30]

Gelatin is a soluble extracellular matrix protein obtained by partial hydrolysis of collagen, the main fibrous protein constituent in bones, cartilages and skin. This protein has chemotactic or adhesive properties: an Arg-Gly-Asp (RGD) aminoacidic sequence is found in the backbone of gelatin and serves as binding site for the cell receptors, thus improving cell adhesion, migration and differentiation.[31,32]

In this study, gelatin was blended to non-cytotoxic polyurethanes derived from vegetable oils[21] with different weight ratios to develop novel bioartificial blends. Microscopic morphology, mechanical and thermal properties, chemical interaction, degradation tests, contact angle, cell adhesion and bioactivity were investigated as a function of the protein content.

Materials and methods

Materials

Gelatin (bovine skin, type B) and hexafluoro-2-propanol (HFIP) were purchased from Sigma-Aldrich. Polyurethanes derived from fatty acids and 4,4'-methylenebis (phenyl isocyanate) (PUs) were synthesized as described in a previous work.[21] All the analytical grade chemicals for preparing Simulated Body Fluid (SBF) and used in the Western Blot analyses were purchased from Sigma Aldrich.

Preparation of Simulated Body Fluid (SBF)

Simulated body fluid (SBF) was prepared to create physiological fluid conditions according to Kokubo.[33] SBF was prepared by dissolving reagent grade chemicals (NaCl, $NaHCO_3$, KCl, $K_2HPO_4.3H_2O$, $MgCl_2.6H_2O$, $CaCl_2$, and Na_2SO_4 into

distilled water). It was buffered to pH 7.25 with 50 mM Tris-HCl. SBF has a composition similar to human blood plasma.

Samples preparation

Gelatin was suspended in HFIP at room temperature under stirring overnight, PU was added and the mixture was stirred at 40 ºC for 30 min until homogeneous solution was obtained. PU/Gelatin films of various blending weight ratios (PU/Gelatin = 100:0, 70:30, 90:10, 0:100) were prepared by casting a 20 wt % blended solution in 10 ml of HFIP. The films were cast onto Petri dishes and then dried at room temperature for about 7 days until the solvent was completely evaporated. To eliminate any residual solvent, cast films were dried at 37 ºC for 48 h and stored in a vacuum desiccator.

Bioactivity evaluation and *in vitro* morphological changes

In order to study the bioactivity and morphological changes in SBF of PU/ Gelatin samples, films were cut into specimens of 5 mm x 20 mm and immersed in 25 ml of SBF. The temperature was kept at 37 ºC in the shaking incubator (180 rpm) for up to 4 weeks and SBF solution was changed every 5 days. After being incubated for various periods of time (1-4 weeks), the specimens were removed from the SBF solutions, rinsed carefully several times with deionized water and subsequently dried for morphological analysis (scanning electron microscopy; SEM) and composition determination (energy-dispersive spectroscopy; EDS).

Morphological Characterization (SEM-EDS)

The surface morphology and compositional changes were observed using a LEO 1430VP SEM-EDS Equipment. Prior to SEM-EDS examination, samples surfaces were coated with a conductive thin gold film.

Western Blot anti-vinculin analyses for cell adhesion

NIH3T3 fibroblast cells were used. Fibroblast cells were cultured in DMEM enriched with 10% fetal bovine serum (FBS), glutamine (2mM), penicillin (100 U/ml) and streptomycin (100 µg/ml) (Euroclone, Italy). Cells were maintained at 37 °C in a

humidified atmosphere with 5% CO_2 on the samples surfaces. Samples were seeded with NIH3T3 cells and cultured for 24 h. Culture medium was then discarded and a lysis solution (SDS 2.5%, Tris-HCl pH 7.4, 0.25 M in bidistilled water) was placed on different samples. Cell proteins were quantified through BCA assay (Thermo Scientific, USA). For electrophoresis, 10 μg of total proteins were used. Samples were diluted with Laemmli reducing buffer (60 mM Tris-Cl pH 6.8, 2% SDS, 10% glycerol, 5% β-mercaptoethanol, 0.01% bromophenol blue), and electrophoresed on 7.5% sodium dodecylsulfate polyacrylamide gels (SDS-PAGE). The proteins were blotted onto nitrocellulose membranes. The membranes were incubated for 1 h in 5% blocking solution (non-fat dry milk in PBS), then incubated overnight with 1:500 dilution of primary antibodies (vinculin-Calbiochem, USA), followed by incubation with appropriate secondary antibody HRP-conjugated (Perkin-Elmer, USA). Proteins were detected by Western Lightning plus-ECL (Perkin-Elmer, USA), and protein bands were then visualized by Bio-Rad VersaDoc™ imaging system (BioRad, Milano, Italy). Cells seeded on cell culture Petri dishes were used as positive control.

Beta-actin antibody (abcam, UK) has been used as loading control for western blot analyses. 10 μg of total proteins were used as performed for vinculin detection.

Contact angle

The hydrophilic/hydrophobic properties of the PU/gelatin blended films were evaluated by contact angle measurements using CAM 200 KSV Instrument, equipped with Tetha software. Static contact angle measurements were carried out adding 5μl-drop of distilled water by a motor driving syringe at room temperature on three different samples of each material and at least five measurements for each sample.

Mechanical tests

Stress-strain curves of PU/Gelatin blended films (10 mm x 5 mm x 0.1 mm, length/width/thickness) were obtained at room temperature by means of a tensile testing machine MTS Qtest/10 Elite Controller, at a crosshead speed of 2 mm/min. At least three specimens of each sample have been used.

Differential Scanning Calorimetry (DSC).

Calorimetric studies were carried out on a TA DSC-Q20 instrument. Samples were accurately weighed (5.5 ± 0.5 mg) and sealed in hermetic aluminium pans. Dry nitrogen gas was purged into the DSC cell at a flow rate of 50 ml/min. DSC analysis was carried out at scaninng rate of 10°C /min. An empty reference pan with the same weight was used as control.

Thermogravimetric Analysis (TGA).

Thermal stability studies of PU/Gelatin blended films were carried out on a TGA Q5 instrument (TA, USA) with N_2 as a purge gas. The heating rate in TGA dynamic mode was 10 °C/min from 25 °C up to 600 °C. Samples of 10 ± 0.5 mg were used.

Infrared Spectroscopy by Attenuated Total Reflection Spectroscopy (ATR-FTIR).

Chemical characterization of PUs, gelatin and PU/Gelatin blended films was performed by ATR-FTIR, using a Frontier PerkinElmer FT-IR spectrophotometer with universal ATR module (Diamond/KRS-5 crystal) in the 4000-400 cm^{-1} wavenumber range. The spectra were analysed by Spectrum 10TM software (PerkinElmer, USA).

Results and discussion

The chemical structures of previously synthesized oleic- and undecylenic acid-derived polyurethanes (PU1-PU4) are shown in Figure 1. These PUs revealed good thermal and mechanical properties and no cytotoxic response[21], which make them promising materials for biomedical purposes. To prepare new bioartificial polymeric materials with good biocompatibility and high performance, blends of synthetic and natural polymers as gelatin were studied. Blends were prepared by mixing gelatin and PUs in HFIP obtaining a homogeneous solution, thus showing compatibility of the two components in HFIP solution. Blended films of PUs/gelatin were prepared by casting and the interaction of gelatin and PUs investigated.

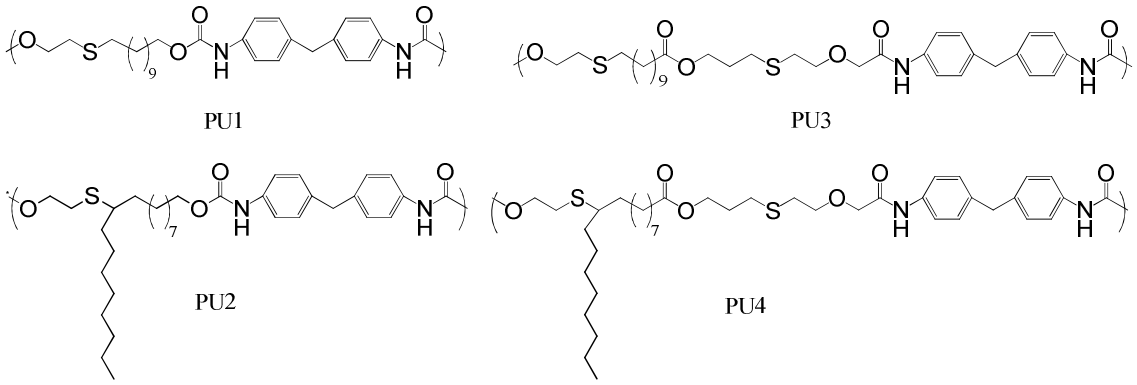

Figure 1. Chemical structures of polyurethanes (PUs)

Morphology of films

Figure 2 shows the SEM images of the blended films of PUs/gelatin with two blending weight ratios: 90:10 and 70:30, prepared by solution casting. The two micrograph images of PU1/gelatin (a) are the only ones showing clear indications of phase segregation of the two components. In all cases is observed that as the blending concentration of gelatin increased, the roughness of the surface increased.

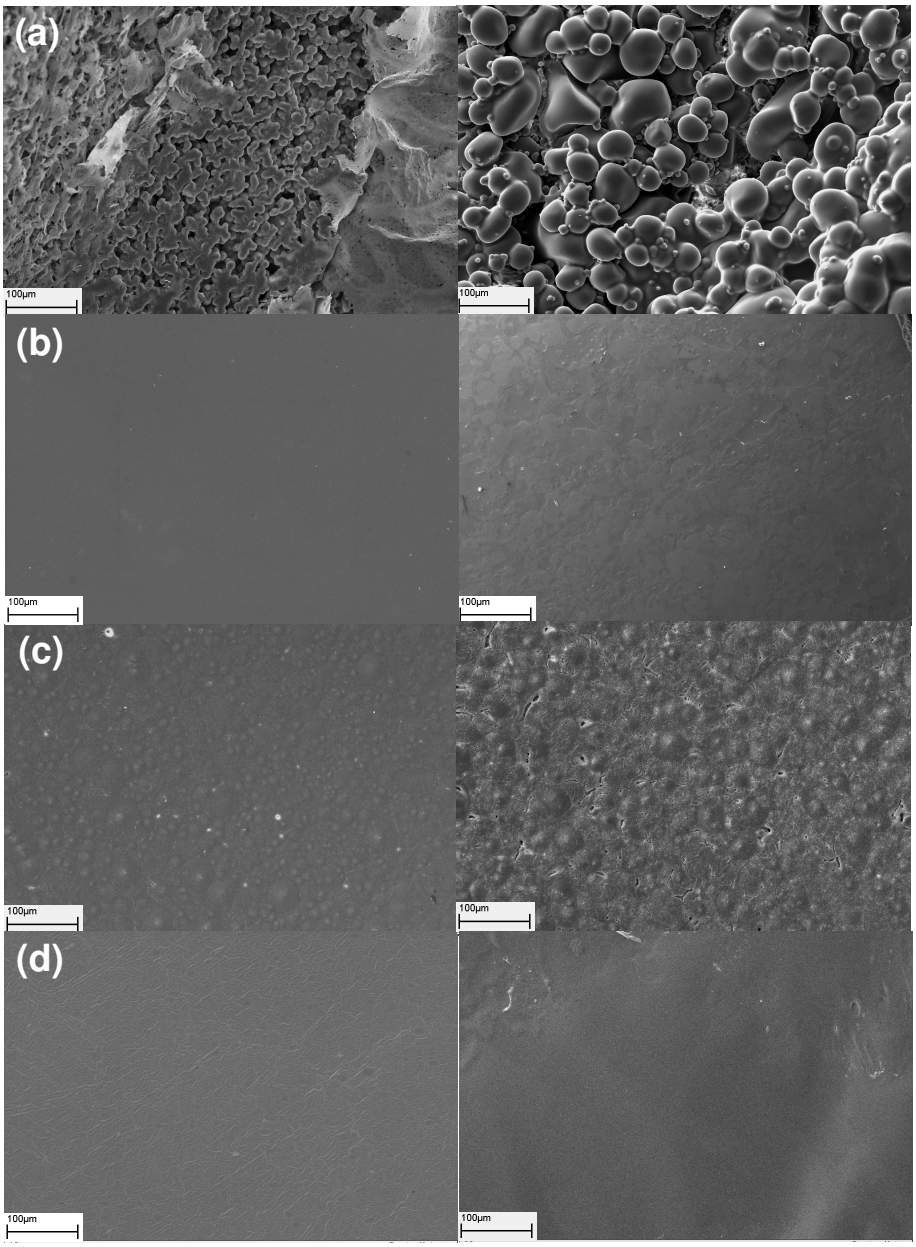

Figure 2. SEM images of 90:10 (left) and 70:30 (right) PU/gelatin blended films:
a) PU1/gelatin; b) PU2/gelatin; c) PU3/gelatin; d) PU4/gelatin

PU1 and PU3 derivatives from undecylenic acid showed higher crystallinity than PU2 and PU4 derivatives from oleic acid due to the presence of long aliphatic pendant chains that hinder macromolecular chain packing. Thus, the higher flexibility of PU2 and PU4 chains benefits the miscibility of these PUs/gelatin blends as it appears in the higher homogeneity observed in the PU2/gelatin and PU4/gelatin micrographs.[34]

Chemical and thermal properties

Chemical characterization of blended PUs/gelatin films was done by IR spectroscopy in the range of 1000-4000 cm^{-1} by ATR-FTIR. As an example, figure 3 shows the IR spectra of blended 90:10 and 70:30 PU1/gelatin films, together with PU3 and gelatin spectra. Characteristic absorption bands of main chain of PU3 were observed. C=O stretching bands of urethane bonds appear at 1701 cm^{-1}, while the NH stretching and bending bands appear at 3323 cm^{-1} and 1525 cm^{-1} respectively. Gelatin diagnostic adsorptions, appear at approximately 1650 cm^{-1} (amide I) due to stretching vibration of the C=O bond, 3297 cm^{-1} and 1540 cm^{-1} (amide II) corresponding to the NH stretching and bending bands respectively, and 1280 cm^{-1} (amide III) corresponding to the stretching vibration of the C-N bond. The presence of the amide III band is indicative of the triple helix structure of gelatin.[35] As can be seen, the spectra of blended films showed common bands of PU1 and gelatin and notably an increase of the amide I and amide III bands is observed with increasing amount of gelatin in the blend.

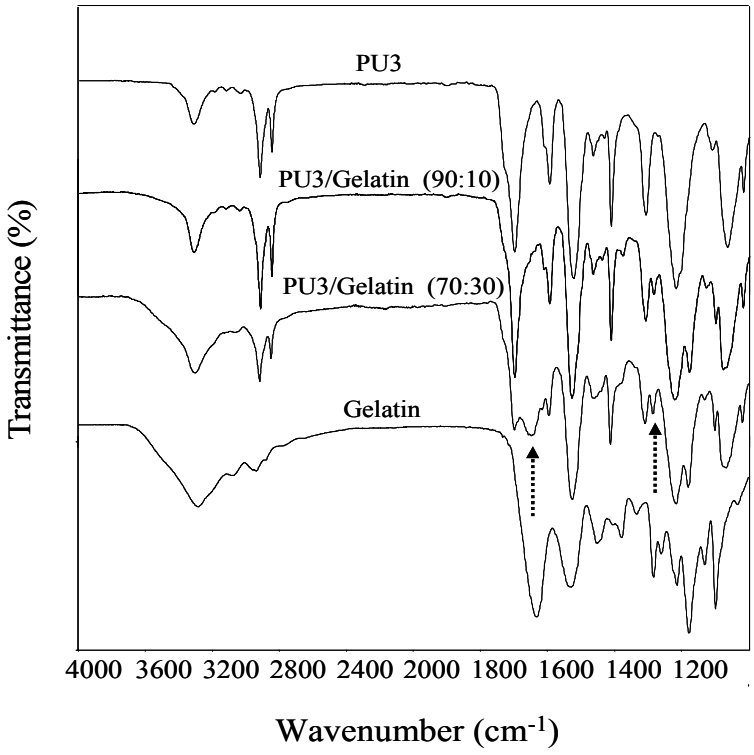

Figure 3. FTIR-ATR spectra of blended PU3/gelatin, PU3 and gelatin.

The thermal degradation behavior of PUs, gelatin and the blended samples were examined by TGA in nitrogen atmosphere. The thermal degradation of the different blends showed a similar behaviour. As an example, the PU4/gelatin thermograms are collected in Figure 4 together with those of PU4 and gelatin. Decomposition curves of PU4/gelatin blends cast films show up to three overlapped degradation events. The first weigth loss (8-10%) was attributed to dehydration of absorbed moisture and/or volatile components evaporation. The second and third steps represent the sequence of pyrolitic reactions.[23]

The thermal gravimetric curves show an event between 250 ºC and 500 ºC which indicates the higher weight loss in all samples, which is characteristic of chemical degradation process resulting from scission of urethane and peptide linkages in the polymer backbone. It is clear from Figure 4 that the thermal stability regions of the blended samples are at a temperature values comprised between those corresponding to the parent components and their stability decrease while increasing the gelatin content.

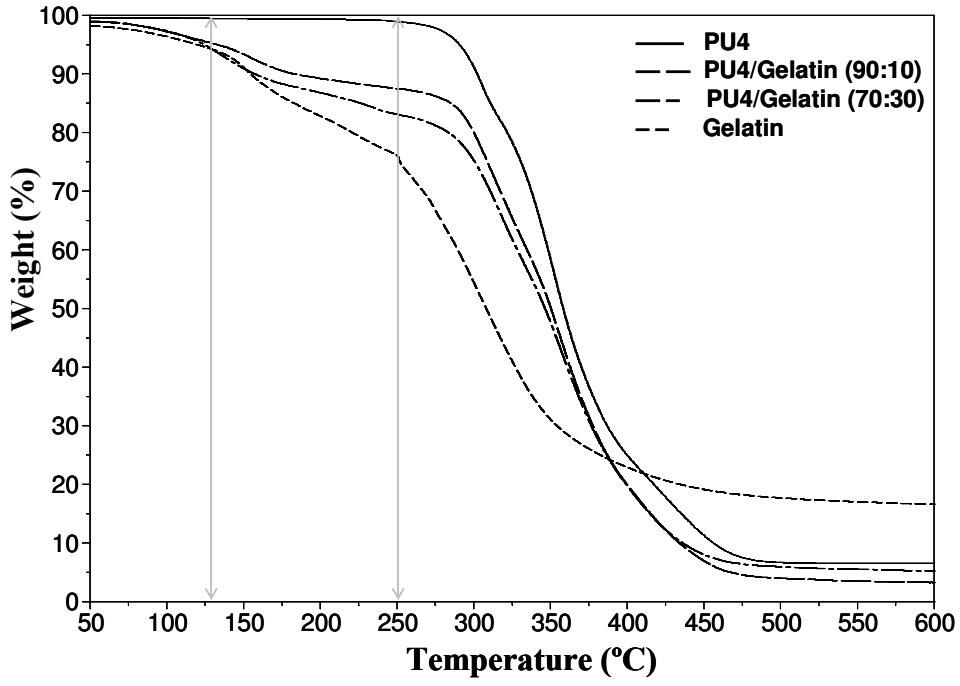

Figure 4. Thermograms of PU4, gelatin and blended PU4/ gelatin.

The effect on thermal transitions Tg and Tm arising from the different precursors was investigated by DSC (Table 1). Figure 5 shows DSC traces for the different PUs/gelatin blends and their parent components. Gelatin (IV) presented a

classical behavior: a glass transition (T_g = 65 ºC) followed by helix coil transition or melting process (T_m = 153 ºC). Gelatin is a denatured collagen and during the denaturation process, the triple helix structure of collagen is broken to form random-coil gelatins. In an aqueous solution or specific organic solvents as HFIP, [35,36] some gelatin chain can form secondary structures (helix) and three dimensional network with zones of intermolecular microcrystalline junctions stabilized by the formation of interchain hydrogen bonds between C=O and N-H groups. In PUs, hydrogen bonding also exists between the same groups, consequently, it is now a well-known strategy to enhance the compatibility of PUs/Gelatin blends by the incorporation of inter-associated hydrogen bonds.[34] The formation of intermolecular hydrogen bonds between PUs and gelatin not only promotes the miscibility of PUs/Gelatin blends but also modifies the properties of the PUs.

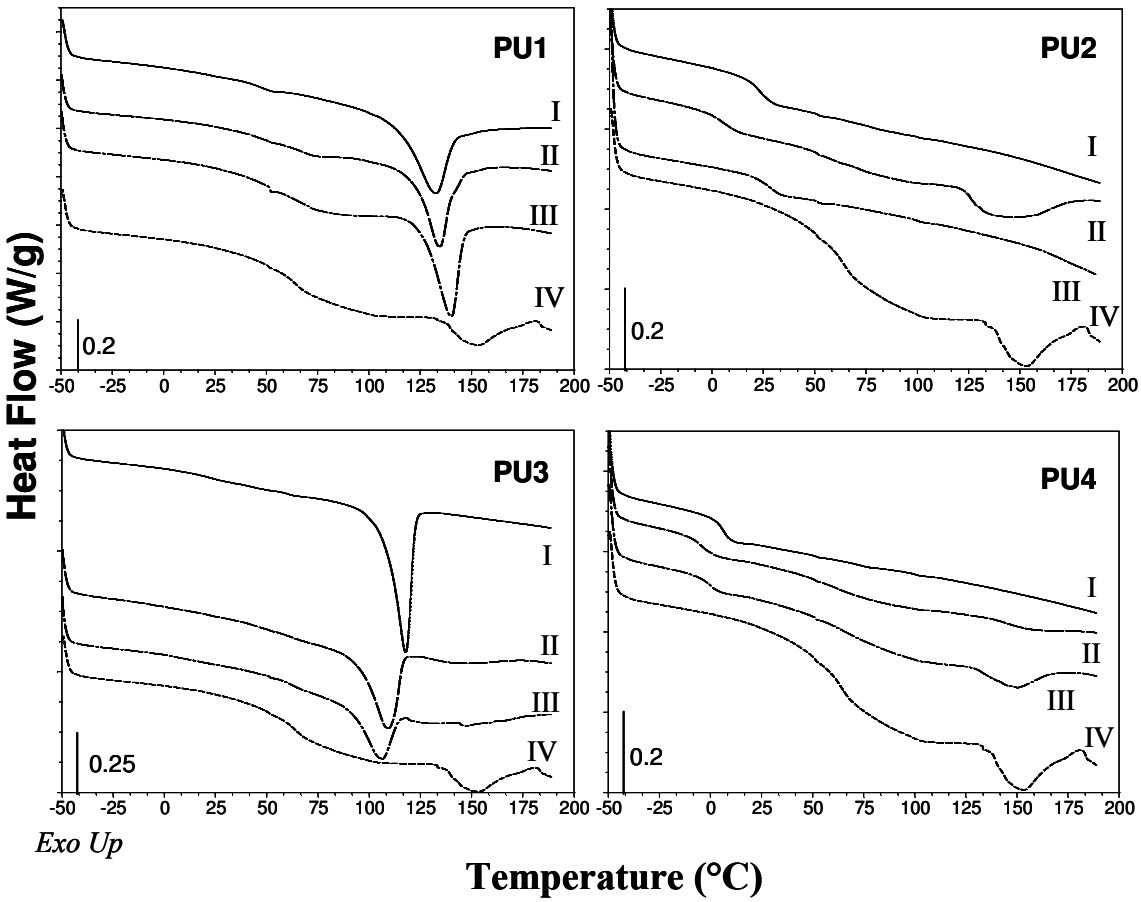

Figura 5. DSC traces of (I) PUs, (II) PUs/gelatin (90:10), (III) PUs/gelatin (70:30) and (IV) gelatin.

The decrease of the melting point of a crystalline polymer component in a blend provides important information about its miscibility and its associated polymer-polymer interaction. In some blends, the hydrogen bonds are so strong that the crystallization of the crystalline components is hindered. Coherently, Figure 5 thermograms of blended PU3/gelatin (II and III) show that the melting point (T_m) and the enthalpy of melting (ΔH_m) of PU3 decrease with increasing gelatin content in the blends, and the crystallization of gelatin is suppressed in both cases. In contrast, the blended PU1/gelatin films (II and III) only show slight changes in Tm and ΔH_m compared to PU1 (I). Moreover, although the endotherm of melting process of gelatin is suppressed, its T_g, remains at 63º C. These results are in accordance with the above mentioned phase segregation of the two components observed by SEM (see Figure 2a).

Literature concerning hydrogen-bonded polymer blends demonstrate that, in general, a positive or negative deviation from linearity of the blend Tg is observed,[34] and that is the case for the blends from amorphous PU2 and PU4 precursors. Moreover, as it can be observed in the thermograms of these blends the melting process of gelatin is diminished or inhibited as above mentioned for PU1 and PU3.

Table 1. Thermal properties of PUs/gelatin blends and parent components

	DSC		
Samples	**T_g (ºC)**	**T_m (ºC)**	**ΔH (J/g)**
Gelatin	63	153	16
PU1	56	133	35
PU1/gelatin (90:10)	63	134	33
PU1/gelatin (70:30)	63	137	32
PU2	25	-	-
PU2/gelatin (90:10)	5	149	10
PU2/gelatin (70:30)	30	-	-
PU3	20	122	42
PU3/gelatin (90:10)	-	108	30
PU3/gelatin (70:30)	-	104	14
PU4	8	-	-
PU4/gelatin (90:10)	-4	154	2
PU4/gelatin (70:30)	0	149	6

Contact angle

Cells adhere and spread more effectively on surfaces with suitable hydrophilicity than on hydrophobic surfaces. Thus, surface wettability, that influences cell adhesion and proliferation, was measured by the water contact angle (Figure 6). Contact angles of the pure PUs show the highest hydrophobicity while the gelatin has a higher wettability. As the concentration of gelatin increases in the blends, water contact angles significantly decrease. These results prove that the addition of a hydrophilic natural polymer such as gelatin improves the hydrophilic properties of PUs/gelatin blends.

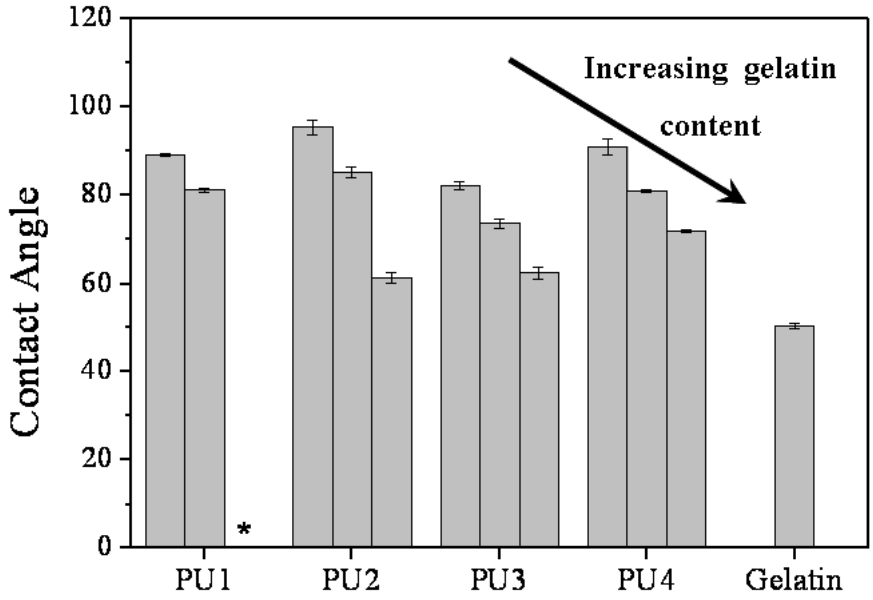

Figure 6. Contact angle values of PUs, gelatin and blended PUs/ gelatin.

* irregular sample surface to measure contact angle

Mechanical properties

In general, the mechanical properties of gelatin materials are not matching the requirements of most biomedical applications. This limitation can be overcome by blending gelatin with other polymers of either natural or synthetic origin.[23,32] In particular, for what concerns polyurethanes, they exhibit much higher elasticity than most of the other polymers used in biomedical applications.[6]

The tensile stress-strain curves of blended PUs/gelatin films with different compositions are shown in Figure 7.

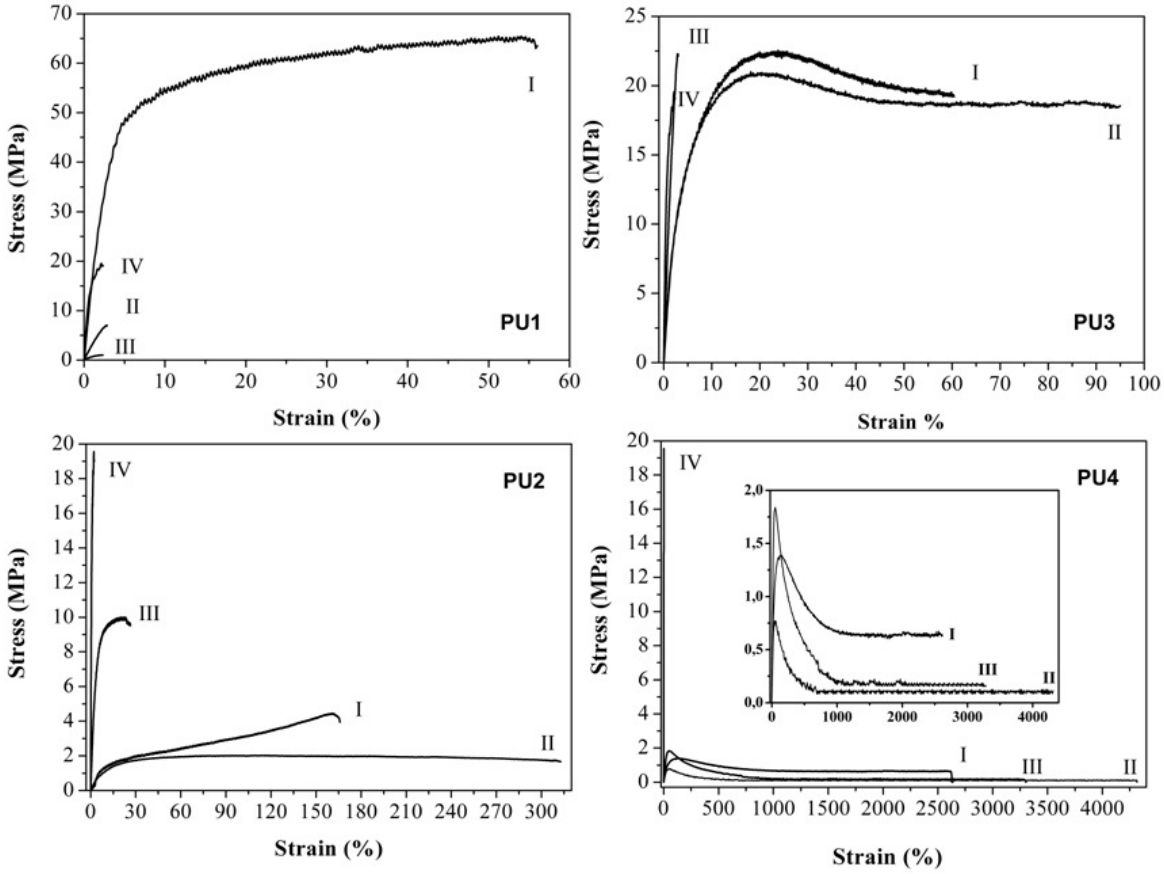

Figure 7. Stress-strain curves of : (I) PUs; (II) PUs/gelatin (90:10); (III) PUs/gelatin (70:30); (IV) gelatin.

As it is evident in Fig. 7 PUs/gelatin blends with composition of 10 wt % of gelatin (II) show a higher elongation at break in all samples, with the exception of PU1/gelatin blend. In this case, which presented phase segregation (see Fig. 2a), both blended PUs/gelatin (II and III) showed lower mechanical properties than their pure components (I and IV). Moreover, the combination of PUs and gelatin with a ratio of 30 wt% (III) increases the strength, but decreased the elongation at break of PU2 and PU3 blends. Only the combination of PU4 and gelatin with a ratio of 30 wt% (III) increases the mechanical properties, strength at yield and elongation at break, thus confirming appropriate interaction between PU4 and gelatin.[32]

Morphology Changes and Bioactivity Evaluation in SBF

Figure 8 exhibits morphological changes in PUs/gelatin blends as well as PUs control, during *in vitro* degradation after 1 week.

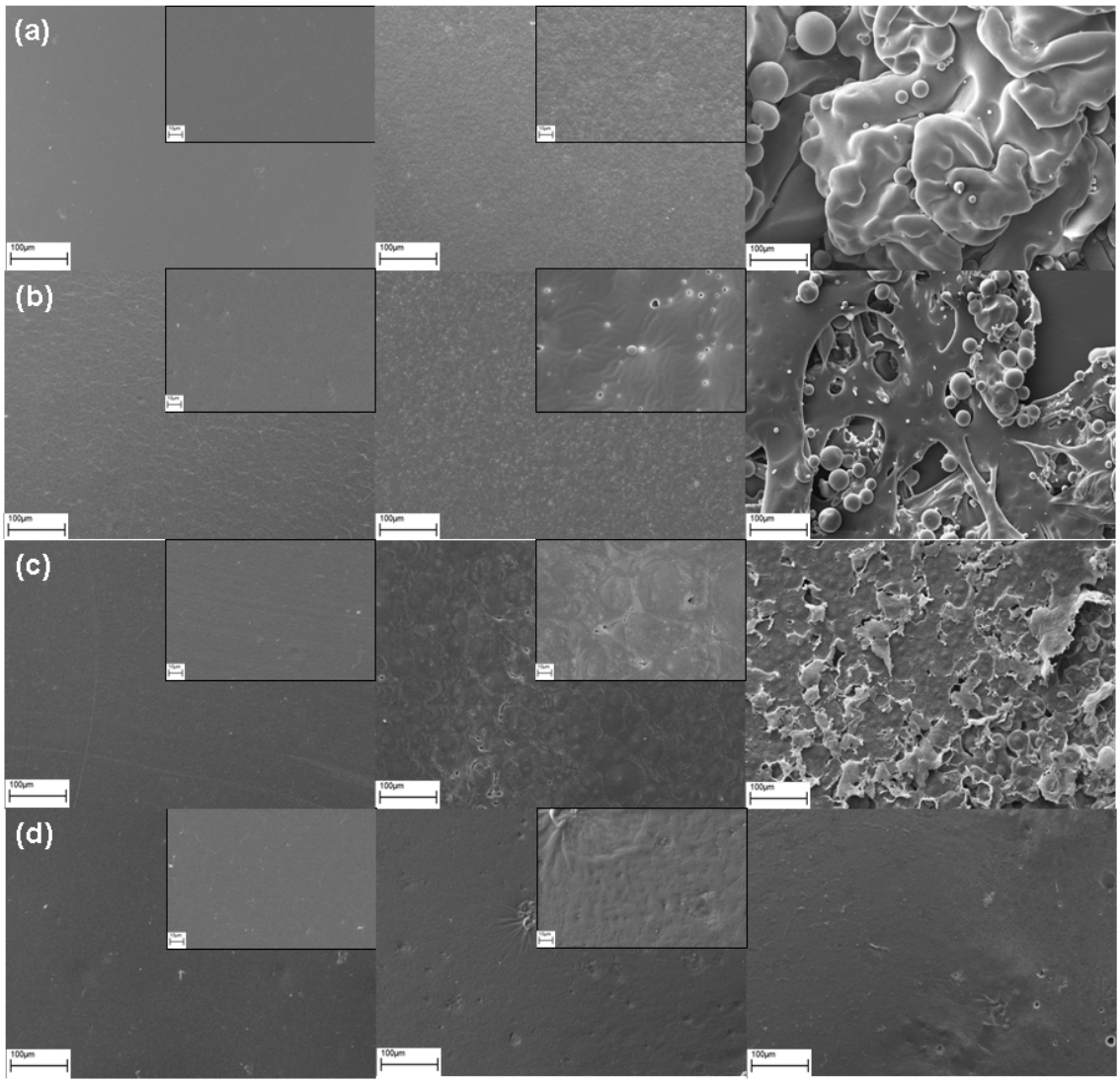

Figure 8. SEM images of degraded PUs (left) and PUs/Gelatin blends 90:10 (middle) and PUs/Gelatin blends 70:30 (right) in SBS solution, after 1 week. a) PU1; b) PU2; c) PU3; d) PU4.

With the exception of PU4/Gelatin blend, in which the erosion rate is lower, it can be seen that the amount of gelatin dominates the morphology of the film. The higher the amount of gelatin loading the higher is the erosion on the surface, which is in

agreement with the hydrophylicity of the blends, with consequently easier water diffusion.

A material is called "bioactive" when it has been designed to induce a specific biological activity.[37] The use of a bioactive material capable to nucleate calcium and phosphate ions on the surface of an implant may be advantageous, as bone formation can be accelerated as compared with the more inert metallic oxide surface of metallic implants. *In vivo* bioactivity can be predicted from *in vitro* tests using a simulated body fluid (SBF) with a similar ion concentration to that of human blood plasma. In our experiments, the original SBF solution was used having the same composition proposed by Kokubo et al.[33] A material that rapidly forms bonelike calcium phosphates on its surface when immersed in SBF will bond to living bone in a short period after implantation. This method can thus be used for screening the bioactivity of materials before *in vivo* animal testing. Recently, biomimetic deposition of calcium phosphate from SBF has been shown to be an effective method for coating many different types of polymers. In addition, the structure of biomimetic calcium phosphate may more closely match the structure of natural bone mineral and, therefore, enhance implant fixation and bone regeneration. The deposition of calcium phosphate crystals upon immersion in SBF has been generally attributed to ionic interactions between the scaffold surface and the SBF medium. In terms of being able to study calcium phosphates mineralization near-biological conditions, gelatin and oils have attracted some attention.[38] In Figure 9, the SEM micrographs of blended films of PUs/Gelatin after bioactivity experiments, are shown.

As can be seen, after two weeks (a-d), a significant difference is observed between the pure PUs and PUs/Gelatin blends. The first do not show mineral nucleation on the surface while the blends do. However, this nucleation was observed on PUs surface after four weeks (e-h). Composition EDS analyses on mineral content of all the samples is showed in Table 2.

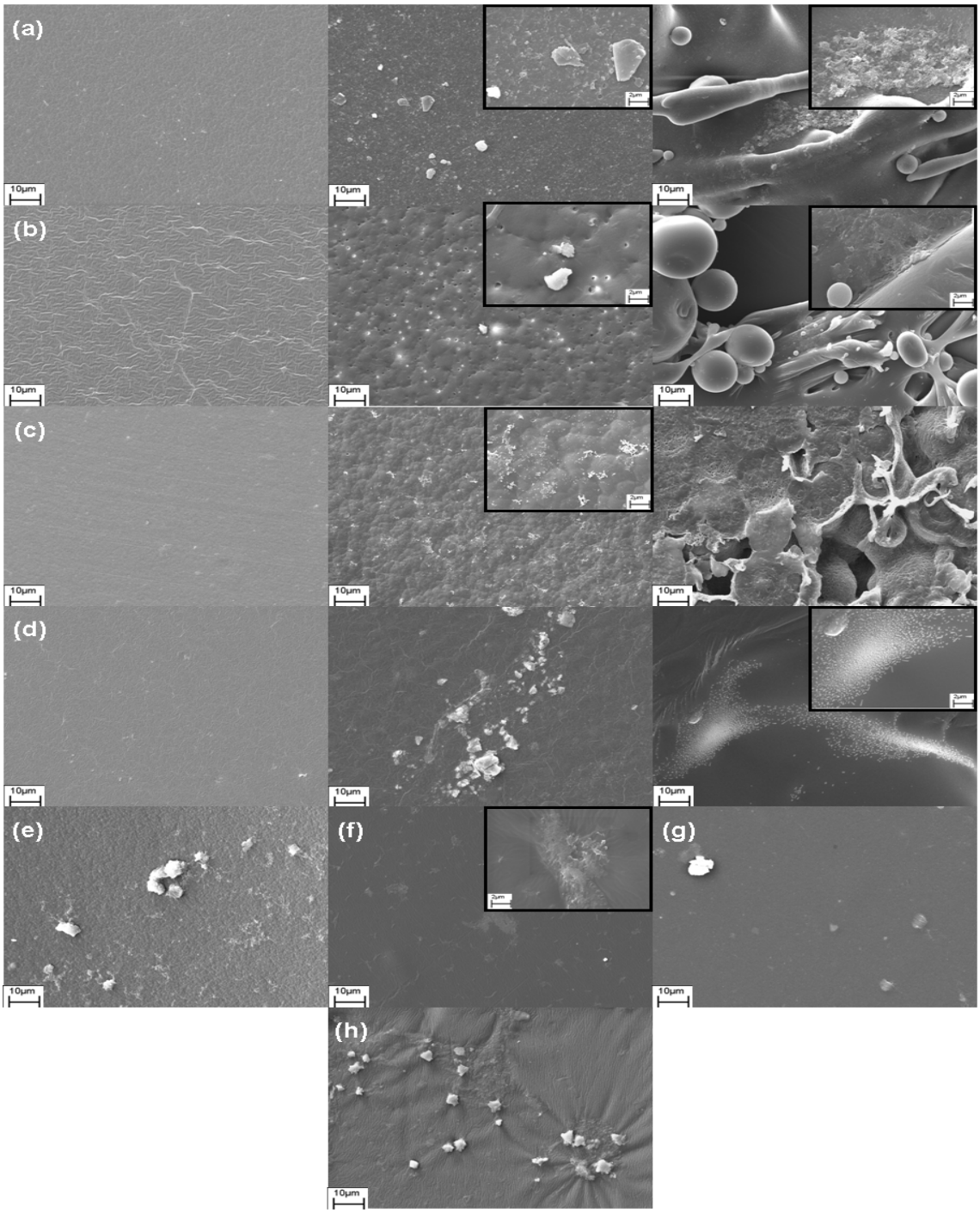

Figure 9. SEM images of PUs (left) and PUs/Gelatin blends 90:10 (middle) and PUs/Gelatin blends 70:30 (right) in SBS solution, after 2 weeks: a) PU1; b) PU2; c) PU3; d) PU4, and SEM images of pure PUs in SBF after 4 weeks: e) PU1; f) PU2; g) PU3; h) PU4.

Table 2. Composition analyses on mineral content by EDS.

Samples	Time	Atomic (%)							Ca / P ratio
		Mg	C	Cl	Na	O	P	Ca	
PU1/gelatin (90:10)	2 weeks	16.9	34	-	-	47	-	1.8	-
PU1/gelatin (70:30)	2 weeks	-	-	-	-	89.42	3.35	7.23	2.15
PU2/gelatin (90:10)	2 weeks	-	-	-	-	97	1.5	1.5	1
PU2/gelatin (70:30)	2 weeks	-	-	-	-	94.38	2.11	3.51	1.66
PU3/gelatin (90:10)	2 weeks	-	-	-	-	94.89	1.9	3.21	1.68
PU3/gelatin (70:30)	2 weeks	-	71.06	0.98	0.78	24.35	-	2.83	-
PU4/gelatin (90:10)	2 weeks	-	-	-	-	90.17	6,52	3.31	0.50
PU4/gelatin (70:30)	2 weeks	-	-	-	-	97.78	1.47	0.75	0.51
PU1	4 weeks	-	-	-	-	-	1.88	0.89	0.47
PU2	4 weeks	-	-	-	-	97.37	1.78	0.85	0.48
PU3	4 weeks	-	-	-	-	98	1.01	0.99	0.98
PU4	4 weeks	-	-	-	-	74.99	11.91	13.1	1.09

The minerals on PU1/Gelatin (90:10) and PU3/Gelatin (70:30) blends surface show the typical atomic composition of calcium phosphates contained in natural bone such as Mg, Na, or Cl which can be introduced into the bonelike calcium phosphate lattice by substitution of one or more Ca atoms. However, the major substituent in biological bonelike calcium phosphates is carbonate which in bone mineral occurs, typically in 5-8wt%.[39] PU1/Gelatin (90:10) and PU3/Gelatin (70:30) blends are the only ones that present C atoms in the compositional analyses by EDS after 2 weeks, thus, carbonate may be the mineral nucleated on surface. Other PUs/Gelatin blends showed

Ca/P ratios typical of biological calcium phosphates.[40] Thus, PU1/Gelatin (70:30) has a Ca/P ratio of 2.15, this ratio is attributed to amorphous calcium phosphate (ACP), Posner[41] proposed that ACP is the initially precipitating phase during bone formation *in vivo*. Ca/P ratio in PU2/Gelatin (90:10) blend is 1, which is the Ca/P ratio found in pathological calcifications corresponding to dicalcium phosphate dihydrate (DCPD) and it is used in calcium phosphates cements for dentistry and other biomedical applications. PU2/Gelatin (70:30) and PU3/Gelatin (90:10) shows Ca/P ratios very close to the value found for stoichiometric hydroxyapatite (1.67), which is a calcium phosphate similar to natural bone. Due to chemical similarities to bone and teeth mineral, hydroxyapatite (HA) is widely used as coating for orthopedic and dental implants. PU4/Gelatin blend shows a Ca/P ratio of 0.5, which corresponds to monocalcium phosphate monohydrate (MCPM) which is used in some calcium phosphate cements in medicine and mineral supplements for foods and beverages. Calcium phosphates nucleation were observed on pure PUs surface after four weeks inmersed in SBF, as can been observed in Table 2, they showed Ca/P ratios of 0.5 (MCPM) and 1 (DCPD). As conclusion, the bioactivity of the PUs is improved with gelatine and PU/Gelatin blends showed mineral nucleation on the surface faster than the PUs.

Western Blot anti-vinculin (131 kDa) analyses for cell adhesion

PUs derived from fatty acids used here to prepare the blends with gelatine, showed to be noncytotoxic.[21] To further investigate the biocompatibility of these materials, and to study the influence of the blended gelatine, cell adhesion assays were performed, by measuring vinculin expression through Western Blot. Vinculin is a protein associate to focal adhesion of cells to substrates and adherent unions between cells and substrates. Focal adhesion quantification is a suitable method to measure biomaterial biocompatibility.[42] For cytocompatibility testing, quantifying the amount of cell attachment should be proportional to the number of attached focal adhesion sites formed. Identifying a focal adhesion complex is possible by labeling any protein within it, using immunocytochemical cell adhesion identification (Western Blot anti-vinculin analyses), which is a sensitive technique, since differences in adhesion to more subtly differing substrates could be detected by the difference in the protein expression. Increasing the expression of vinculin promotes cell adhesion and reduces cell motility.

In Figure 10 a higher vinculin expression is observed for amorphous PUs (PU2 and PU4) in comparison with semicrystalline PUs (PU1 and PU3). As expected, blending of PUs and gelatin improve cell attachment compared to pure PUs.

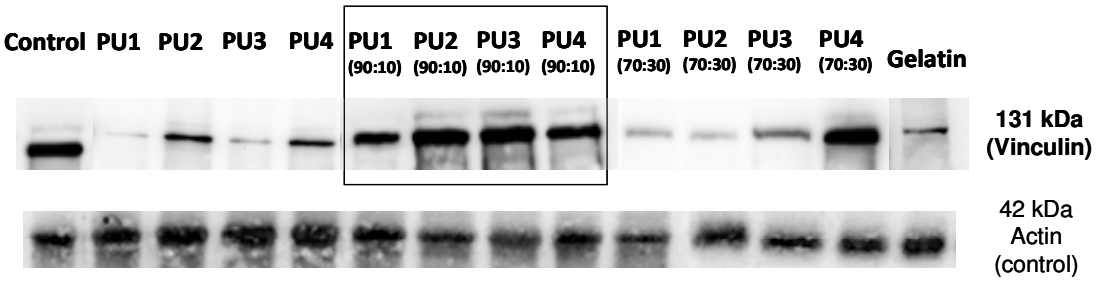

Figure 10. Western blot anti-vinculin (131 kDa) analyses on NIH3T3 fibroblast-like cells seeded on different substrates for 24 h.

These results reflect the fact that cells require cell adhesions ligands (gelatin) for adhesion, but they also demonstrate that there might be an optimal ligand concentration and indicate that cell adhesion decrease, in most cases, in blends with a high concentration of gelatin. PUs/Gelatin blends with composition of 10 wt% of gelatin have higher expression of vinculin (comparable with positive control) than blends with composition of 30 wt% of gelatin. Only the combination of PU4 and gelatin with a ratio of 30 wt% presents a higher vinculin expression, comparable with control, in the blends. This could be attributed to the lower erosion rate presented on the surface of this blend (Figure 8 d). Neff et al. demonstrated that an intermediate RGD concentration on the surface provides maximun cell adhesion of fibroblasts, indicating that excessive peptide levels on the surface causes a decrease in cell adhesion.[43]

Conclusions

In this study, gelatin was blended to proprietary non-cytotoxic polyurethanes (PUs) derived from vegetable oils with different weight ratios. Higher blend miscibility was observed for the amorphous PUs, derived from oleic acid due the higher flexibility of their chains. Results demonstrate that the properties of PU/Gelatin films were strongly influenced by the concentration of gelatine in the films. The hydrophilic

gelatine improves the hydrophilic properties of the of the PU/Gelatin blends with consequently easier water diffusion and a higher erosion on the surface. The bioactivity of the PUs is improved with gelatin, thus PU/Gelatin films showed mineral nucleation on the surface faster than the PUs. Western blot analysis showed that adhesions ligands (gelatin) improved cell adhesion. Gelatin/PU films prepared would eventually be suitable for biomedical applications, such as orthopedic and dental implants.

Acknowledgement

The authors express their thanks to CICYT (Comisión Interministerial de Ciencia y Tecnología) MAT2011-24823) for financial support for this work.

References

[1] Wirpsza Z. Polyurethanes: Chemistry, technology and applications, Ellis Norwood, London 1993.

[2] Król P. Synthesis methods, chemical structures and phase structures of linear polyurethanes. Properties and applications of linear polyurethanes in polyurethane elastomers, copolymers and ionomers, Prog Mater Sci 2007;52:915-1015.

[3] Chattopadhyay DK, Raju KVSN. Structural engineering of polyurethane coatings for high performance applications, Prog Polym Sci 2007;32:352-418.

[4] Del Rio E, Lligadas G, Ronda JC, Galià M, Meier MAR, Cádiz V. Polyurethanes from polyols obtained by ADMET polymerization of a castor oil-based diene: characterization and shape memory properties. J Polym Sci: Part A Polym Chem 2011;49:518–525.

[5] Vozzi G, Rechichi A, Dini F, Salvadori C, Vozzi F, Burchielli S, Carlucci F, Arispici M, Ciardelli G, Giusti P, Ahluwalia A.. PAM-microfabricated polyurethane scaffolds: in vivo and in vitro preliminary studies. Macromol Biosci 2008;8:60–68.

[6] Vermette P, Griesser HJ, Laroche G, Guidoin R. Polyurethanes in biomedical applications, Landes Bioscience Press, Texas, USA. 2001.

[7] Silvestri A, Serafini PM, Sartori S, Ferrando P, Boccafoschi F, Milione S, Conzatti L, Ciardelli G. Polyurethane-based biomaterials for shape-adjustable cardiovascular devices. J Appl Polym Sci 2011;122:3661–3671.

[8] Zhang JY, Beckman EJ, Hu J, Yang GG, Agarwal S, Hollinger JO. Synthesis, biodegradability, and biocompatibility of lysine diisocyanate-glucose polymers. Tissue Eng 2002;8:771-785.

[9] Li B, Davidson J M, Guelcher SA. The effect of the local delivery of platelet-derived growth factor from reactive two-component polyurethane scaffolds on the healing in rat skin excisional wounds. Biomaterials 2009;30:3486-3494.

[10] Hafeman AE, Li B, Yoshii T, Zienkiewicz K, Davidson JM, Guelcher SA. Injectable biodegradable polyurethane scaffolds with release of platelet-derived growth factor for tissue repair and regeneration. Pharm Res. 2008, 25, 2387-2399.

[11] Guan J, Sacks MS, Beckman EJ, Wagner WR. Synthesis, characterization, and cytocompatibility of elastomeric, biodegradable poly(ester-urethane)ureas based on poly(caprolactone) and putrescine. J Biomed Mater Res 2002;61:493-503.

[12] Fujimoto KL, Guan J, Oshima H, Sakai T, Wagner WR. In vivo evaluation of a porous, elastic, biodegradable patch for reconstructive cardiac procedures. Ann Thorac Surg 2007;83:648-654.

[13] Gorna K, Gogolewski S. Preparation, degradation, and calcification of biodegradable polyurethane foams for bone graft substitutes. J Biomed Mater Res A 2003;67:813-827.

[14] Adhikari R, Gunatillake PA, Griffiths I, Tatai L, Wickramaratna M, Houshyar S, Moore T, Mayadunne RTM, Field J, McGee M, Carbone T. Biodegradable injectable polyurethanes: synthesis and evaluation for orthopaedic applications. Biomaterials 2008;29:3762-3770.

[15] Zunfeng L, Xiang W, Xiaoying Y, Dongping L, Chen J, Ruimin S, Xueping L, Fangxing L. Synthesis and characterization of novel blood-compatible soluble chemically cross-linked polyurethanes with excellent mechanical performance for biomedical applications. Biomacromolecules 2005;6:1713-1721.

[16] Lligadas G, Ronda JC, Galià M, Cádiz, V. Polyurethane networks from fatty acid-based aromatic triols: Synthesis and characterization. Biomacromolecules 2007;8:1858-1864

[17] Andjelkovic DD, Larock RC. Novel rubbers from cationic copolymerization of soybean oils and dicyclopentadiene 1. Synthesis and characterization. Biomacromolecules 2006;7:927-936.

[18] Guner FS, Yagci Y, Erciyes T. Polymers from triglyceride oils. Prog Polym Sci 2006;31:633-670.

[19] Kong X, Narine SS. Physical properties of polyurethane plastic sheets produced from polyols from canola oil. Biomacromolecules 2007;8:2203-2209.

[20] Lligadas G, Ronda JC, Galià M, Cádiz, V. Plant oils as platform chemicals for polyurethane synthesis: current state-of-the-art. Biomacromolecules 2010;11:2825-2835.

[21] Gonzalez-Paz RJ, Lluch C, Lligadas G, Ronda JC, Galià M, Cádiz, V. A Green approach toward oleic and undecylenic acid-derived polyurethanes. J Polym Sci Part A: Polym Chem 2011;49:2407-2416.

[22] Thakore IM, Desai S, Sarawade BD, Devi S. Studies on biodegradability, morphology and thermomechanical properties of LDPE/modified starch blends. Eur Polym J 2001;7:151–60.

[23] Kim SU, Heo DN, Lee JB, Kim JR, Park SH, Jeon SH, Kwon IK. Electrospun gelatin/polyurethane blended nanofibers for wound healing. Biomed Mater 2009;4: 044106.

[24] Chiellini E, Cinelli P, Fernandes EG, Kenawy ES, Lazzeri A. Gelatin-based blends and composites. morphological and thermal mechanical characterization. Biomacromolecules 2006;2:806-811.

[25] Nirmala R, Nam K, Navamathavan R, Park S-J, Kim H. Hydroxyapatite mineralization on the calcium chloride blended polyurethane nanofiber via biomimetic method. nanoscale. Res Lett 2011;6:2-8.

[26] Detta N, Errico C, Dinucci D, Puppi D, Clarke DA, Reilly GC, Chiellini F. Novel electrospun polyurethane/gelatin composite meshes for vascular grafos. J Mater Sci Mater Med 2010;21:1761–1769.

[27] Cascone MG, Lazzeri L, Barbani N, Polacco G, Pollicino A, Giusti P. dehydrothermally cross-linked collagen–poly(vinyl alcohol) blends: mechanical, biological and surface properties. J Mater Sci: Mater Med 1997;7:297–300.

[28] Ciardelli G, Chiono V. Materials for Peripherals nerve regeneration. Macromol Biosci 2006;6:13-26.

[29] Elbert DL, Hubbell JA. Surface treatments of polymers for compatibility. Annu Rev Mater Sci 1996;26:365-94.

[30] Horbett TA. The role of adsorbed proteins in animal cell adhesion. Colloid Surface B: Biointerfaces 1994;2:225-240.

[31] Anselme K. Osteoblast adhesion on biomaterials. Biomaterials 2000;21:667-681.

[32] Hajiali H, Shahgasempour S, Naimi-Jamal MR, Peirovi H. Electrospun PGA/gelatin nanofibrous scaffolds and their potential application in vascular tissue engineering, Int J Nanomedicine 2011;6:2133–2141.

[33] Ebisawa Y, Kokubo T, Ohura K, Yamamuro T. Bioactivity of CaO·SiO2-based glasses: in Vitro evaluation. J Mater Sci: Mater Med 1990;1:239-244.

[34] He Y, Zhu B, Inoue Y. Hydrogen bonds in polymers blends. Prog Polym Sci 2004; 29:1021-1051.

[35] Chandrasekaran AR, Venugopla J, Sundarrajan S, Ramakrishna S. Fabrication of nanofibrous scaffold with improved bioactivity for cultured of human dermal fibroblast for skin regeneration. Biomed Mater 2011;6:015001.

[36] Roccatone D, Fioroni M, Zacharias M., Colombo G. Effect of hexafluoroisopropanol alcohol on the structure of melittin: A molecular dynamics simulation study. Protein Sci 2005;14:2582–2589.

[37] Williams DF. Editor. Definitions in biomaterials. Amsterdam–Oxford–NewYork–Tokyo: Elsevier; 1987.

[38] Schweizer S, Taubert A. Polymer-controlled, Bio-inspired calcium phosphate mineralization from Aqueous solution. Macromol Biosci 2007;7:1085-1099.

[39] Kumta PN, Sfeir C, Lee D, Olton D, Choi D. Nanostructured calcium phosphates for biomedical applications: novel síntesis and characterization. Acta Biomaterialia 2005;1: 65-83.

[40] Dorozhkin SV, Epple M. Biological and medical significance of calcium phosphates. Angew Chem Int Ed 2002;41:3130-3146.

[41] Termine JD, Posner AS. Infrared determination of the percentage of crystallinity in apatitic calcium phosphate. Nature 1966;211:268-270.

[42] Owen GRh, Meredith DO, ap Gwynn I, Richards RG. Focal adhesión quantification-a new assay of material biocompatibility?: Review. Eur Cell Mat 2005;9:85-96.

[43] Neff JA, Tresco PA, Caldwell KD. Surface modification for controlled studies of cell-ligand interactions. Biomaterials 1999;20:2281-2286.

CHAPTER V

Cytocompatible polyurethanes from fatty acids through covalent immobilization of collagen

Cytocompatible Polyurethanes from Fatty Acids through Covalent Immobilization of Collagen

Rodolfo J. González-Paz[1], Gerard Lligadas[1], Juan C. Ronda[1], Marina Galià[1], Ana M. Ferreira [2], Francesca Boccafoschi[3], Gianluca Ciardelli[2,4], Virginia Cádiz[1].

[1]Department of Analytical and Organic Chemistry, Rovira i Virgili University, Campus Sescelades, Marcel.lí Domingo s/n, 43007 Tarragona, Spain.

[2]Department of Mechanical and Aerospace Engineering, Politecnico di Torino, Corso Duca degli Abruzzi, 24, 10129, Turin, Italy.

[3]Department of Health Sciences, Università del Piemonte Orientale, Via Solaroli, 17, Novara, Italy.

[4] CNR-IPCF UOS Pisa Via Moruzzi 1, 56124 Pisa, Italy

Summary

Polyurethanes derived from fatty acids were modified by grafting polymerization of acrylic acid initiated by plasma treatment and further covalent immobilization of collagen using EDC/NHS as coupling agent. Scanning electron microscopy, X-Ray photoelectron spectroscopy, optical microscopy, colorimetric titration methods and contact angle measurements confirmed the surface changes at each stage of treatment, both in terms of morphology and chemical composition. The results for osteoblastic cells (MG63) cultured in vitro proved that PUs modified with collagen had better cytocompatibility that the control PUs.

Introduction

Polymer surfaces play a key role in biomedical interactions as the response of a biological environment to a synthetic material is dictated by the adsorption of biological molecules at the hybrid interface. Moreover, as degradation generally proceeds from the surface into the bulk, the chemical composition of the surface layers affect the rates and mechanism of biodegradation.[1]

Vegetable oils have a number of excellent properties, including low toxicity and high biodegradability; which have been utilized in producing valuable polymeric materials, such as polyurethanes (PUs).[2-4] PUs are extensively used for biomedical applications because of their excellent mechanical properties and good biocompatibility.[5] PUs are frequently used in the fabrication of scaffolds for tissue engineering as they are available in a wide variety of composition, properties, form, and can be easily shaped into complex structures.[6,7] Besides, PUs can be modified by the introduction of biomolecules that can enhance their cell, blood or tissue compatibility.[1]

For the engineering of hard tissues, the scaffolds should have an adequate structure to maintain the spaces required for cell ingrowths and matrix formation during in vitro culturing. Moreover, they must provide sufficient temporary mechanical support, matching the mechanical properties of the host tissue as closely as possible, to bear in vivo stresses and loading.[8] Mechanical forces play a crucial role in remodeling, and repair of load-bearing tissues, such as bone and cartilage.[9,10] In a previous work the synthesis, characterization and cytocompatibility of novel crosslinked polyurethanes derived from fatty acids were described,[11] in order to promote their integration with the biological environment. These crosslinked PUs had similar mechanical properties (Young`s modulus and strain at break) to those of cancellous bone.[12] Also, satisfactory human osteoblasts cell viability and adhesion on PUs surface were observed.

Currently, one promising and widely investigated approach to design materials in tissue engineering applications[13,14] is focused on the design of biomimetic materials, capable of eliciting specific cellular responses and directing new tissue formation mediated by biomolecular recognition. Usually, biomolecular recognition of the material by the cells is achieved by incorporating cell-binding peptides in the form of native long chain of extracellular matrix (ECM) proteins, such as fibronectin, laminin, vitronectin and collagen via chemical or physical surface modification. Several methods have been used to modify surface properties of PUs to enhance cell compatibility, such as peptides or collagen grafting, through wet chemical modification or plasma assisted immobilization. Among these methods, functionalisation with collagen is widely used and has good effect on improving cell adhesion and growth on PUs surface.[15-17]

The most reliable methods to attach a biomolecule to a PUs surface are adsorption via electrostatic interactions and covalent binding. Covalent immobilizations offer several advantages by providing the most stable bond between the compound and the PUs surface, extending the half-life of the biomolecule.[15] Often, the use of a hydrophilic spacer layer between the solid polymer and the biomolecule is beneficial in covalent immobilization. The reasons probably include increased mobility for exposing the bioactive epitote, and, due to the larger separation (compared with direct immobilization), a reduced strength of the interfacial forces exerted by the polymer upon the bioactive molecules, forces that can induce denaturation of attached proteins.[1] In particular plasma-induced graft polymerization is one of the most commonly used techniques to create the hydrophilic spacer layers. Plasma is a high energy state of matter, in which a gas is partially ionized into charged species, electrons, and neutral molecules. Plasma is a particularly useful technique for the functionalization of surfaces, as it can provide modification of the top nanometers of polymer surface without using solvents or generating chemical waste and with less degradation and roughening of the material than many wet chemical treatments. By plasma exposure radical groups are formed on the polymer surface and then the desired monomer may be polymerized, resulting in the formation of a grafted brushed spacer layers on top of the surface.[15, 16]

In this work crosslinked PUs films derived from fatty acids were grafted with acrylic acid using argon plasma. Plasma-induced polymerization of acrylic acid produces a poly (acrylic acid)-like (PAA) layer. Carboxyl groups formed were used to covalently bind collagen. Collagens are the most abundant proteins in the extracellular matrix; they are the major structural element of all connective tissues, such as bone, tendon and cartilage.[18,19]

The aim of this study was to accomplish a general strategy (plasma treatment) to modify PUs derived from fatty acids to obtain a novel material by immobilising on the surface collagen molecules, selected for their well known biological activity. The influence of the chemical structure of crosslinked PUs on the surface modification, the immobilization of collagen and the cytocompatibility was also studied.

Materials and Methods

Thermosetting polyurethane films (PUs) derived from fatty acids (undecenoic and oleic acids) were synthesized as described in a previous work, using two triols derived from undecenoic acid (a) and oleic acid (b). (Scheme 1).[11]

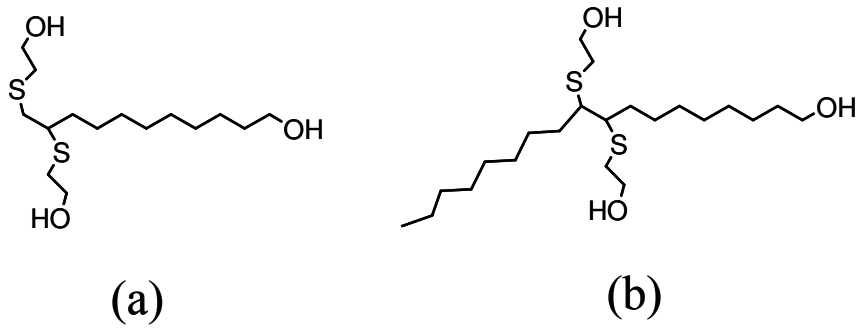

Scheme 1. Structures of undecenoic based (a) and oleic based (b) triols used as PUs precursors.

After reaction of triol (a) or (b) with 4,4'-methylenebis(phenylisocyanate) (MDI), PU1 and PU2 were obtained. Collagen type I was extracted from tibias and femurs of New Zeland's rabbit bones.[20] Acrylic acid (AA) was purchased from Sigma-Aldrich (Milan, Italy) and purified by distillation. 1-ethyl-3-(3-dimethylaminopropyl) carbodiimide (EDC) was purchased from Lancaster (UK), and N-hydroxysuccinimide (NHS) from Sigma-Aldrich (Milan, Italy), as well as ethylenediaminetetraacetic acid (EDTA), acetic acid, ethanol, sodium hydroxide and pepsin. Toluidine Blue (TBO) and Sirius red kit dyes for carboxylic groups and collagen molecules quantification were purchased from Sigma Aldrich (Milan, Italy) and Sircol Biocolor (United Kingdom) respectively.

Bone demineralization and collagen type I extraction:

Femurs and tibias were obtained from adult New Zealand rabbits with average weights of 4.0-5.0 Kg in accordance with the ethical standards of the Local Ethical Committee (CNR-IFC, Pisa-Italy). Bones were decalcified using a solution of 0.5M EDTA at pH 7.5 during 4 weeks at 4 °C, pulverized in a steel mill (IKA A11) refrigerated with liquid nitrogen to obtain a fine powder after 1 minute and solubilised with 0.5M acetic acid/pepsin (0.5% w/w). The supernatant (soluble collagen) was centrifuged at 3000 rpm for 10 minutes and freeze-dried (Scanvac, CoolSafe) at -20ºC for 24h.

Surface modification

Plasma treatment:

Films of PUs with 1mm of thickness and 25 cm^2 of surface area were washed with EtOH/H_2O (50% v/v) and dried at room temperature. The Ar plasma was applied to the PUs films using a reactor DiemerElectronic, Pico Low Pressure Plasma System, to activate the surface by free radical formation for a further grafting of acrylic acid (AA) molecules. The PUs samples were exposed to 15 ccm flow Ar plasma at 100W and 200W of power for 15 min, maintaining the plasma reactor chamber pressure at 0.06 mBar. Grafting reaction was carried out in the presence of monomer vapours into the reactor, in the same conditions as plasma activation. Finally the residual monomers and homopolymers were removed by an extensively wash with distilled water at the end of the treatment.

Collagen type I coupling:

The chemical functionalization after plasma treatment of PUs films with Collagen type I was performed by immersing the samples for 20h in 0.2 mM aqueous solution (pH 5) of 1-ethyl-3-(3-dimethylaminopropyl) carbodiimide (EDC), in the presence of 0.12 mM of N-hydroxysuccinimide (NHS) at 4 °C for 20 h. The NHS facilitates the amidation on the acrylic acid-grafted PUs surface, by the formation of intermediate succinimidyl ester groups (Scheme 2).[21] These activated samples were washed with distilled water and then immersed into a Collagen type I solution 0.1 % w/v; pH 8 at 4 °C for 20 h, thus allowing the reaction between the amine groups of collagen and the active succinimidyl ester groups and forming stable amide linkages on PUs surface.

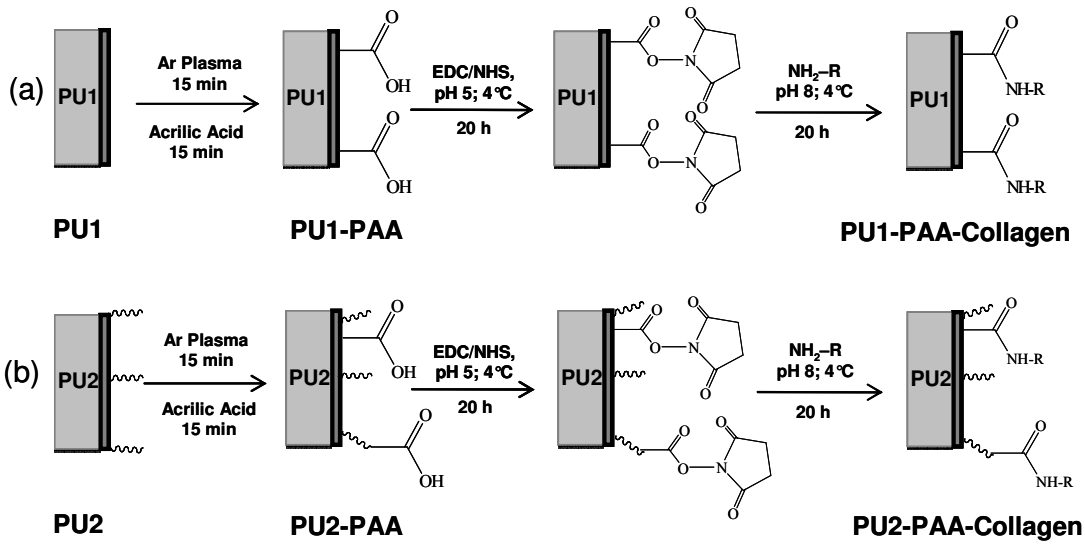

Scheme 2. Schematic representation of the collagen covalent immobilization on the PUs surface after plasma treatment: (a) PU1 derived from undecenoic acid and (b) PU2 derived from oleic acid containing dangling chains.

Colorimetric titration method to determine surface density of functional groups

Quantification of the carboxyl groups after AA grafting/polymerization

The carboxylic group concentration on the PUs surface after the AA grafting/polymerization treatment was determined by colorimetric titration method using toluidine blue O (TBO).[22] The PUs films with a surface area of 0.2 cm^2 were immersed into a 0.05 mM TBO aqueous solution with pH of 10. The formation of ionic complex between COOH groups and the cationic dye was allowed to proceed for 12 h at room temperature. With the aim to remove the unbound TBO molecules from the PUs-AA surface, the samples were rinsed with 0.1mM NaOH solution (pH 10). TBO bound to the surface of PUs-AAc samples was desorbed by incubation in 1 mL 50% (v/v) acetic acid solution for 10 min. The absorbance at 632 nm was recorded by a UV–Vis spectrophotometer (PerkinElmer, Lambda 25). The amount of carboxyl groups was calculated using a calibration curve from different concentrations (0.0025, 0.005, 0.0175, 0.025 % w/v) of TBO/50% acetic acid solution recorded at the same conditions. The calculation is based on the assumption that 1 mol TBO corresponds exactly to 1 mol carboxyl groups. The colorimetric protocol was performed in triplicate for each kind of sample.

Quantification of collagen immobilized on PUs films

The amount of collagen immobilized on PUs surfaces was determined quantitatively using Sirius kit red-based colorimetric micro assay.[23] PUs films with immobilized were cut into pieces of 1 cm^2 area and put into 1.5 ml tubes. Then 1 ml Sirius red dye was added to each well, and the films were stained for 30 min under gentle mechanical shaking. During this time a collagen-dye complex was formed. Thereafter, the dye solution was removed by suction and the stained samples were washed twice with 0.75 ml of iced-cold acid-salt wash reagent (containing acetic acid, sodium chloride and surfactants) to remove the unbound dye for 10 min. The washing solution was drained and wasted, removing any fluid from the lip of the eppendorf tubes. The bound dye was dissolved adding 1 ml of the alkali reagent (0.5M sodium hydroxide) to the PUs and mixed into a vortex for 10 min. The collagen bound dye was transferred into a 96 micro well plate and optical density was measured at 560 nm with a UV-Vis scanning spectrophotometer (PerkinElmer, Lambda 25). The density of collagen bonded to PUs was obtained converting the measured absorbance (560 nm) of the immobilized collagen using a linear calibrated standard curve of collagen type I from bovine skin reference at different concentrations (0.00125, 0.0025, 0.005, 0.010, 0.020 % w/v) in 0,5M of acetic acid solution. The colorimetric protocol was performed in triplicate for each kind of sample.

Surface analysis

X-Ray photoelectron spectroscopy (XPS)

Atomic composition and surface chemistry of treated and non-treated samples were analyzed by a X-ray Photoelectron Spectroscopy/ Electron Spectroscopy for Chemical Analysis (XPS/ESCA) using PHI 5000 Versaprobe instrument, with a power of 25.6 W and a scanning surface of 500 x 500 micronm. Overlapping peaks were resolved into their individual components by XPSPEAK 4.1 software.

Contact angle measurements

The wettability of the samples treated and non-treated were evaluated by contact angle measurements using CAM 200 KSV Instrument, equipped with Tetha software. Static contact angle measurements were carried out adding a drop of 3µl of bi-distilled

water by a motor driving syringe at room temperature on three different samples of each material and at least three measurements for each sample.

Scanning Electron Microscopy (SEM)

The surface morphology changes on samples after treatment were observed using a LEO 1430VP SEM Equipment. Prior to SEM examination, samples surface were coated with a conductive thin gold film.

Optical Microscopy

Sirius Red staining method was used for analysing the immobilization of collagen on the PUs surface. It is a strong anionic dye whose sulfonic acid groups interact with the basic groups of collagen staining it red.[24] This helped us to determine the effective immobilization of the collagen molecules and viewed under a NIKON microscope and stereo zoom microscope smz1500 with DS CAMERA HEAD DS-Fi1. Collagen is stained red on a yellow background in the PUs scaffolds.

Cytocompatibility tests

Cell Lines

MG63 osteoblast cells were used. Cells were cultured in DMEM enriched with 10% fetal bovine serum (FBS), glutamine (2mM), penicillin (100 U/ml) and streptomycin (100 µg/ml) (Euroclone, Italy). Cells were maintained at 37° C in a humidified atmosphere with 5% CO_2 and used at 10^5 x cm^2 on the samples' surfaces.

MTS assay (MG63)

To evaluate cell viability, MTS assay was performed (CellTiter 96® Aqueous Non-Radioactive Cell Proliferation Assay, Promega, Italy). Briefly, cells were cultured on different surfaces for 24 h. A MTS solution was added to culture medium. After 3 h, culture medium was removed and the solution was read in UV-VIS spectroscopy (V-630 UV-Vis Spectrophotometer, Jasco, USA) at 490 nm. The absorbance was directly proportional to viable cells amount. Cells seeded on cell culture Petri dishes were used as positive control.

Scanning Electron Microscopy (SEM)

After 24 h., SEM was performed according to the following procedure: the medium was removed, samples were washed twice in 0.15M cacodylate buffer and fixed for 30 minutes at 4°C with Karnowsky solution (2% paraformaldehyde and 2,5% gluteraldehyde in 0.15M cacodylate buffer, pH 7.2-7.4). Following fixation, samples were treated for 30 minutes with 1% osmium tetroxide in 0.15M cacodylate buffer solution. Samples were then dehydrated with graded ethanol (from 50% to 100%), soaked for 30 minutes in hexamethyldisilazane, dried and sputter-coated with gold-palladium. Images were collected at different magnifications (SEM, Leo 1450VP, LeoCo.LTD).

Results and Discussion

Plasma treatment was used to create functionalization on PUs surface by attachment of new chemical groups useful for the coupling of molecules that enhance the cell growth, spreading and proliferation. Usually, with this treatment, only the outermost layers are modified and likewise the further functionalization with macromolecules. Therefore, the amount of modified material is not sufficient to apply conventional bulk analysis methods and more sensitive surface analysis techniques must be used to obtain information at a molecular level.

Plasma treatment.

To test the effects of plasma treatment on the PUs, contact angle measurements, quantification of carboxyl groups and SEM, were performed.

The decrease in the contact angle is an index of the magnitude of the chemical changes occurring on the film surface due to plasma-induced polymerization of acrylic acid, which renders the surface more hydrophilic with respect to the virgin film, because of the presence of carboxylic groups. Table 1 summarizes the change of water contact angles upon exposing the PU films to Ar plasma at different power.

Table 1. Contact angles variation after plasma treatment and collagen coupling. Quantification of carboxylic groups (C_1) and collagen groups (C_2).

Sample	Contact angle	C_1 [μg/cm^2]	C_2 [μg/cm^2]
PU1	85.66 ± 0.35	–	–
PU1-PAA (100W)	79.35 ± 0.26	3.5 ± 0.3	–
PU1-PAA (200W)	75.73 ± 5.96	3.1 ± 0.9	–
PU1-PAA-Collagen	57.9 ± 1.30	–	10.5 ± 0.3
PU2	86.98 ± 0.29	–	–
PU2-PAA (100 W)	77.38 ± 0.08	4.6 ± 0.5	–
PU2-PAA (200 W)	75.46 ± 4.08	3.7 ± 0.7	–
PU1-PAA-Collagen	54.3 ± 1.80	–	12.8 ± 0.9

At higher plasma power (200W) a little increase in hydrophilicity was observed for both PUs, but a high standard deviation on contact angle measurements was produced. This fact could be explained by a non-homogeneous chemical modification. With regards to the coupling step, it should be taken into account that under plasma conditions, carboxylic compounds can decarboxylate. The fragmentation of the monomer in the plasma reactor is undesirable because it decreases the amount of carboxylic groups in the functional coating, limiting the posterior coupling of biomolecules.[18]

Table 1 also shows the concentrations of carboxylic acid groups grafted onto PUs surface. They were determined by colorimetric titration method using TBO dye. The maximum number of carboxylic groups onto PUs surfaces was obtained by plasma power of 100W, with concentrations of 3.5 μg/cm^2 and 4.6 μg/cm^2 for PU1 and PU2 respectively. It is worth noting that a higher concentration of carboxylic groups was obtained for PU2, with long aliphatic side chains, which produce a higher number of reactive sites, so facilitating grafting of AA. These concentrations are high enough to introduce a continuous bioactive protein layer on the surface.[25,26] Lower concentrations

were obtained by plasma power of 200 W. These results suggest that decarboxylation process occurs during plasma treatment at 200W producing a non-homogeneous chemical surface modification on PUs.

In addition to chemical surface modification, a very important approach to manipulate protein-surface interactions and cell behaviors on PUs surfaces is surface morphology.[1,27] Figure 1 shows the variation on surface morphology of PUs films before plasma treatment (a and d) and after plasma treatment, PUs-PAA at plasma power of 100 W (b and e) and 200 W (c and f), observed by SEM. Micrographs b) and e) show a higher organization of surface roughness than c) and f), probably due to the decarboxylation process above mentioned and a greater etching of the surface during plasma treatment at 200 W.

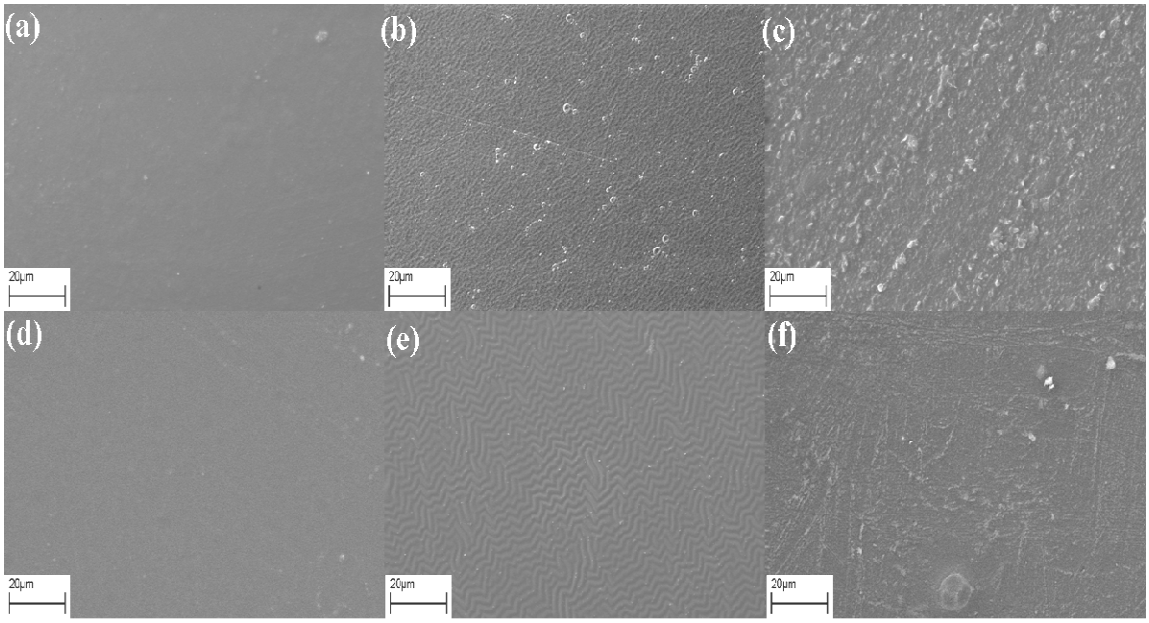

Figura 1. a) PU1, b) PU1-PAA (100W), c) PU1-PAA (200W), d) PU2, e) PU2-PAA (100W), f) PU2-PAA (200W).

Substrates with morphological features, such as grooves or ridges will expose more surface area for possible interaction with proteins. Grooves and ridges are among the most studied morphological patterns related to cell morphology control and protein-surface interactions.[28,29] The most important phenomenon is that cell spreading, alignment, and migration can be oriented along grooves/ridges. A slight variation on surface morphological patterns is observed on PU1 and PU2 after plasma treatment power at 100 W, in Figure 1 (b) and (e). Regular micro patterns like ridges/grooves are

formed in contrast with the irregular surface morphology observed on PU1 and PU2 after plasma treatment power at 200W, in Figure 1 (c) and (f).

According to all the above results only the PUs treated at 100 W were used for a further collagen coupling.

Collagen type I coupling

In the last years different surface activation processes for collagen immobilization on plasma-polymerized acrylic acid (pPAA) films have been investigated. The reaction with the EDC/NHS resulted in higher activation of the pPAA surfaces. On the other hand in the collagen case only the EDC/NHS activation promotes protein coupling.[19] In order to evaluate the efficiency of covalent immobilization and surface changes after collagen coupling on PUs-PAA surfaces, SEM, optical microscopy, contact angle measurements and collagen quantification by colorimetric titration were carried out. The surface morphology of PUs-PAA and PUs-PAA-Collagen is shown in Figure 2.

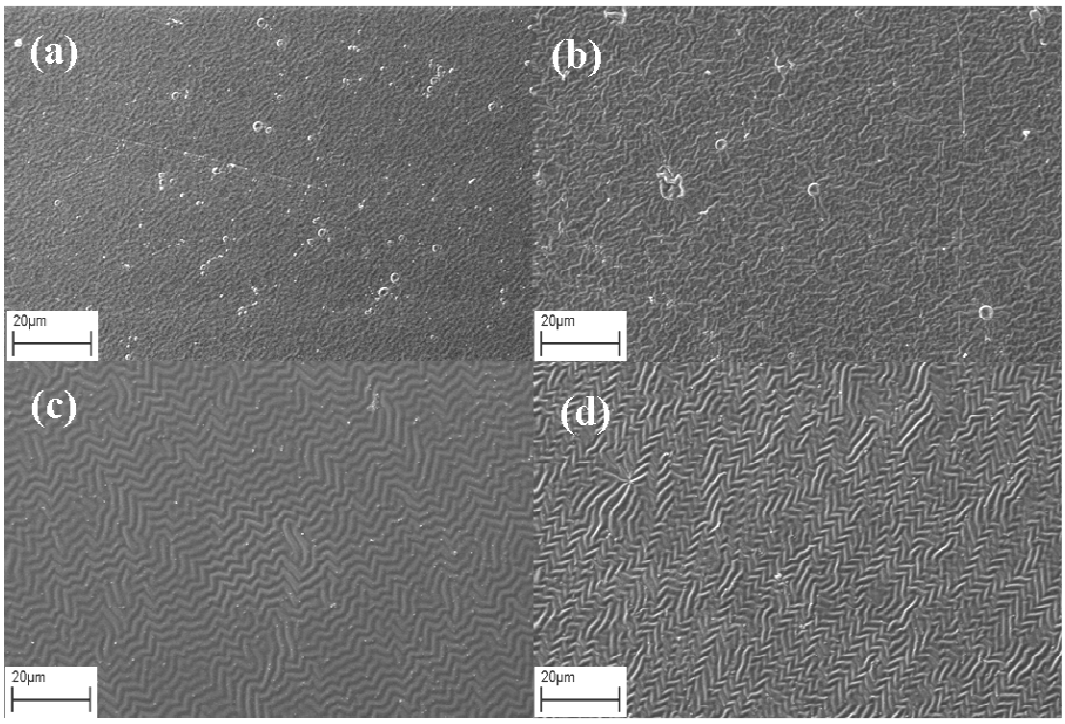

Figure 2. Surface morphology variation of PUs-PAA films after collagen immobilization obtained by SEM: a) PU1-PAA, b) PU1-PAA-Collagen, c) PU2-PAA , d) PU2-PAA-Collagen.

The PUs-PAA-Collagen surfaces present the roughest morphology (Figure b and d), probably due to the presence of immobilized collagen molecules. To confirm it, samples were stained with Sirius red, to determine the effective immobilization of the collagen, and examined under a NIKON microscope (Figure 3).

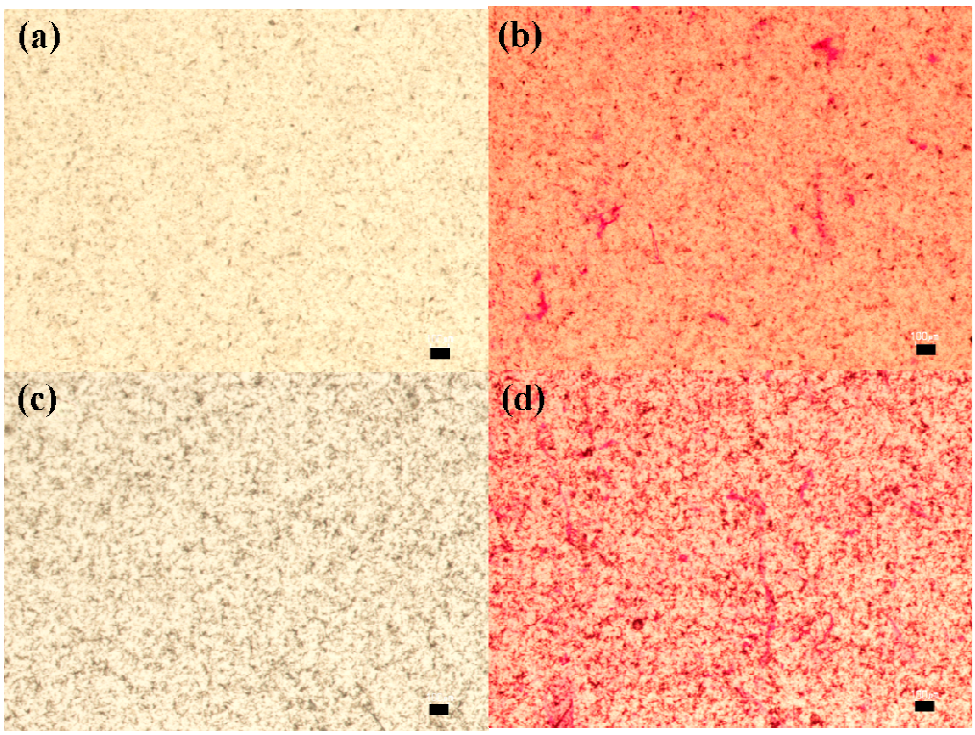

Figure 3. Collagen staining on PUs-PAA-Collagen films using Sirius red dye: a) PU1-PAA, b) PU1-PAA-Collagen, c) PU2-PAA, d) PU2-PAA-Collagen. Scale bar (100 μm).

The strong anionic SO_3^- groups in the dye strongly interact with the basic groups of collagen, thus collagen molecules are strongly and selectively stained by Sirius red.[23,24] As it can be seen in Figure 3, the presence of collagen is clear in b) and d), and PU2-PAA-Collagen (d) shows a higher red stained compared to PU1-PAA-Collagen (b). Moreover, the Sirius red-based colorimetric titration allow to measure the surface density of bonded collagen, (Table 1). A higher density of collagen molecules is detected for PU2-PAA-Collagen. This result agrees with the greater surface density of carboxylic groups on the precursor sample (see Table 1) and the optical microscope picture.

By increasing the amount of grafted PAA, the amount of collagen absorption was also increased. This is attributed to both the higher amount of available adsorption sites and to the three-dimensional PAA brush structure. However, the increase of the quantity of collagen was not proportional to the amount of carboxylic acid groups. The excess of collagen found, could be due to additional collagen deposits onto the primarily immobilized collagen.[30] It is reported[31] that the amount of collagen present in a monolayer is 0.1 to 0.5 μg/cm^2, therefore, we can infer that the PUs-PAA-Collagen surfaces are covered by many layers of collagen molecules.

The wettability of the control and modified PUs films was studied using water contact angles (Table 1). Surface hydrophilicity of the modified PU films was obviously enhanced compared with the control film. The unmodified PU surface showed a relatively high contact angle. As is well known a hydrophobic polymer is unfavorable for cell attachment.[32] Many works reported that cells attached and spread more easily and effectively on hydrophilic surfaces (water contact angle of 40º-70º) than on hydrophobic surfaces.[25,33-35] The hydrophilicity of PU films surface increases dramatically after grafting with AA and collagen immobilization. The change of the contact angle of samples immobilized by collagen confirms that the reaction was successful, causing the surface to be more hydrophilic as a function of collagen content on the surface (see Table 1).

XPS analysis allows quantification of the chemical modification of the surface and determines the atomic composition of a material top several nanometers. Thus, the alteration of the surface chemical composition of PU2 was investigated by XPS at each stage of surface modification. XPS results for the virgin PU2, PU2-PAA and PU2-PAA-Collagen are summarized in Table 2 and shown in Figure 4. Table 2 gives the elemental composition of the films.

Table 2. XPS atomic composition (%) and ratios.

Sample	O	N	C	S	O/C	N/C
PU2	20.6	3	74.5	1.9	0.27	0.04
PU2-PAA	39.4	-	60.6	-	0.65	-
PU2-PAA-Collagen	25.9	13	61.1	< 0.1	0.42	0.21

The measured oxygen-to-carbon (O/C) ratio is maximum for PU2-PAA, consistent with the presence of the PAA layer, rich in carboxyl groups, and is near to PAA theoretical O/C ratio of 0.67.[25] The oxygen and carbon composition have values close to those predictable for a pure PAA sample (40 and 60 % respectively).[18] The nitrogen and sulfur composition are not present, indicating that the PAA layer has a thickness which is above XPS sampling depth. As the sampling depth of XPS in polymer matrix usually is about 7 nm, it could be concluded that the thickness of the PAA layer exceed 6-7 nm.[36] The nitrogen-to carbon (N/C) ratio is higher in PU2-PAA-Collagen, according to a surface rich in amide groups, and the atomic composition is close to that found in a pure collagen sample.[37] Thus, it can be concluded that the thickness of the immobilized collagen multilayer exceed XPS sampling depth.

The deconvolution of the core level C_{1s} peaks on virgin PU2 (a) and PU2-PAA (b), (Figure 4) shows three peaks around 285, 286 and 289 eV which may be assigned, to the presence of aliphatic C-H and C-C bonds, C-O and C-N bonds, and COOR and COOH groups respectively.[18] Likewise, the deconvolution of the core level O_{1s} peaks on virgin PU2 (a) and PU2-PAA (b), (Figure 4) shows two contributions around 532 and 533 eV, corresponding to the presence of O=C, and O-C and O-H bonds respectively.[38] As can be seen in Figure 4, the relative intensity of COOH or COOR, C-O and O-H groups increases after plasma treatment (b), indicating the effective grafting of PAA layer on PU surface. After collagen immobilization (Figure 4 c) a new peak in the deconvolution of the core level C_{1s} appears at 288 eV, which is typically attributed to an amide group (NH-C=O), characteristic of the peptide bond.[18,25,39]

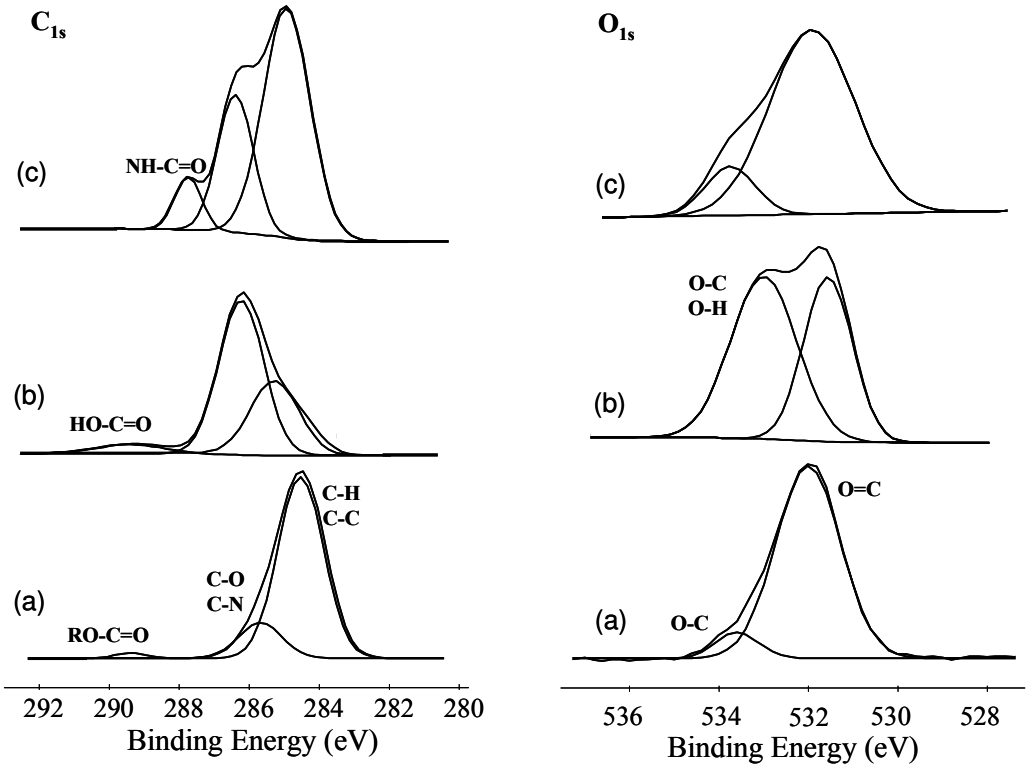

Figure 4. Relative intensity of the deconvoluted C_{1s} and O_{1s} core levels spectra of: a) PU2, b) PU2-PAA and c) PU-PAA-Collagen.

Cytocompatibility test

Cytocompatibility of polymers is very closely related to cell behaviour on contact with them and particularly to cell adhesion to their surface. The immobilization of the bioactive molecules (collagen) on PUs surface, after they were grafted with PAA, provides the possibility of cytocompatibility improvement. Colorimetric MTS test (Figure 5), measuring the mitochondrial activity of MG63 osteoblast cells in the presence of different substrates after 24 h, gives an indication about cell viability (%) on surface-modified samples (PUs-PAA-Collagen) with respect to unmodified samples (PUs) and the positive control (Control). Cell viability on surface-modified samples significantly increased after the immobilization of collagen molecules on PUs surface. PU2-PAA-Collagen showed a superior cell viability than the control, probably due to the higher amount of immobilized collagen molecules on surface.

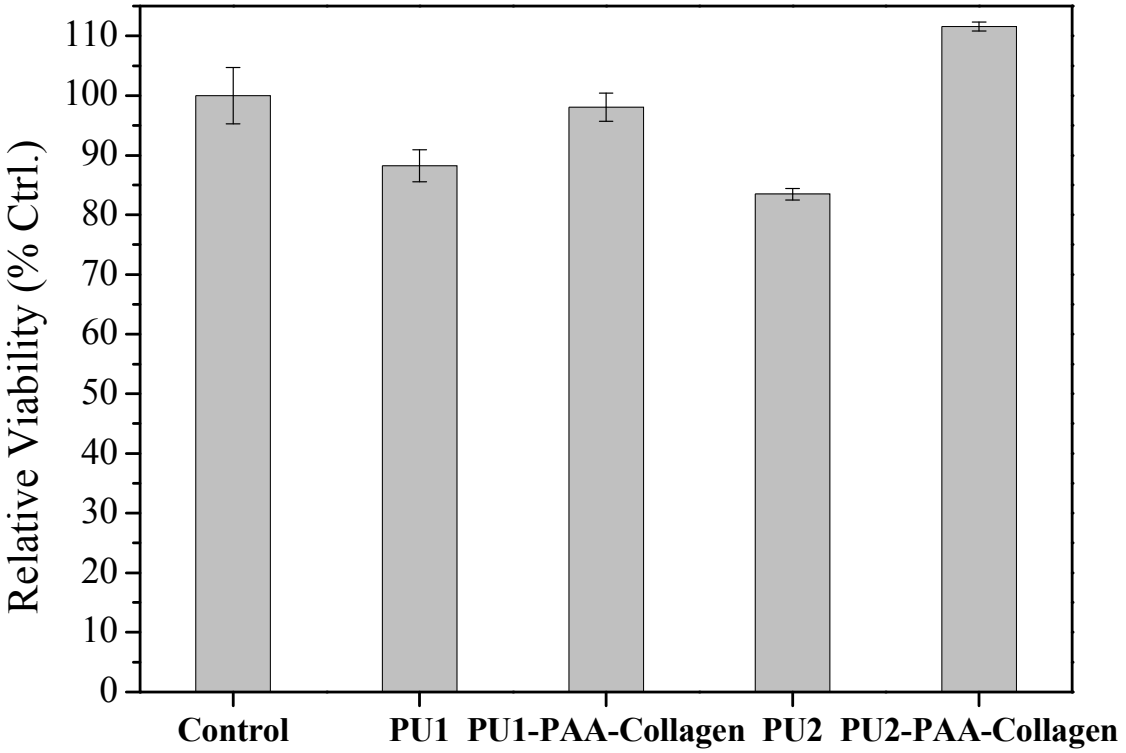

Figure 5. MTS test results after 24 h incubations.

Surface characteristics of materials, such as morphology, chemistry, surface energy, hydrophilicity, and the presence of bioactive molecules play an essential part in osteoblast adhesion on biomaterials. Thus, adhesion and spreading belong to the first phase of cell-material interactions and the quality of this first phase will influence the cell`s capacity to proliferate and to differentiate itself on contact with the implant.[35] Figure 6 shows the morphology of MG63 osteoblast cells on surface-modified samples (b and d) respect to unmodified samples (a and c) after 24 h, observed under SEM. As shown, cells on PU2 (c) show more round-shaped and non-homogenously distributed on the surface, presenting cell clusters while cells on PU1 show a better cell spreading and distribution on the surface (a). Micrographs (b) and (d), show an enhanced cell adhesion and cell spreading after plasma treatment and covalent immobilization of collagen on PUs. These cells seeded on the collagen modified PUs displayed flattened and spreading morphology.

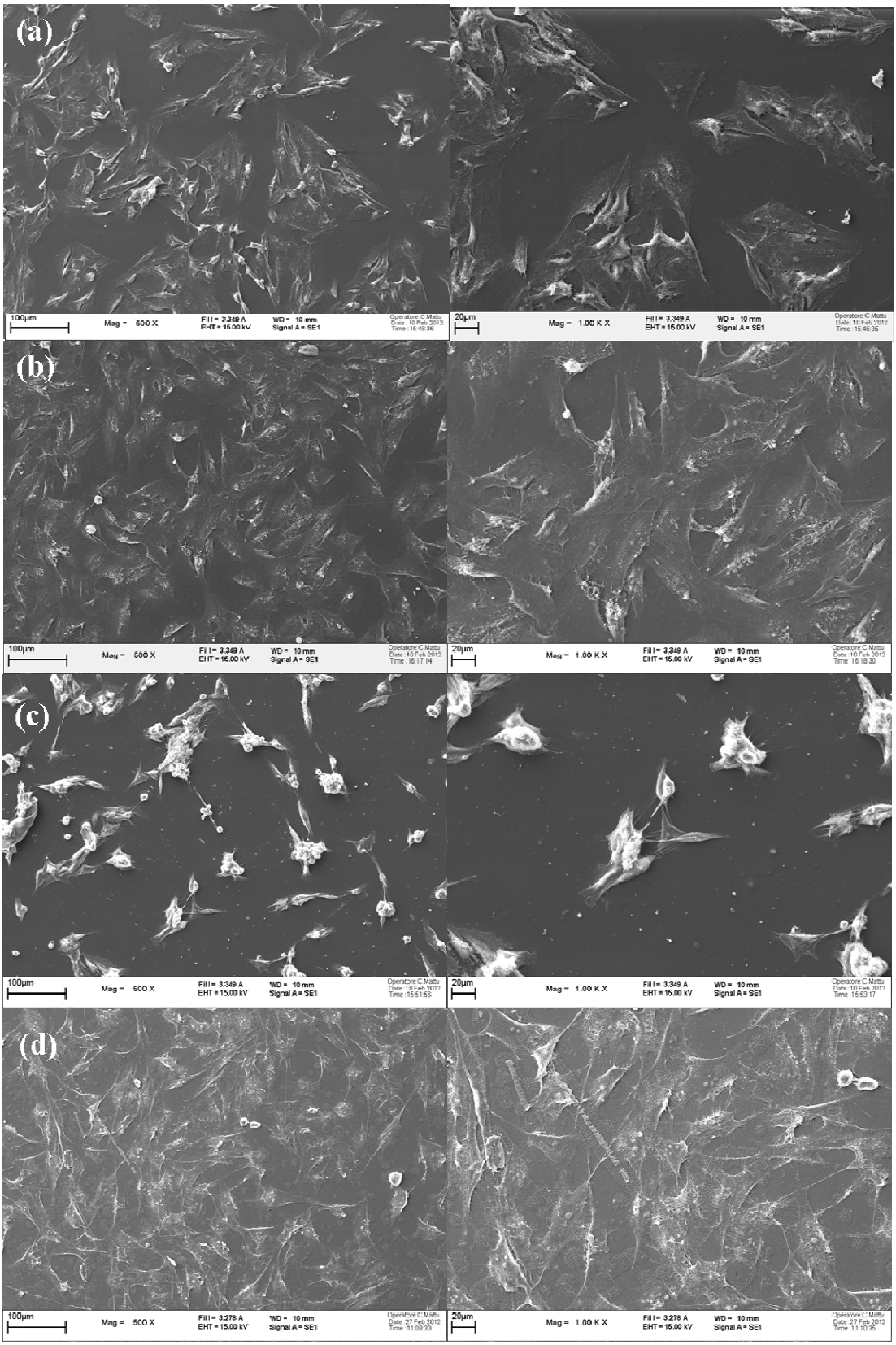

Figure 6. SEM micrographs at different scale (100 μm left and 20 μm right) of MG63 osteoblast cell seeded on: a) PU1, b) PU1-PAA-Collagen, c) PU2 and d) PU2-PAA-Collagen after 24 h.

Cell migration depends on the dynamic interplay between the cells substrate and cytoskeleton. Firstly, the cell develops a protrusion of its leading edge to form a lamellipodium, then cell creates filopodias or cytoplasmic projections that extend beyond the leading edge of lamellipodia in migrating cells. Thus, the cell generates the traction and energy required for cell movement. Filopodia form focal adhesions with the substratum, linking it to the cell surface. In Figure 7 it is possible to detect cells filopodias (black arrows) on surfaces-modified PU1-PAA-Collagen (a) and PU2-PAA-Collagen (b). Cell movement is also regulated by surface morphology as grooves or ridges. Usually, the migration is oriented along grooves/ridges formed on the surface. This behaviour is observed in SEM micrograph (b) (white arrows).These results agree with the contact guidance phenomenon described on osteoblastic cells, where the organization of surface roughness is an important parameter to consider.[16,35]

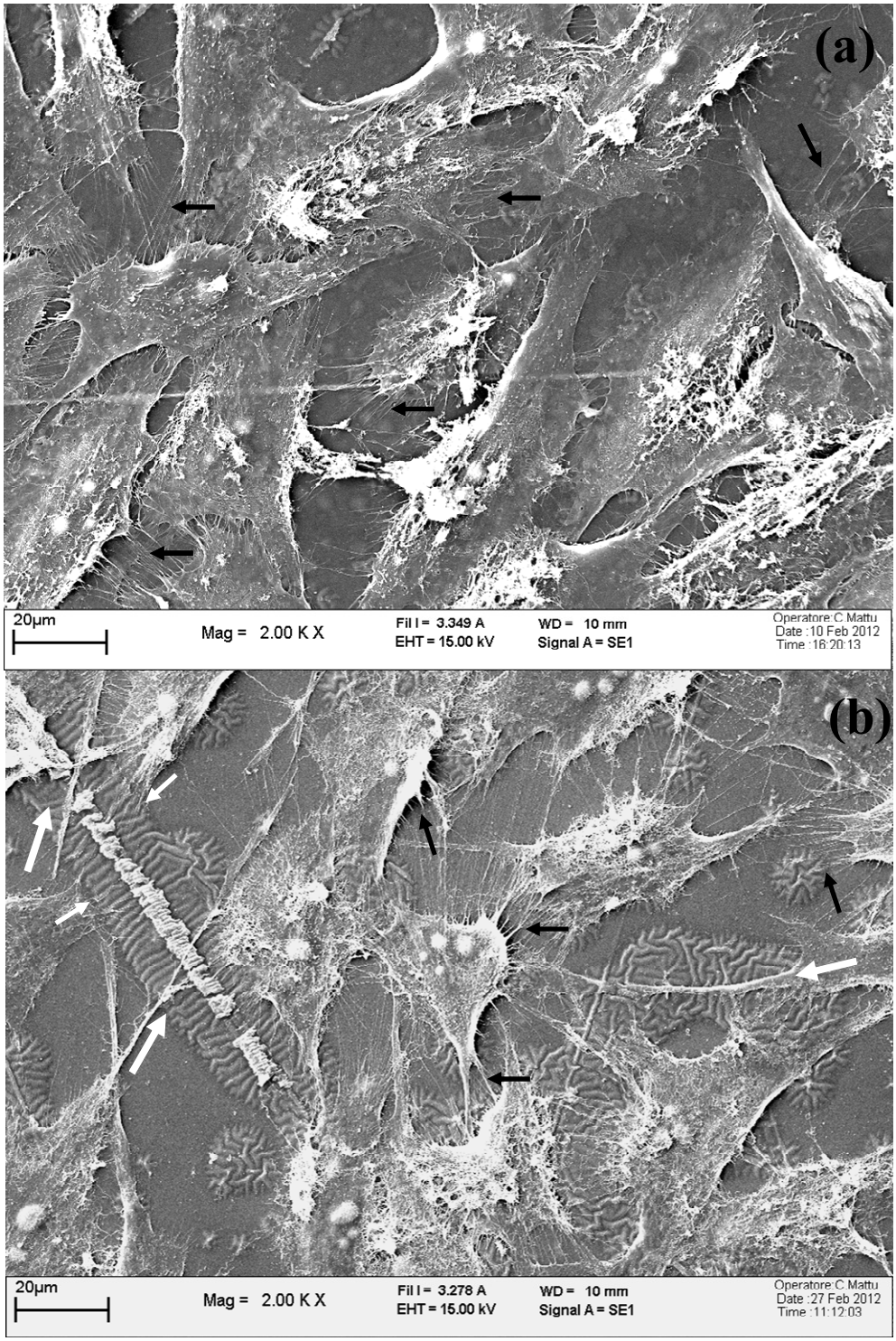

Figure 7. SEM micrographs of morphological aspects of MG63 osteoblast cell seeded on surface-modified samples: (a) PU1-PAA-Collagen and (b) PU2-PAA-Collagen.

Conclusions

Results obtained in this study suggest that plasma assisted acrylic acid monomer polymerisation is an attractive way to introduce carboxylic groups on fatty acid based polyurethane surfaces. Plasma treatment at 100 W proves to be an effective procedure to graft acrylic acid moieties on the PU surfaces but treatment at 200 W produces some decarboxylation, so reducing the number of active sites. Bioactive molecule such as collagen was successfully immobilized on the PU-PAA surface by EDC/NHS as coupling agent. By increasing the amount of grafted PAA, the quantity of collagen adsorption was also increased. Protein immobilization in multilayer was achieved. All characterization confirms the surface changes at each stage of treatment, both in terms of morphology and chemical composition. Morphological and chemical composition changes after plasma treatment and subsequently coupling of collagen molecules had a positive effect on modifying the cytocompatibility of PUs from fatty acids. It was also shown that a higher amount of immobilized collagen on PUs-PAA surface resulted in a better cytocompatibility of the material. It is possible to assume that both PUs can be used as valid substrate to create biomimetic materials and interfaces for biomedical implants and scaffolds for tissue engineering, but the use of PU2 is preferable to obtain higher PAA grafting, coupling of collagen and consequent positive activation of cellular processes.

Acknowledgements

The authors express their thanks to CICYT (Comisión Interministerial de Ciencia y Tecnología) (MAT2011-24823) for financial support for this work.

References

[1] P.Vermette, H.J. Griesser, G. Laroche, R. Guidoin, Polyurethanes in Biomedical Applications, Landes Bioscience Press, Texas, USA. 2001, p.176, p.192, p.185.

[2] F.S. Guner, Y. Yagci, T. Erciyes, Polymers from Triglyceride Oils, Prog. Polym. Sci. 31 (2006) 633-670.

[3] G. Lligadas, J.C. Ronda, M. Galià, V. Cádiz, Poly(ether urethane) networks from renewable resources as candidate biomaterials: Synthesis and characterization, Biomacromolecules 8 (2007) 686-692.

[4] R.J. Gonzalez-Paz, C. Lluch, G. Lligadas, J.C. Ronda, M. Galià, V. Cadiz, A green approach toward oleic and undecylenic acid-derived polyurethanes. J. Polym. Sci. Part A, Polym. Chem. 49 (2011) 2407-2416.

[5] J.P. Santerre, K. Woodhouse, G. Laroche, R.S. Labow, Understanding the biodegradation of polyurethanes: From classical implants to tissue engineering materials, Biomaterials 26 (2005) 7457-7470.

[6] L. Zunfeng, W. Xiang, Y. Xiaoying, L. Dongping, J. Chen, S. Ruimin, L. Xueping, L. Fangxing, Synthesis and characterization of novel blood-compatible soluble chemically cross-linked polyurethanes with excellent mechanical performance for biomedical applications, Biomacromolecules 6 (2006) 1713-1721.

[7] R. Adhikari, P.A. Gunatillake, I. Griffiths, L. Tatai, M Wickramaratna, S. Houshyar, T. Moore, R.T.M. Mayadunne, J. Field, M. McGee, T. Carbone, Biodegradable injectable polyurethanes: Synthesis and evaluation for orthopaedic applications. Biomaterials 29 (2008) 3762–3770.

[8] D. Puppi, F. Chiellini, A.M. Piras, E. Chiellini, Polymeric materials for bone and cartilage repair. Prog. Polym. Sci. 35 (2010) 403–440.

[9] R.L. Duncan, C.H. Turner, Mechanotransduction and the functional response of bone to mechanical strain. Calcif. Tissue Int. 57 (1995) 344–358.

[10] K. Noris-Suarez, J. Lira-Olivares, A.M. Ferreira, J.L. Feijoo, N. Suarez, M.C. Hernandez, E. Barrios, In vitro deposition of hydroxyapatite on cortical bone collagen stimulated by deformation-induced piezoelectricity, Biomacromolecules 8 (2007) 941-948.

[11] R.J. Gonzalez-Paz, G. Lligadas, J.C. Ronda, M. Galià, V. Cádiz, Thiol-yne reaction on alkyne-derivatized fatty acids: Biobased polyols and cytocompatibility of derived polyurethanes, Polym. Chem. 3 (2012) 2471-2478

[12] D. W. Hutmacher, J. T. Schantz, C.X.F. Lam, K.C. Tan, T.C. Lim, State of the art and future directions of scaffold-based bone engineering from a biomaterials perspective, J. Tissue Eng. Regen. Med. 1 (2007) 245-260.

[13] D. Puppi, F. Chiellini, A.M. Piras, E. Chiellini, Polymeric materials for bone and cartilage repair, Prog. Polym. Sci. 35 (2010) 403-440.

[14] S. Van Vlierberghe, P. Dubruel, and E. Schacht, Biopolymer-based hydrogels as scaffolds for tissue engineering applications: A review, Biomacromolecules 12 (2011) 1387-1408.

[15] J.M. Goddard, J.H. Hotchkiss, Polymer surface modification for the attachment of bioactive compounds. Prog. Polym. Sci. 32 (2007) 698-725.

[16] Z. Ma, Z. Mao, C. Gao, Surface modification and property analysis of biomedical polymers used for tissue engineering. Colloids Surf. B: Biointerfaces 60 (2007) 137-157.

[17] L. Yan-Hui, H. Yu-Dong, The study of collagen inmobilization on polyurethane by oxygen plasma treatment to enhance cell adhesion and growth. Surf. Coat. Technol. 201 (2007) 5124-5127.

[18] S. Sartori, A. Rechichi, G. Vozzi, M. D`Acunto, E. Heine, P. Giusti, G. Ciardelli, Surface modification of a synthetic polyurethane by plasma glow discharge: Preparation and characterization of bioactive monolayers. React. Funct. Polym. 68 (2008) 809-821.

[19] S. Strola, G. Ceccone, D. Gilliand, A. Valsesia, P. Lisboa, F. Rossi, Comparison of surface activation processes for protein immobilization on plasma-polymerized acrylic acid films, Surf. Interface Anal. 42 (2010) 1311-1315.

[20] A.J. Bailey, T.J. Sims, L. Knott, Int. J. Biochem. Cell Biol. 34 (2002) 176-182.

[21] P.D. Drumheller, J.A. Hubbell, Surface immobilization of adhesion ligands for investigations of cell-substrate interactions, The Biomedical Engineering Handbook, Second Edition, J.D. Bronzino (Ed.), CRC Press LLC, Boca Raton, 2000, p. 110.

[22] Y. Liu, T. He, C. Gao, Colloids Surf. B: Biointerfaces 46 (2005) 117-126.

[23] Y. Zhu, M.B. Chan-Park, Density quantification of collagen grafted on biodegradable polyester: Its application to esophageal smooth muscle cell. Anal. Biochem. 363 (2007) 119-127.

[24] A.R. Chandrasekaran, J. Venugopal, S. Sundarrajan S. Ramakrishna, Fabrication of a nanofibrous scaffold with improved bioactivity for culture of human dermal fibroblasts for skin regeneration. Biomed. Mater. 6 (2011) 015001.

[25] Y. Xia, F. Boey, S.S. Venkatraman, Surface modification of poly(L-lactic acid) with biomolecules to promote endothelialization, Biointerphases 5 (2010) 32-40.

[26] C. Jyh-Ping, S. Chien-Hao, Surface modification of electrospun PLLA nanofibers by plasma treatment and cationized gelatin immobilization for cartilage tissue engineering, Acta Biomaterialia 7 (2011) 234-243.

[27] K.C. Dee, D.A. Puleo, R. Bizius, An introduction to tissue-biomaterial interactions, John Wiley & Sons, Inc., Hoboken, New Jersey, 2002, p.40.

[28] A. Curtis, C. Wilkinson, Topographical control of cells, Biomaterials 18 (1997) 1573-1583.

[29] R.G. Flemming, C.J. Murphy, G.A. Abrams, S.L. Goodman, P.F. Nealey, Effects of synthetic micro- and nano-structured surfaces on cell behavior, Biomaterials 20 (1999) 573-588.

[30] I. Bisson, M. Kosinski, S. Ruault, B. Gupta, J. Hilborn, F. Wurm, P. Frey, "Acrylic acid grafting and collagen immobilization on poly(ethylene terephthalate) surfaces for adherence and growth of human bladder smooth muscle cells. Biomaterials 23 (2002) 3149-3158.

[31] T.A. Horbett, Principles underlying the role of adsorbed plasma-proteins in blood interactions with foreign materials, Cardiovasc. Pathol. 2 (1993) S137–S148.

[32] D.M.E. Margarett, J.G. Steel, Polymer surface chemistry and a novel attachment mechanism in corneal epithelial cells. J. Biomed. Mater. Res. 40 (1998) 621-630.

[33] P.B. van Wachem, T. Beugelling, J. Feijen, A. Bantjes, J.P. Detmers, W.G. van Aken, Interaction of cultured human endothelial cells with polymeric surfaces of different wettabilities. Biomaterials 6 (1985) 403-408.

[34] P. Clark, P. Connolly, G.R. Moores, Cell guidance by micropatterned adhesiveness in vitro. J. Cell Sci. 103 (1992) 287-292.

[35] K. Anselme, Osteoblast adhesión on biomaterials, Biomaterials 21 (2000) 667-681.

[36] Z. Ding, J. Chen, S. Gao, J. Chang, J. Zhang, E.T. Kang, Immobilization of chitosan onto poly-l-lactic acid film surface by plasma graft polymerization to control the morphology of fibroblast and liver cells, Biomaterials 25 (2004) 1059-1067.

[37] R. Chena, C. Huanga, Q. Kea, C. Heb, H. Wangb, X. Mob, Preparation and characterization of coaxial electrospun thermoplastic polyurethane/collagen compound nanofibers for tissue engineering applications, Colloids and Surf. B: Biointerfaces 79 (2010) 315-325.

[38] N.H. Tran, G.R. Dennis, A.S. Milev, G.S. Kamali Kannangara, M.A. Wilson, R.N. Lamb, Interactions of sodium montmorillonite with poly(acrylic acid), J. Colloid Interf. Sci. 290 (2005) 392-396.

[39] H. Thissen, G. Johnson, P.G. Hartley, P. Kingshott, H.J. Griesser, Biomaterials 27 (2006) 35-43.

CHAPTER VI

Enhancement of fatty acid-based polyurethanes cytocompatibility by non-covalent anchoring of chondroitin sulfate

Enhancement of Fatty Acid-based Polyurethanes Cytocompatibility by Non-covalent Anchoring of Chondroitin Sulfate

Rodolfo J. González-Paz[1], Gerard Lligadas[1], Juan C. Ronda[1], Marina Galià[1], Ana M. Ferreira[2], Francesca Boccafoschi[3], Gianluca Ciardelli[2,4], Virginia Cádiz[1].

[1]Department of Analytical and Organic Chemistry, Rovira i Virgili University, Campus Sescelades, C/Marcel.lí Domingo s/n, 43007 Tarragona, Spain.

[2]Department of Mechanical and Aerospace Engineering, Politecnico di Torino, Corso Duca degli Abruzzi, 24, 10129, Turín, Italy.

[3]Department of Health Siences, Università del Piemonte Orientale, Via Solaroli, 17, Novara, Italy.

[4]CNR-IPCF USO Pisa Via Moruzzi 1, 56124 Pisa, Italy.

Abstract.

For tissue engineering purpose biopolymer chondroitin sulfate (CS), one of the major components of cartilage and bone extracellular matrix, was immobilized onto the surface of amino-functionalized polyurethane (PU) films derived from naturally occurring oleic and 10-undecenoic acids. The amino-functionalized PUs were prepared by aminolysis with 1,6-hexamethylenediamine of synthesized PUs containing methyl ester groups. FTIR-ATR, XPS, SEM and water contact angle measurements were used to confirm the surface changes at each step of treatment, both in morphologies and chemical composition. Cytotoxicity and cell morphology analysis using osteoblast cell line MG63 showed that PU-CS films are suitable materials for cell growth, spreading, and differentiation.

Introduction

Biomedical applications have been the primary driver in establishing the science of biocompatible and biodegradable polymers.[1] Tissue engineering has attracted a great deal of attention, and become one of the major fields in biotechnology, because of its potential as a new method in the treatment of damaged or lost human tissue and organs. In tissue engineering, scaffolds play an important role by serving as substrates for bone regeneration, cell attachment, and physical supports for the formation of new tissues.

Whereas demands for new biomedical polymeric materials continue to grow, needs for renewable and biodegradable alternatives of traditional polymers to embrace the challenges in environmental protection and future shortage of petroleum supplies are fueling a new phase of development of the area. In fact, rapid depletion of fossil and petroleum resources, skyrocketing of petrol price, and increasing emission of greenhouse gases have brought the chemical industry, grown on the basis of fossil resources, to a crossroads. Crisis inspires changes, and in this context, actual chemists are being forced to release the chemical industry from its dependence on depleting resources.

Many biological and chemical processes have hitherto been demonstrated powerful for production of polymers, fuels and chemicals from biorenewable resources, with the utilization of carbohydrates and lipids as a major interest.[2] Plant oils as annually renewable platform chemicals are good candidates for the preparation of potentially biocompatible polymers as they are natural body components. Nevertheless, it is important to mention that biobased does not necessarily entail biodegradable.[3] Nowadays there is a broad palette of chemical pathways for the preparation of linear and crosslinked polymers based on triglyceride and fatty acid molecules being polyurethanes (PUs) the most studied system.[4, 5] PUs are popularly used in cardiovascular and other biomedical applications due to their good biocompatibility as well as mechanical properties.[6] However, cellular adhesion on PUs surface is relatively poor and their use in tissue-engineered products is limited. Conventional blending approach with bioactive molecules has been investigated to improve polyurethane performance in tissue engineering.[7,8]. Because the interaction between living cells and materials occurs mainly on the interfacial layer, many surface modification methods with biological molecules

known to mediate cellular attachment have been developed to alter the surface properties of PUs, for improving the cytocompatibility of the materials without alteration of the bulk properties.[9] These include glow discharge or gas plasma treatment,[10,11] protein coating, gelatin impregnation, and hyaluronic acid or collagen immobilization.[12,13,14] Anchoring bioactive molecules on PUs surface is particularly interesting approach because overcomes phase compatibility problems and avoids usual alteration of bulk properties associated with simple blending.

Our group recently applied thiol-yne coupling reaction to alkyne-derivatized fatty acids methyl esters derived from naturally occurring oleic (OL) and 10-undecenoic (UD) acids to prepare diols and polyols suitable for PU technology.[15] OL and UD are the major products of high oleic sunflower oil saponification and castor oil pyrolysis, respectively.The resulting biobased diols were then polymerized with 4,4'-methylenebis(phenylisocyanate) (MDI) to produce the corresponding thermoplastic PUs containing pendant ester groups (Scheme 1).

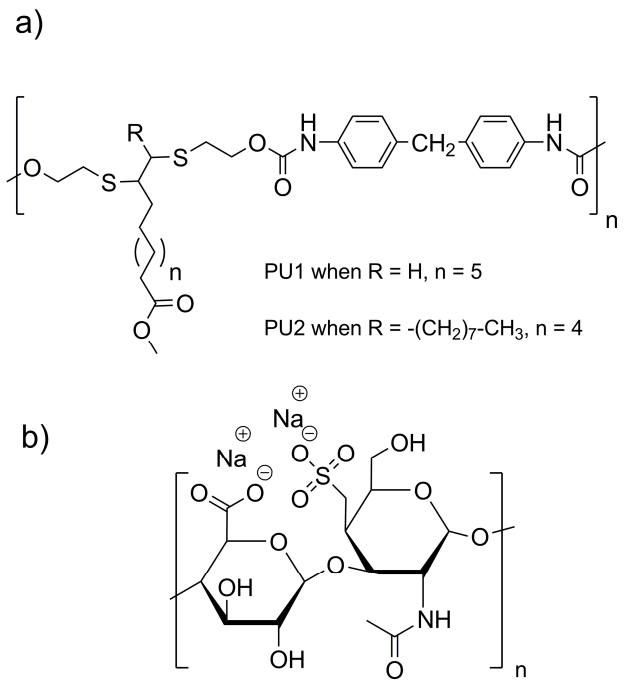

Scheme 1. Chemical structure of a) polyurethanes PU1 and PU2 and b) polysaccharide chondroitin-4-sulfate

In this work we are seeking to improve the cytocompatibility properties of these PUs by anchoring chondroitin sulfate sodium salt (CS, Scheme 1) as a bioactive molecule. CS is a glycosaminoglycan found in the body, mainly in cartilage, in cancellous and compact bones, as a component of the extracellular matrix network (ECM) that plays an important role in regulating the expression of the chondrocyte phenotype and on osteogenetic differentiation.[16] It comprises alternating units of β-1,3-linked glucuronic acid and *N*-acetyl-galactosamine (GalNAc) with sulfate groups at either the 4 or the 6 position of the GalNAc. CS is also involved in intracellular signaling, cell recognition, and the connection of extracellular matrix components to cell-surface glycoproteins.[17] The effects of CS modification on PUs chemical composition, surface properties and osteoblast cell line MG63 adhesion were evaluated in vitro in the search of applications in orthopedic medicine as bone grafts or bone substitute materials.

Experimental Section

Materials.

Thermoplastic PUs, PU1 and PU2, were synthesized as previously described from MDI and biobased diols synthesized via thiol-yne coupling from alkyne-derivatized UD and OL, respectively.[15] Chondroitin-4-sulfate sodium salt (CS) from bovine trachea was purchased from Biochemika. 1,6-Hexamethylenediamine (HMDA) and other auxiliary compounds were purchased from Sigma-Aldrich and were used as received. Double distilled water was used in all the experiments

Aminolysis of PU films.

PU films of 0.5 mm of thickness and 25 cm^2 of surface area prepared by casting from THF solution, were washed with water/ethanol (50% v/v) to clean dirt, with large amount of water and then dried at room temperature under reduced pressure for 12 h. Films were immersed into 0.06 g/ml of HMDA/PrOH solution for 3 or 6 min at 37 ºC, rinsed with a large quantity of water to remove free HMDA for 24 h and finally dried under reduced pressure at 30°C for 12h.[18]

Determination of amine groups.

The Acid Orange 7 (AO7) dye assay was used to label the amino groups on the aminolyzed PU surfaces for quantification purposes.[19] Briefly, samples of defined size (0.25 cm^2) were immersed in 1 ml of a solution of 500 μmol/l AO7 in distilled water at pH 3 (diluted HCl). After shaking for 24 h at room temperature, samples were thoroughly washed with water diluted HCl at the same pH. The amount of bound dye was quantified after detachment in 1 ml of distilled water at pH 12 (diluted NaOH). The detachment was achieved after 15 min of shaking at room temperature. Optical density of the solution was measured spectrometrically at a wavelength of 492 nm using UV-Vis Spectra PerkinElmer, Lambda 25 spectrometer. The concentration of amine groups was determined with help of a calibration curve under assumption that one amine group is complexed with one equivalent value of Acid Orange II. A standard curve was created for 100 μM, 10 μM, 5 μM, 1 μM, 500 nM, and 100 nM concentrations of dye. Triplicate colorimetric measurements were performed for each sample.

Anchoring of CS to aminolyzed PU (PU-NH2) films. PU-NH2 films were treated with 0.012M HCl solution for 1 min, washed with a large amount of water, and subsequently incubated in a CS deionized water solution (2 mg/ ml, pH 6) for 10 min. Finally, PU-CS films were rinsed with deionized water for 10 min and dried under reduced pressure at 30°C for 12h**.**

Staining and determination of CS density on PU-CS.

Taylor`s Blue staining method was used for visualization of the anchored CS on PU-CS surfaces. A Nikon microscope and stereo zoom microscope smz1500 with DS camera Head DS-Fi1 was used. Quantification of CS density on film surfaces was carried out following a colorimetric protocol described by Rider.[20] Briefly, Taylor's Blue solution was prepared as follows: 3.04 g glycine with 2.37 g NaCl were dissolved in 95 mL 0,1 M HCl, 16 mg of 1,9-dimethylmethylene blue dye were gradually added over a period of about 2 min and deionized water was added for making the solution up to 1 L. Films were cut into squared samples with a surface of 1 cm^2 and dipped into Taylor's Blue solution for 90 minutes. The tubes containing the dipped samples were centrifuged at 12000 rpm for 10 min and subsequentely Taylor's Blue solution was

removed and drained off. A 1 ml of 3M GuHCl in PBS, pH 7.5 (Guanidine hydrochloride) as a dissociating agent was added to each sample with the aim to induce the release of the bound dye 1,9-dimethylmethylene molecules and CS groups. A vortex was used for 10 minutes to facilitate the dye dissolution into the solution. Dissociation turn the coloration of dissociating reagent from transparent to blue. After 30 min, dissociating reagent absorbance at 653 nm was measured using an optical spectrophotometer (Perkin Elmer Instrument Lambda 40). Measure absorbance was set against dissociation reagent for the blanks, calibration curve standards and test samples. The colorimetric protocol was be performed in triplicate for each kind of sample. CS density on modified samples was calculated through a calibration curve. This was prepared performing the described protocol to previously prepared CS solutions at known concentrations (1-2-3-4 μg/mL).

Instrumentation.

The FTIR spectra were recorded on an IR Perkin-Elmer Frontier spectrophotometer with an attenuated total reflectance (ATR) device (Germanium crystal). Spectra were taken with a resolution of 4 cm^{-1} and averaged over 36 scans. The wettability of samples was evaluated by contact angle measurements using CAM 200 KSV Instrument, equipped with Tetha software. Static contact angle measurements were carried out adding a drop 3μl-drops of bi-distilled water by a motor driving syringe at room temperature on three different samples of each material and at least three measurements for each sample. Surface morphologies were observed using a LEO 1430VP SEM Equipment. Prior to SEM examination, samples surface were coated with a conductive thin gold film. Atomic composition and surface chemistry were investigated by a X-ray Photoelectron Spectroscopy/Electron Spectroscopy for Chemical Analysis (XPS/ESCA) using PHI 5000 Versaprobe instrument, wih a power of 25.6 W and a scanning surface of 500 x 500 micronm. Overlapping peaks were resolved into their individual components by XPSPEAK 4.1 software.

Cell culture

Synthesized PUs were examined as polymeric supports for growth of MG63 osteoblast cells. Cells were cultured in Dulbecco's modified Eagle's medium enriched with 10% fetal bovine serum (FBS), glutamine (2mM), penicillin (100 U/ml) and streptomycin (100 µg/ml) (Euroclone, Italy). Cells were maintained at 37° C in a humidified atmosphere with 5% CO_2. The cells were seeded at a density of $10^5/cm^2$ on the PUs surface. Cell adhesion and viability were assayed by a colorimetric MTS assay after 24 h. The morphology of cell attachment on the scaffolds was observed by scanning electronic microscopy.

MTS assay and cell attachment

To evaluate cell viability, MTS assay was performed. Cells were cultured on different surfaces for 24 hours. A [3-(4,5-dimethylthiazol-2-yl)-5-(3-carboxymethoxyphenyl)-2-(4-sulfophenyl)-2H-tetrazolium, inner salt (MTS) solution was added to culture medium. After 3 h, culture medium was removed and the solution was analyzed by UV-VIS spectroscopy (V-630 UV-Vis Spectrophotometer, Jasco, USA) at 490 nm. The absorbance was directly proportional to viable cells amount. To study the morphology of cell attachment, the 24 h cell-cultured PU films were washed twice in 0.15M cacodylate buffer and fixed for 30 minutes at 4°C with Karnowsky solution (2% paraformaldehyde and 2.5% glutaraldehyde in 0.15M cacodylate buffer, pH 7.2-7.4). Following fixation, samples were treated for 30 minutes with 1% osmium tetroxide in 0.15M cacodylate buffer solution. Samples were then dehydrated with graded ethanol (from 50% to 100%), soaked for 30 minutes in hexamethyldisilazane. Completely dried samples were sputter-coated with gold-palladium and observed using scanning electron microscopy (SEM, Leo 1450VP, LeoCo.LTD). Images were collected at different magnifications.

Results and Discussion

Diol synthesis and PU preparation

In a recent study, photoinitiated thiol-yne addition was used as a key reaction step to functionalize 10-undecynoic (UDY) and 9-octadecynoic acids (OLY) with hydroxyl moieties. Two biobased diols, UDYM-diol and OLYM-diol, containing methyl ester groups were obtained in high yields as viscous oils. UDYM-diol and OLYM-diol were combined with MDI in DMF solution at 50ºC for 24h using tin (II) 2-ethylhexanoate as a catalyst accepted by FDA.[21] The chemical structures of the corresponding linear PUs were assessed by FTIR and NMR spectroscopy. Characteristic IR absorption bands of the main chain were observed. Thus, the C=O stretching and NH stretching and bending bands arising from urethane linkages appear at 1701 cm^{-1}, 3320 cm^{-1} and 1532 cm^{-1} respectively. Moreover, the C=O stretching band of dangling methyl ester groups appear at 1730 cm^{-1}. ^{1}H and ^{13}C NMR spectra were in all cases in full concordance with the expected chemical structures of PUs. Table 1 shows the molecular weight, polydispersity, and solubility of the PUs synthesized.

Table 1. Polycondensation results and solubility of thermoplastic PUs

			SEC [a]		Solubility [b]			
	Diol	Yield (%)	M_n (g/mol)	M_w/M_n	H_2O	DMSO	$CHCl_3$	THF
PU1	UDYM-diol	93	18,900	1.5	-	+	+	+
PU2	OLYM-diol	98	48,100	1.7	-	+	+	+

[a] Number molecular weight determined by SEC in THF using polystyrene standards.

[b] Solubility at 25ºC: + soluble, - insoluble.

Modification of PU surface via aminolysis

The surface modification of polyester-type PUs and polyesters via aminolysis is a well known procedure.[22,23,24] However, the major drawback of this methodology is that aminolysis treatment partially sacrifices the molecular weight of the polymer. As illustrated in Scheme 2, as a previous step to immobilize CS we took advantage of methyl ester groups to functionalize PUs surface with amine (NH_2) groups by the aminolysis reaction with 1,6-hexamethylenediamine (HMDA) at 37ºC. In this case a reduction of molecular weight is avoided since ester groups are pendant moieties. At a given concentration of 0.06 g/ml of HMDA in PrOH, aminolysis of PU1 and PU2 films was carried out for 3 and 6 min to determine optimal reaction conditions.

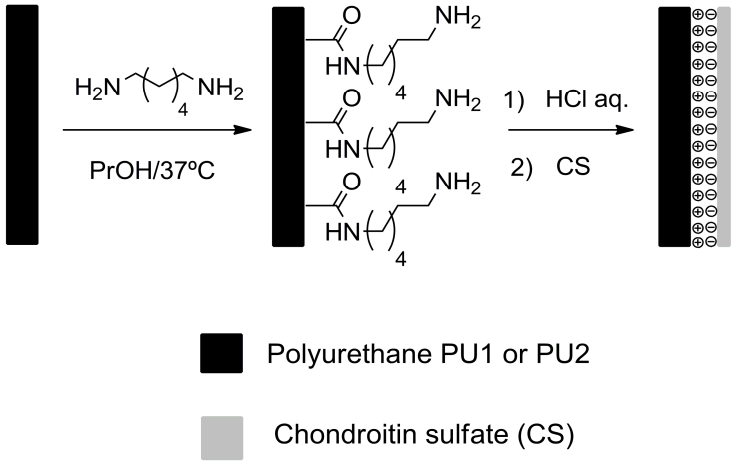

Scheme 2. Schematic diagram showing PU surface aminolysis of ester groups and ionic CS immobilization.

The success of the aminolysis treatment was verified qualitatively by FTIR-ATR and water contact-angle whereas a quantitative determination of surface NH_2 groups was carried out by UV spectroscopy using AO7 dye. FTIR-ATR spectra of PU1 and PU1-NH_2 after 3 and 6 min of aminolysis treatment are shown in Figure 1.

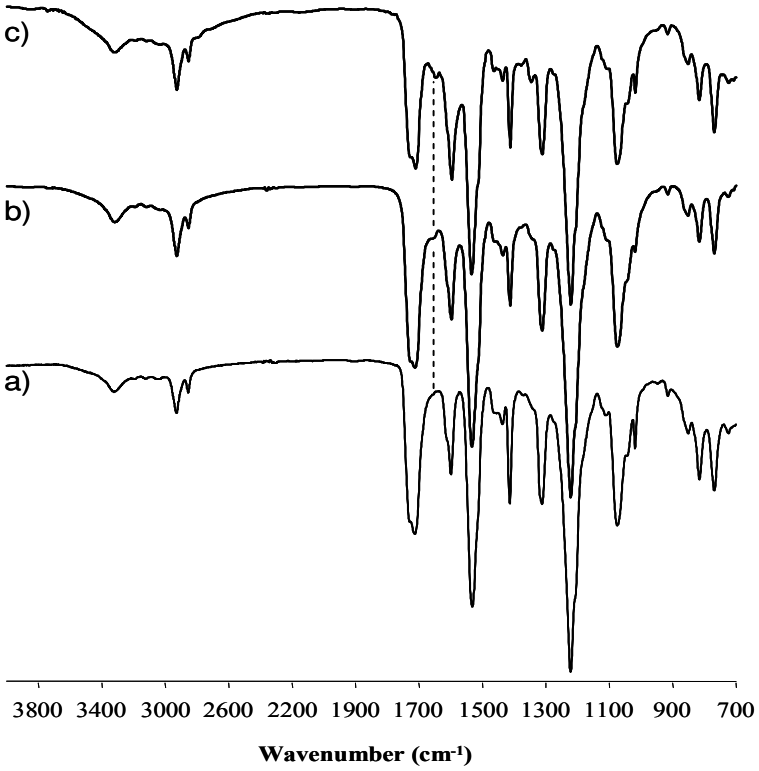

Figure 1. FTIR-ATR spectra of PU1 a) before and after aminolyis treatment with HMDA for b) 3 min and c) 6 min.

In the 3200-3500 cm^{-1} region, PU-NH_2 spectrum was almost the same as that of PU1 control because primary amine N-H stretching bands were overlapped by the urethane N-H absorption bands. The presence of amine groups on the PU1 aminolyzed surface could be confirmed by N-H bending absorbance of primary amine groups occurring at 1630 cm^{-1}. The water contact angle measurement of PU1, PU2, PU1-NH_2, and PU2-NH_2 shown in Figure 2 also confirmed the introduction of hydrophilic -NH_2 groups on PUs surface. Both PU-NH_2 films showed a slight decrease in water contact angle in contrast to virgin PU films. The decrease of contact angle is an index of the chemical changes occurring on the film surfaces, which renders the surface more hydrophilic with respect to the original films.

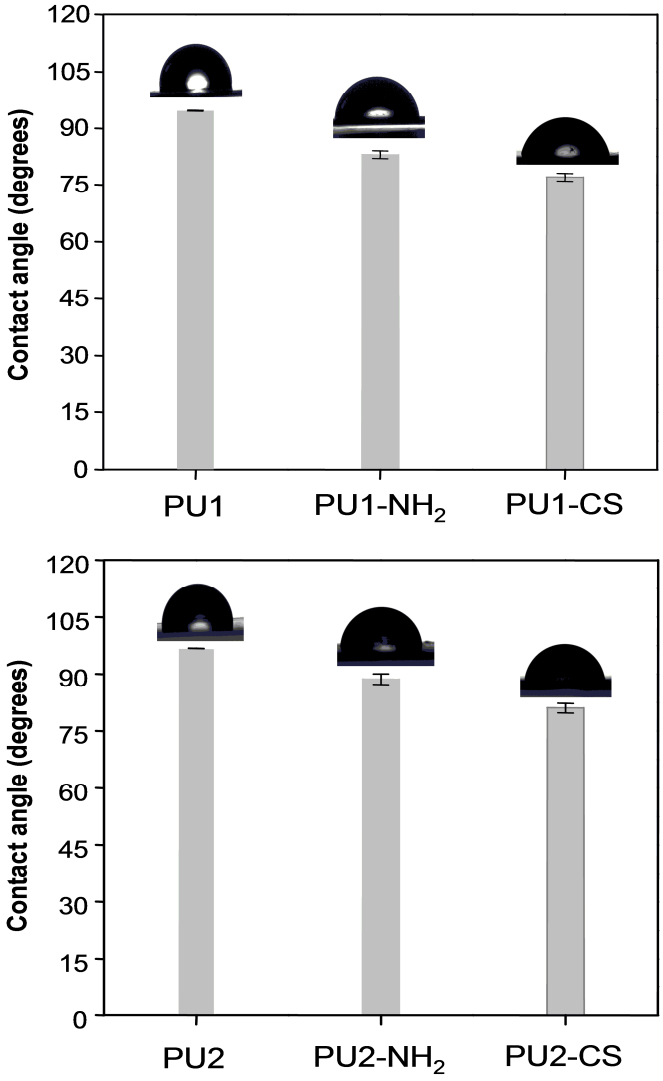

Figure 2. Contact angle values for control PUs, samples after aminolysis treatment treatment with HMDA, and after CS immobilization.

The quantitative determination of NH_2 groups density on PUs-NH_2 films was measured using AO7 dye. PU1-NH_2 showed the highest surface NH_2 density (4.3 ± 0.09 μg/cm^2) at aminolysis time of 6 min. On the other hand, PU2-NH_2 showed higher NH_2 groups density (3.2 ± 0.2 μg/cm^2) after 3 min than after 6 min of aminolysis treatment. When aminolysis time was increased to 6 min amino groups concentration on PU2-NH_2 surface decreased to 2.2 ± 0.7 μg/cm^2. This is possibly due to the presence of long aliphatic side chain in PU2 backbone that provides higher free volume, thus both amino groups of HMDA can react easily between methyl ester groups, decreasing the free primary amino groups concentration on surface and promoting the crosslinking of PU2 chains at long time treatment. On the basis of SEM images, these results suggest that in

the later case high surface porosity occurred in some extend probably due to a strong crosslinking between PU2 chains on the surface at too long aminolysis treatment. SEM micrographs shown in Figure 3 illustrate the surface morphology changes of PU1 and PU2 films before and after 3 and 6 min aminolysis treatment.

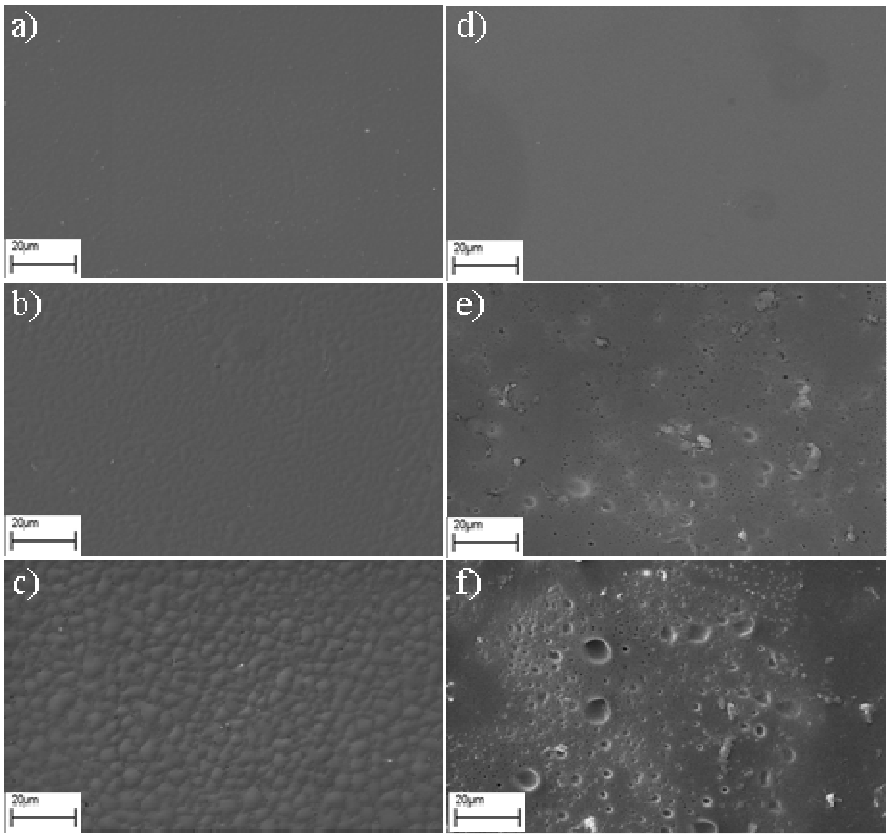

Figure 3. SEM micrographs of control PU1 and PU2 (a and d), samples after 3 min (b and e) and 6 min (c and f) aminolysis treatment treatment with HMDA.

As shown in Figure 3a and d, the surface of virgin PUs obtained by casting was smooth. After 3 min aminolysis treatment (Figure 3b and e) both PU surfaces maintained a regular and homogeneous morphology only disrupted by some small pores in PU2. As can be seen in Figure 3c and f, 6 min aminolysis treatment clearly modified PU surface in both systems. PU1 surface became rougher whereas in the case of PU2 many deep pores appeared.

Ionic Immobilization of CS on PU-NH_2

Water contact angle data demonstrated that the introduction of NH_2 groups onto PU films surface improves the poor hydrophilicity of the studied fatty acid-derive PUs but also provide the necessary active sites through which other biocompatible components such as proteins, polysaccharides, cell growth factors, or peptides can be further immobilized. As illustrates Scheme 2, after aminolysis and taking advantage of NH_2 group's basicity, we anchored the polysaccharide CS on PU surface via non covalent ionic interactions. First, PU-NH_2 films were treated with a 0.012M HCl solution to ensure a positive charged state on the surface of the material. Then, films were incubated in a CS aqueous solution. The alteration of surface wettability and XPS were used to evaluate the success of the immobilization process. As can be seen in Figure 2, PU1-CS and PU2-CS surfaces become less hydrophobic after CS was anchored as their water contact angles decrease to about 77º and 82º for PU1-CS and PU2-CS respectively. XPS analysis of PU2 results are in agreement with contact angle values and also confirmed the CS immobilization.

Table 2. XPS elemental surface composition (%) of PU2, PU2-NH_2 and PU2-CS.

Sample	O_{1s}	N_{1s}	C_{1s}	S_{2p}	Na_{1s}	O/C	N/C	N/S
PU2	13	3.5	80	3.5	-	0.16	0.044	1.0
PU2-NH_2	11.9	6.2	78.4	3.5	-	0.15	0.08	1.7
PU2-CS	21.1	6.0	68.6	3.6	0.7	0.3	0.09	1.6

Table 2 shows the surface composition of the virgin PU2 and modified PU2-NH_2 and PU2-CS films. Consistently with the fact that the CS is an oxygen-rich molecule compared with the virgin PU2 and PU-NH_2, containing oxygen atoms in both the sugar ring and pendant alcohol groups, PU2-CS exhibited the highest O concentration.The O/C ratio is directly associated with the surface density of the immobilized CS on surface. From Table 2, we noted that PU2-CS showed O/C ratio much smaller than CS respective theoretic value (O/C=1.0). The stoichiometry does not reach the value expected from CS atomic composition, because the thickness of the CS

layer is thinner than the XPS sampling depht, including the PU2-NH_2 substrate. As the sampling depht of XPS in polymer matrix usually is about 7 nm, it could be concluded that the thickness of the immobilized CS layer do not exceed 6-7 nm.[25]

S_{2p} core-level spectra for PU2 and PU2-CS shown in Figure 4 also confirm polysaccharide anchoring. The S_{2p} peak for PU2 consists of only one component, a thioether (S-C) peak at 164.3 eV. On the other hand, S_{2p} peak for PU2-CS can be curve-fitted into two peak components with binding energies at about 164.4 and 166.8 eV, attributable to the S-C and and S=O species, respectively. The above results and the increase of the C_{1s} signal area at 286.3 eV associated to C-O linkages are consistent with the fact that CS was successfully immobilized on the PU surfaces.

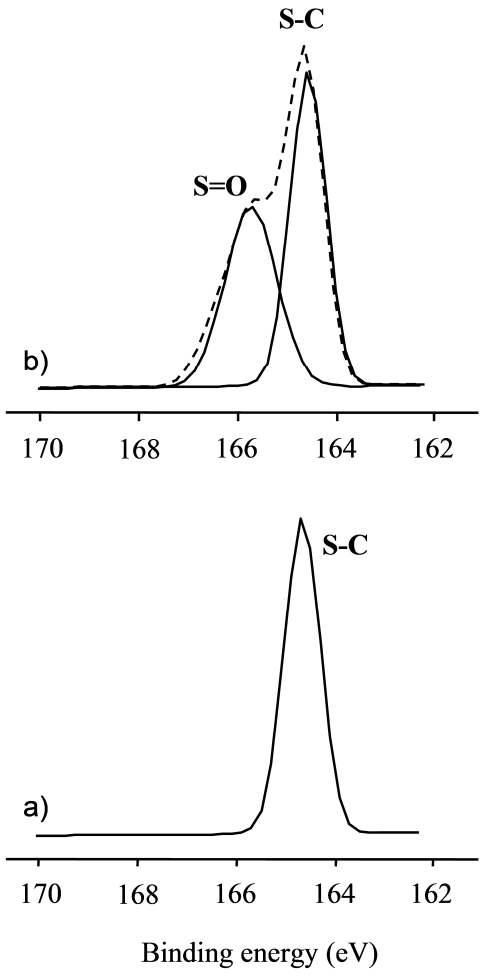

Figure 4. High-resolution S_{2p} peaks of ESCA spectra for a) PU2 and b) PU2-CS.

The surface morphologies of PUs-CS were studied by SEM to compare with initial morphologies. Figure 5 shows how after CS immobilization, the roughness of surface increased significantly and a rolling showing can be appreciated. Moreover, some CS aggregates of approximately 1 μm appeared.

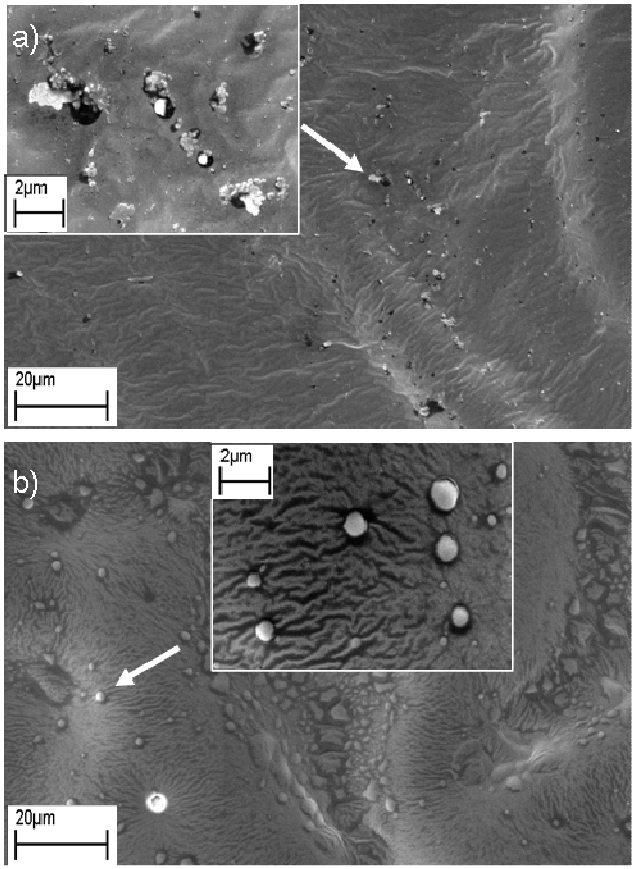

Figure 5. SEM micrographs of a) PU1-CS and b) PU2-CS.

To microscopically visualize the CS layer on PU-NH_2 surfaces and further quantify its concentration, optical microscopy was performed on control PUs and PUs-CS stained with 1,9-dimethylmethylene blue (DMMB) dye. Cationic DMMB dye is well known for binding to sulfate and carboxyl groups present in glycosaminoglycan chains.[26] Figure 6 shows how PUs-CS stained blue on a white background. The intense staining provides another evidence of CS immobilization. The CS density ($\mu g/cm^2$) values were determined colorimetrically following a procedure reported by Rider.[20] The immobilized amount of CS on PU1 and PU2 was determined to be 1.5 ± 0.07 $\mu g/cm^2$ and 0.8 ± 0.02 $\mu g/cm^2$, respectively.

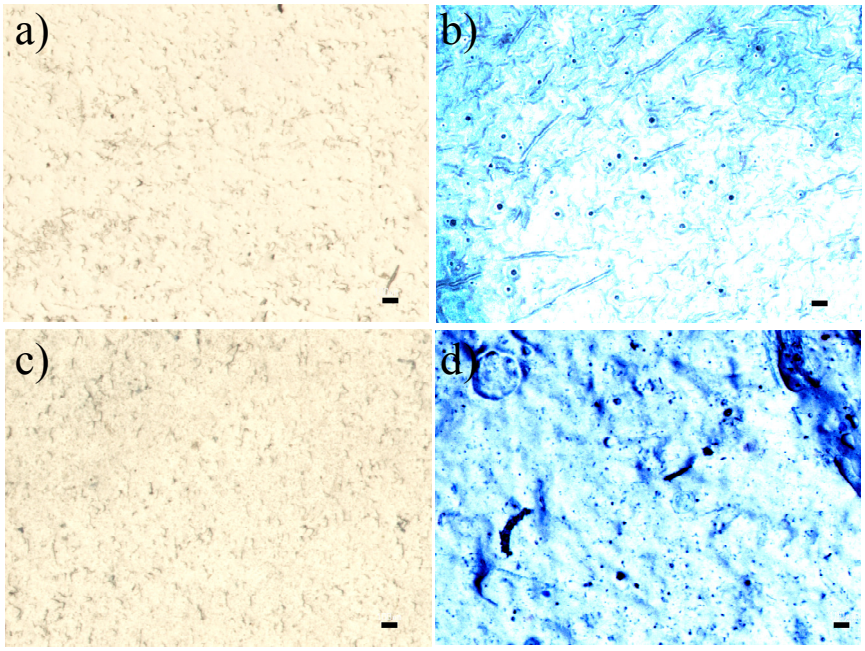

Figure 6. Optical microscopy images of a) PU2, b) PU2-CS, c) PU1, and d) PU1-CS stained with DMMB dye. Scale bar (100μm)

Cell culture on the CS-modified PUs

Cytocompatibility of the control PUs and PU-CS was evaluated by testing the viability of cells in contact with the polymer surfaces. In this study, a MTS assay with osteoblast cell line MG63 was used. MG63 cells are derived from a human osteosarcoma and express a number of features characteristics of osteoblasts.[27] Figure 7 shows the viabilities of osteoblasts seeded on PU1, PU2, PU1-CS, PU2-CS films and under control conditions (absence of materials, standard plastic culture plates). The introduction of the CS on PUs suface markedly enhanced the cell viabilities. MTS for PU1 increased from 76% to 112% after CS immobilization, whereas and increment of 10% was obtained for PU2-CS versus PU2. These results can be related with the fact that CS is promoting osteblast cell adhesion and enhance osteoblast cell attachment via ligand-acceptor interaction.[28] Another possible cause may be that the hydrophilic CS facilitates the penetration of the medium into the surface, such that the cells attach easily to the surface and grow well.

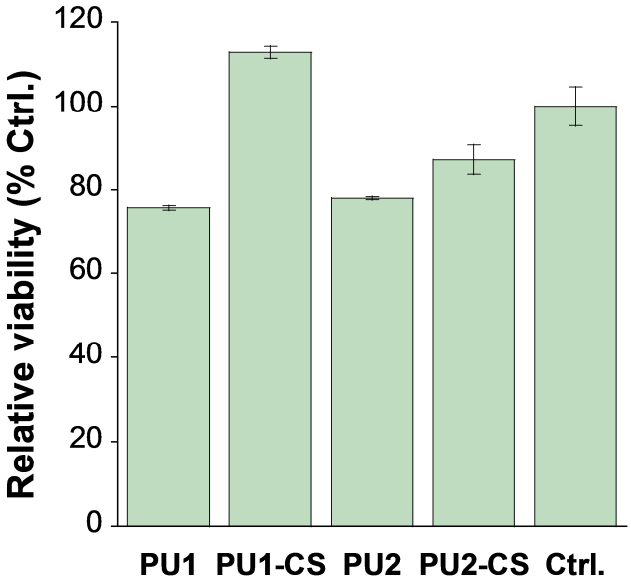

Figure 7. MTS cytotoxicity results for control and PUs before and after CS immobilization.

Cell morphology on the various PUs surfaces was analyzed by SEM. As can be seen in Figure 8, cells successfully attached to all samples after 24h.

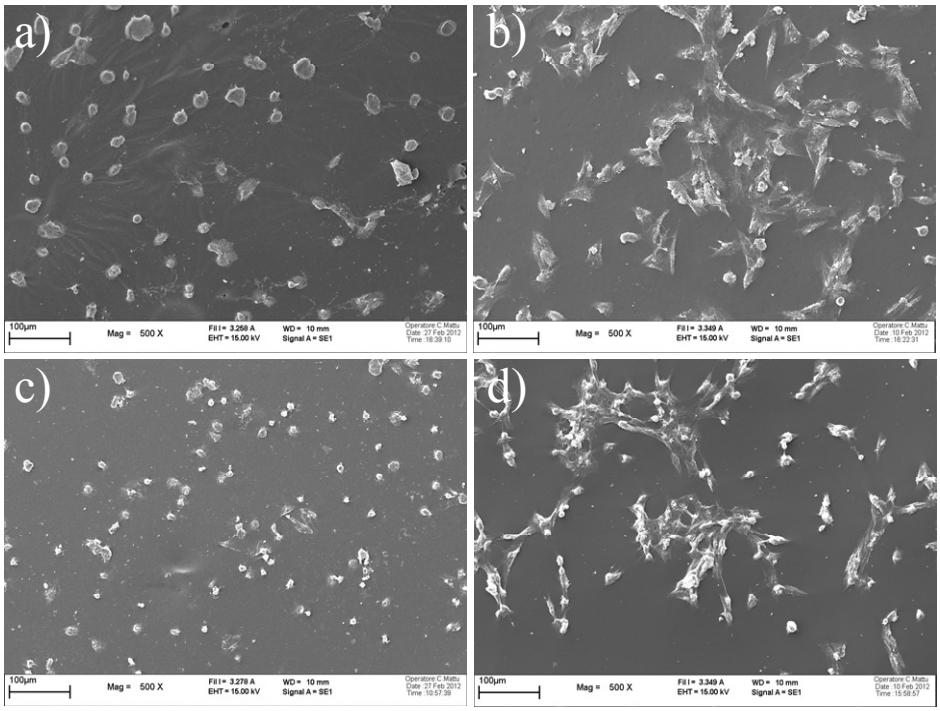

Figure 8. SEM micrographs of MG63 cells cultured for 24 h on PU1 a) before and b) after, and PU2 c) before and d) after CS immobilization.

In agreement with MTS data, best results were obtained for PUs-CS. On the control PUs, although cells could adhere, cell morphology observations evidenced no cell division or cell spreading after 24 h. On the contrary, cell clusters could be found. On both PU1-CS and PU2-CS surfaces, cells were well attached and spread out, displaying a flat configuration and normal morphology. However, the absolute cell number was not high enough to cover the entire surface, leaving some bare areas not occupied by the cells. Nevertheless, this morphology generally indicates that the materials are favorable for cell growth, spreading, and differentiation. In summary, cell viability and attachment on the studied fatty acid-based PUs was significantly improved by anchoring CS on their surface.

Conclusions

In this paper, in order to provide a convenient way to immobilize the polysaccharide CS on polyurethane (PU) films derived from naturally occurring oleic and 10-undecenoic acids, free amino groups have been introduced by aminolysis with HMDA of pendant methyl ester groups present in the PUs. The variation of FTIR-ATR, XPS, water contact angle and morphology showed that CS was successfully immobilized ionic on the surface of polyurethanes. CS immobilization not only improved the hydrophilicity, but also greatly improved cytocompatibility in comparison with base PUs. Hence, it can be concluded that the CS immobilization is a promising way to enhance biological activity of fatty acid-derived PUs.

Acknowledgements

The authors express their thanks to CICYT (Comisión Interministerial de Ciencia y Tecnología) (MAT2011-24823) for financial support for this work.

References

[1] Biomimetic, Bioresponsive, and Bioactive Materials: An Introduction to Integrating Materials with Tissues, M. Santin and G. J. Phillips Ed., John Wiley & Sons , Inc., Hoboken, New Jersey 2012.

[2] U. Biermann, U. Bornscheuer, M. A. R. Meier, J. O. Metzger and H. J. Schäfer, Angew. Chem. Int. Ed. 2011, 50, 3854.

[3] M. Desroches, M. Escouvois, R. Auvergne, S. Caillol, B. Boutevin, Polym. Rev. 2012, 52, 38.

[4] L. Montero de Espinosa, M. A. R. Meier, Eur. Polym. J. 2011, 47, 837.

[5] G. Lligadas, J. C. Ronda, M. Galià, V. Cádiz, Biomacromolecules 2010, 11, 2825.

[6] Biomedical Applications of Polyurethanes, P. Vermette, H. J. Griesser, G. Laroche and R. Guidoin, Eurekah.com, Georgetown, Texas, U.S.A, 2001.

[7] Q. Lv, C. Cao, H. Zhu, Biomaterials 2003, 24, 3915.

[8] M. C. Popescu, C. Vasile, D. Macocinschi, M. Lungu, O. Cracinunescu, Int. J. Biol. Macromol. 2010, 47, 646.

[9] J. M. Goddard, J. H. Hotchkiss, Prog. Polym. Sci. 2007, 32, 698.

[10] S. K. Williams, T. Carter, P. K. Park, D. G. Rose, T. Schneider, B. E. Jarrell, J. Biomed. Mater. Res. 1992, 26, 103.

[11] S. Sartori, A. Rechichi, G. Vozzi, M. D'Acunto, E. Heine, P. Giusti, G. Ciardelli, React. Funct. Polym. 2008, 68, 809.

[12] F. Hess, R. Jerusalem, O. Reijnders, C. Jerusalem, S. Steeghs, B. Braun, P. Grande, Biomaterials 1992, 13, 657.

[13] P. C. Lee, L. L. H. Huang, L. W. Chen, K. H. Hsieh, C. L. Tsai, J. Biomed. Mater. Res. 1996, 32, 645.

[14] F. Xu, J. C. Nacker, W. C. Crone, K. S. Masters, Biomaterials 2008, 29, 150.

[15] R. J. González-Paz, G. Lligadas, J. C. Ronda, M. Galià, V. Cádiz, Polym. Chem. 2012, 3, 9, 2471-2478.

[16] W. Schneiders, C. Rentsch, S. Rehberg, S. Rein, H. Zwipp, S. Rammelt, Mater. Sci. Eng. C, 2012, 32, 1926.

[17] S. Ayad, R. P. Boot-Handford, M. J. Humphries, K. E. Kadler, C. A. Shuttleworth, In The Extracellular Matrix-Facts Book; Academic Press: San Diego, CA, 1994.

[18] Y. Zhu, Y. Sun, Coll. Surf. B Biointerfaces 2004, 36, 49.

[19] E. Uchida Y. Uyama, Y. Ikada, Langmuir 1993, 9, 1121.

[20] C. C. Rider, In Methods in Molecular Biology: Glycoanalysis Protocols, E F Hounsell Ed., Humana Press Inc., Totowa, NJ., Vol 76, 131-143, 1998.

[21] FDA (Food and Drugs Administration). Resinous and polymeric coatings. In: Title 21, Chapter I, Part 175, Subpart C, Sec. 175,300. USA, 2002.

[22] Y. Zhu, C. Gao, T. He, J. Shen, Biomaterials 2004, 25, 423-430.

[23] Y. Zhu, C. Gao, X. Liu, J. Shen, Biomacromolecules 2002, 3, 1312.

[24] Y. Zhu, C. Gao, X. Liu, T. He, J. Shen, Tissue. Eng. 2004, 10, 53.

[25] Z. Ding, J. Chen, S. Gao, J. Chang, J. Zhang, E.T. Kang, Biomaterials 2004, 25, 1059.

[26] B. O. Enobakhare, D. L. Bader, D. A. Lee, Anal. Biochem. 1997, 243, 1189.

[27] Clover, J.; Gowen, M. Bone 1994, 15, 585.

[28] J.W. Lee, R. Juliano, Mol. Cells 2004, 17, 188.

GENERAL CONCLUSIONS

General conclusions

- Using thiol-ene (TEC) and thiol-yne (TYC) as a key step, novel routes to obtain diols and triols derived from oleic and 10-undecenoic acids are described.

- Prepared diols and triols were combined with MDI to produce the corresponding thermoplastic and thermosetting polyurethanes, which revealed good thermal and mechanical properties.

- Polyurethanes (PUs) showed no cytotoxic response, which indicates that these materials could be useful as polymeric supports for tissue engineering.

- The blending of PUs with gelatin resulted in an improving of the hydrophilicity, bioactivity and cell adhesivity of the PUs.

- Plasma treatment with acrylic acid was used as a previous step to covalently immobilize collagen on PUs surface. Collagen had a positive effect on the cytocompatibility of the PUs.

- Chondroitin sulfate was successfully ionically immobilized on the surface of polyurethanes. Chondroitin sulfate immobilization improved hydrophilicity, and cytocompatibility in comparison with base polyurethanes.

APPENDICES

Appendix A: List of abbreviations

AA	Acrylic acid
ACP	Amorphous calcium phosphate
AIBN	2,2`-azobis(2-methylpropionitrile)
AO7	Acid orange 7 or IUPAC name: (sodium 4-[(2E)-2-(2-oxonaphthalen-1-ylidene)hydrazinyl] benzenesulfonate
ATR	Attenuated total reflection
Cm-SH	7-mercapto-4-methylcoumarin
CS	Chondroitin sulfate
DCPD	Dicalcium phosphate dihydrate
DMF	Dimethylformamide
DMMB	1,9-dimethylmethylene blue or IUPAC name: (3,7'-bis(dimethylamino)-1,9-dimethyldiphenothiazin-5-ium chloride
DMEM	Dubelcco`s modified eagle medium
DMPA	2,2-dimethoxy-2-phenylacetophenone
DMSO	Dimethyl sulfoxide
DMTA	Dynamic mechanical thermal analysis
DSC	Differential scanning calorimetry
E	Young`s modulus
E_a	Activation energy
ECM	Extracellular matrix
EDS	Energy dispersive spectroscopy
EDC	1-ethyl-3-(3-dimethylaminopropyl) carbodiimide
EDTA	Ethylenediaminetetraacetic acid
FBS	Fetal bovine serum
FDA	Food and drugs administration
FTIR	Fourier transform infrared spectroscopy
GalNAc	N-acetyl-galactosamine
gHSQC	Gradient-selected heteronuclear single quantum correlation
HA	Hydroxyapatite
HEPES	4-(2-hydroxyethyl)-1-piperazineethanesulfonic acid
HFIP	Hexafluoroisopropanol

HMDA	1,6-Hexamethylenediamine
ΔH	Melting enthalpy
MCPM	Monocalcium phosphate monohydrate
MDI	4,4`-methylenebis(phenylisocyanate)
M_n	Number average molecular weight
MTT	3-(4,5-dimethylthiazol-2-yl)-2,5-diphenyltetrazolium bromide
MTS	3-(4,5-dimethylthiazol-2-yl)-5-(3-carboxymethoxyphenyl)-2-(4-sulfophenyl)-2H-tetrazolium, inner salt
M_w	Weight average molecular weight
NHS	N-hydroxysuccinimide
NMR	Nuclear magnetic resonance
OL	Oleic acid
OLA	Allyl oleate
OLM	Methyl oleate
OLY	9-octadecynoic acid
OLYM	Methyl 9-Octadecynoate
PAA	Polyacrylic acid
PBS	Phosphate buffered saline
pPAA	Plasma-polymerized acrylic acid
PUs	Polyurethanes
RGD	Arginine-Glycine-Aspartame
SBF	Simulated body fluid
SDS-PAGE	Sodium dodecylsulfate polyacrylamide gels
SEC	Size exclusion chromatography
SEM	Scanning electron microscopy
TBO	Toluidine Blue O or IUPAC name (7-amino-8-methyl-phenothiazin-3-ylidene)dimethyl-ammonium
TEC	Thiol-ene coupling
T_g	Glass transition temperature
TGA	Thermogravimetric analysis
THF	Tetrahydrofuran
T_m	Melting temperature
T_{max}	Temperature of maximum weight loss
TMX	Thermanox

TPUs	Thermoplastic polyurethanes
TYC	Thiol-yne coupling
$T_{5\%}$	Temperature of 5% weight loss
UD	10-undecenoic acid
UDA	Allyl 10-undecenoate
UDM	Methyl 10-undecenoate
UV-VIS	Ultraviolet-visible
UDY	10-undecynoic acid
UDYM	Methyl 10-undecynoate
XPS	X-Ray photoelectron spectroscopy
ε	Strain at break
σ	Stress at break

Appendix B: List of publications

Authors: R.J. González-Paz, C. Lluch; G. Lligadas, J.C. Ronda, M. Galià; V. Cádiz.
Title:"A Green Approach toward Oleic and Undecylenic Acids-Derived Polyurethanes"
Ref.: J. Polym. Sci. Part A: Polym. Chem. 49, 2407-2416, 2011.

Authors: R.J. González-Paz; G. Lligadas, J.C. Ronda; M. Galià,V. Cádiz.
Title: "Thiol-yne Reaction on Alkyne-derivatized Fatty Acids: Biobased Polyols and Cytocompatibility of derived Polyurethanes"
Ref.: Polym. Chem. 3, (9), 2471-2478, 2012.

Authors: R. J. González-Paz, G. Lligadas, J.C. Ronda, M. Galià, A. M. Ferreira Duarte, F. Boccafoschi, G. Ciardelli, V. Cádiz.
Title: "Study on the interaction between gelatin and polyurethanes derived from fatty acids".
Ref.: J. Biomed. Mat. Res. Part A, (In Press).

Authors: R. J. González-Paz, G. Lligadas, J. C. Ronda, M. Galià, A. M. Ferreira Duarte, F. Boccafoschi, G. Ciardelli, V. Cádiz.
Title: "Enhancement of Fatty Acid-based Polyurethanes Cytocompatibility by Non-covalent Anchoring of Chondroitin Sulfate"
Ref.: Macromol. Biosci. (In Press)

Authors: R. J. González-Paz, G. Lligadas, J. C. Ronda, M. Galià, A. M. Ferreira Duarte, F. Boccafoschi, G. Ciardelli, V. Cádiz.
Title: "Cytocompatible polyurethanes from fatty acids through covalent immobilization of collagen"
Ref.: Submitted to React. Funct. Polym.

Authors: R. J. González-Paz, G. Lligadas, J. C. Ronda, M. Galià, V. Cádiz.
Title: "Thiol-yne Reaction of Alkyne-derivatized Fatty Acids: Thiol-Reactive Linear Polyurethanes"
Ref.: To be submitted.

Appendix C: Stages and meeting contributions

Authors: C. Lluch, R. J. González-Paz, G. Lligadas, J.C. Ronda, M. Galià, V. Cádiz.
Oral communication: "Thiol-ene/ Thiol-Yne Coupling Reactions of Fatty Acid" Derivatives.
Congress: V Congreso de Jóvenes Investigadores en polímeros (JIP).
Place: Calella de Palafrugell, Spain **Data:** May, 2009

Autores: C. Lluch, R. J. González-Paz, G. Lligadas, J.C. Ronda, M. Galià, V. Cádiz.
Oral communication: "Polyurethanes and Polyanhydrides from Thiol-ene Functionalized Castor Oil Derivatives".
Congress: MACRO 2010, 43rd World Polymer Congress, Polymers science in the Service of Society.
Place: Glasgow, England **Data:** July, 2010

Authors: R. J. González-Paz, K. Noris-Suárez, G. González, J. L. Feijoo, J. Lira-Olivares.
Poster presentation: "Biomimetic growth of hydroxyapatite nanocrystals inside self-assembled collagen fibers".
Congress: International Bone Tissue Engineering
Place: Hannover, Germany **Data:** October, 2010

Authors: G. Lligadas, C. Lluch, R. J. González-Paz, E. Rio, J.C. Ronda, M. Galià, V. Cádiz.
Oral Communication: "Green aproaches Toward Plant-Derived Monomers and Polymers Via Thiol-ene Click Chemistry".
Congress: 4th Workshop on Fats and Oils as Renewable Feedstock for the Chemical Industry.
Place: Karlsruhe, Germany **Data:** April, 2011

Authors: R. J. González-Paz, G. Lligadas, J. C. Ronda, M. Galià, V. Cádiz

Poster presentation: "Oleic and undecylenic acids-based diols and derived polyurethanes via thiol-ene coupling".

Congress: European Polymer Congress

Place: Granada, Spain **Data:** June, 2011

Authors: Z. Beyazkilic, R. J. González-Paz, G. Lligadas, J. C. Ronda, M. Galià, V. Cádiz

Poster presentation: "Thiol-yne coupling to undecylenic acid derivatives. Synthesis of polyurethanes".

Congress: European Polymer Congress

Place: Granada, Spain **Data:** June, 2011

Authors: R. J. González-Paz, G. Lligadas, J. C. Ronda, M. Galià, A. M. Ferreira, F. Boccafoschi, G. Ciardelli, V. Cádiz

Oral communication: "Polyurethanes derived from fatty acids and their interactions with gelatin"

Congreso: European Materials Research Society Fall Meeting

Place: Warsaw, Poland **Data:** September, 2012

Stays abroad

Organization: Politecnico di Torino

Departament: Departament of Mechanical and Aerospace Engineering.

Host center: Biomedical Laboratory.

Cities: Torino, Alessandria. **Country:** Italy

Length: 122 days **Year:** 2011-2012